

The genomics of  
stress-induced life cycle  
decisions in nematodes

Thesis by  
James Siho Lee

In Partial Fulfillment of the Requirements for  
the Degree of  
Doctor of Philosophy in Biology

The Caltech logo, featuring the word "Caltech" in a bold, orange, sans-serif font, centered within a light orange rectangular background.

CALIFORNIA INSTITUTE OF TECHNOLOGY  
Pasadena, California

2019  
(Defended September 25, 2018)



© 2018

James Siho Lee

ORCID: 0000-0002-4959-7237

## ACKNOWLEDGEMENTS

Nowadays, I find myself struggling to remember the people I wish I could thank the most. So, this section is here so that I will never forget the people who helped me along my PhD. (Part of me thinks I would otherwise, because it all seems so unreal.) Animals make decisions based on their environment, and my environment in Caltech was a very good one:

I would like to thank my classmates Alicia Rogers, Benji Uy, Greg Donaldson, and Katie Schretter, who are my role models in life and science; my friends Christopher Gilson, Eugene Shvarts, Haley Stepp, Jennifer Chen, Millie Grimes, and Sarah Gao, whose visits were the cure for my struggles; my mentors Amir Sapir, Mihoko Kato, Ryoji Shinya, and Tsui-Fen Chou, who helped me find myself as a scientist; my committee members Bruce Hay, Ellen Rothenberg, Eric Davidson, and Joseph Parker, who embody everything that I hope to be; my advisor Paul Sternberg, the Wormy Wonka to this wild, one of a kind laboratory, and who taught me everything my family didn't; my family, who taught me everything Paul didn't; my lab: the post-docs who showed me the way, and the grad students with whom we made fun of the post-docs; and my partner Pei-Yin Shih, who is the kindest person I know. I am incredibly lucky to have her support.

Finally, I dedicate this thesis to my grandfather, Jin Sung Koo. He saw the connections that tied every living thing together—he saw the picture in ways geneticists dream of.

## ABSTRACT

Organisms including bacteria, insects, and mammals make decisions to alter aspects of their development based on signals from the environment. The roundworm *Caenorhabditis elegans* can escape environmental collapse by halting reproductive growth and entering the stress-resistant dauer larval stage. Dauer larvae are spore-like and have specialized behaviors for finding and stowing onto carrier animals for dispersal. The decision to enter dauer is an anticipatory decision that is based on the inputs of food, pheromone, and temperature.

Here, I show that touch is an overlooked input into the dauer entry decision. Using quantitative dauer entry assays on CRISPR knock-ins and existing mutants in mechanosensation, I demonstrate that gentle, harsh, and piezo touch promote dauer entry. By measuring pheromone sensation and signal transmission in mechanosensation-defective mutants, I show that mechanosensation likely inputs into the decision in parallel with pheromone. Further confirmation that touch promotes dauer entry is provided using direct mechanical stimulation of *C. elegans*, and I provide a plausible role for touch in sensing dauer-promoting weather and crowding conditions.

Using RNA-seq, I also show that 8,042 genes are differentially expressed between dauer and reproductive development. Within this dataset, we observed the striking up-regulation of 64 neuropeptide genes (encoding 215 peptides) during dauer. By comparison, the entire human genome contains 97 neuropeptide genes (encoding 270 peptides). In particular, we observed coordinated up-regulation of

the FMRFamide-like neuropeptides (FLPs). Using *sbt-1* mutants to knock down neuropeptide processing, we demonstrate that peptidergic signaling promotes the dauer entry decision, promotes vigorous waving during the dauer-specific nictation behavior (carrier animal-hitchhiking), and is necessary for switching from repulsion to CO<sub>2</sub> (a carrier animal cue) in non-daughters to CO<sub>2</sub> attraction in daughters. By testing individual neuropeptides using CRISPR knockouts and existing strains, we show that 7 FLPs promote dauer entry while 4 FLPs inhibit. I therefore propose plausible roles for these FLPs in acting downstream of and/or modulating the sensation of food, pheromone, temperature, and touch inputs. We also demonstrate that FLP-10/FLP-17, which are expressed in the CO<sub>2</sub>-sensing BAG neuron, promote CO<sub>2</sub> chemotaxis and nictation in daughters. These findings reveal that neuropeptides can alter decision-making and behavior during *C. elegans* dauer entry. Through a meta-analysis, we discovered similar up-regulation of FLPs in the dauer-like infective juveniles of diverse parasitic nematodes, suggesting that this may be an ancient mechanism for expanding the behavioral repertoire of nematodes.

Further utilizing our RNA-seq dataset, I identified several markers for conveniently tracking and manipulating the dauer entry decision. These include *col-183* (which tracks dauer fate in the hypodermis), *ets-10* (neurons and intestine), *nhr-246* (intestine and muscle), and *led-1* (reproductive fate in hypodermis). Using condition shift experiments, we demonstrate that the dauer markers label animals during dauer-commitment. We show that these markers can be used to manipulate the entry decision by driving the reproduction-promoting

gene *daf-9*/Cytochrome P450 under the control of the dauer-commitment markers. We further demonstrate that the markers can be used to track tissue coordination and its breakdown in partial dauer mutants, and propose strategies for using the markers to identify the intercellular signals that coordinate the dauer entry decision.

I have discovered that the *C. elegans* dauer entry decision is more complex than previously realized, I have shown that *C. elegans* dauers obtain new behaviors through FLP signaling, and I have engineered tools for conveniently tracking and manipulating the dauer entry decision. My findings may illuminate how animals make robust decisions in uncertain environments, and have implications for how densely information and behaviors can be packed into a nervous system.

## PUBLISHED CONTENT AND CONTRIBUTIONS

**Lee JS**, Shih PY, Schaedel ON, Quintero-Cadena P, Rogers AK and Sternberg PW (2017) FMRFamide-like peptides expand the behavioral repertoire of a densely connected nervous system. *Proceedings of the National Academy of Sciences USA* 114(50): E10726-E10735. doi: 10.1073/pnas.1710374114

J.S.L. participated in designing research, performing experiments, contributing new reagents, analyzing data, and writing the manuscript.

## TABLE OF CONTENTS

Acknowledgements.....	iii
Abstract .....	iv
Published Content and Contributions.....	vii
Table of Contents.....	viii
List of Illustrations and/or Tables.....	x
Chapter 1: Introduction .....	1
Thesis overview .....	2
Figures .....	21
References .....	25
Chapter 2: <i>Caenorhabditis elegans</i> can use mechanosensation to predict environmental collapse.....	36
2.1 Abstract .....	37
2.2 Introduction .....	38
2.3 Results .....	40
2.4 Discussion .....	47
2.5 Materials and Methods.....	51
2.6 Figures .....	54
2.7 References .....	65
Chapter 3: FMRFamide-like peptides expand the behavioral repertoire of a densely connected nervous system .....	75
3.1 Abstract .....	76
3.2 Introduction .....	78
3.3 Results .....	81
3.4 Discussion .....	98
3.5 Materials and Methods.....	103
3.6 Figures .....	116
3.7 References .....	135
Chapter 4: Genetic markers enable the verification and manipulation of the <i>Caenorhabditis elegans</i> dauer entry decision.....	150
4.1 Introduction .....	151
4.2 Results .....	153
4.3 Discussion .....	160
4.4 Materials and Methods.....	163
4.5 Figures .....	168
4.6 References .....	182
Appendix A: Extremophile nematodes in and around Mono Lake.....	186
A.1 Abstract .....	187
A.2 Introduction .....	188
A.3 Results .....	191
A.4 Discussion .....	199

A.5 Materials and Methods.....	202
A.6 Figures.....	205
A.7 References .....	234



## LIST OF ILLUSTRATIONS AND/OR TABLES

<i>Figure</i>	<i>Page</i>
1.1 Life cycle and dauer entry decision of <i>C. elegans</i> .....	21
1.2 Conceptual framework of the dauer entry decision .....	22
1.3 Model for signal input during the decision, and for circuit changes during dauer entry .....	23
2.1 The dauer entry life cycle decision is modulated by mechanosensation .....	54
2.2 <i>mec-4</i> and <i>mec-10</i> CRISPR alleles are putative nulls .....	56
2.3 <i>mec-4</i> promotes dauer entry .....	57
2.4 Touch and pheromone are parallel inputs into the dauer entry decision .....	59
2.5 <i>mec-4</i> and <i>trp-4</i> act additively with <i>pezo-1</i> to promote dauer entry ...	62
2.6 Direct mechanical stimulation promotes dauer entry .....	63
2.7 Model of the complex dauer entry decision .....	64
3.1 39% of the <i>C. elegans</i> genome is differentially expressed during dauer and reproductive development. ....	116
3.2 <i>daf-9(dh6)</i> RNA-seq dataset summaries .....	118
3.3 Differential expression was detected at high accuracy and single-cell resolution .....	119
3.4 Clustering revealed six common expression profiles during dauer and reproductive development. ....	122
3.5 Enriched GO terms and KEGG pathways in clusters 1 to 6. ....	123
3.6 Differential expression of the neuronal effector genome of <i>C. elegans</i> during dauer and reproductive development .....	125
3.7 Nictation initiation and the proportion of time spent nictating are not significantly affected in <i>sbt-1</i> null mutants .....	126
3.8 Neuropeptide signaling promotes dauer entry and dispersal	

behaviors .....	127
3.9 FMRFamide-like peptides are coordinately up-regulated during dauer development .....	128
3.10 FMRFamide-like peptides are coordinately up-regulated during dauer development .....	130
3.11 FMRFamide-like peptides are coordinately up-regulated in host-seeking infective juveniles of parasitic nematodes.....	132
3.12 Model of circuit changes during dauer development via non-synaptic FLP signaling.....	134
4.1 Expression profiles of collagen genes .....	168
4.2 <i>col-183</i> , <i>ets-10</i> , <i>nrh-246</i> and <i>led-1(F53F1.4)</i> Genetic markers demonstrates dauer- or reproductive-specific expression pattern ....	169
4.3 Expression profiles of transcription factors.....	171
4.4 <i>ets-10</i> expression pattern in non-dauer stages (L4-adult) .....	173
4.5 <i>nhr-246</i> expression pattern in non-dauer stage (embryo-L1) .....	175
4.6 Expression profiles of genes that are down-regulated in dauer.....	176
4.7 The appearance of fluorescence correlates with the dauer-commitment decision and stays on in dauer .....	177
4.8 Overexpressing <i>daf-9</i> in the hypodermis during commitment increases the reproduction decision .....	178
4.9 Partial dauers mis-express dauer markers .....	180

<i>Table</i>	<i>Page</i>
2.1 Expression pattern and allele effects of mechanosensation genes .....	61

<i>Appendix Figure</i>	<i>Page</i>
A.1 Nematodes were isolated from in and around Mono Lake .....	205
A.2 Pictures of three sampling sites around Mono Lake .....	207
A.3 Nematodes isolated from the three sites are diverse in morphology.....	208
A.4 The nematodes isolated are phylogenetically and morphologically diverse .....	211

A.5 Nematodes isolated from the three sites are diverse in morphology .....	214
A.6 Percent of sequence identify of each isolate compared to its closest related species.....	215
A.7 Phylogenetic tree of species a (based on LSU sequence).....	216
A.8 Phylogenetic tree of species a (based on SSU sequence).....	217
A.9 Phylogenetic tree of species b (based on LSU sequence) .....	218
A.10 Phylogenetic tree of species b (based on SSU sequence).....	219
A.11 Phylogenetic tree of species c (based on LSU sequence).....	220
A.12 Phylogenetic tree of species c (based on SSU sequence).....	221
A.13 Phylogenetic tree of species d (based on LSU sequence) .....	222
A.14 Phylogenetic tree of species d (based on SSU sequence).....	223
A.15 Phylogenetic tree of species e (based on LSU sequence).....	224
A.16 Phylogenetic tree of species e (based on SSU sequence).....	225
A.17 Phylogenetic tree of species f (based on LSU sequence) .....	226
A.18 Phylogenetic tree of species g (based on SSU sequence).....	227
A.19 Phylogenetic tree of species h (based on SSU sequence).....	228
A.20 Species g and h SSU sequence alignment .....	229
A.21 Characteristics of <i>Auanema tufa</i> .....	230
A.22 <i>Auanema tufa</i> is resistant to arsenic .....	232

### Appendix Table

3.1 Metadata of our <i>daf-9(dh6)</i> RNA-seq experiment	
3.2 Normalized expression values for each detected gene in the RNA-seq dataset	
3.3 Differentially expressed genes from the twelve pairwise comparisons	
3.4 Genes in clusters 1 to 6	
3.5 Differentially expressed neuronal effector genes	

	<i>Page</i>
A.1 Detailed information of the soil samples collected .....	212

*Appendix Video*

- 3.1 Wild type nictation
- 3.2 *sbt-1(-)* nictation
- 3.3 Wild type CO<sub>2</sub> response
- 3.4 Wild type control gas response
- 3.5 *sbt-1(-)* CO<sub>2</sub> response
- 3.6 *sbt-1(-)* control gas response

*Chapter 1***INTRODUCTION**

## 1.1 Thesis overview

### **Most of life undergoes developmental decisions**

Most of the life on the planet undergoes developmental decisions. By altering aspects of their development, organisms such as bacteria, fungi, nematodes, insects, plants, and mammals can adapt their metabolism, physiology, and reproductive strategy to meet resource availability (1-6). Several examples can be found from various taxa:

- Bacteria can sporulate, become competent to uptake DNA, or transcriptionally respond to predicted changes in environment (1, 7).
- Saprophytic *Arthrobotrys oligospora* fungi can develop carnivorous traps when they are starved for nitrogen (5, 8).
- Plants can change their growth and competition strategies in response to being blocked out from sunlight by neighboring plants (3, 9).
- Insects can switch from solitary to social forms in response to crowding (2). Eusocial insects can also generate queen and worker castes based on nutrition input (2, 10).
- Fish and reptiles can change their sex based on environmental temperature (11-13) or mate availability (14).
- Mammals can change their fur color (15) and immune system (16, 17) to deal with predators and pathogens. In addition, the embryos of various species can suspend development when environmental conditions are unsuitable for pregnancy (4, 18).

Developmental decisions can be stochastic (19), driven by internal cues (20, 21), or determined by environmental signals (22). However, even if the individual is not responding to the environment *per se* during stochastic or internally-driven decisions, the structure of the decision (including its dynamic range, bias, and rate of switching) faces selection from the environment (1, 23). In other words, even these decisions are responses to and anticipations of the environment that are conditioned by evolution (1). (This has been demonstrated using yeast engineered to switch stochastically between two states facing antagonistic selection. Yeast that were engineered as fast-switchers outgrew slow-switchers in fluctuating environments, while slow-switchers dominated in stable environments (24).) Therefore, understanding how the environment inputs into an organism's developmental decision is key to fully understanding the decision. In my thesis, I have taken an ethological approach to studying the *Caenorhabditis elegans* dauer entry life cycle decision, using genomics, quantitative genetics, and behavioral studies.

### **The enduring larva**

One of the best-studied life cycle decisions is the *Caenorhabditis elegans* dauer entry decision (25, 26). Under favorable conditions, *C. elegans* roundworms develop through four larval stages—L1, L2, L3, and L4—to become a reproductive adult. However, declining food, temperature, and crowding conditions promote L1 larvae to enter the pre-dauer L2d stage. If conditions improve, L2d animals can

decide to resume reproductive development, while un-improved conditions cause L2d to enter the dauer larval stage (**Figure 1.1**).

Dauers are spore-like larvae that cease feeding and aging (27). This is accomplished in part by halting their reproductive growth and shifting their metabolism to favor long-term utilization of lipids (28, 29). Dauers have a stress-resistant, impermeable cuticle and can survive dessication for several days—even surviving losses of up to 98% of their body water (6, 25, 30). These factors contribute to dauers having a lifespan of approximately 8 months, which is 10 times longer than that of non-dauers (31).

### **Half a year to make a decision**

L2d larvae make the dauer entry decision based on the inputs of food, pheromone, and temperature (32). The pheromones consist of small-molecule ascarosides (based on the sugar ascarylose) that are constitutively secreted, and can therefore be used to measure population density (33). Food, pheromone, and temperature are sensed by seven amphid sensory neurons, which convert these inputs into insulin and TGF- $\beta$  signals (34). Specifically, food promotes the release of insulin and TGF- $\beta$ , while pheromone and temperature inhibit. These signals are integrated in at least one cell—the neuroendocrine XXX cell (35). When insulin and TGF- $\beta$  levels are high, the XXX initiates amplification of dafachronic acid (DA) growth hormone across the animal body, thus ensuring the decision to resume reproductive development (dauer bypass). How the XXX cell promotes dauer entry



when insulin and TGF- $\beta$  levels are low is not well understood. Therefore, some questions that remain are:

- Is the XXX cell the only point of integration? XXX was identified as a site of integration because of its expression of *daf-9*/Cytochrome P450, which contributes to the synthesis of DA growth hormone (36, 37). However, it is likely not the sole site of integration since laser ablation of XXX during L1 produces a weak dauer entry phenotype, especially compared to *daf-2*/insulin receptor and *daf-7*/TGF- $\beta$  mutants (38). In addition, the steps of DA production are distributed among various tissues, with intestine (*daf-36*/Rieske oxygenase), pharynx and head neurons (*dhs-16*/3-hydroxysteroid dehydrogenase), and hypodermis (*dhs-16* and *daf-9*) expressing components of the synthesis pathway (39). Therefore, integration of insulin and TGF- $\beta$  signals may occur in these tissues as well.
- Do any signals instruct the decision to enter dauer other than the reduction of insulin and TGF- $\beta$ ? The field has mostly focused on insulin and TGF- $\beta$  (as well as the inputs of food, pheromone, and temperature) because these components of the decision architecture were discovered using forward genetic screens and genetic interaction tests for strong dauer-constitutive and dauer-defective phenotypes (36, 37, 40-43). However, while these screens were performed to saturation, they did not reveal components of the decision that were redundant or modulatory. For

instance, the pheromone receptors *daf-37*, *daf-38*, *srbc-64*, *srbc-66*, *srg-36*, and *srg-37* were not identified in the initial screens because they redundantly sense the ascaroside pheromones (44-46). In addition, in **Chapter 2** I demonstrate that touch is an overlooked input into the dauer entry decision, likely because it modulates the decision. Therefore, it is possible that other environmental inputs and intercellular signals play a role in the dauer entry decision. In **Chapter 4**, several genetic markers for conveniently tracking the dauer entry decision are described, and strategies for using these markers for identifying additional intercellular signals are discussed.

- Is the dauer entry decision simply made by the absence of DA? And are dauer programs driven in all tissues when DA levels are low? *daf-9* mutants form partial dauers that develop incomplete cuticles, which lack the wild type resistance to SDS detergent, so there appear to be some programs that require non-DA input (47). How these tissue-specific programs can be teased apart is discussed in **Chapter 4**.
- How is the decision integrated? For instance, are dauer-promoting and dauer-inhibiting signals from the environment summed up over time, and if so, how is the information stored? Are environmental signals weighted differently based on their frequency and strength (perhaps to filter out spurious signals)? These are likely the

questions that will require the most work in the future to resolve.

One strategy that would be effective in addressing these questions is to use convenient markers of the decision (**Chapter 4**) as high-throughput read-outs to test the dynamics of the decision. Since mechanical stimuli input into the decision (**Chapter 2**), and because its delivery (e.g. via vibrations or acoustic speakers) can be dynamically controlled (48), these inputs can be applied in bursts or as a stable signal, pulsed early during integration or late, and so forth in order to test how the resulting decision rates change.

Notably, L2d larvae spend 17 hours integrating environmental inputs to make the dauer entry decision (35). If the 3 week lifespan of *C. elegans* is scaled to the lifespan of humans, then L2d larvae spend 2.7 worm years making the decision. Or, if we consider that a 3 hour pulse of favorable conditions can trigger dauer bypass (35), then the decision-making period scales to half a year. In other words, the dauer entry decision can occupy a considerable proportion of the *C. elegans* lifespan. This is likely because the natural environment of *C. elegans* is noisy, consisting of a complex mix of microbes, invertebrates, and predators that can add to, alter, and corrupt the signals that *C. elegans* uses to assess its surroundings (8, 49, 50). When decisions need to be made in uncertain environments, trends in incoming signals must be integrated over time to average out the noise and to make an informed decision (51). (An everyday example of this occurs when one begins to suspect that it has started to rain: The first drop could be from anything (air conditioning unit, guttation from trees, drain pipe), but five

drops later and rain may be looking likely. By collecting trends in the data (e.g. frequency between drops) and integrating against a threshold (e.g. “five drops means rain is likely”), an appropriate response can be made despite uncertainty in the environment.)

In addition to dealing with uncertainty, the dauer entry decision likely aims to predict whether environmental conditions will continue to support growth. Entry into L2d, which stores more fat and has a longer intermolt than L2, allows *C. elegans* to anticipate an unfavorable environment, and provides the animal with developmental flexibility in case the environment does or does not collapse (52) (**Figure 1.1**). In this way, dauer entry may be similar to diapause in insects such as the mosquito *Culex pipiens* and the monarch butterfly *Danaus plexippus*, where diapause is triggered by stimuli (photoperiod and temperature) that signal the advent of an unfavorable condition (winter) (22, 53-55).

Based on current observations, the dauer entry decision can likely be conceptualized in terms of a drift diffusion model. Drift diffusion models of a decision assume that the decision is made by accumulating noisy evidence towards a decision-triggering threshold, and describe the accumulation of the evidence as a diffusion process (56, 57). Since these models resemble the algorithm that broke the Enigma code in World War II, they represent computationally fast and effective methods for dealing with uncertain information (51, 56, 57). In addition these models have been used to successfully describe decision-making in various animals. The dauer entry decision, therefore, likely fits a drift diffusion model with a reproductive development-triggering threshold that

can be reached by accumulating favorable stimuli, and which defaults to dauer entry when the decision times out at the end of the L2d integration period (**Figure 1.2**). This is because it appears that entry into dauer cannot be locked in before the end of L2d integration (at 33 hours post hatch), whereas a 3 hour pulse of favorable conditions at any time during integration can initiate dauer bypass (35). In this framework, the timed-out dauer entry decision relies on low levels of insulin and TGF- $\beta$  (though other intercellular signals may be revealed; see above), and is locked-in by the absence of DA but also some non-DA inputs.

### **Touch is an overlooked input into the dauer entry decision**

Touch is an important sensory modality that is present in every organism that has been observed (58-60). In humans, touch is the first sense that develops, and it can be used to assess social as well as physical aspects of the environment through distinct nerve fibers (61, 62). Social touch plays an important role during human development, affecting infant feeding behavior, stress response, weight gain, and even word detection during the early stages of vocabulary assembly (61, 62). Interpersonal touch can also affect human behaviors, including compliance, social participation, and resource sharing (e.g. tipping of waitstaff) (63). Remarkably, touch alone can communicate emotions such as anger, fear, disgust, sympathy, happiness, love, and sadness (64, 65).

(Correspondingly, perhaps, art and literature has depicted touch as a fundamental aspect of humanity. Touch is shown to literally impart humanity in

Michelangelo's *The Creation of Adam*, whose visual motif is repeated in such films as *E.T.* Other works visit this idea of touch as an inextricable part of humanity, such as Alfonso Cuarón's space-locked *Gravity* and Denis Villeneuve's existential *Blade Runner 2049*. We see this idea inverted in the common symbolism of gloves being used to hide or deny one's true self, such as in Disney's *Frozen* or Nicolas Winding Refn's *Drive*. It is likely no mistake that the phrase "human touch" combines the two words to describe things that are authentically human, and that things that move us are said to be "touching.")

If touch is fundamental to humans, there is evidence that it plays a similarly large role in other organisms as well. Touch can be used to convey social information (e.g. population density) in bacteria, plants, and insects (2, 9, 66), and is important for the growth and development of invertebrates and vertebrates (61). For instance, the development of nurturing behavior in rats has been shown to depend on mechanical stimuli received during early growth (67), and mating behaviors are dependent on mechanosensation in *C. elegans* and *Drosophila melanogaster* (68, 69). Importantly, the molecular mechanisms of touch are conserved, and the same mechanotransducers are present in the genomes of invertebrates and mammals:

- **Degenerin/epithelial Na<sup>+</sup> channel (DEG/ENaC) family:**

Degenerin/epithelial Na<sup>+</sup> channels and their accessory proteins are involved in *C. elegans* gentle touch (*mec-2*, *mec-4*, *mec-6*, *mec-10*), harsh touch (*degt-1*), and nose touch (*deg-1*, *delm-1*, *delm-2*); *D. melanogaster* nociception (*pickpocket*); and texture discrimination in

mice (SLP3) (60, 70).

- **Transient receptor potential channel (TRP) family:** TRPs are a diverse family, consisting of seven subfamilies: TRPA (ankyrin), TRPC (canonical), TRPML (mucolipin), TRPM (melastatin), TRPN (NOMPC-like), TRPP (polycystin), and TRPV (vanilloid) (71).
  - TRPA: The TRPA homologs *trpa-1* in *C. elegans*, *painless* in *D. melanogaster*, and TRPA1 in mammals share roles in touch and nociception (60).
  - TRPN: The TRPN1 homolog *trp-4* in *C. elegans* is required for nociception (72), and shares roles with its *D. melanogaster* homolog *nompC* in touch and proprioception (70, 73, 74). Homologs of TRPN1 are found in zebrafish and amphibians, but not in mammals (60).
  - TRPV: In *C. elegans* the TRPV channels *ocr-2* and *osm-9* are involved in nose touch. TRPV4 in mammals has modest effects on touch sensitivity (60).
- **Transmembrane channel-like (TMC) family:** TMCs are multipass membrane channels, and *Tmc1* and *Tmc2* in mice are necessary for hair cell mechanosensation (75). In *C. elegans* *tmc-2* is expressed in PVD harsh touch mechanosensory neurons, and is therefore a putative mechanoreceptor channel (76).
- **Piezo family:** Piezos are large ion channels (over 2,000 amino acids long) that are involved in touch sensing in flies and mammals (77, 78).

Its role in *C. elegans* is unknown.

In the wild, *C. elegans* can use olfaction (79) and mechanosensation to navigate the complex environments it is found in (usually rotting vegetation and fruits) (80). In these habitats, *C. elegans* can encounter bacteria, fungus, insects, carriers, predators, and other nematodes. *C. elegans* can sense several types of touch including gentle touch, harsh touch, nose touch, and food texture (70), and these have been shown to affect ethologically relevant behaviors such as dwelling on food (81) and predator-avoidance (82).

Gentle touch is sensed in *C. elegans* by six touch receptor neurons (ALML, ALMR, AVM, PLML, PLMR, PVM) whose processes extend along the length of the animal, and whose activities resemble the Pacinian corpuscles in human skin that detect the onset and offset of light force (83). Gentle touch is therefore likely analogous to low-threshold, discriminative touch in humans, which detects light touch, hair movements, vibrations, quivering, and social touch (60, 84, 85). On the other hand, harsh touch is sensed by nine neurons in *C. elegans* (ADE, AQR, BDU, FLP, PDE, PHA, PHB, PVD, SDQR) and is likely analogous to high-threshold nociception, which detects physically damaging forces (60, 72, 86). Nose touch and texture discrimination likely represent harsh touch that is modulated by other neurons that respond to context. (e.g. (87)).

In **Chapter 2**, I demonstrate that gentle and harsh touch are used to modulate the dauer entry decision in *C. elegans*. I also provide a plausible role for mechanosensation in assessing weather and crowding conditions that promote



dauer entry. My findings reveal that the decision is more complex than previously recognized, and raises the intriguing possibility that other cues such as light, O<sub>2</sub>/CO<sub>2</sub>, pH, and osmotic stress may input into the decision as well. Furthermore, I discuss evidence that suggests that touch may be a common modulator of developmental decisions in organisms across biology. Due to noise in the environment, it is conceivable that multiple inputs are necessary for accurately assessing the environment in order to make appropriate developmental decisions.

### **Acquiring new behaviors with a constrained nervous system**

The dauer is the most commonly observed stage of *C. elegans* in nature, since *C. elegans* feeds on transient microbial communities that collapse approximately every three of their generations (88, 89). In other words, *C. elegans* growth can be characterized by short periods of boom followed by potentially long periods of bust, during which time dauers must migrate to find improved conditions. It has been noted that soil nematodes can cover a distance of 15 cm on their own (90), but aided by vectors such as wind and carrier animals (e.g. isopods and slugs), *C. elegans* dauers are able to effectively disperse to dramatically different environments (91, 92). In fact, *C. elegans* has even been shown to migrate between continents, likely aided by large vectors such as humans (6, 91).

Dauers have two behaviors that aid in finding carrier animals. The first is nictation—a hitchhiking behavior where dauers stand on their tails and wave their

bodies (93). Dauers can nictate individually or in large amassed groups that have been termed dauer towers (88, 94). Nictation increases the likelihood of attaching onto a passing animal, and has been shown to affect the rate that *C. elegans* are transported by flies and isopods (93, 95). Conceivably, dauers may even nictate to draw the attention of animals in order to be eaten, as it has been shown that dauers can safely harbor in the intestines of slugs after being consumed by them (80, 96).

The second behavior that dauers use for dispersal is CO<sub>2</sub> chemotaxis. While non-dauers are repelled by CO<sub>2</sub>, dauers are attracted, and in other nematode species the CO<sub>2</sub> produced by three mealworms is enough to elicit taxis behavior (97, 98). Non-dauers are likely repelled by CO<sub>2</sub> since it can signal the presence of predators (e.g. mites and springtails) or crowding (80). On the other hand, dauers are likely to take the risk in order to find carriers, especially since they can survive (and benefit from) being eaten by some animals (96).

Both nictation and CO<sub>2</sub> chemotaxis are dauer-specific behaviors, indicating that the neural state of dauers and non-dauers are different. However, this acquisition of behaviors is surprising given that *C. elegans* has a numerically simple nervous system of only 302 neurons (99). By comparison, the human eye alone carries over 120 million neurons (100, 101), and that the simple gill withdrawal reflex in *Aplysia* sea slugs requires the activity of around 300 neurons (102). In addition, the *C. elegans* nervous system is densely interconnected—almost any two neurons in *C. elegans* are connected by three degrees of (synaptic) separation (103). In other words, there are no synaptically

compartmentalized circuits that *C. elegans* can switch between during dauer and non-dauer that could explain the differences in their behavior and neural state.

Therefore, one way that *C. elegans* generates a new neural state during dauer is by rewiring its neurons (104). Specifically, the processes of ADE, AFD, ASG, ASI, AWC, and IL2 sensory neurons change their positions and morphologies during dauer. The reconfiguration of IL2, involving dendritic arborization and axonal remodeling, is necessary for the acquisition of nictation behavior (93). The role of rewiring in the other neurons is unknown, but based on the functions of these neurons, it can be presumed that these changes affect sensitivity to temperature (AFD), chemicals (ASG, ASI, AWC), and harsh touch (ADE) (105).

In **Chapter 3**, I demonstrate another method that *C. elegans* use to generate a new neural state in dauer. I show that *C. elegans* neuropeptides are massively up-regulated during dauer entry, and that this peptidergic signaling promotes the dauer entry decision, promotes vigorous waving during nictation, and is necessary for the switch to CO<sub>2</sub> preference in dauers.

Neuropeptides are evolutionarily ancient signaling molecules that likely pre-date the classical neurotransmitters, such as acetylcholine and dopamine (106-108). Neuropeptides are short sequences of amino acids that can act as transmitters, neuromodulators, and hormones. Other than a few instances (e.g. insulin-like peptides), neuropeptides bind G-protein coupled receptors to affect their target cells (109). After binding to their receptor, neuropeptides can modulate

the response amplitude, polarity, sensitivity, gene expression, and signaling repertoire of a target neuron (110, 111). Neuropeptides can also diffuse to facilitate signaling between synaptically unconnected neurons (103, 112). Through privileged ligand-receptor communication channels, neuropeptides can shape which circuits are active in the nervous system, the membership of these circuits, and their functions (103).

The *C. elegans* genome encodes for three families of neuropeptides—the insulin-related peptides (40 *ins* genes), the neuropeptide-like proteins (47 *nlp* genes), and the FMRFamide-like peptides (31 *flp* genes) (113):

- **Insulin-like neuropeptides (*ins*):** Insulin neuropeptides have evolutionarily conserved roles in regulating growth and metabolism in Metazoa (106). In *C. elegans*, signaling through DAF-2/insulin-like receptor promotes reproductive growth (113). Perhaps as a result, few of the *ins* genes were up-regulated during dauer entry (**Chapter 3**). In fact, the only *ins* gene that was up-regulated between dauer-commitment and reproductive development was *ins-1*, which likely antagonizes DAF-2 signaling and increases dauer entry (114).
- **Neuropeptide-like proteins (*nlp*):** The NLPs are a miscellaneous group of non-INS, non-FLP neuropeptides (113) that likely function in several independent processes. We observed the up-regulation of 25 of 47 *nlp* genes during dauer entry (Chapter 3). The specific roles of these neuropeptides during dauer remain untested.
- **FMRFamide-related peptides (*flp*):** FLPs are present across the

animal kingdom and have conserved roles in regulating feeding and reproduction in nematodes, arthropods, mollusks, and vertebrates (106, 115-117). The FLP family is especially expanded in the phylum Nematoda (118), and the FLPs in *C. elegans* represent the largest family of neuropeptides yet described (119). Strikingly, we observed that the *flp* neuropeptides are coordinately up-regulated during *C. elegans* dauer entry (**Chapter 3**). In addition, we discovered that *flp-8*, *flp-10*, *flp-11*, *flp-17*, *flp-21*, *flp-25*, and *flp-26* promote dauer entry, while *flp-2*, *flp-6*, *flp-18*, and *flp-34* inhibit dauer entry. Therefore, FLPs act redundantly and with opposed effects to modulate dauer entry. Conceivably, these *flp* neuropeptides could act downstream of and/or modulate the sensation of food, pheromone, temperature, and touch inputs (**Figure 1.3A**). As downstream signals, the FLPs could act as intercellular signals in addition to insulin and TGF- $\beta$  to instruct the dauer entry decision. As modulators of input sensation, the FLPs could potentially be secreted by the sensory neurons to cross-talk with other modalities (120). For instance, cross-modal communication could allow one modality to compensate for defects or uncertainty in another (by, for instance, increasing sensitivity to mechanical stimuli to help assess crowding when pheromone cannot reliably be measured). Similarly, cross-modal communication could allow evidence to be corroborated or screened from the decision.

We also observed that FLP-10/FLP-17, which are expressed in

the CO<sub>2</sub>-sensing BAG neuron, promote CO<sub>2</sub> chemotaxis and nictation in dauers. While the functions of the other FLPs during dauer remain untested, I suspect that they dramatically change the neural state of dauers by altering the composition and function of the active circuits in the nervous system (103). For example, FLP-10 signaling likely produces a dauer-specific circuit where the BAG neuron signals directly to DVA, HSN, and SDQ—which express the FLP-10 receptor EGL-6 (113, 118)—whereas these neurons are not connected in a single circuit in non-dauers (99) (**Figure 1.3B**). Interestingly, this FLP-10 circuit would allow the BAG neuron to signal to the ALM gentle touch neuron, as well as the AQR, FLP, PDE, and SDQR harsh touch neurons. I speculate that the role of this may be to suppress nociception and touch avoidance while the dauer performs CO<sub>2</sub> chemotaxis, so that mechanical contact with a carrier animal does not result in avoidance.

Therefore, the coordinated up-regulation of the FLPs likely functions to switch the neural state of *C. elegans* during dauer. In **Chapter 3**, I demonstrate that this strategy may reflect an ancient mechanism for expanding the behavioral repertoire of nematodes, and, from this framework, attempt to explain the expansion of the *flp* genes in Nematoda.

Conceivably, using neuropeptides to generate new neural states could be a crucial strategy in other organisms that lack highly compartmentalized nervous systems (e.g. species in Cnidaria, Ctenophora, and Echinodermata that possess

nerve nets). It is also plausible that this may have been a dominant strategy during early animal life, when complexity in the nervous system was low (121). Furthermore, neuropeptides are likely important for switching neural states within local regions of a compartmentalized brain. Indeed, the neuropeptide NPY (an evolutionary relative of the FLPs (109, 117)) fine-tunes the activity of the retina, perhaps playing a neuroprotective role (122). Because of their wide array of modulatory functions, and their ability to signal beyond the physical connectome, neuropeptides likely underlie many neural state changes, such as in sleep, post-traumatic stress disorder, and depression (123, 124).

### **The genomics of the dauer entry decision**

Forward genetic screens have been useful in studying the dauer entry decision, revealing much of the core components of the decision. Using genomics, I have expanded the study of dauer by analyzing gene families that were prioritized based on our RNA-seq. I then tested the role of these genes in the integration of environmental signals and the acquisition of dispersal behaviors.

I studied how *C. elegans* use mechanosensation to increase the accuracy of the dauer entry decision (**Chapter 2**). Modulation of the decision from senses that assess various aspects of the environment could minimize uncertainty and allow *C. elegans* to make robust developmental decisions. Touch is also an important modality for growth and development in organisms across biology, so it is conceivable that it modulates the developmental decisions of other organisms

as well.

I also discovered how a coordinated class of neuropeptides, the FMRFamides, modulates the entry decision, and allows *C. elegans* to acquire dispersal behaviors after it decides to enter dauer (**Chapter 3**). Cross-modal communication by the FLPs may be an important aspect of the computation of the decision. Behavioral repertoire expansion by the FLPs allows adaptive behaviors to be expressed at the right time, despite lack of compartmentalization in the *C. elegans* nervous system.

Using data from our RNA-seq timecourse, I identified genetic markers that can be used for tracking and manipulating the dauer entry decision (**Chapter 4**). These tools will likely be useful for testing the dynamics of the decision, and for identifying any intercellular signals that work in addition to insulin, TGF- $\beta$ , and DA.

My findings have revealed that the dauer entry decision is more complex than previously recognized, and may illuminate how animals make robust decisions in uncertain environments. In addition, my findings have revealed how animals acquire new behaviors, even with a physically constrained nervous system. It is remarkable how much *C. elegans* can achieve with a “little brain” of 302 neurons, and it is clear that dauers have much to reveal about how densely information and behaviors can be packed into a nervous system.



## 1.2 Figures

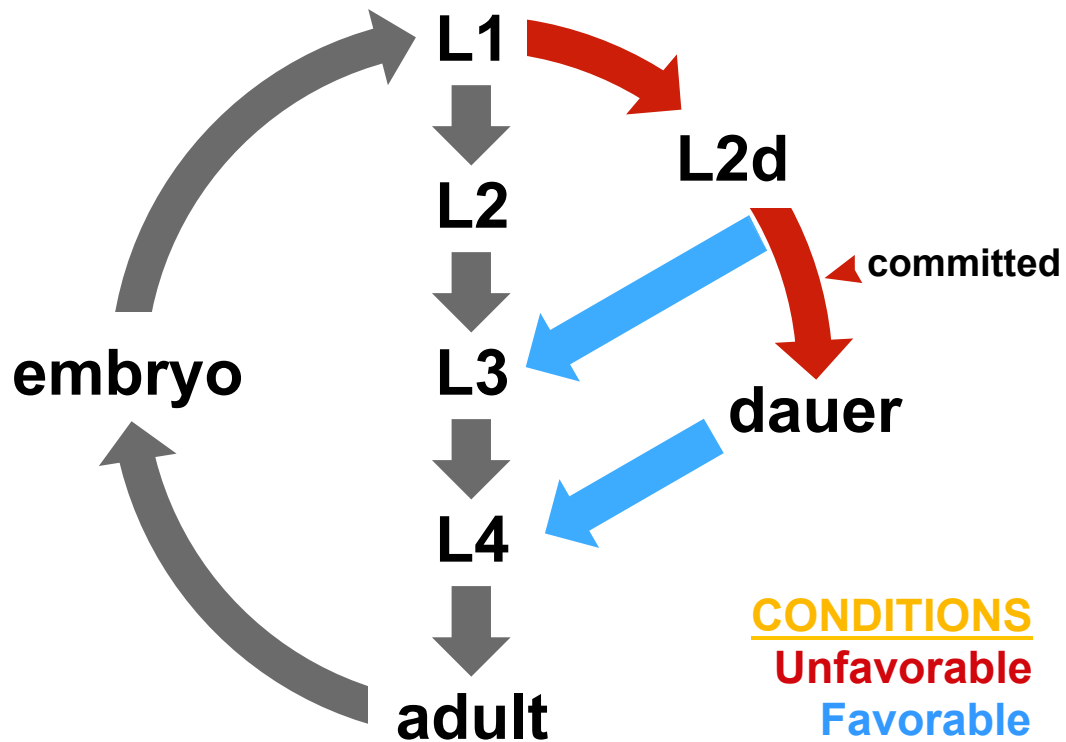


**Figure 1.1.** Life cycle and dauer entry decision of *C. elegans*. The arrowhead indicates the dauer-commitment time point (approximately halfway between the start of L2d and molt into dauer), after which the decision to enter dauer cannot be reversed. Red indicates dauer development under unfavorable conditions, and blue indicates the two possible paths out of dauer development under favorable conditions. Grey indicates reproductive development.

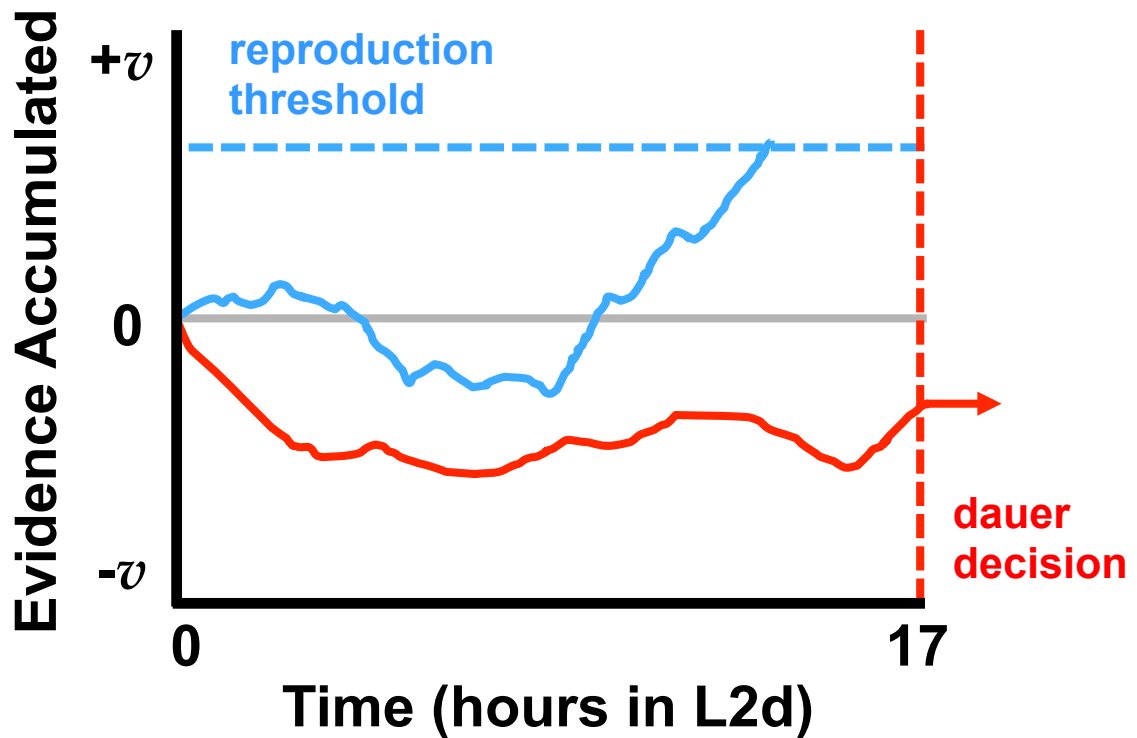


**Figure 1.2.** Conceptual framework of the dauer entry decision. Lines do not represent real data, but are drawn to highlight the accumulation of noisy evidence. Evidence in favor of a favorable environment is given a positive value ( $+v$ ) and evidence for an unfavorable environment is negative ( $-v$ ). The blue line describes a possible path for an animal that decided to resume reproductive development after accumulating enough evidence to pass the reproduction threshold. The red line represents an animal that entered dauer as a result of the decision timing out.

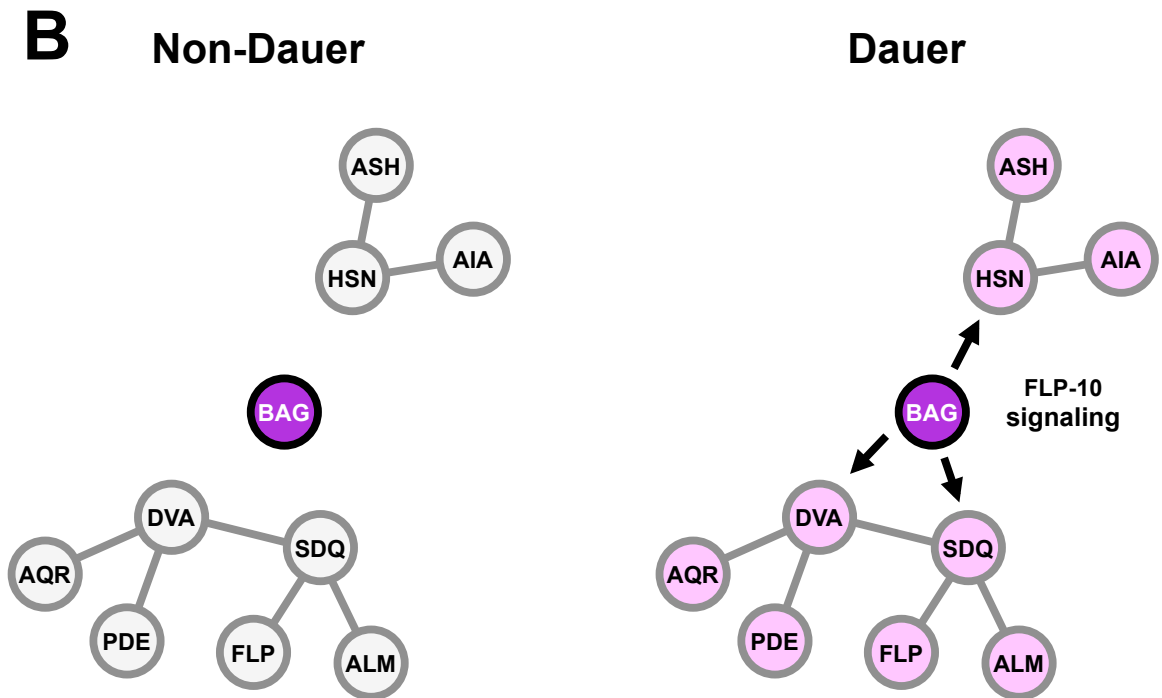
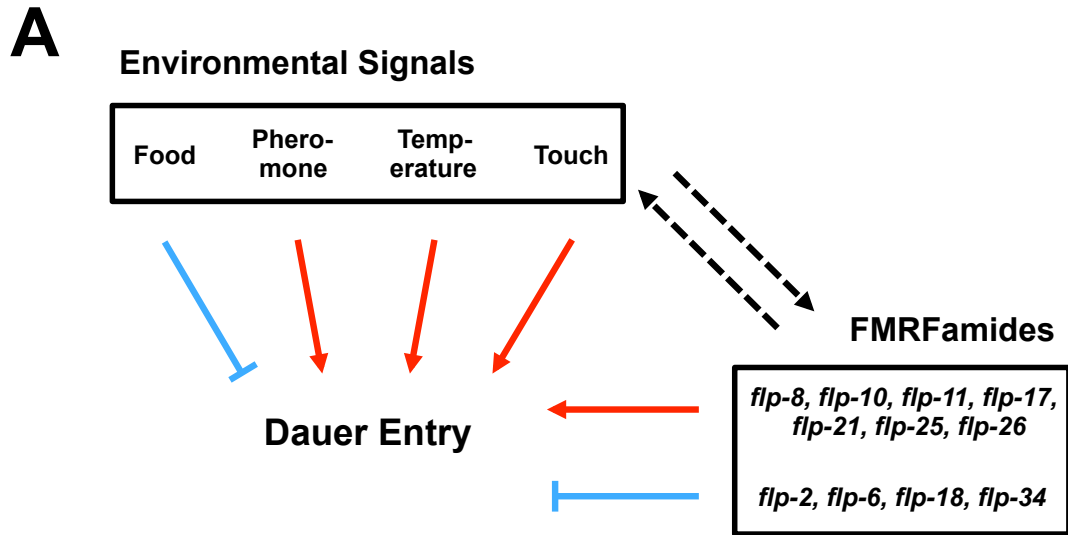


**Figure 1.3.** Model for signal input during the decision, and for circuit changes during dauer entry. (A) Red and blue indicate dauer-promoting and dauer-inhibiting effects, respectively. Dashed arrows indicate the possibility of flp neuropeptides acting downstream of the environmental inputs, and/or modulating the sensation of the environmental signals. (B) Circuit changes via non-synaptic FLP-10 signaling between the CO<sub>2</sub>-sensing BAG neuron and FLP-10 receiving neurons. This figure is a zoomed-in version of Figure 3.12 in Chapter 3.

### 1.3 References

1. Perkins TJ & Swain PS (2009) Strategies for cellular decision-making. *Mol Syst Biol* 5:326.
2. Simpson SJ, Sword GA, & Lo N (2011) Polyphenism in insects. *Current biology : CB* 21(18):R738-749.
3. Gruntman M, Gross D, Majekova M, & Tielborger K (2017) Decision-making in plants under competition. *Nat Commun* 8(1):2235.
4. Renfree MB & Fenelon JC (2017) The enigma of embryonic diapause. *Development* 144(18):3199-3210.
5. Vidal-Diez de Ulzurrun G & Hsueh YP (2018) Predator-prey interactions of nematode-trapping fungi and nematodes: both sides of the coin. *Appl Microbiol Biotechnol* 102(9):3939-3949.
6. Kiontke K & Sudhaus W (2006) Ecology of Caenorhabditis species. *WormBook : the online review of C. elegans biology*:1-14.
7. Tagkopoulos I, Liu YC, & Tavazoie S (2008) Predictive behavior within microbial genetic networks. *Science* 320(5881):1313-1317.
8. Hsueh YP, *et al.* (2017) Nematophagous fungus *Arthrobotrys oligospora* mimics olfactory cues of sex and food to lure its nematode prey. *eLife* 6.
9. de Wit M, *et al.* (2012) Plant neighbor detection through touching leaf tips precedes phytochrome signals. *Proceedings of the National Academy of Sciences of the United States of America* 109(36):14705-14710.
10. Chandra V, *et al.* (2018) Social regulation of insulin signaling and the evolution of eusociality in ants. *Science* 361(6400):398-402.
11. Janzen FJ & Phillips PC (2006) Exploring the evolution of environmental sex determination, especially in reptiles. *J Evol Biol* 19(6):1775-1784.
12. Ospina-Alvarez N & Piferrer F (2008) Temperature-dependent sex determination in fish revisited: prevalence, a single sex ratio response pattern, and possible effects of climate change. *PLoS one* 3(7):e2837.

13. Woodward DE & Murray JD (1993) On the Effect of Temperature-Dependent Sex Determination on Sex Ratio and Survivorship in Crocodilians. *Proceedings of the Royal Society of London. Series B: Biological Sciences* 252(1334):149.
14. Hobbs JP, Munday PL, & Jones GP (2004) Social induction of maturation and sex determination in a coral reef fish. *Proc Biol Sci* 271(1553):2109-2114.
15. Mills LS, *et al.* (2013) Camouflage mismatch in seasonal coat color due to decreased snow duration. *Proceedings of the National Academy of Sciences of the United States of America* 110(18):7360-7365.
16. Fusco G & Minelli A (2010) Phenotypic plasticity in development and evolution: facts and concepts. Introduction. *Philosophical transactions of the Royal Society of London. Series B, Biological sciences* 365(1540):547-556.
17. Gilbert SF (2000) *Developmental Biology*. (Sinauer Associates, Sunderland (MA)).
18. Ptak GE, *et al.* (2012) Embryonic diapause is conserved across mammals. *PloS one* 7(3):e33027.
19. Ackermann M (2015) A functional perspective on phenotypic heterogeneity in microorganisms. *Nat Rev Microbiol* 13(8):497-508.
20. Zimova M, Mills LS, Lukacs PM, & Mitchell MS (2014) Snowshoe hares display limited phenotypic plasticity to mismatch in seasonal camouflage. *Proc Biol Sci* 281(1782):20140029.
21. Hu CK & Brunet A (2018) The African turquoise killifish: A research organism to study vertebrate aging and diapause. *Aging Cell* 17(3):e12757.
22. Hand SC, Denlinger DL, Podrabsky JE, & Roy R (2016) Mechanisms of animal diapause: recent developments from nematodes, crustaceans, insects, and fish. *Am J Physiol Regul Integr Comp Physiol* 310(11):R1193-1211.
23. Avery SV (2006) Microbial cell individuality and the underlying sources of heterogeneity. *Nat Rev Microbiol* 4(8):577-587.
24. Acar M, Mettetal JT, & van Oudenaarden A (2008) Stochastic switching as a survival strategy in fluctuating environments. *Nature genetics* 40(4):471-475.

25. Cassada RC & Russell RL (1975) The dauerlarva, a post-embryonic developmental variant of the nematode *Caenorhabditis elegans*. *Developmental biology* 46(2):326-342.
26. Hu PJ (2007) Dauer. *WormBook : the online review of C. elegans biology*:1-19.
27. Klass M & Hirsh D (1976) Non-ageing developmental variant of *Caenorhabditis elegans*. *Nature* 260(5551):523-525.
28. Oriordan VB & Burnell AM (1990) Intermediary Metabolism in the Dauer Larva of the Nematode *Caenorhabditis-Elegans* .2. The Glyoxylate Cycle and Fatty-Acid Oxidation. *Comp Biochem Phys B* 95(1):125-130.
29. Wadsworth WG & Riddle DL (1989) Developmental regulation of energy metabolism in *Caenorhabditis elegans*. *Developmental biology* 132(1):167-173.
30. Erkut C, *et al.* (2013) Molecular strategies of the *Caenorhabditis elegans* dauer larva to survive extreme desiccation. *PloS one* 8(12):e82473.
31. Vanfleteren JR & Braeckman BP (1999) Mechanisms of life span determination in *Caenorhabditis elegans*. *Neurobiol Aging* 20(5):487-502.
32. Golden JW & Riddle DL (1984) The *Caenorhabditis elegans* dauer larva: developmental effects of pheromone, food, and temperature. *Developmental biology* 102(2):368-378.
33. Butcher RA, Ragains JR, Kim E, & Clardy J (2008) A potent dauer pheromone component in *Caenorhabditis elegans* that acts synergistically with other components. *Proceedings of the National Academy of Sciences of the United States of America* 105(38):14288-14292.
34. Fielenbach N & Antebi A (2008) *C. elegans* dauer formation and the molecular basis of plasticity. *Genes & development* 22(16):2149-2165.
35. Schaedel ON, Gerisch B, Antebi A, & Sternberg PW (2012) Hormonal signal amplification mediates environmental conditions during development and controls an irreversible commitment to adulthood. *PLoS biology* 10(4):e1001306.
36. Gerisch B, Weitzel C, Kober-Eisermann C, Rottiers V, & Antebi A (2001) A hormonal signaling pathway influencing *C. elegans* metabolism, reproductive development, and life span. *Developmental cell* 1(6):841-851.

37. Jia K, Albert PS, & Riddle DL (2002) DAF-9, a cytochrome P450 regulating *C. elegans* larval development and adult longevity. *Development* 129(1):221-231.
38. Ohkura K, Suzuki N, Ishihara T, & Katsura I (2003) SDF-9, a protein tyrosine phosphatase-like molecule, regulates the L3/dauer developmental decision through hormonal signaling in *C. elegans*. *Development* 130(14):3237-3248.
39. Antebi A (2015) Nuclear receptor signal transduction in *C. elegans*. *WormBook : the online review of C. elegans biology*:1-49.
40. Gottlieb S & Ruvkun G (1994) daf-2, daf-16 and daf-23: genetically interacting genes controlling Dauer formation in *Caenorhabditis elegans*. *Genetics* 137(1):107-120.
41. Riddle DL, Swanson MM, & Albert PS (1981) Interacting genes in nematode dauer larva formation. *Nature* 290(5808):668-671.
42. Thomas JH, Birnby DA, & Vowels JJ (1993) Evidence for parallel processing of sensory information controlling dauer formation in *Caenorhabditis elegans*. *Genetics* 134(4):1105-1117.
43. Vowels JJ & Thomas JH (1992) Genetic analysis of chemosensory control of dauer formation in *Caenorhabditis elegans*. *Genetics* 130(1):105-123.
44. Kim K, *et al.* (2009) Two chemoreceptors mediate developmental effects of dauer pheromone in *C. elegans*. *Science* 326(5955):994-998.
45. McGrath PT, *et al.* (2011) Parallel evolution of domesticated *Caenorhabditis* species targets pheromone receptor genes. *Nature* 477(7364):321-325.
46. Park D, *et al.* (2012) Interaction of structure-specific and promiscuous G-protein-coupled receptors mediates small-molecule signaling in *Caenorhabditis elegans*. *Proceedings of the National Academy of Sciences of the United States of America* 109(25):9917-9922.
47. Albert PS & Riddle DL (1988) Mutants of *Caenorhabditis elegans* that form dauer-like larvae. *Developmental biology* 126(2):270-293.
48. Chen X & Chalfie M (2014) Modulation of *C. elegans* touch sensitivity is integrated at multiple levels. *J Neurosci* 34(19):6522-6536.



49. Diaz SA, *et al.* (2014) Diverse and potentially manipulative signalling with ascarosides in the model nematode *C. elegans*. *BMC Evol Biol* 14(1):46.
50. Torr P, Heritage S, & Wilson MJ (2004) Vibrations as a novel signal for host location by parasitic nematodes. *International journal for parasitology* 34(9):997-999.
51. Ratcliff R & McKoon G (2008) The diffusion decision model: theory and data for two-choice decision tasks. *Neural Comput* 20(4):873-922.
52. Avery L (2014) A model of the effect of uncertainty on the *C. elegans* L2/L2d decision. *PloS one* 9(7):e100580.
53. Diniz DFA, de Albuquerque CMR, Oliva LO, de Melo-Santos MAV, & Ayres CFJ (2017) Diapause and quiescence: dormancy mechanisms that contribute to the geographical expansion of mosquitoes and their evolutionary success. *Parasites & vectors* 10(1):310.
54. Goehring L & Oberhauser KS (2002) Effects of photoperiod, temperature, and host plant age on induction of reproductive diapause and development time in *Danaus plexippus*. *Ecological Entomology* 27(6):674-685.
55. Denlinger DL (2002) Regulation of diapause. *Annu Rev Entomol* 47:93-122.
56. Shadlen MN & Roskies AL (2012) The neurobiology of decision-making and responsibility: reconciling mechanism and mindedness. *Frontiers in neuroscience* 6:56.
57. Gold JI & Shadlen MN (2007) The neural basis of decision making. *Annu Rev Neurosci* 30:535-574.
58. Hsiao S G-RM (2011) Touch. in *Neurobiology of Sensation and Reward*, ed JA G (CRC Press/Taylor & Francis, Boca Raton (FL)).
59. Liang X, Sun L, & Liu Z (2017) Overview of Mechanosensory Transduction. *Mechanosensory Transduction in Drosophila Melanogaster*, eds Liang X, Sun L, & Liu Z (Springer Singapore, Singapore), pp 1-12.
60. Lumpkin EA, Marshall KL, & Nelson AM (2010) The cell biology of touch. *J Cell Biol* 191(2):237-248.
61. Ardiel EL & Rankin CH (2010) The importance of touch in development. *Paediatr Child Health* 15(3):153-156.

62. Cascio CJ, Moore D, & McGlone F (2018) Social touch and human development. *Dev Cogn Neurosci*.
63. Gallace A & Spence C (2010) The science of interpersonal touch: an overview. *Neurosci Biobehav Rev* 34(2):246-259.
64. Hertenstein MJ, Holmes R, McCullough M, & Keltner D (2009) The communication of emotion via touch. *Emotion* 9(4):566-573.
65. Hertenstein MJ, Keltner D, App B, Bulleit BA, & Jaskolka AR (2006) Touch communicates distinct emotions. *Emotion* 6(3):528-533.
66. Blango MG & Mulvey MA (2009) Bacterial landlines: contact-dependent signaling in bacterial populations. *Curr Opin Microbiol* 12(2):177-181.
67. Gonzalez A, Lovic V, Ward GR, Wainwright PE, & Fleming AS (2001) Intergenerational effects of complete maternal deprivation and replacement stimulation on maternal behavior and emotionality in female rats. *Dev Psychobiol* 38(1):11-32.
68. Barr MM & Sternberg PW (1999) A polycystic kidney-disease gene homologue required for male mating behaviour in *C. elegans*. *Nature* 401(6751):386-389.
69. Eberl DF, Duyk GM, & Perrimon N (1997) A genetic screen for mutations that disrupt an auditory response in *Drosophila melanogaster*. *Proceedings of the National Academy of Sciences of the United States of America* 94(26):14837-14842.
70. Schafer WR (2015) Mechanosensory molecules and circuits in *C. elegans*. *Pflugers Arch* 467(1):39-48.
71. Nilius B & Owsianik G (2011) The transient receptor potential family of ion channels. *Genome biology* 12(3):218.
72. Li W, Kang L, Piggott BJ, Feng Z, & Xu XZ (2011) The neural circuits and sensory channels mediating harsh touch sensation in *Caenorhabditis elegans*. *Nat Commun* 2:315.
73. Kernan M, Cowan D, & Zuker C (1994) Genetic dissection of mechanosensory transduction: mechanoreception-defective mutations of *Drosophila*. *Neuron* 12(6):1195-1206.

74. Walker RG, Willingham AT, & Zuker CS (2000) A *Drosophila* mechanosensory transduction channel. *Science* 287(5461):2229-2234.
75. Pan B, *et al.* (2013) TMC1 and TMC2 are components of the mechanotransduction channel in hair cells of the mammalian inner ear. *Neuron* 79(3):504-515.
76. Smith CJ, *et al.* (2010) Time-lapse imaging and cell-specific expression profiling reveal dynamic branching and molecular determinants of a multi-dendritic nociceptor in *C. elegans*. *Developmental biology* 345(1):18-33.
77. Kim SE, Coste B, Chadha A, Cook B, & Patapoutian A (2012) The role of *Drosophila* Piezo in mechanical nociception. *Nature* 483(7388):209-212.
78. Ranade SS, *et al.* (2014) Piezo2 is the major transducer of mechanical forces for touch sensation in mice. *Nature* 516(7529):121-125.
79. Bargmann CI (2006) Chemosensation in *C. elegans*. *WormBook : the online review of C. elegans biology*:1-29.
80. Schulenburg H & Felix MA (2017) The Natural Biotic Environment of *Caenorhabditis elegans*. *Genetics* 206(1):55-86.
81. Sawin ER, Ranganathan R, & Horvitz HR (2000) *C. elegans* locomotory rate is modulated by the environment through a dopaminergic pathway and by experience through a serotonergic pathway. *Neuron* 26(3):619-631.
82. Maguire SM, Clark CM, Nunnari J, Pirri JK, & Alkema MJ (2011) The *C. elegans* touch response facilitates escape from predacious fungi. *Current biology : CB* 21(15):1326-1330.
83. O'Hagan R, Chalfie M, & Goodman MB (2005) The MEC-4 DEG/ENaC channel of *Caenorhabditis elegans* touch receptor neurons transduces mechanical signals. *Nature neuroscience* 8(1):43-50.
84. McGlone F, Wessberg J, & Olausson H (2014) Discriminative and affective touch: sensing and feeling. *Neuron* 82(4):737-755.
85. Tan PL & Katsanis N (2009) Thermosensory and mechanosensory perception in human genetic disease. *Hum Mol Genet* 18(R2):R146-155.

86. McClanahan PD, Xu JH, & Fang-Yen C (2017) Comparing *Caenorhabditis elegans* gentle and harsh touch response behavior using a multiplexed hydraulic microfluidic device. *Integr Biol (Camb)* 9(10):800-809.
87. Chatzigeorgiou M & Schafer WR (2011) Lateral facilitation between primary mechanosensory neurons controls nose touch perception in *C. elegans*. *Neuron* 70(2):299-309.
88. Felix MA & Duveau F (2012) Population dynamics and habitat sharing of natural populations of *Caenorhabditis elegans* and *C. briggsae*. *BMC biology* 10:59.
89. Petersen C, Dirksen P, Prah S, Strathmann EA, & Schulenburg H (2014) The prevalence of *Caenorhabditis elegans* across 1.5 years in selected North German locations: the importance of substrate type, abiotic parameters, and *Caenorhabditis* competitors. *BMC Ecol* 14:4.
90. Robinson A (2004) Nematode behavior and migrations through soil and host tissue. *Nematology - Advances and Perspectives*, ed Chen ZX, Chen, S.Y., Dickson, D.W. (Tsinghua University Press, Beijing, China), pp 380-405.
91. Frezal L & Felix MA (2015) *C. elegans* outside the Petri dish. *eLife* 4.
92. White JH (1953) Wind-borne Dispersal of Potato-Root Eelworm. *Nature* 172:686.
93. Lee H, *et al.* (2012) Nictation, a dispersal behavior of the nematode *Caenorhabditis elegans*, is regulated by IL2 neurons. *Nature neuroscience* 15(1):107-112.
94. Penkov S, *et al.* (2014) A wax ester promotes collective host finding in the nematode *Pristionchus pacificus*. *Nat Chem Biol* 10(4):281-285.
95. Lee D, Lee H, Kim N, Lim DS, & Lee J (2017) Regulation of a hitchhiking behavior by neuronal insulin and TGF-beta signaling in the nematode *Caenorhabditis elegans*. *Biochem Biophys Res Commun* 484(2):323-330.
96. Petersen C, *et al.* (2015) Travelling at a slug's pace: possible invertebrate vectors of *Caenorhabditis* nematodes. *BMC Ecol* 15:19.
97. Hallem EA, *et al.* (2011) A sensory code for host seeking in parasitic nematodes. *Current biology : CB* 21(5):377-383.

98. Hallem EA, Rengarajan M, Ciche TA, & Sternberg PW (2007) Nematodes, bacteria, and flies: a tripartite model for nematode parasitism. *Current biology : CB* 17(10):898-904.
99. White JG, Southgate E, Thomson JN, & Brenner S (1986) The structure of the nervous system of the nematode *Caenorhabditis elegans*. *Philosophical transactions of the Royal Society of London. Series B, Biological sciences* 314(1165):1-340.
100. Masland RH (2012) The neuronal organization of the retina. *Neuron* 76(2):266-280.
101. Kennedy B & Malicki J (2009) What drives cell morphogenesis: a look inside the vertebrate photoreceptor. *Dev Dyn* 238(9):2115-2138.
102. Zecevic D, *et al.* (1989) Hundreds of neurons in the *Aplysia* abdominal ganglion are active during the gill-withdrawal reflex. *J Neurosci* 9(10):3681-3689.
103. Bargmann CI (2012) Beyond the connectome: how neuromodulators shape neural circuits. *BioEssays : news and reviews in molecular, cellular and developmental biology* 34(6):458-465.
104. Albert PS & Riddle DL (1983) Developmental alterations in sensory neuroanatomy of the *Caenorhabditis elegans* dauer larva. *The Journal of comparative neurology* 219(4):461-481.
105. Inglis PN, Ou G, Leroux MR, & Scholey JM (2007) The sensory cilia of *Caenorhabditis elegans*. *WormBook : the online review of C. elegans biology*:1-22.
106. Jekely G (2013) Global view of the evolution and diversity of metazoan neuropeptide signaling. *Proceedings of the National Academy of Sciences of the United States of America* 110(21):8702-8707.
107. Kennedy MW & Harnett W (2001) *Parasitic Nematodes: Molecular Biology, Biochemistry, and Immunology* (CABI Pub.).
108. Senatore A, Reese TS, & Smith CL (2017) Neuropeptidergic integration of behavior in *Trichoplax adhaerens*, an animal without synapses. *J Exp Biol* 220(Pt 18):3381-3390.
109. Mirabeau O & Joly JS (2013) Molecular evolution of peptidergic signaling systems in bilaterians. *Proceedings of the National Academy of Sciences of the United States of America* 110(22):E2028-2037.

110. Nusbaum MP, Blitz DM, Swensen AM, Wood D, & Marder E (2001) The roles of co-transmission in neural network modulation. *Trends in neurosciences* 24(3):146-154.
111. Salio C, Lossi L, Ferrini F, & Merighi A (2006) Neuropeptides as synaptic transmitters. *Cell Tissue Res* 326(2):583-598.
112. Landgraf R & Neumann ID (2004) Vasopressin and oxytocin release within the brain: a dynamic concept of multiple and variable modes of neuropeptide communication. *Frontiers in neuroendocrinology* 25(3-4):150-176.
113. Li C & Kim K (2008) Neuropeptides. *WormBook : the online review of C. elegans biology*:1-36.
114. Pierce SB, *et al.* (2001) Regulation of DAF-2 receptor signaling by human insulin and ins-1, a member of the unusually large and diverse *C. elegans* insulin gene family. *Genes & development* 15(6):672-686.
115. Cardoso JC, Felix RC, Fonseca VG, & Power DM (2012) Feeding and the rhodopsin family g-protein coupled receptors in nematodes and arthropods. *Frontiers in endocrinology* 3:157.
116. Dockray GJ (2004) The expanding family of -RFamide peptides and their effects on feeding behaviour. *Experimental physiology* 89(3):229-235.
117. Elphick MR & Mirabeau O (2014) The Evolution and Variety of RFamide-Type Neuropeptides: Insights from Deuterostomian Invertebrates. *Frontiers in endocrinology* 5:93.
118. Li C & Kim K (2014) Family of FLP Peptides in *Caenorhabditis elegans* and Related Nematodes. *Frontiers in endocrinology* 5:150.
119. McVeigh P, Geary TG, Marks NJ, & Maule AG (2006) The FLP-side of nematodes. *Trends Parasitol* 22(8):385-396.
120. Rabinowitch I, *et al.* (2016) Neuropeptide-Driven Cross-Modal Plasticity following Sensory Loss in *Caenorhabditis elegans*. *PLoS biology* 14(1):e1002348.
121. Sakarya O, *et al.* (2007) A post-synaptic scaffold at the origin of the animal kingdom. *PloS one* 2(6):e506.

122. Santos-Carvalho A, Alvaro AR, Martins J, Ambrosio AF, & Cavadas C (2014) Emerging novel roles of neuropeptide Y in the retina: from neuromodulation to neuroprotection. *Prog Neurobiol* 112:70-79.
123. Reichmann F & Holzer P (2016) Neuropeptide Y: A stressful review. *Neuropeptides* 55:99-109.
124. Nath RD, Chow ES, Wang H, Schwarz EM, & Sternberg PW (2016) C. elegans Stress-Induced Sleep Emerges from the Collective Action of Multiple Neuropeptides. *Current biology : CB* 26(18):2446-2455.

*Chapter 2****CAENORHABDITIS ELEGANS* CAN USE MECHANOSENSATION  
TO PREDICT ENVIRONMENTAL COLLAPSE**

(This work was done in collaboration with Chin-Sang I., Brugman K., and Shih P.Y.)



## 2.1 Abstract

Animals make decisions to alter aspects of their development based on signals from the environment. The roundworm *Caenorhabditis elegans* can escape environmental collapse by entering a spore-like dauer larval stage. Food, pheromone, and temperature have long been known to input into the dauer entry decision, but some inputs are clearly missing in models of the decision. Here we report a role for mechanosensation as an overlooked input into the decision. We show that gentle, harsh, and piezo touch promote dauer entry, using quantitative entry assays on CRISPR knock-ins and existing mutants in mechanosensation. We demonstrate that touch and pheromone likely work in parallel to promote dauer entry, by examining pheromone sensation and signal transmission in mechanosensation-defective mutants. We confirm that direct mechanical stimulation of *C. elegans* promotes dauer entry, and we provide a plausible role for mechanosensation in sensing dauer-promoting weather and crowding conditions. Our findings reveal that the dauer entry decision is more complex than previously recognized, and illuminates how animals can make robust decisions, even with a numerically simple nervous system.

## 2.2 Introduction

Most if not all organisms undergo developmental decisions to survive in changing environments (1, 2). By altering aspects of their development, organisms including bacteria (3, 4), insects (5), plants (6, 7), and mammals (8, 9) can adapt their metabolism, physiology, and reproductive strategy to meet resource availability. In this way, *Caenorhabditis elegans* roundworms can escape environmental collapse by becoming dauer larvae (10). Dauers are spore-like, stress-resistant, and capable of long-range dispersal (11-13). In addition, dauers have a remodeled nervous system and cease feeding, reproduction, and aging, making dauer entry one of the most dramatic postembryonic switches to be reported (14-16).

Dauer entry is a complex decision, requiring multiple inputs from food, pheromone, and temperature to assess the quality of the environment (17). Seven amphid sensory neurons (**Figure 2.1A**) transduce these signals over an integration period of several hours, presumably to extract trend information on the environment's decline (18-20). Dauer entry is therefore an anticipatory decision that aims to predict whether environmental conditions will continue to support growth.

Despite being one of the best studied life cycle decisions, no satisfying model of dauer entry exists (but see (12, 18)), likely because a complete accounting of all of the inputs into the decision has not been made (21). We therefore investigated the possibility that mechanosensory inputs affect the dauer entry decision. Indeed, mechanosensation is useful for assessing population

density in plants and bacteria (7, 22), and can be used to self-assess growth rate in insects (23). In the wild, *C. elegans* is found in rotting vegetation, where it can come into contact with bacteria, fungi, insects, predators, and other nematodes (24). *C. elegans* can use several types of touch, including discriminative gentle touch (25, 26) and nociceptive harsh touch (27, 28), to help navigate through such complex physical environments (29, 30). Conceivably, information captured by mechanosensation could complement food, pheromone, and temperature signals to assess crowding, nutrition status, or other cues.

Using quantitative dauer entry assays, we demonstrate that CRISPR mutants and existing strains of mechanosensation-defective animals make inaccurate dauer entry decisions. By examining pheromone sensation and signal transmission, we find that pheromone and touch work in parallel pathways to promote dauer entry. Using direct mechanical stimulation, we further demonstrate that mechanosensation promotes dauer entry. Finally, we provide a plausible role for mechanosensation in assessing weather and crowding conditions that promote dauer entry. Our findings reveal that *C. elegans* use mechanosensation to enhance the accuracy of their dauer entry decision, demonstrating that the decision is more complex than previously recognized.

## 2.3 Results

### The dauer entry life cycle decision is modulated by mechanosensation.

Gentle touch in *C. elegans* is sensed by the ALM, AVM, PLM, and PVM touch receptor neurons (TRNs) (25). The MEC-3/LIM homeodomain transcription factor is necessary for the differentiation of the TRNs during development (31). Using pheromone to induce dauer entry (19, 32), we tested the ability of *mec-3(e1338)* null mutants to enter dauer, relative to wild type. We observed that *mec-3(e1338)* entered dauer at a 3.4-fold lower rate than wild type (*mec-3(e1338)* dauer entry rate = 16%, N = 147; wild type dauer entry rate = 55%, N = 245) (**Figure 2.1B-C**). This data suggests that MEC-3, and likely the TRNs, promotes dauer entry.

Mechanotransduction in the TRNs relies on the MEC-4/ MEC-10/MEC-2/MEC-6 channel complex (33). The MEC-4 channel subunit is essential for the activity of this complex, and is expressed exclusively in the TRNs (25, 34). Additionally, MEC-4 is believed to be required specifically for mechanotransduction, since other ionic currents are unaffected in *mec-4* nulls (33). Using CRISPR, we knocked in a 43-nucleotide stop cassette (35) into the *mec-4* gene to generate 3 putative null alleles: *sy1124*, *sy1125*, and *sy1126* (**Figure 2.2**). We observed that the pheromone-induced dauer entry of these mutants occurred at an average 2.0-fold lower rate than wild type (e.g. *mec-4(sy1124)* dauer entry = 21%, N = 315; wild type dauer entry = 58%, N = 520) (**Figure 2.1B-C, Figure 2.3**).

We also tested the canonical *mec-4(u253)* null allele (36), which demonstrated a 126-fold decrease in dauer entry (*mec-4(u253)* dauer entry = 0%,

N = 267; wild type dauer entry = 47%, N = 446). The stronger phenotype of the *u253* allele may indicate that *sy1124*, *sy1125*, and *sy1126* are loss-of-function alleles instead of nulls, or could be due to genetic background effects in the *mec-4(u253)* strain.

Furthermore, we observed that *mec-4(e1611)* gain-of-function mutants have a 2.0-fold increased dauer entry rate as compared to wild type (*mec-4(e1611)* dauer entry = 79%, N = 228; wild type dauer entry = 37%, N = 167). Although the *e1611* gain-of-function allele causes neurodegeneration in the TRNs through hyperactivity of the mechanotransduction channel (37), the AVM touch neuron is not fully degenerated until adulthood (38). It is therefore likely that mechanotransduction is hyperactive in the AVM during the dauer entry decision in *mec-4(e1611)* animals. These data suggest that MEC-4 promotes dauer entry through the activity of the mechanotransduction channel.

We further confirmed this by testing the MEC-10 subunit of the channel complex, which regulates the ionic activity of the complex (39). We used CRISPR to generate 2 putative null alleles of *mec-10*: *sy1127*, and *sy1129* (**Figure 2.2**), and observed that they entered dauer at an average 1.9-fold lower rate than wild type (e.g. *mec-10(sy1127)* dauer entry = 35%, N = 341; wild type dauer entry = 58%, N = 520) (**Figure 2.1B-C**).

We also tested the *mec-10(e1515)* point mutant, which dramatically reduces the mechanoreceptor current (MRC) of the transduction complex (39). *mec-10(e1515)* mutants entered dauer at a 37.9-fold lower rate than wild type (*mec-10(e1515)* dauer entry = 1%, N = 181; wild type dauer entry = 42%, N =

241). Furthermore, the loss-of-function allele *mec-10(ok1104)*, which only mildly decreases the peak MRC of the channel complex (39), did not significantly affect dauer entry (*mec-10(ok1104)* dauer entry = 38%, N = 236; wild type dauer entry = 46%, N = 299). These data suggest that MEC-10 promotes dauer entry through the MRC of the transduction complex.

MEC-18/Firefly luciferase-like protein and MEC-19/novel membrane protein modulate gentle touch (40, 41). We observed that *mec-18(u228)* decreased dauer entry by 5.1-fold (*mec-18(u228)* dauer entry = 9%, N = 167; wild type dauer entry = 46%, N = 418) and *mec-19(ok2504)* modestly decreased dauer entry by 1.4-fold (*mec-19(ok2504)* dauer entry = 44%, N = 233; wild type dauer entry = 60%, N = 430) (**Figure 2.1B-C**). These data further indicate that gentle touch promotes dauer entry.

We also tested the role of harsh touch on dauer entry by assaying the *trp-4(sy695)* and *trp-4(sy696)* putative null alleles (42). The TRP-4/TRPN channel subunit is expressed in the ADE, DVA, and PDE harsh touch neurons and regulates posterior harsh touch (27). We observed that *trp-4(sy695)* and *trp-4(sy696)* decreased dauer entry by an average 3.9-fold (e.g. *trp-4(sy695)* dauer entry = 10%, N = 143; wild type dauer entry = 50%, N = 294) (**Figure 2.1B-C**). These data suggest that harsh touch mediated by TRP-4 promotes dauer entry.

Since *mec* and *trp-4* mutants disrupt the function of several neurons, we used *ceh-17(np1)* nulls to test the effects of an incomplete nervous system on the dauer entry decision. The CEH-17 transcription factor is necessary for the proper axonal outgrowth of the ALA and 4 SIA neurons (43, 44), neither of which have

known functions in dauer entry or mechanosensation. We observed that *ceh-17(np1)* did not significantly affect dauer entry, relative to wild type (*ceh(np1)* dauer entry = 39%, N = 185; wild type dauer entry = 49%, N = 239) (**Figure 2.1B**). Therefore, the effects of the *mec* and *trp-4* mutants on dauer entry are likely beyond those of an incomplete nervous system. These data indicate that the dauer entry decision is modulated by gentle and harsh touch.

### **Touch and pheromone are parallel inputs into the dauer entry decision**

To understand how the dauer entry decision is affected in touch mutants, we tested the dauer entry dose-response of *mec-4*, *trp-4*, and *mec-4;trp-4* mutants to pheromone. Using concentrations of 0.25%, 0.75%, and 2.25% pheromone to drive dauer entry, we observed a logarithmic dose-response to pheromone in wild type, as expected (45), with an EC50 of 0.64% ( $R^2 = 0.99$ ) (**Figure 2.4A**). *mec-4(sy1124)* mutants demonstrated an EC50 of 2.22% ( $R^2 = 0.99$ ), corresponding to a decreased dose-response to pheromone across 0.75%-2.25%. *trp-4(sy695)* mutants demonstrated an EC50 of 0.98% ( $R^2 = 0.99$ ), corresponding to a modest decrease in dose-response across all concentrations. The *mec-4(sy1124);trp-4(sy695)* double mutant demonstrated a similar dose-response to that of the *mec-4(sy1124)* single, with an EC50 of 2.07% ( $R^2 = 0.99$ ). The decreased dose-response of the mutants suggests that *mec-4* and *trp-4* affect dauer entry by modulating pheromone sensation, or by affecting the decision as a parallel input to pheromone.

Aside from dauer entry, another method for assaying pheromone sensation

is to measure *str-3* gene expression in the ASI neuron (46). STR-3 is a chemosensory receptor, and its expression in the ASI is repressed by sensation of pheromone in ASI and ASK. As a result, *str-3::gfp* is useful for identifying mutants that disrupt pheromone sensation and signal transmission (47, 48). We observed that STR-3::GFP fluorescence in the ASI did not vary between L2d animals with wild type *mec-4*, null *mec-4(sy1124)*, and gain-of-function *mec-4(e1611)* (**Figure 2.4B-C**). In addition, STR-3::GFP fluorescence was the same between wild type, *mec-4(sy1124)*, and *mec-4(e1611)* young adults (**Figure 2.4D**). Furthermore, STR-3::GFP levels did not vary in wild type adults that were mechanically stimulated via drop test (49) (**Figure 2.4E**). These data suggest that touch does not affect pheromone sensation or signal transmission. A simple interpretation is that touch affects the dauer entry decision as a parallel input to pheromone.

#### ***mec-4* and *trp-4* act additively with *pezo-1* to promote dauer entry**

Despite being the major mechanotransducer in mammals (50, 51), the role of PEZO-1/Piezo in *C. elegans* remains unclear. In addition, *pezo-1* is expressed in neurons but not the TRNs (**Table 2.1**). We used CRISPR to generate 3 loss-of-function alleles of *pezo-1*: *sy1184*, *sy1199*, and *sy1200*, and we observed that *pezo-1(sy1199)* decreased dauer entry by 2.0-fold (*pezo-1(sy1199)* dauer entry = 28%, N = 172; wild type dauer entry = 57%, N = 1039) (**Figure 2.5**). This data suggest that *pezo-1* acts similarly to the *mec-4* and *trp-4* mechanotransducers and promotes dauer entry.



*mec-4(sy1124);pezo-1(sy1200)* double mutants decreased dauer entry by 2.5-fold (dauer entry = 23%, N = 137; wild type dauer entry = 57%, N = 1039), though this effect was not significantly different from the effect of the *mec-4* and *pezo-1* single mutants (**Figure 2.5**). On the other hand, *mec-4(sy1124);trp-4(sy695);pezo-1(sy1184)* triple mutants decreased dauer entry by 4.2-fold (dauer entry = 14%, N = 190; wild type dauer entry = 57%, N = 1039) (**Figure 2.5**). The effect of the *mec-4;trp-4;pezo-1* triple mutant was significantly greater than the effect of the single mutants, as well as the *mec-4;trp-4* double. These data suggest that *mec-4* and *trp-4* act additively with *pezo-1* to modulate dauer entry.

### **Direct mechanical stimulation promotes dauer entry**

We investigated whether direct mechanical stimulation of animals could drive them into dauer entry. We used two methods for inducing mechanosensation: (1) we added 150-212  $\mu\text{m}$  glass beads to dauer entry plates to increase the roughness of the culture surface, and (2) we used a servo shaker to gently agitate culture plates every 10 to 20 seconds.

We observed that the addition of 0.2 to 0.6  $\text{mg}/\text{cm}^2$  glass beads did not affect wild type dauer entry (dauer entry without beads = 64%, N = 215; dauer entry with beads = 64%, N = 325) (**Figure 2.6A**). However, we observed that gently agitating sensitized *daf-2(e1370)* mutants—which enter dauer mildly at room temperature (52)—increased dauer entry by 1.8-fold (*daf-2(e1370)* dauer entry = 52%, N = 762; *daf-2(e1370)* with vibration = 94%, N = 458) (**Figure 2.6B**). These results suggest that direct mechanical stimulation, at least from vibration,

can promote the dauer entry decision. A caveat is that the vibration may have increased the temperature that the *daf-2(e1370)* animals were exposed to, which may also account for the observations.

## 2.4 Discussion

Developmental decisions allow organisms to survive in changing environments (2). One of the best studied developmental decisions is *C. elegans* dauer entry. The principal regulators of this decision have been identified through genetic analysis of dauer-constitutive and -defective mutants, which highlighted the major inputs of food and pheromone (53-58). However, no satisfying model of the entry decision exists, likely because all of the inputs have not been identified (21).

Indeed, the known inputs into the dauer entry decision—food, pheromone, and temperature—are not the only cues that nematodes are exposed to in the wild, and in some cases these cues may be unreliable for assessing the environment. For instance, pheromones may be quenched by organic matter in soils (59), and may be used as dishonest signals to manipulate other nematodes into disadvantageous dauer decisions (60, 61).

Here we have demonstrated a role for mechanosensation as an overlooked modulator of the dauer entry decision. *C. elegans* can sense several types of touch, presumably to help navigate its natural environments where it can come into contact with bacteria, fungus, insects, carriers, predators, and other nematodes (62). These types of touch include gentle touch, harsh touch, nose touch, and food texture sensation (30). Gentle touch is likely analogous to low-threshold, discriminative touch in humans, which helps to detect light touch, hair movements, vibrations, quivering, and social touch (26, 63, 64). On the other hand, harsh touch is likely analogous to high-threshold nociception, which detects physically damaging forces (26-28). Curiously, the major mechanotransducers in

nematodes are MEC-4/10 and TRP-4, while the major mechanotransducer in mammals is Piezo.

Using quantitative dauer entry assays on CRISPR knock-ins and existing mutants of gentle touch (*mec-3*, *mec-4*, *mec-10*, *mec-18*, and *mec-19*), harsh touch (*mec-3* and *trp-4*), and piezo touch (*pezo-1*), we showed that mechanosensation promotes the dauer entry decision. We further confirmed this using direct mechanical stimulation, and demonstrated that vibration can promote dauer entry. We mostly did not observe large effect sizes for the mechanosensation-defective single mutants, and this is to be expected since the principal regulators of the decision have already been identified. Therefore, mechanosensation is a modulator of the decision, much like temperature which enhances pheromone-induced dauer entry (17).

Because of the moderate effect size of *trp-4(sy695)* on dauer entry, the *mec-4(sy1124);trp-4(sy695)* phenotype could not be used to determine if *mec-4* and *trp-4* act additively or in the same pathway (65). However, close connections between the harsh touch and gentle touch neurons suggest it is likely that *mec-4* and *trp-4* act in the same circuit pathway to modulate dauer entry: The harsh touch PDE neuron is directly gap junctioned to the gentle touch PVM, and is gap junctioned to the gentle touch PLM via PVC (66, 67). In addition, the harsh touch DVA is gap junctioned to the gentle touch ALM and PLM via PVR and PVC/PVR, respectively. On the other hand, we demonstrated that *mec-4* and *trp-4* act additively with *pezo-1* to promote dauer entry, indicating that there are parallel pathways for mechanosensation to input into the decision.

We propose that mechanosensation could be used to assess at least two conditions that correlate with dauer entry: humidity and crowding. First, humidity is sensed, in part, by MEC-10 (68), and has been suggested by some groups to promote dauer entry (21). Moreover, moisture has been shown to affect the dispersal of parasitic nematodes (69), suggesting it may affect dauer dispersal as well. Indeed, we and others have shown that dauers and parasitic nematodes share common strategies for dispersal (32, 70). Thus, while dauers can survive dessication for a few days (13), it may be advantageous for *C. elegans* to enter dauer when humidity levels are favorable for dispersal.

Second, *C. elegans* can sense crowding via pheromone signals (71), which can be inaccurate (59-61). We speculate that *C. elegans* could also measure crowding via contact-dependent signaling, such as in bacteria (22), plants (7), and insects (5). We have shown that touch and pheromone likely act in parallel to affect the dauer entry decision, and it is conceivable that they might jointly assess crowding in order to increase the accuracy of the decision.

The input of mechanosensation into dauer entry has revealed the decision to be more complex than previously recognized. This growing complexity raises the intriguing possibility that other cues such as light,  $O_2/CO_2$ , pH, and osmotic stress may input into the decision as well (**Figure 2.7**). This hypothesis is supported by recent findings that the dauer entry decision is modulated by noxious stimuli, which may facilitate pheromone signaling (48). It is plausible that multiple inputs assessing various aspects of the environment may be crucial for making robust developmental decisions in *C. elegans*. Finally, since mechanosensation is

important for growth and development in invertebrates to vertebrates (72), and is used to make developmental decisions in fungi (73), plants (7), and insects (5), we speculate that mechanosensation may be a common input into developmental decisions across biology.

## 2.5 Materials and Methods

### Animal strains

*C. elegans* strains were grown using standard protocols with *Escherichia coli* OP50 as a food source (74). The wild type strain was N2 (Bristol). Strains obtained from the *Caenorhabditis* Genetics Center (CGC) include CB1515 *mec-10(e1515)*, RB1115 *mec-10(ok1104)*, TU228 *mec-18(u228)*, RB1925 *mec-19(ok2504)*, and IB16 *ceh-17(np1)* 3x outcrossed. TQ526 *mec-3(e1338)* 4x outcrossed, TQ253 *mec-4(u253)*, and TQ1243 *mec-4(e1611)* 6x outcrossed were gifts from the Xu laboratory. PS4492 *trp-4(sy695)* 7x outcrossed and PS4493 *trp-4(sy696)* 6x outcrossed were generated in the Sternberg laboratory.

### CRISPR-generated strains

CRISPR alleles of *mec-4*, *mec-10*, and *pezo-1* were generated by knocking in the 43-nucleotide stop cassette: GGAAGTTTGTCCAGAGCAGAGGTGACTAAGTGATAAgctagc (35).

PS7913 *mec-4(sy1124)*, PS7914 *mec-4(sy1125)*, and PS7915 *mec-4(sy1126)* were generated using the guide RNA ACGACGTGCCGGTTTTGTGG. Flanking sequences (Left) CCGAACCACCCACCACCCCTGCACCCACCA (Right) CAAAACCGGCACGTCGTCGAGGAAAACGTG. PS8039 *trp-4(sy695);mec-4(sy1124)* was generated by crossing PS7913 males to PS4492.

PS7916 *mec-10(sy1127)* and PS7918 *mec-10(sy1129)* were generated using the guide RNA TATACAATTTATCAATCAGG. Flanking sequences (Left) TTCTAATCTGTGCTATACAATTTATCAATC

(Right) AGGCGGTCGCTGTGATTCAGAAAGTATCAGA.

PS8111 *pezo-1(sy1199)*, PS8112 *pezo-1(sy1200);mec-4(sy1124)*, and PS8084 *trp-4(sy695);pezo-1(sy1184);mec-4(sy1124)* were generated using the guide RNA CCAGAAGCTCGTAAGCCAGG. Putative flanking sequences

(Left) CGCTGTTTCTGAACCAGAAAGCTCGTAAGCC

(Right) AGGAGGCACTGAAGAAACGGATGGTGATGA.

### **Dauer entry assay**

Pheromone-induced dauer entry assays were performed as previously described (32). The conditions used to induce dauer entry were: 20  $\mu$ L of 8% w/v heat-killed OP50 and incubation at 25.5°C for 48 hours, with approximately 50 animals per plate. For phenotypic screening (**Figure 2.1B**), we used 1.5% pheromone to induce approximately 50% dauer entry in wild type in order to detect increased or decreased dauer entry in mutants.

### **Mechanical perturbation of animals**

*Glass beads*: 2 to 6 mg of autoclaved glass beads (Millipore Sigma G1145, 150-212  $\mu$ m) were added to the surface of 0.75% pheromone dauer entry plates, to an approximate density of 0.2 to 0.6 mg/cm<sup>2</sup>. Dauer entry was assayed as above.

*Vibration assay*: We used the *daf-2(e1370)* sensitized mutant, which enters dauer modestly at room temperature (52). We attached culture plates containing *daf-2(e1370)* animals to a servo shaker and gently agitated every 10 to 20



seconds at room temperature for 48 hours.

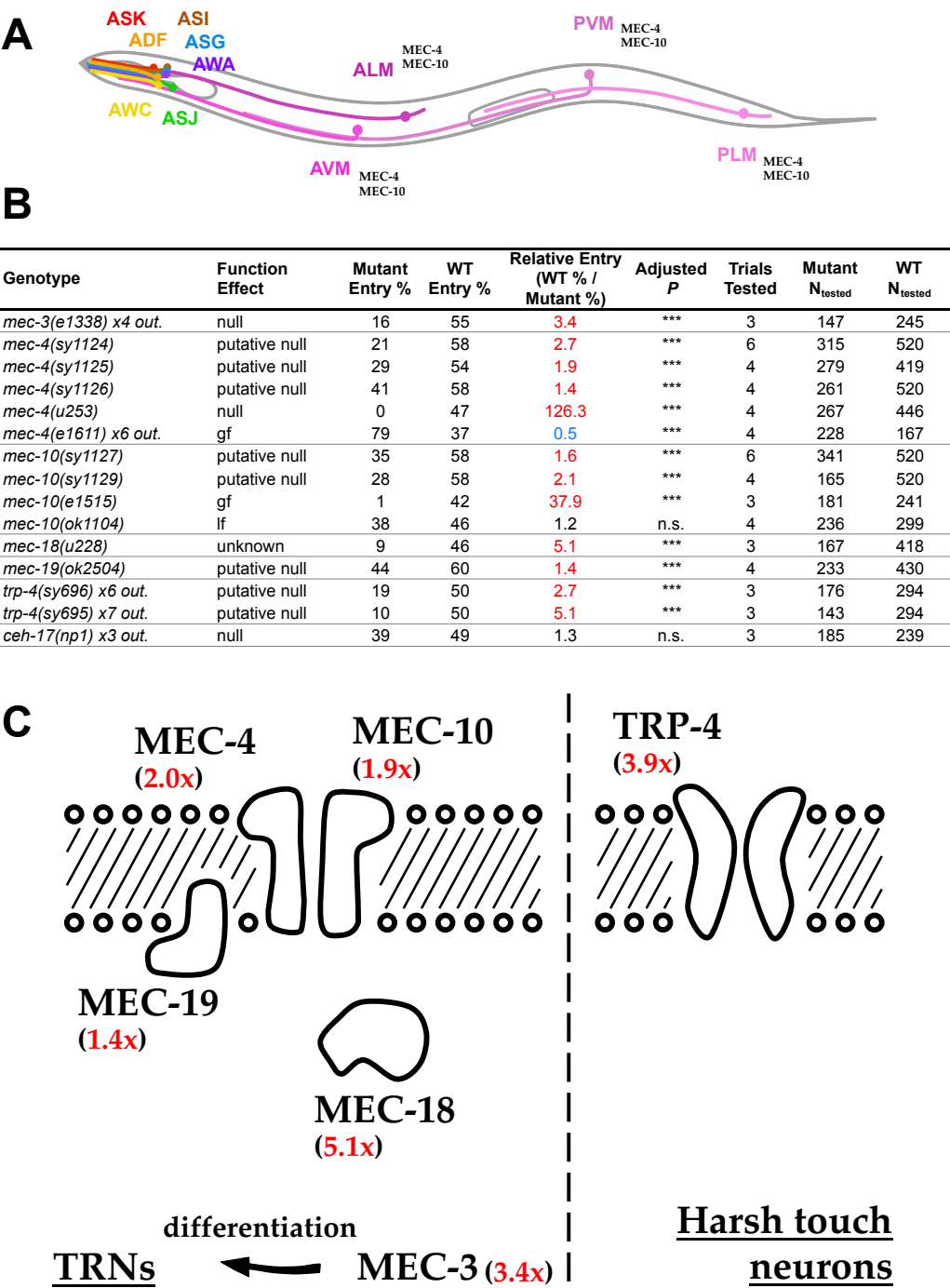
### **Drop test assay**

Culture plates were parafilmed, put in a cardboard box, and dropped as in (49): from a height of 5 cm, 30 times, with a 10 second interstimulus interval.

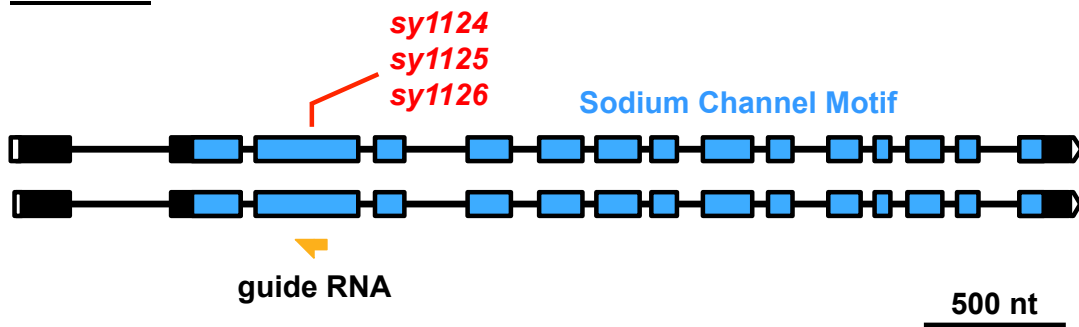
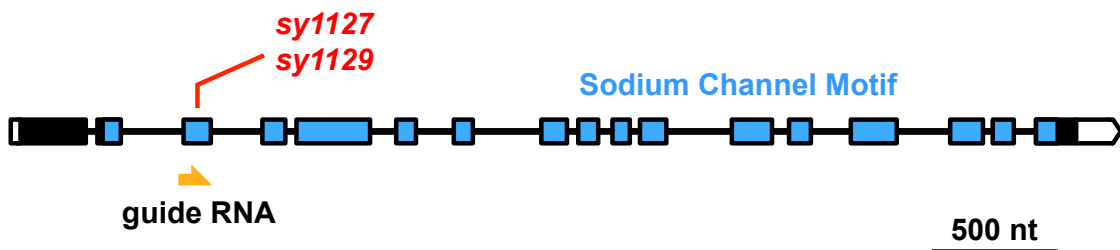
### **Pheromone sensitivity assay**

For measurements in L2d, larvae were grown on 2.25% pheromone dauer entry plates for 23 to 27 hours at 25.5°C. For measurements in young adults, 20 L4 animals were picked onto seeded NGM plates the day before the assay. For the drop test assay, 15 L4 animals were picked the day before the assay. Fluorescence measurements of STR-3::GFP in the ASI neuron were made using ZEISS ZEN software. Average fluorescence intensities were obtained from regions drawn around the ASI and image backgrounds, and fluorescence was corrected by subtracting the background. All fluorescence intensities were normalized to measurements from the same-day CX3596 *str-3::gfp* control.

2.6 Figures and tables



**Figure 2.1. The dauer entry life cycle decision is modulated by mechanosensation. (A)** Schematic of the gentle touch mechanosensory neurons (magenta) and amphid neurons (rainbow) of *C. elegans*. The expression of MEC-4 and MEC-10 mechanoreceptors in the gentle touch neurons is indicated. **(B)** Dauer entry rates of *mec* mutants. *P* calculated via nonparametric permutation test and adjusted using Bonferroni correction. out., outcrossed. **(C)** Schematic of gentle (left) and harsh (right) touch neurons. Top, ECM; bottom, cytoplasm. Numbers in parentheses represent the relative dauer entry rate of wild type to mutant. Red, dauer entry promoting.

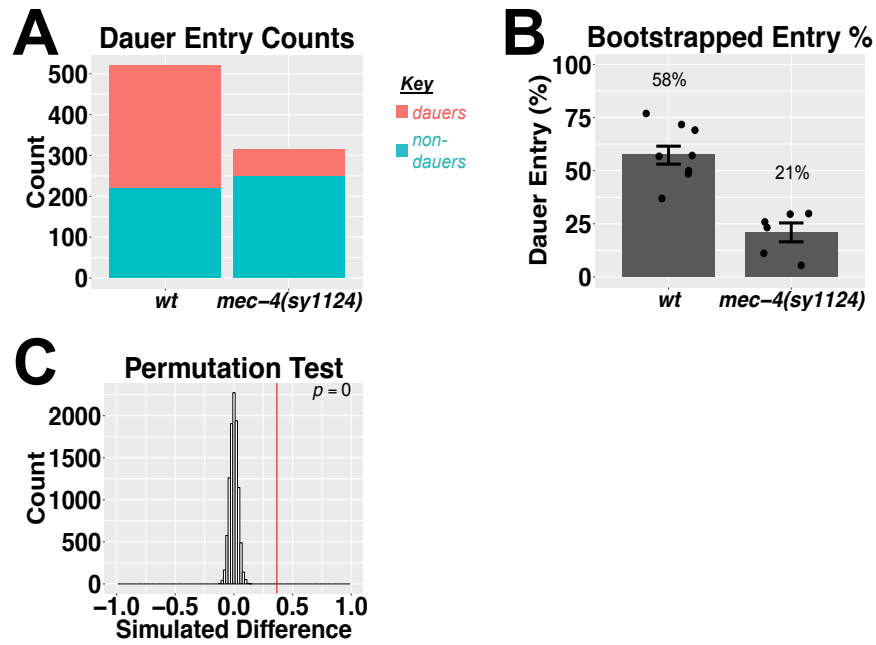
**mec-4****mec-10**

sy1124 – 1126, 1127, 1129

STOP-IN allele: GGGAAGTTTGTCCAGAGCAGAGGTGACTAAGTGATAAgctagc

**Figure 2.2. *mec-4* and *mec-10* CRISPR alleles are putative nulls.** Gene models of *mec-4* and *mec-10*. The location of the sy CRISPR alleles are indicated in red. White, untranslated regions; black, exons; blue, sodium channel-encoding exon regions; lines, introns. Arrow indicates the direction of the guide RNA.

# *mec-4(sy1124)*



# *mec-4(e1611)*

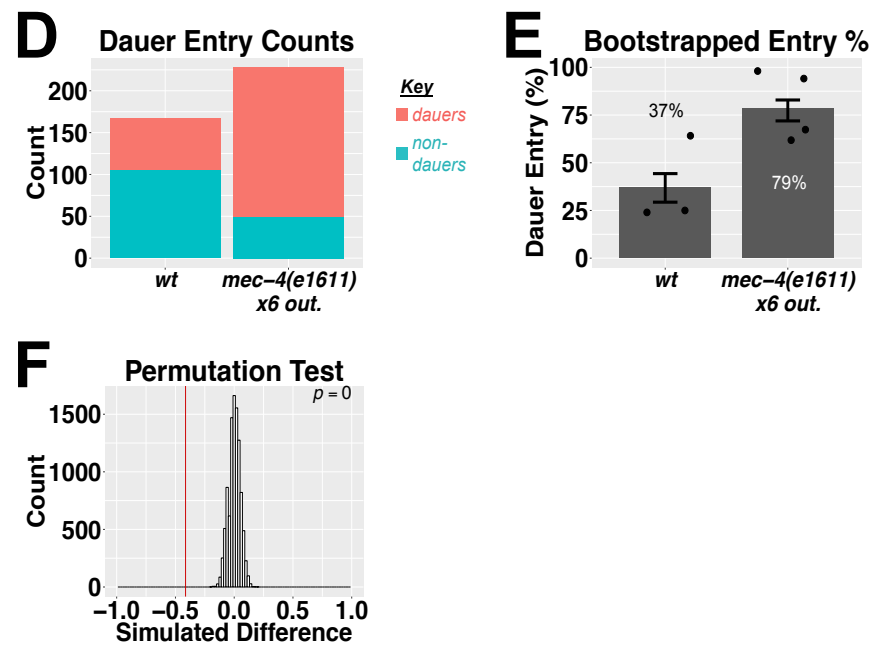
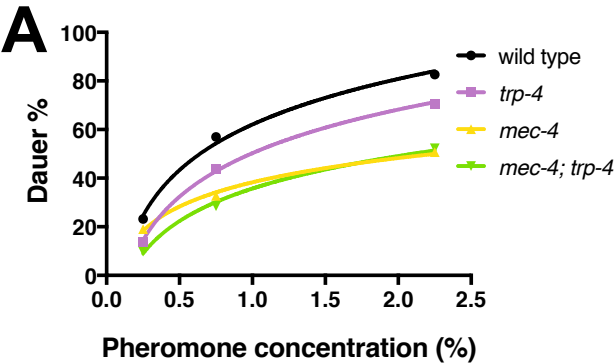


**Figure 2.3. *mec-4* promotes dauer entry.** (A, D) The number of animals that decided to enter dauer (red) or reproductive development (blue) for the wild type control, (A) *mec-4(sy1124)* nulls, and (D) *mec-4(e1611)* gain-of-function mutants. (B, E) Representation of dauer entry counts as percentages. Points, independent trials; bar, bootstrapped dauer entry percentage; whiskers, 95% confidence interval. (C, F) Histogram of the 9,999 simulated differences between wild type and (C) *mec-4(sy1124)* nulls or (F) *mec-4(e1611)* gain-of-function mutants in non-parametric permutation tests. Red line, observed difference.



**0.25%**

	wild type	<i>mec-4</i>	<i>trp-4</i>	<i>mec-4; trp-4</i>
wild type				
<i>mec-4</i>	n.s.			
<i>trp-4</i>	*	n.s.		
<i>mec-4; trp-4</i>	*	n.s.	n.s.	

**0.75%**

	wild type	<i>mec-4</i>	<i>trp-4</i>	<i>mec-4; trp-4</i>
wild type				
<i>mec-4</i>	***			
<i>trp-4</i>	**	*		
<i>mec-4; trp-4</i>	***	n.s.	**	

**2.25%**

	wild type	<i>mec-4</i>	<i>trp-4</i>	<i>mec-4; trp-4</i>
wild type				
<i>mec-4</i>	***			
<i>trp-4</i>	***	***		
<i>mec-4; trp-4</i>	***	n.s.	***	

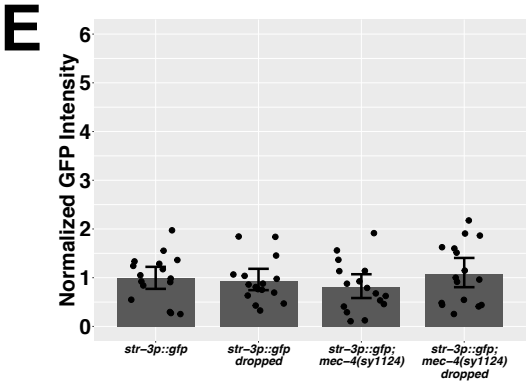
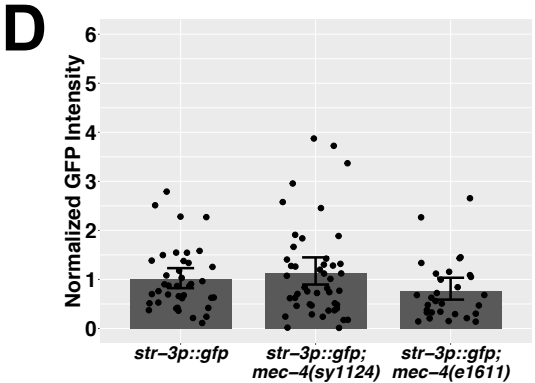
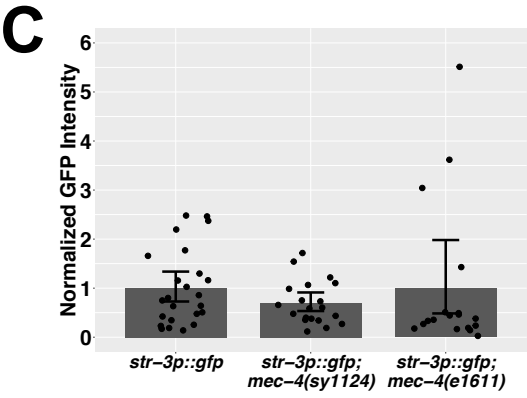


**Figure 2.4. Touch and pheromone are parallel inputs into the dauer entry decision.** **(A)** Pheromone dose-response curve of dauer entry for wild type, *mec-4(sy1124)* nulls, *trp-4(sy695)* nulls, and *mec-4(sy1124);trp-4(sy695)* double mutants. Points represent averages from 3-17 independent trials. Pairwise adjusted *P* values are indicated in the matrices corresponding to each pheromone concentration point. Shades of green, increasing statistical confidence. **(B)** Representative image of *str-3::gfp* fluorescence in the ASI neuron of *mec-4(wt)* L2d larvae. **(C-D)** STR-3::GFP intensity in (C) L2d and (D) adult animals. **(E)** STR-3::GFP intensity in adults mechanically stimulated via dropping. Points, individual animals; bar, bootstrapped mean intensity; whiskers, 95% confidence interval.



Gene	Protein Type	Expression	Strain	Allele	Protein Effect	Function Effect	Phenotype	Citation
<i>mec-3</i>	LIM homeodomain protein	AlZ, ALM, AVM, FLP, PLM, PVD, PVM, VNC	TQ526	<i>mec-3(e1338)</i>	Insertion and frameshift	Putative loss-of-function or null	TRNs fail to differentiate	Way & Chalfie 1989; Xue, Tu, & Chalfie 1993; Bounoutas <i>et al.</i> Chalfie 2009; Kubanek <i>et al.</i> Goodman 2018
<i>mec-4</i>	DEG / ENaC channel	ALM, AVM, PLM, PVM	TU253	<i>mec-4(u253)</i>	Deletion	Null	Abolished mechanoreceptor currents	Hong, Mano, & Driscoll 2000; O'Hagan, Chalfie, & Goodman 2005
			TQ1243	<i>mec-4(e1611)</i>	T442A	Gain-of-function	Touch insensitivity, touch cell degeneration	Driscoll & Chalfie 1991
			CB1339	<i>mec-4(e1339)</i>	G230E	Loss-of-function	Partially touch insensitive	O'Hagan, Chalfie, & Goodman 2005; Chalfie & Sulston 1981
<i>mec-10</i>	DEG / ENaC channel	ALM, AVM, FLP, PLM, PVD, PVM, tail neuron	CB1515	<i>mec-10(e1515)</i>	S105F	Gain-of-function	Touch insensitive (but weaker than <i>u20</i> , <i>u390</i> , <i>u332</i> , <i>e1715</i> )	Huang & Chalfie 1994; Arnadottir <i>et al.</i> Chalfie 2011
			RB1115	<i>mec-10(ok1104)</i>	Deletion	Loss-of-function	Partially touch insensitive (weaker than <i>e1515</i> )	Arnadottir <i>et al.</i> Chalfie 2011
<i>mec-18</i>	Firefly luciferase-like	ALM, AVM, PLM, PVM	TU228	<i>mec-18(u228)</i>	Uncurated	Unknown	Partial abnormality in mechanosensation	WormBase; CGC
<i>mec-19</i>	Novel membrane protein	ALM, AVM, FLP, PLM, PVD, PVM	RB1925	<i>mec-19(ok2504)</i>	Deletion	Putative null	Enhanced <i>mec-4(d)</i> degeneration	Barstead <i>et al.</i> Zapf 2012; Chen <i>et al.</i> Chalfie 2016
<i>pezo-1</i>	Piezo-type mechanosensitive ion channel	head neurons, HOA, HOB, male tail interneurons, PCS, CAN, ray neurons, spermatheca, vulval muscle	PS8111	<i>pezo-1(sy1199)</i>	Insertion, stop, and frameshift	Putative loss-of-function or null	Male mating defective (falling off), reduced fecundity	Brugman & Sternberg <i>unpublished</i>
<i>trp-4</i>	TRPN channel pore-forming subunit	ADE, CEP, DVA, DVC, PDE	PS4492	<i>trp-4(sy695)</i>	Deletion	Putative null	Abnormal body bends	Li <i>et al.</i> Xu 2011
			PS4493	<i>trp-4(sy696)</i>	Deletion	Putative null	Abnormal body bends	Li <i>et al.</i> Xu 2011
<i>ceh-17</i>	Q <sub>50</sub> paired-like homeodomain protein	ALA, DA8, DB5, DNC, head muscle, RMED, SIA, SIBV, VNC	IB16	<i>ceh-17(np1)</i>	Deletion	Null	ALA and SIA axonal outgrowth impaired	Pujol <i>et al.</i> Brunet 2000; Buskirk & Sternberg 2007

**Table 2.1. Expression pattern and allele effects of mechanosensation genes.**

Magenta, gentle touch receptor neurons; Orange, harsh touch receptor neurons.

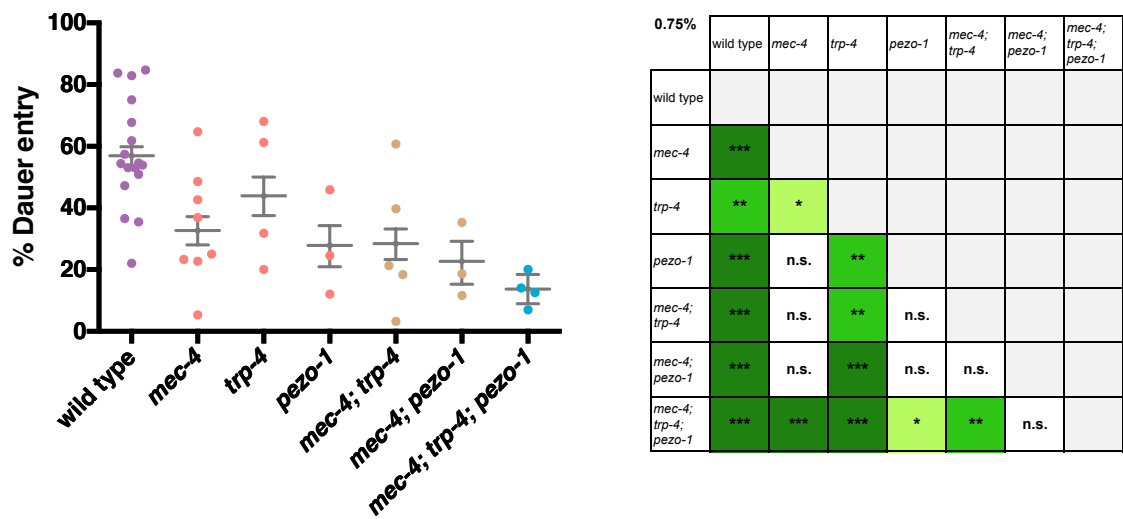


**Figure 2.5. *mec-4* and *trp-4* act additively with *pezo-1* to promote dauer entry.**

Dauer entry *mec-4*, *trp-4*, and *pezo-1* at 0.75% pheromone. Points, independent trials; center line, bootstrapped dauer entry percentage; whiskers, 95% confidence interval.

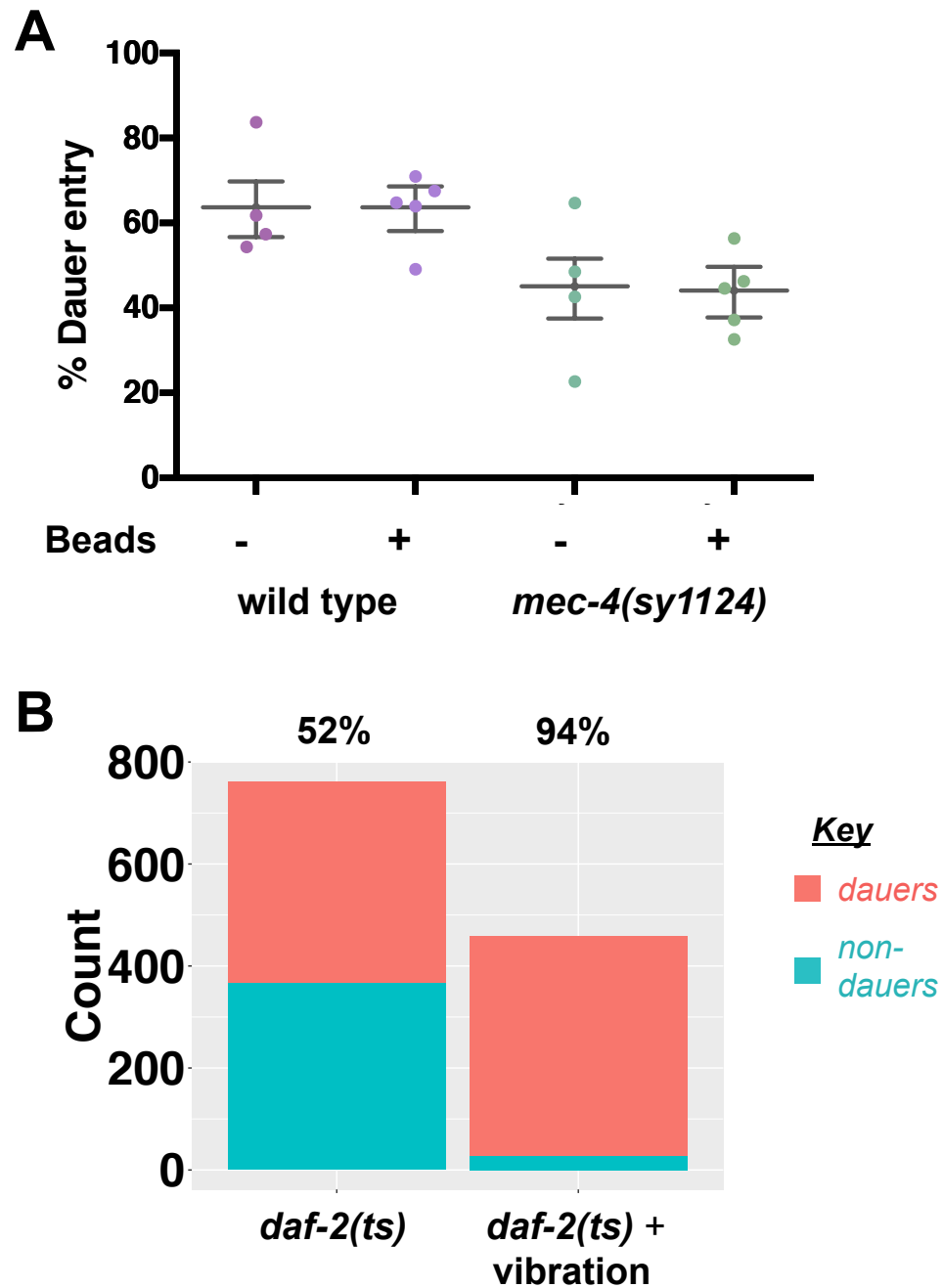


**Figure 2.6. Direct mechanical stimulation promotes dauer entry. (A)** Dauer entry percentages for wild type animals grown with glass bead perturbation. **(B)** Dauer entry for *daf-2(e1370)* with vibration perturbation. Counts were pooled from three independent trials.

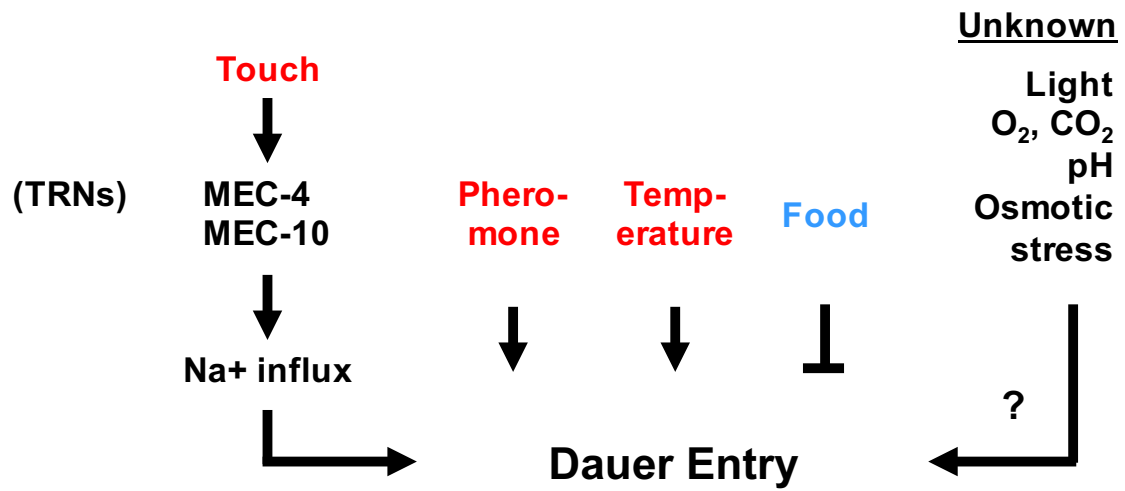


**Figure 2.7. Model of the complex dauer entry decision.** Red, dauer-promoting inputs; blue, dauer-inhibiting.

## 2.7 References

1. Ackermann M (2015) A functional perspective on phenotypic heterogeneity in microorganisms. *Nat Rev Microbiol* 13(8):497-508.
2. Fusco G & Minelli A (2010) Phenotypic plasticity in development and evolution: facts and concepts. Introduction. *Philosophical transactions of the Royal Society of London. Series B, Biological sciences* 365(1540):547-556.
3. Perkins TJ & Swain PS (2009) Strategies for cellular decision-making. *Mol Syst Biol* 5:326.
4. Tagkopoulos I, Liu YC, & Tavazoie S (2008) Predictive behavior within microbial genetic networks. *Science* 320(5881):1313-1317.
5. Simpson SJ, Sword GA, & Lo N (2011) Polyphenism in insects. *Current biology : CB* 21(18):R738-749.
6. Gruntman M, Gross D, Majekova M, & Tielborger K (2017) Decision-making in plants under competition. *Nat Commun* 8(1):2235.
7. de Wit M, *et al.* (2012) Plant neighbor detection through touching leaf tips precedes phytochrome signals. *Proceedings of the National Academy of Sciences of the United States of America* 109(36):14705-14710.
8. Ptak GE, *et al.* (2012) Embryonic diapause is conserved across mammals. *PloS one* 7(3):e33027.
9. Renfree MB & Fenelon JC (2017) The enigma of embryonic diapause. *Development* 144(18):3199-3210.

10. Cassada RC & Russell RL (1975) The dauerlarva, a post-embryonic developmental variant of the nematode *Caenorhabditis elegans*. *Developmental biology* 46(2):326-342.
11. Felix MA & Duveau F (2012) Population dynamics and habitat sharing of natural populations of *Caenorhabditis elegans* and *C. briggsae*. *BMC biology* 10:59.
12. Fielenbach N & Antebi A (2008) *C. elegans* dauer formation and the molecular basis of plasticity. *Genes & development* 22(16):2149-2165.
13. Kiontke K & Sudhaus W (2006) Ecology of *Caenorhabditis* species. *WormBook : the online review of C. elegans biology*:1-14.
14. Albert PS & Riddle DL (1983) Developmental alterations in sensory neuroanatomy of the *Caenorhabditis elegans* dauer larva. *The Journal of comparative neurology* 219(4):461-481.
15. Klass M & Hirsh D (1976) Non-ageing developmental variant of *Caenorhabditis elegans*. *Nature* 260(5551):523-525.
16. Vanfleteren JR & Braeckman BP (1999) Mechanisms of life span determination in *Caenorhabditis elegans*. *Neurobiol Aging* 20(5):487-502.
17. Golden JW & Riddle DL (1984) The *Caenorhabditis elegans* dauer larva: developmental effects of pheromone, food, and temperature. *Developmental biology* 102(2):368-378.
18. Avery L (2014) A model of the effect of uncertainty on the *C. elegans* L2/L2d decision. *PloS one* 9(7):e100580.

19. Golden JW & Riddle DL (1984) A pheromone-induced developmental switch in *Caenorhabditis elegans*: Temperature-sensitive mutants reveal a wild-type temperature-dependent process. *Proceedings of the National Academy of Sciences of the United States of America* 81(3):819-823.
20. Schaedel ON, Gerisch B, Antebi A, & Sternberg PW (2012) Hormonal signal amplification mediates environmental conditions during development and controls an irreversible commitment to adulthood. *PLoS biology* 10(4):e1001306.
21. Karp X (2016) Working with dauer larvae. *WormBook : the online review of C. elegans biology*:1-19.
22. Blango MG & Mulvey MA (2009) Bacterial landlines: contact-dependent signaling in bacterial populations. *Curr Opin Microbiol* 12(2):177-181.
23. Nijhout HF & Callier V (2015) Developmental mechanisms of body size and wing-body scaling in insects. *Annu Rev Entomol* 60:141-156.
24. Frezal L & Felix MA (2015) *C. elegans* outside the Petri dish. *eLife* 4.
25. Chalfie M & Sulston J (1981) Developmental genetics of the mechanosensory neurons of *Caenorhabditis elegans*. *Developmental biology* 82(2):358-370.
26. Lumpkin EA, Marshall KL, & Nelson AM (2010) The cell biology of touch. *J Cell Biol* 191(2):237-248.
27. Li W, Kang L, Piggott BJ, Feng Z, & Xu XZ (2011) The neural circuits and sensory channels mediating harsh touch sensation in *Caenorhabditis elegans*. *Nat Commun* 2:315.

28. McClanahan PD, Xu JH, & Fang-Yen C (2017) Comparing *Caenorhabditis elegans* gentle and harsh touch response behavior using a multiplexed hydraulic microfluidic device. *Integr Biol (Camb)* 9(10):800-809.
29. Maguire SM, Clark CM, Nunnari J, Pirri JK, & Alkema MJ (2011) The *C. elegans* touch response facilitates escape from predacious fungi. *Current biology : CB* 21(15):1326-1330.
30. Schafer WR (2015) Mechanosensory molecules and circuits in *C. elegans*. *Pflugers Arch* 467(1):39-48.
31. Way JC & Chalfie M (1989) The *mec-3* gene of *Caenorhabditis elegans* requires its own product for maintained expression and is expressed in three neuronal cell types. *Genes & development* 3(12A):1823-1833.
32. Lee JS, *et al.* (2017) FMRFamide-like peptides expand the behavioral repertoire of a densely connected nervous system. *Proceedings of the National Academy of Sciences of the United States of America* 114(50):E10726-E10735.
33. O'Hagan R, Chalfie M, & Goodman MB (2005) The MEC-4 DEG/ENaC channel of *Caenorhabditis elegans* touch receptor neurons transduces mechanical signals. *Nature neuroscience* 8(1):43-50.
34. Lai CC, Hong K, Kinnell M, Chalfie M, & Driscoll M (1996) Sequence and transmembrane topology of MEC-4, an ion channel subunit required for mechanotransduction in *Caenorhabditis elegans*. *J Cell Biol* 133(5):1071-1081.



35. Sternberg PW, Wang H, Park H, & Liu J (2018) An efficient genome editing strategy to generate putative null mutants in *Caenorhabditis elegans* using CRISPR/Cas9. *bioRxiv*.
36. Hong K, Mano I, & Driscoll M (2000) In vivo structure-function analyses of *Caenorhabditis elegans* MEC-4, a candidate mechanosensory ion channel subunit. *J Neurosci* 20(7):2575-2588.
37. Brown AL, Fernandez-Illescas SM, Liao Z, & Goodman MB (2007) Gain-of-function mutations in the MEC-4 DEG/ENaC sensory mechanotransduction channel alter gating and drug blockade. *J Gen Physiol* 129(2):161-173.
38. Calixto A, Jara JS, & Court FA (2012) Diapause formation and downregulation of insulin-like signaling via DAF-16/FOXO delays axonal degeneration and neuronal loss. *PLoS Genet* 8(12):e1003141.
39. Arnadottir J, O'Hagan R, Chen Y, Goodman MB, & Chalfie M (2011) The DEG/ENaC protein MEC-10 regulates the transduction channel complex in *Caenorhabditis elegans* touch receptor neurons. *J Neurosci* 31(35):12695-12704.
40. Chen Y, Bharill S, O'Hagan R, Isacoff EY, & Chalfie M (2016) MEC-10 and MEC-19 Reduce the Neurotoxicity of the MEC-4(d) DEG/ENaC Channel in *Caenorhabditis elegans*. *G3 (Bethesda)* 6(4):1121-1130.
41. Topalidou I, van Oudenaarden A, & Chalfie M (2011) *Caenorhabditis elegans* *aristaless/Arx* gene *alr-1* restricts variable gene expression.

*Proceedings of the National Academy of Sciences of the United States of America* 108(10):4063-4068.

42. Li W, Feng Z, Sternberg PW, & Xu XZ (2006) A C. elegans stretch receptor neuron revealed by a mechanosensitive TRP channel homologue. *Nature* 440(7084):684-687.
43. Pujol N, Torregrossa P, Ewbank JJ, & Brunet JF (2000) The homeodomain protein CePHOX2/CEH-17 controls antero-posterior axonal growth in C. elegans. *Development* 127(15):3361-3371.
44. Van Buskirk C & Sternberg PW (2010) Paired and LIM class homeodomain proteins coordinate differentiation of the C. elegans ALA neuron. *Development* 137(12):2065-2074.
45. Schroeder NE & Flatt KM (2014) In vivo imaging of Dauer-specific neuronal remodeling in C. elegans. *J Vis Exp* (91):e51834.
46. Peckol EL, Troemel ER, & Bargmann CI (2001) Sensory experience and sensory activity regulate chemosensory receptor gene expression in Caenorhabditis elegans. *Proceedings of the National Academy of Sciences of the United States of America* 98(20):11032-11038.
47. Kim K, *et al.* (2009) Two chemoreceptors mediate developmental effects of dauer pheromone in C. elegans. *Science* 326(5955):994-998.
48. Neal SJ, *et al.* (2016) A Forward Genetic Screen for Molecules Involved in Pheromone-Induced Dauer Formation in Caenorhabditis elegans. *G3 (Bethesda)* 6(5):1475-1487.

49. Rose JK, Sangha S, Rai S, Norman KR, & Rankin CH (2005) Decreased sensory stimulation reduces behavioral responding, retards development, and alters neuronal connectivity in *Caenorhabditis elegans*. *J Neurosci* 25(31):7159-7168.
50. Geng J, Zhao Q, Zhang T, & Xiao B (2017) In Touch With the Mechanosensitive Piezo Channels: Structure, Ion Permeation, and Mechanotransduction. *Curr Top Membr* 79:159-195.
51. Ranade SS, *et al.* (2014) Piezo2 is the major transducer of mechanical forces for touch sensation in mice. *Nature* 516(7529):121-125.
52. Gems D, *et al.* (1998) Two pleiotropic classes of daf-2 mutation affect larval arrest, adult behavior, reproduction and longevity in *Caenorhabditis elegans*. *Genetics* 150(1):129-155.
53. Gerisch B, Weitzel C, Kober-Eisermann C, Rottiers V, & Antebi A (2001) A hormonal signaling pathway influencing *C. elegans* metabolism, reproductive development, and life span. *Developmental cell* 1(6):841-851.
54. Gottlieb S & Ruvkun G (1994) daf-2, daf-16 and daf-23: genetically interacting genes controlling Dauer formation in *Caenorhabditis elegans*. *Genetics* 137(1):107-120.
55. Jia K, Albert PS, & Riddle DL (2002) DAF-9, a cytochrome P450 regulating *C. elegans* larval development and adult longevity. *Development* 129(1):221-231.

56. Riddle DL, Swanson MM, & Albert PS (1981) Interacting genes in nematode dauer larva formation. *Nature* 290(5808):668-671.
57. Thomas JH, Birnby DA, & Vowels JJ (1993) Evidence for parallel processing of sensory information controlling dauer formation in *Caenorhabditis elegans*. *Genetics* 134(4):1105-1117.
58. Vowels JJ & Thomas JH (1992) Genetic analysis of chemosensory control of dauer formation in *Caenorhabditis elegans*. *Genetics* 130(1):105-123.
59. Torr P, Heritage S, & Wilson MJ (2004) Vibrations as a novel signal for host location by parasitic nematodes. *International journal for parasitology* 34(9):997-999.
60. Bose N, *et al.* (2014) Natural variation in dauer pheromone production and sensing supports intraspecific competition in nematodes. *Current biology : CB* 24(13):1536-1541.
61. Diaz SA, *et al.* (2014) Diverse and potentially manipulative signalling with ascarosides in the model nematode *C. elegans*. *BMC Evol Biol* 14(1):46.
62. Schulenburg H & Felix MA (2017) The Natural Biotic Environment of *Caenorhabditis elegans*. *Genetics* 206(1):55-86.
63. McGlone F, Wessberg J, & Olausson H (2014) Discriminative and affective touch: sensing and feeling. *Neuron* 82(4):737-755.
64. Tan PL & Katsanis N (2009) Thermosensory and mechanosensory perception in human genetic disease. *Hum Mol Genet* 18(R2):R146-155.
65. Huang LS & Sternberg PW (2006) Genetic dissection of developmental pathways. *WormBook : the online review of C. elegans biology*:1-19.

66. Chen BL, Hall DH, & Chklovskii DB (2006) Wiring optimization can relate neuronal structure and function. *Proceedings of the National Academy of Sciences of the United States of America* 103(12):4723-4728.
67. White JG, Southgate E, Thomson JN, & Brenner S (1986) The structure of the nervous system of the nematode *Caenorhabditis elegans*. *Philosophical transactions of the Royal Society of London. Series B, Biological sciences* 314(1165):1-340.
68. Russell J, Vidal-Gadea AG, Makay A, Lanam C, & Pierce-Shimomura JT (2014) Humidity sensation requires both mechanosensory and thermosensory pathways in *Caenorhabditis elegans*. *Proceedings of the National Academy of Sciences of the United States of America* 111(22):8269-8274.
69. dos Santos CN, *et al.* (2011) Seasonal dynamics of cyathostomin (Nematoda - Cyathostominae) infective larvae in *Brachiaria humidicola* grass in tropical southeast Brazil. *Veterinary parasitology* 180(3-4):274-278.
70. Viney ME (2009) How did parasitic worms evolve? *BioEssays : news and reviews in molecular, cellular and developmental biology* 31(5):496-499.
71. Ludewig AH & Schroeder FC (2013) Ascaroside signaling in *C. elegans*. *WormBook : the online review of C. elegans biology*:1-22.
72. Ardiel EL & Rankin CH (2010) The importance of touch in development. *Paediatr Child Health* 15(3):153-156.

73. Vidal-Diez de Ulzurrun G & Hsueh YP (2018) Predator-prey interactions of nematode-trapping fungi and nematodes: both sides of the coin. *Appl Microbiol Biotechnol* 102(9):3939-3949.
74. Brenner S (1974) The genetics of *Caenorhabditis elegans*. *Genetics* 77(1):71-94.

*Chapter 3***FMRFAMIDE-LIKE PEPTIDES EXPAND THE BEHAVIORAL  
REPERTOIRE OF A DENSELY CONNECTED NERVOUS SYSTEM**

**Lee JS\***, Shih PY\*, Schaedel ON, Quintero-Cadena P, Rogers AK and Sternberg PW  
(2017) FMRFamide-like peptides expand the behavioral repertoire of a densely  
connected nervous system. *Proceedings of the National Academy of Sciences USA*  
114(50): E10726-E10735. doi: 10.1073/pnas.1710374114  
\*Equal contribution

### 3.1 Abstract

Animals, including humans, can adapt to environmental stress through phenotypic plasticity. The free-living nematode *Caenorhabditis elegans* can adapt to harsh environments by undergoing a whole-animal change, involving exiting reproductive development and entering the stress-resistant dauer larval stage. The dauer is a dispersal stage with dauer-specific behaviors for finding and stowing onto carrier animals, but how dauers acquire these behaviors, despite having a physically limited nervous system of 302 neurons, is poorly understood. We compared dauer and reproductive development using whole-animal RNA-seq at fine time points, and at sufficient depth to measure transcriptional changes within single cells. We detected 8,042 differentially expressed genes during dauer and reproductive development, and observed striking up-regulation of neuropeptide genes during dauer entry. We knocked down neuropeptide processing using *sbt-1* mutants, and demonstrate that neuropeptide signaling promotes the decision to enter dauer over reproductive development. We also demonstrate that during dauer, neuropeptides modulate the dauer-specific nictation behavior (carrier animal-hitchhiking), and is necessary for switching from repulsion to CO<sub>2</sub> (a carrier animal cue) in non-dauers to CO<sub>2</sub> attraction in dauers. We tested individual neuropeptides using CRISPR knockouts and existing strains, and demonstrate that the combined effects of *flp-10* and *flp-17* mimic the effects of *sbt-1* on nictation and CO<sub>2</sub> attraction. Through meta-analysis, we discovered similar up-regulation of neuropeptides in the dauer-like infective juveniles of diverse parasitic nematodes, suggesting the anti-parasitic target potential of SBT-1. Our findings reveal that



under stress, increased neuropeptide signaling in *C. elegans* enhances their decision-making accuracy, and expands their behavioral repertoire.

### 3.2 Introduction

Stress during development can have long-lasting effects on animal physiology and behavior. For instance, trauma during early human childhood can lead to difficulties with coping against depression and anxiety in adults (1-4). Phenotypic plasticity allows animals to adapt to stresses from the environment (5). Examples of phenotypic plasticity include the production of new antibodies by the mammalian immune system (6), temperature-dependent sex determination in reptiles (7, 8), and crowding-induced cannibalism in the spadefoot toad (5, 9).

The free-living bacterivore *Caenorhabditis elegans* can adapt to stressful conditions by exiting reproductive development and entering the stress-resistant dauer larval stage (10-12). In reproductive development, *C. elegans* develops through four larval stages (L1, L2, L3, and L4) to become a reproductive adult. Declining food, temperature, and crowding conditions, however, promote L1 entry into pre-dauer L2d. If conditions improve, L2d commit to reproductive development through amplification of dafachronic acid growth hormone across the animal body (13). Unimproved conditions cause L2d to commit to dauer development, through a process that is not well understood. Following this event, L2d larvae molt into dauer larvae and halt their feeding.

Dauers are less metabolically active than non-dauers, and can survive long periods of starvation by utilizing stored lipids, in lieu of aerobic respiration (14, 15). Morphologically, they have a highly impermeable cuticle that allows them to resist environmental assaults (10). In addition, they have a rewired nervous system (16, 17), and specialized dispersal behaviors for finding and stowing onto

carrier animals (18, 19). Dauer lifespans are ten times longer than those of non-dauers (20), and dauers can resume reproductive development with an unaffected adult lifespan once they recover under favorable conditions (21). Thus, dauers have much to reveal about the biological control of longevity, stress-resistance, and neural state.

The genetic and anatomical tractability of *C. elegans* make it an advantageous model for studying phenotypic plasticity in a whole organism. Previous systems-level studies have analyzed the *C. elegans* transcriptome during molt into dauer, during dauer, and during recovery from dauer (22-24). However, the transcriptome of L2d during the dauer entry decision has not been characterized, likely because L2d lack strong distinguishing traits that can be used to isolate them (25). Furthermore, dauer and reproductive development have not been compared under parallel growth conditions, which has limited the discovery of genes that are differentially expressed between the two developments.

Therefore, we have used techniques from our previous analysis of *daf-9(dh6)* loss-of-function animals (13) to add crucial detail to dauer development. Using dafachronic acid, we controlled the developmental decisions of *daf-9(dh6)* L2d, under parallel conditions. We coupled this with our previous timing of *daf-9(dh6)* development to collect pure populations of uncommitted L2d, dauer-committed L2d, L3-committing L2d, dauers, and L4. We performed whole-animal RNA-seq on these populations, revealing 8,042 differentially expressed genes during dauer and reproductive development. Through enrichment analysis, we observed

striking up-regulation of neuropeptide genes during dauer-commitment. Using the *sbt-1(ok901)* null mutant to knock down neuropeptide processing (26), we demonstrate that peptidergic signaling promotes the dauer entry decision, promotes coordination during nictation (a hitchhiking behavior), and is necessary for switching from CO<sub>2</sub> repulsion in non-dauers to CO<sub>2</sub> attraction in dauers.

Testing individual neuropeptides using CRISPR knockouts and existing strains, we demonstrate uncoordinated nictation and CO<sub>2</sub> avoidance phenotypes in *flp-10(n4543) flp-17(n4894)* double mutants, similar to *sbt-1(ok901)*. Through a meta-analysis, we discovered similar up-regulation of neuropeptides in the dauer-like infective juveniles of diverse parasitic nematodes, suggesting the anti-parasitic target potential of SBT-1. Our results reveal that the *C. elegans* nervous system responds to environmental stress by increasing neuropeptide signaling to enhance decision-making, and to enable specialized dispersal behaviors. The expansion of the neuropeptide genes, especially the FMRFamide-like neuropeptide (*flp*) genes, in nematodes has been a puzzle (27, 28), and our results provide one reasonable explanation.

### 3.3 Results

#### RNA-seq was used to investigate dauer and reproductive development

Our previous analysis of the *daf-9(dh6)* null mutant in (13) allowed us to sequence cDNA from large quantities of dauer- and reproductive-developing animals. Briefly, *C. elegans* DAF-9 is a cytochrome P450 enzyme that synthesizes the growth hormone dafachronic acid (DA) (29, 30). Commitment to reproductive development only occurs when the level of DA in the animal body is high enough to trigger feedback amplification of DA across the entire organism, thus locking the developmental decision (13). *daf-9(dh6)* null mutants cannot produce their own DA, and therefore constitutively form dauers unless synthetic DA is added to induce reproductive development (13, 30, 31). We previously characterized the timing of development in *daf-9(dh6)* animals: dauer-commitment occurs at 33 hours post hatch (hph), followed by molt into dauer at 48 hph (13). However, if DA is added at 24 hph, *daf-9(dh6)* L2d commit to reproductive development by 27 hph, and molt into L4 at 34 hph.

Using these conditions, we grew synchronized populations of dauer-developing *daf-9(dh6)* by withholding synthetic DA, and we collected L2d animals (at 24 hph and 26 hph), dauer-committed L2d (at 34 hph), and fully developed dauers (at 60 hph) for RNA sequencing (**Figure 3.1A**). In parallel, we added synthetic DA to a sub-culture, forcing it into reproductive development, and from which we collected L3-committing larvae (at 26 hph) and L4 (at 34 hph) for sequencing. We sequenced each sample using two biological replicates, at an average depth of 100 million reads (the sum of the replicates) (**Appendix Table 3.1**). Since *C.*

*C. elegans* animals contain 959 cells (32), and each cell likely expresses 100,000 mRNA transcripts (33, 34), we estimated that we had sequenced one read for every transcript in the whole animal at each time point. Therefore, we expected to detect signals from transcripts as long as they were not expressed in few cells at low abundance. For each sample, we detected between 20,519 to 22,672 expressed genes, of the total 20,362 coding and 24,719 non-coding genes of the *C. elegans* genome (35, 36) (**Figure 3.2A** and **Appendix Table 3.2**).

### **PCA analysis revealed the extent of variation between developmental stages**

We analyzed the variation between our transcriptomes using principal component analysis (PCA) (**Figure 3.2B-C**). Replicate samples had similar PC scores to each other, indicating that our biological replicates were well correlated in their gene expression. Our analysis also revealed that the largest sources of variation between our transcriptomes were the differences between dauer-commitment/differentiation versus the remaining time points (principal component 1, 65% of overall variation), and the difference between 24 hph L2d and 26 hph L2d (principal component 2, 17% of overall variation). Along the first two principal components, 24 hph L2d and L4 demonstrated close similarity, as did 26 hph L2d and L3-committing larvae, as well as dauer and dauer-committed larvae.

### **8,042 genes are differentially expressed during dauer and reproductive development**

Using the differential gene expression analysis program DESeq (37, 38), we performed pairwise comparisons between 24 hph L2d and 26 hph L2d to identify gene expression changes during L2d sensory integration, between L2d and dauer-committed larvae for changes during dauer-commitment, and between L2d and dauer larvae for changes during differentiation and maintenance of dauer (**Figure 3.1B**). With our reproductive development samples, we performed pairwise comparisons between L2d and L3-committing larvae for changes during commitment to reproductive development, and between L2d and L4 for changes during reproductive growth. In addition, our design allowed us to perform pairwise comparisons between age-matched dauer- and reproductive-developing animals at 26 hph (L2d versus L3-committing larvae) and 34 hph (dauer-committed larvae versus L4) to identify gene expression changes specific to one developmental track (**Figure 3.1C**). We avoided sequencing an age-matched reproductive sample for 60 hph dauer since reproductive animals at 60 hph are gravid and inappropriate for studying a stage-specific transcriptome. In total, we performed twelve pairwise comparisons between our dauer and reproductive time points. In each comparison, we detected between 484 to 2,276 up-regulated genes, and 280 to 2,824 down-regulated genes (**Figure 3.1D** and **Appendix Table 3.3**). Overall, we observed 8,042 differentially expressed genes from the twelve comparisons. These genes corresponded to 7,866 coding genes and 77 ncRNA genes, indicating that 39% of the *C. elegans* protein-coding genome is differentially expressed during dauer and reproductive development.

## Differential expression was detected at high accuracy and single-cell resolution

To analyze the resolution of our RNA-seq dataset, we used WormBase anatomical-level gene expression data to search our 8,042 differentially expressed genes for genes previously reported to have tissue-specific expression. We detected transcriptional changes in 47 epithelial system genes (of 74 total epithelium-specific genes in WormBase), 56 muscular system genes (of 89 total), 181 alimentary system genes (of 310 total), 108 reproductive system genes (of 233 total), 139 nervous system genes (of 599 total), 9 amphid sensillum genes (of 62 total), and 1 XXX cell gene (of 4 total) (**Figure 3.3A**). This analysis suggests that we could detect differential expression from within tissues and single cells. Indeed, we constructed fluorescent transcriptional reporters for *col-40* and *srt-41*, which were up-regulated in our data during dauer development, and we observed previously unreported, specific expression for the two genes in the hypodermis and the AWC neuron, respectively (**Figure 3.3B-O**).

We examined the accuracy of our dataset by comparing to SAGE data published by Jones, *et al.* (2001), and microarray data published by Wang & Kim (2003), which have identified genes that are enriched in wild type dauers versus mixed-populations or post-dauer adults, respectively (24, 39). When tested for differential expression in our data, 141 (45%) of the dauer-enriched genes from (39) were significantly up-regulated at dauer-commitment and dauer, relative to L2d and L4 (**Figure 3.3P**). Similarly, 312 (69%) of the dauer-enriched genes from (24) were significantly up-regulated at dauer-commitment and dauer. Thus, our



calculations for differential expression (negative binomial testing at a Benjamini-Hochberg controlled false discovery rate  $< 0.01$ ) may have been more stringent than the calculations in (24, 39). Other differences may be explained by gene expression changes that are only observable between dauer and post-dauer, and by differences in the *daf-9(dh6)* strain we used versus the wild type strain. Nonetheless, we conclude from this analysis that *daf-9(dh6)* and wild type transcriptomes demonstrate high comparability, and that our differential expression testing is conservative.

### **Clustering revealed six common expression profiles during dauer and reproductive development**

Soft clustering is a sensitive method for identifying common expression profiles within a dataset (40, 41). We performed soft clustering on our 8,042 differentially expressed genes to group the genes by similarities in their expression profiles. This revealed six clusters (clusters 1-6), indicating that differential gene expression through dauer and reproductive development can be described by six common expression profiles (**Figure 3.4**): the expression levels of 1,102 genes gradually decreased into dauer (cluster 1), 1,921 genes gradually increased into dauer (cluster 2), 1,025 genes increased transiently at 26 hph (cluster 3), 1,497 genes increased transiently during dauer-commitment (cluster 4), 1,332 genes decreased after dauer-commitment (cluster 5), and 1,165 genes increased in L4 (cluster 6) (**Appendix Table 3.4**).

The genes from clusters 2 and 4 encompass 3,418 genes likely involved in commitment, differentiation, and maintenance of dauer. These highly dauer-specific genes represent a 7.6-fold expansion over the 449 ‘dauer-enriched’ genes described previously (24). In addition, the genes from clusters 1, 3, 5, and 6 encompass 4,624 genes whose expressions are largely excluded during dauer-commitment and dauer.

We examined the six clusters for enriched biochemical pathways and gene ontology (GO) terms using KEGG biochemical pathway data (42-44), and the PANTHER Classification System (45). We observed that cluster 1 (genes with decreasing expression into dauer) was enriched for the “peroxisome” KEGG pathway, suggesting that peroxisomal activity is reduced in dauers (**Figure 3.4**). This is consistent with the reduction of ascarocide pheromone production in dauers (46), since a key step of ascarocide biosynthesis occurs via peroxisomal  $\beta$ -oxidation (47). In fact, cluster 1 contains genes for the  $\beta$ -oxidation enzymes ACOX-1, MAOC-1, and DHS-28, which perform 3 of the 4 steps of ascarocide side chain biosynthesis (47).

Cluster 2 (genes with increasing expression into dauer) was enriched for the “FoxO signaling pathway” and “longevity regulating pathway – worm” KEGG pathways, as may be expected from the extended longevity of dauers (20), and the role of FOXO signaling in modulating longevity and stress resistance (11) (**Figure 3.4** and **Appendix Table 3.4**). We observed 13 members (18%) of the “longevity regulating pathway – worm” in cluster 2, including members in the branches of the pathway that respond to environmental cues, dietary restriction,

oxidative stress, germline state, and the mitochondrial unfolded protein response to affect lifespan (42-44). The remaining input into the longevity regulating pathway, the hypoxia branch, did not have any members in cluster 2. This suggests the intriguing possibility that the extreme longevity of dauer arises from the simultaneously enhanced activity of five of the six branches of the longevity pathway.

We also observed enrichment of the “neuropeptide signaling pathway” GO term in cluster 2 (**Figure 3.4**), suggesting that neuropeptides modulate the dauer-commitment decision and/or neural functions downstream of the decision. Indeed, some neuropeptides have been shown to affect dauer biology: insulin signaling via DAF-28, INS-4, and INS-6 promotes reproductive growth over dauer development, and INS-1 and INS-18 antagonize this pathway (reviewed in (48)). In addition, FMRFamide signaling via FLP-18 acts in parallel with the TGF- $\beta$  signaling pathway to inhibit dauer development (49). Furthermore, *ins-3*, *6*, *18*, *20*, *27-28*, *31*, *34*, and *daf-28* have been shown to affect the fraction of time that is spent nictating in dauer (50).

In cluster 3 (genes with increased expression at 26 hph), we observed enrichment for biomolecule synthesis and turnover pathways, including the “proteasome,” “lysosome,” “fatty acid degradation,” and “fatty acid elongation” KEGG pathways (**Figure 3.4**, **Figure 3.5**, and **Appendix Table 3.4**). This observation may reflect the developmental uncertainty in L2d, and perhaps represents a bet-hedging strategy of cycling biomolecules in preparation for either commitment decision. Consistent with the prediction of developmental uncertainty,

genes with the “molting cycle” GO term were enriched (2.9-fold enrichment,  $p = 2.54 \times 10^{-14}$ ) among the genes up-regulated in 26 hph L2d versus 24 hph L2d (**Appendix Table 3.3**), despite molt into dauer, one of the two possible molts from L2d, occurring 22 hours later at 48 hph.

In cluster 4 (genes with increased expression at dauer-commitment), we observed enrichment of the “neuroactive ligand-receptor interaction” and “calcium signaling pathway” KEGG pathways (**Figure 3.4**, **Figure 3.5**, and **Appendix Table 3.4**). Together with cluster 2, this indicates that several genes with neuronal functions have increased expression during dauer-commitment and dauer.

Genes that are down-regulated during dauer-commitment are likely repressed to exclude non-dauer physiologies, and indeed, our enrichment data for cluster 5 (genes with decreased expression after dauer-commitment) are consistent with the reduction of TCA cycle activity in favor of long-term lipid metabolism in dauer (51), as we observed enrichment of the “fatty acid degradation” and “citrate cycle (TCA cycle)” KEGG pathways (**Figure 3.5** and **Appendix Table 3.4**).

Cluster 6 (genes with increased expression at L4) was enriched for terms related to translation and respiration, including the “mitochondrial electron transport, ubiquinol to cytochrome c” GO term and the “ribosome” KEGG pathway (**Figure 3.4**), which likely reflects growth during reproductive development and gametogenesis in the L4 (52-54).

### **Differential expression of the neuronal genome during dauer development**

Our KEGG and GO enrichment analyses indicated the strong involvement of neuronal effector genes during dauer-commitment and dauer. To investigate this further, we examined the expression of the neuronal genome of *C. elegans* during dauer and reproductive development. The neuronal genome of *C. elegans* encodes 3,114 genes from 30 gene classes, including the calcium channels, neurotransmitters, G protein-coupled receptors (GPCRs), and CO<sub>2</sub> receptors (55). We detected the differential expression of 606 neuronal genes during dauer and reproductive development, corresponding to 19% of the total neuronal genome, with members from all of the 30 gene classes (**Figure 3.6**).

Five gene classes were enriched in one of the soft clusters 1 to 6, indicating that for these classes, a high proportion of their members followed a certain expression profile during dauer and reproductive development (**Appendix Table 3.5**). The extracellular immunoglobulin and leucine rich repeat domain gene class was over-represented in cluster 1 (decreasing expression into dauer), with 2.8-fold enrichment and  $p = 6.42 \times 10^{-3}$ . The neuropeptide gene class was over-represented in cluster 2 (increasing expression into dauer), with 3.1-FE and  $p = 6.32 \times 10^{-21}$ . Finally, the GPCR (2.9-FE,  $p = 2.41 \times 10^{-8}$ ), CO<sub>2</sub> and O<sub>2</sub> receptor (4.9-FE,  $p = 7.86 \times 10^{-5}$ ), and potassium channel gene classes (3.0-FE,  $p = 2.84 \times 10^{-3}$ ) were over-represented in cluster 4 (increased expression at dauer-commitment).

GPCR gene expression increases sharply during dauer-commitment, before neuropeptide gene expression reaches its peak during dauer (**Figure 3.6**). In addition, the 34 GPCRs in cluster 4 include 1 biochemically de-orphanized neuropeptide GPCR (*npr-11*) and 9 putative neuropeptide GPCRs (*ckr-1*,

*frpr-7*, -19, *npr-17*, -31, C01F1.4, F13H6.5, Y37E11AL.1, and Y70D2A.1) (27, 55) (**Appendix Table 3.5**). This suggests that neuropeptide receptors are up-regulated during dauer-commitment in anticipation of increasing neuropeptide gene expression during dauer-commitment and dauer.

Notably, the neuropeptide gene class was the only class that was enriched for increasing expression into dauer. We observed extensive up-regulation of the neuropeptides during dauer development: in dauer-commitment (34 hph) versus L2d (24 hph), 60 of the 118 total neuropeptide genes were up-regulated while 9 were down-regulated (**Figure 3.9A**). Similarly, at dauer-commitment (34 hph) versus L4 (34 hph), 43 neuropeptide genes were up-regulated while 10 were down-regulated (**Figure 3.10A**), and in dauer (60 hph) versus L2d (24 hph), 64 neuropeptide genes were up-regulated while 9 were down-regulated (**Figure 3.10B**). The up-regulation of 64 neuropeptide genes during dauer versus L2d is remarkable, as it corresponds to the majority of all neuropeptide genes in the *C. elegans* genome. Furthermore, the 64 genes encode for 215 putative or biochemically isolated peptides (48). By comparison, the human genome contains a total of 97 neuropeptide genes that encode for 270 peptides (56).

### **Peptidergic signaling downstream of SBT-1 promotes dauer entry and nictation coordination, and is necessary for CO<sub>2</sub> chemoattraction in dauer**

Neuropeptides become functional transmitters and neuromodulators only after they are cleaved from longer proneuropeptide chains (48) (**Figure 3.7A**). SBT-1/7B2 is a chaperone for the proprotein convertase EGL-3/PC2, which

cleaves proneuropeptides (57), and as a result, *sbt-1(ok901)* null mutants have reduced levels of mature neuropeptides compared to wild type (26) (**Figure 3.7B**). Previously, *sbt-1(ok901)* mutants were reported to possess aldicarb resistance and extended lifespans (58, 59), but to our knowledge, no functions for *sbt-1* in dauer biology have been reported.

Because we observed up-regulation of neuropeptides starting from dauer commitment, we tested the ability of *sbt-1(ok901)* mutants to enter dauer, using crude pheromone to induce dauer entry. Under the same dauer-inducing conditions, wild type animals entered dauer 49% of the time, while *sbt-1(ok901)* mutants entered dauer 16.5% of the time (**Figure 3.8A**). We also observed that expressing *sbt-1* genomic DNA in *sbt-1(ok901)* mutants (under the control of the endogenous promoter) rescued the dauer entry phenotype in two independent lines: rescue line 1 entered dauer 46% of the time, and rescue line 2 entered dauer 37% of the time (**Figure 3.8A**). These results suggest that the net effect of peptidergic signaling downstream of SBT-1 promotes dauer entry over reproductive development.

We examined if neuropeptides play a role during dauer, when the majority of the *C. elegans* neuropeptide genes were expressed the highest in our dataset. *C. elegans* dauers have been found to associate with invertebrate carriers, likely for transportation to new niches (60). Nictation, where dauers stand on their tail and wave their body, and CO<sub>2</sub> chemoattraction are two dauer-specific behaviors that likely enable dauers to migrate toward and attach onto carriers (18, 61). We tested *sbt-1(ok901)* nictation on micro-dirt chips, which provide substrates for dauers to

nictate on, and observed that the average nictation duration doubled in *sbt-1(ok901)* mutants ( $\mu$  = 28.90 seconds, max = 139.63 seconds) as compared to wild type ( $\mu$  = 14.44 s, max = 32.32 s). Moreover, the phenotype was rescued by *sbt-1* genomic DNA expression under the endogenous promoter (line 1:  $\mu$  = 14.35 s and max = 78.00 s, line 2:  $\mu$  = 14.50 s and max = 52.27 s) (**Figure 3.8B**). We observed a difference in the degree of three-dimensional movement during nictation in wild type and *sbt-1(ok901)* mutant animals that may explain the increased duration of nictation in *sbt-1(ok901)* mutants: while wild type animals displayed a wide range of motion and fell back to the chip easily, *sbt-1(ok901)* animals displayed a limited range of motion and slow, uncoordinated waving that likely increased stability during nictation (**Appendix Video 3.1** and **3.2**). We did not observe significant differences in other components of the nictation behavior, such as initiation frequency and the proportion of time spent nictating (19) (**Figure 3.7**).

CO<sub>2</sub> has been shown to be attractive to dauers and repulsive to non-dauers (18, 62). Using chemotaxis assays, we observed attraction to CO<sub>2</sub> in wild type dauers (chemotaxis index = 0.59) and repulsion to CO<sub>2</sub> in *sbt-1(ok901)* dauers (chemotaxis index = -0.53) (**Figure 3.8C**). We further performed CO<sub>2</sub> acute avoidance assays by delivering CO<sub>2</sub> directly to the nose of forward-moving dauers and scoring reversal. While wild type dauers did not avoid CO<sub>2</sub> (avoidance index = -0.11), we observed rapid reversal in *sbt-1(ok901)* mutants in response to CO<sub>2</sub> (avoidance index = 0.64). In addition, the CO<sub>2</sub> repulsion phenotype of *sbt-1(ok901)* was rescued by *sbt-1* genomic DNA (line 1: avoidance index = 0.04, line 2: avoidance index = 0.06) (**Figure 3.8D** and **Appendix Video 3.3-3.6**). Together,



our results indicate that the neuropeptides downstream of SBT-1 modulate proper nictation coordination, and are necessary for the correct CO<sub>2</sub> preference switch from aversion in non-dauers to attraction in dauers. To our knowledge, we have reported for the first time the genetic control of the CO<sub>2</sub> preference switch in dauer.

### **The 31-gene *flp* family is coordinately up-regulated during dauer development**

The *C. elegans* genome encodes for three families of neuropeptides: the FMRFamide-like peptides (31 *flp* genes), the insulin related peptides (40 *ins* genes) and the neuropeptide-like proteins (47 *nlp* genes) (48). In dauer-commitment versus L2d, we observed the up-regulation of almost all of the *flp* genes, with significant increases in expression for *flp-1-2*, *4-9*, *11-22*, *24-28*, and *32-34* (28 of 31 total) (**Figure 3.9A** and **Appendix Table 3.3**). In contrast, a smaller proportion of *ins* and *nlp* genes were up-regulated during dauer-commitment versus L2d: *ins-1*, *17-18*, *24*, *28*, *30*, and *daf-28* (7 of 40 total); and *nlp-1-3*, *6*, *8-15*, *17-18*, *21*, *35*, *37-38*, *40-42*, *47*, *ntc-1*, *pdf-1*, and *snet-1* (25 of 47). Similar results were observed during dauer-commitment versus L4 (**Figure 3.10A**), and dauer versus L2d (**Figure 3.10B**). Therefore, the *flp* genes, more than the *ins* or *nlp* genes, are coordinately up-regulated during dauer development.

We quantified this coordination in *flp* gene expression by pairing every combination of the 31 *flp* genes and scoring the correlation between the expression of each pair of genes across our RNA-seq dataset. The average correlation score between the *flp* genes was 0.88, with possible scores ranging

from -1 (perfectly anti-correlated) to 1 (perfectly correlated) (**Figure 3.9B**). By comparison, the average correlation scores for random sets of 31 genes (mimicking the size of the *flp* family) were distributed around a bootstrapped mean of 0.02. In addition, the *ins* and *nlp* genes had an average score of 0.21 and 0.28, respectively. Furthermore, we obtained similar results when we expanded our correlation analysis to include expression data from 246 publically available RNA-seq datasets describing a broad range of *C. elegans* life stages and experimental conditions (23) (**Figure 3.10C-D**). Using dotplot analysis (63), we examined whether the 31 *flp* genes share regions of sequence similarity (**Figure 3.10E**). We observed that there are no regions of shared sequence among the *flp* genes that extends beyond 20 nucleotides, with only two regions sharing a 20-nucleotide match (between *flp-2* and *flp-22*, and between *flp-27* and *flp-28*). Therefore, it is unlikely that the high correlation between *flp* gene expressions was caused by any cross-mapping of RNA-seq reads among the 31 *flp* genes, since our sequenced reads were 50 to 100 base pairs in length. Together, these results strongly suggest that the *flp* genes are co-regulated and are coordinately up-regulated during dauer development.

### **FLPs modulate the dauer entry decision, nictation, and CO<sub>2</sub> chemoattraction**

We investigated whether FLP neuropeptides modulate the dauer entry decision by assaying 4 CRISPR-generated knockout alleles and 19 available *flp* alleles, corresponding to mutations in 18 *flp* genes. We induced dauer entry using crude pheromone and compared the dauer entry percentage of each genotype to the

wild type control. We recapitulated the previously reported increased dauer entry phenotype of *flp-18(db99)* as a positive control (49). We observed increased dauer entry in three additional *flp* mutants: *flp-2(ok3351)*, *flp-6(ok3056)*, and *flp-34(sy810)*. Furthermore, we detected decreased dauer entry in 8 mutants: *flp-1(yn4)*, *flp-8(pk360)*, *flp-10(ok2624)*, *flp-11(tm2706)*, *flp-17(n4894)*, *flp-21(pk1601)*, *flp-25(gk1016)*, and *flp-26(gk3015)* (**Figure 3.9C**). These results suggest that FLPs can act redundantly and with opposed effects on dauer entry.

*flp-10* and *flp-17* are expressed in the CO<sub>2</sub> sensing BAG neuron (64, 65), and act synergistically with the neurotransmitter acetylcholine, which promotes the nictation behavior (19), to inhibit egg-laying (66). Because of these connections to nictation and CO<sub>2</sub>-sensing, we examined nictation and CO<sub>2</sub> chemoattraction in *flp-10(n4543) flp-17(n4894)* double mutant animals. Using the micro-dirt chip, we observed an average nictation duration of 14.44 seconds for wild type, and an increased average duration of 25.02 seconds in *flp-10(n4543) flp-17(n4894)* mutants (**Figure 3.9D**). For CO<sub>2</sub> avoidance, we observed that *flp-10(n4543) flp-17(n4894)* mutants displayed increased reversal behavior in response to CO<sub>2</sub> (avoidance index = 0.56) as compared to wild type (avoidance index = -0.11) (**Figure 3.9E**). These data suggest that *flp-10* and *flp-17* contribute to SBT-1 functions in mediating nictation coordination and the switch to CO<sub>2</sub> attraction in dauers.

***flp* genes are coordinately up-regulated in parasitic nematode IJs**

The infective juvenile (IJ) dispersal stage of parasitic nematodes is similar to dauer in several ways: both are non-feeding stages with a resistant cuticle (67), and both recognize and exploit carriers/hosts similarly (18, 68). One gene class that has been shown to affect dauers and IJs is the neuropeptide-encoding set of genes (27, 48). To investigate if the coordinated up-regulation of *flp* genes is a strategy shared by dauers and IJs, we performed a meta-analysis on *flp* gene expression in IJs of the semi-obligate animal parasite *Strongyloides stercoralis*, the obligate animal parasite *Ancylostoma ceylanicum*, the obligate plant parasite *Globodera pallida*, and the filarial parasite *Brugia malayi*. We selected these distantly related parasitic species because the orthologs/analogs of *C. elegans flp* genes have been identified in these nematodes (69). In addition, the transcriptomes of these species had been collected using RNA-seq, from stages during, before, and after IJ (70-73).

There are 21 *flp* genes in *S. stercoralis*, 25 in *A. ceylanicum*, 14 in *G. pallida*, and 13 in *B. malayi*. We observed that each *flp* gene was expressed at its highest level during the IJ or post-infection IJ in *S. stercoralis*, *A. ceylanicum*, and *G. pallida*, and was expressed lowly in other stages, including the egg, the first larval, third larval, fourth larval, and adult stages (**Figure 3.11B-D**). Specifically, *S. stercoralis* expressed 16 *flp* genes highly in IJ, and 5 highly in the post-infection IJ (**Figure 3.11B**); *A. ceylanicum* expressed 18 *flp* genes highly in IJ, and 5 highly in the post-infection IJ (**Figure 3.11C**); and *G. pallida* expressed 14 *flp* genes highly in IJ (**Figure 3.11D**).

By contrast, only 4 of the 13 *flp* genes in *B. malayi* were expressed at high levels in the IJ. The expressions of the remaining *flp* genes were specialized to other stages, such as the microfilariae and the adult male (**Figure 3.11E**). Unlike the other three parasitic nematodes, *B. malayi* spends its life cycle entirely within its hosts. Notably, the IJs of *B. malayi* infect humans through the aid of a mosquito vector (74). This differs from the IJs of *S. stercoralis*, *A. ceylanicum*, and *G. pallida*, which must find and infect their hosts (**Figure 3.11**). We therefore observe that *C. elegans* dauers and the host-seeking IJs of *S. stercoralis*, *A. ceylanicum*, and *G. pallida* share a strategy of coordinately up-regulating the *flp* family.

### 3.4 Discussion

In the wild, *Caenorhabditis elegans* feeds on transient microbial communities that collapse approximately every three generations (75). To persist, *C. elegans* can enter the stress-resistant dauer larval stage, which can seek improved conditions by stowing onto carrier animals (60). We sequenced cDNA from dauer- and reproductively-developing animals by culturing *daf-9(dh6)* animals under identical conditions apart from exposure to DA. This allowed us to collect the first transcriptomes, to our knowledge, of L2d during dauer-commitment and commitment to reproductive development. Our design also allowed us to compare dauer and reproductive development to identify gene expression changes along, and between, the two tracks. We have demonstrated that 8,042 genes are differentially expressed during dauer and reproductive development, including the up-regulation of 51% of the neuropeptide genes during dauer-commitment.

Neuropeptides are short sequences of amino acids that are derived from longer proneuropeptide chains, and can act as transmitters and neuromodulators. As neuromodulators, they can control the activity, polarity, sensitivity, and signaling repertoire of neurons (76, 77). Neuropeptides can also diffuse to facilitate signaling between synaptically unconnected neurons (78, 79). Through these modulatory functions, neuropeptides can shape which circuits are active in the nervous system, the membership of these circuits, and their functions (79).

*C. elegans* encodes three families of neuropeptides: the insulin-like peptides (INS), the neuropeptide-like proteins (NLP), and the FMRFamide-related peptides (FLP) (48). We have shown that the *flp* genes are coordinately up-regulated during

dauer-commitment. On the other hand, few of the *ins* genes, and approximately half of the *nlp* genes are up-regulated during dauer-commitment. The low level of *ins* up-regulation is not surprising since insulins have conserved roles in growth and metabolism in Metazoa (80). In addition, signaling through the *C. elegans* insulin-like receptor DAF-2 promotes reproductive growth (48). Indeed, the only *ins* gene that was up-regulated between dauer-commitment and L4 was *ins-1*, which is known to increase dauer entry, likely by antagonizing DAF-2 signaling (28). Likewise, the *nlp* genes would not be expected to be up-regulated as a family either, since the NLPs are a miscellaneous group of non-INS, non-FLP neuropeptides (48) that likely function in several independent processes. On the other hand, FLPs have conserved roles in regulating feeding and reproduction in nematodes, arthropods, mollusks, and vertebrates (80-83). These roles correlate well with the inhibition of feeding and reproduction, and the activation of specialized food-seeking behaviors in dauer. Therefore, the coordinated up-regulation of the *flp* family may function to generate a wide response to stress that is centered on feeding and reproduction control.

We took advantage of the knockdown of neuropeptide processing in *sbt-1(ok901)* null mutants (26) to investigate the function of the neuropeptides during dauer development. We have shown that the net effect of peptidergic signaling downstream of *sbt-1* is to promote dauer entry, perhaps by encoding pro-dauer information from the sensed environment, or by modulating the food, temperature, and pheromone signaling pathways to affect the threshold (13) for dauer entry. We have also assayed 23 *flp* mutants and observed increased dauer

entry in 4 mutants and decreased entry in 8 mutants. These results suggest that FLPs can act redundantly and with opposed effects on dauer entry, perhaps to fine-tune the entry decision in response to environmental signals.

Following dauer entry, dauer larvae demonstrate behaviors and preferences that are not observed in non-dauers. For instance, dauers are the only stage that can nictate (10, 19), and are attracted to CO<sub>2</sub> while non-dauers are repelled (18, 84). These changes indicate that dauers possess a different neural state from non-dauers, likely involving different or altered circuits in the nervous system. Yet, *C. elegans* possesses only 302 neurons that are densely interconnected (79, 85), with no synaptically compartmentalized circuits to switch between during dauer and non-dauer. To overcome this constraint, dauers can rewire their neurons to access new behaviors (16, 19). We observed that in addition to this strategy, peptidergic signaling downstream of *sbt-1* promotes coordination during nictation, and is necessary for the switch from CO<sub>2</sub> repulsion to CO<sub>2</sub> attraction in dauer. We have also shown that the combined effects of *flp-10* and *flp-17* strongly promote nictation coordination and the switch to CO<sub>2</sub> attraction. Therefore, we have demonstrated that neuropeptides change the neural state of *C. elegans* during dauer, possibly by altering the composition and function of the active circuits in the nervous system (**Figure 3.12**).

Considering these results, it is notable how many neuropeptides are up-regulated during dauer development. By dauer, 64 neuropeptide genes encoding 215 peptides are up-regulated, and by comparison, the entire human genome only contains 97 neuropeptide genes encoding 270 peptides (56). Indeed, the



neuropeptide gene families are expanded in *C. elegans* (48), and the FLP neuropeptides are especially expanded in the phylum Nematoda (27). We observed that FLPs are involved in establishing the *C. elegans* dauer neural state, and RNAi knockdown experiments have also shown that FLPs regulate the IJ dispersal behaviors of *G. pallida* (*flp-12*), *Meloidogyne incognita* (*flp-18*), and *Steinernema carpocapsae* (*flp-21*) (86, 87), indicating that they are involved in establishing the IJ neural state as well. Because we observed coordinated up-regulation of the FLPs during dauer, and in the IJs of the distantly related nematodes *S. stercoralis*, *A. ceylanicum*, and *G. pallida*, we speculate that the computational challenges of dauer and IJ were the driving force for *flp* expansion in Nematoda. This hypothesis is supported by the lack of such expansion in the nematodes *Trichinella spiralis* and *Trichuris muris* (69), which do not possess dauer or IJ stages (88, 89), and only encode 4 *flp* genes each. Therefore, *flp* expansion may have provided ancestral nematodes the means to overcome their constrained nervous systems (90) in order to effectively adapt to stress during dauer and IJ.

Our genetic data and meta-analysis also suggest that SBT-1 would be a potent target for anthelmintic control. Since *sbt-1* nulls are strongly defective in dauer entry and dispersal behaviors, we predict that targeting SBT-1 in parasitic nematodes will severely impair dispersal and host-seeking in their IJs. While RNAi against individual FLPs can affect IJ dispersal (86, 87), our meta-analysis indicates that multiple FLPs are up-regulated in several types of parasitic nematodes. We propose that inhibition of SBT-1 could be used to efficiently knock down multiple FLPs at once, and in a wide range of parasitic nematodes. SBT-1 would also be

an excellent target, since nematode SBT-1 is distinct in sequence from vertebrate 7B2 (57), reducing the risks of cross-species effects.

Altogether, we have investigated phenotypic plasticity in a whole organism by studying *C. elegans* adaptation to stress during development. We uncovered the transcriptional dynamics of *C. elegans* during dauer development, and discovered a strategy of massively up-regulating neuropeptide expression. This strategy functions to enhance the dauer entry decision and expand the behavioral repertoire of dauers, and appears to be evolutionarily shared by dauers and host-seeking IJs, suggesting SBT-1 as a potent anthelmintic target.

### 3.5 Materials and Methods

#### Animal strains

*C. elegans* strains were grown using standard protocols with the *E. coli* strain OP50 (for plate cultures) or HB101 (for liquid cultures) as a food source (91). The wild type strain was N2 (Bristol). PS5511 *daf-9(dh6); dhEx24* was a gift from the Antebi lab. Strains obtained from the *Caenorhabditis* Genetics Center (CGC) include: NY16 *flp-1(yn4)*, VC2324 *flp-6(ok3056)*, RB1990 *flp-7(ok2625)*, PT501 *flp-8(pk360)*, RB1989 *flp-10(ok2624)*, FX02706 *flp-11(tm2706)*, RB1863 *flp-12(ok2409)*, AX1410 *flp-18(db99)*, RB2188 *flp-20(ok2964)*, RB982 *flp-21(ok889)*, VC1982 *flp-25(gk1016)*, and VC3017 *flp-26(gk3015)*. AX1129 *flp-21(pk1601)* was a gift from the De Bono lab. MT15933 *flp-17(n4894)* and MT15973 *flp-10(n4543); flp-17(n4894)* were gifts from the Horvitz lab. PS7112 *sbt-1(ok901)* was outcrossed 6 times from CGC RB987; PS7370 *flp-2(ok3351)* was outcrossed 3 times from CGC VC2591; PS7378 W07E11.1 & *flp-2(gk1039)* was outcrossed 3 times from CGC VC2490; PS7379 *flp-3(ok3265)* was outcrossed 3 times from CGC VC2497; PS6813 *flp-13(tm2427)* was outcrossed 3 times from the Mitani strain FX02427; and PS7221 *flp-34(ok3071)* was outcrossed 3 times from CGC RB2269.

#### Transgenic strains

*sbt-1* genomic DNA rescue strains were generated by injecting 15 ng/μL of *sbt-1* genomic DNA (amplified by PCR with forward primer CTGTGAAGCGCTCATCTGAA and reverse primer

TTCAGGCAAATCCATCATCA), 50 ng/μL coelomocyte-specific *ofm-1p::rfp* co-injection marker, and 135 ng/μL 1 kb DNA ladder (New England Biolabs, Beverly, MA) carrier DNA into the adult gonads of *sbt-1(ok901)* animals, followed by integration into the genome by X-ray (92, 93). Two independent integration lines were generated: PS7274 *sbt-1(ok901); ls444[sbt-1p::sbt-1; ofm-1p::rfp]* (line 1, outcrossed 2 times) and PS7275 *sbt-1(ok901); ls445[sbt-1p::sbt-1; ofm-1p::rfp]* (line 2, outcrossed 3 times).

### Transcriptional reporter strains

Transcriptional reporter constructs were built using fusion PCR (1). The promoter regions of *srt-41* and *col-40* were fused to *mCherry::unc-54* 3'UTR (amplified from pGH8 from Addgene). The flanking sequences of the amplified *srt-41* promoter were GCACAGTTTTAAGTTTTTCTGTCTT and TGCTGCCAACCTGTTCTG. The flanking sequences of the amplified *col-40* promoter were ATGATGACCGCCTGATTTTC and AATTATTGTAGTAAAGGGGGAAGTC. Injection mixtures were prepared at a concentration of 20 ng/μL reporter construct, 50 ng/μL *unc-119(+)* rescue construct, and 130 ng/μL 1 kb DNA ladder carrier DNA. Transgenic animals were obtained by microinjecting the mixtures into the adult gonads of *unc-119(ed4)* animals (2, 3). The fluorescent transcriptional reporter strains that were generated are:

**PS7128** *unc-119(ed4); syEx1534[srt-41p::mCherry; unc-119(+)]* and

**PS6727** *unc-119(ed4); syEx1338[col-40p::mcherry; unc-119(+)]*

### CRISPR-generated strains

CRISPR mutagenesis with co-conversion (94) was used to generate the deletion strains. Guide RNA (gRNA) target sequences of 19 bp (corresponding to sequence upstream of an NGG PAM site) were cloned into pRB1017 single-guide RNA (sgRNA) vector (Addgene). Four distinct gRNA sequences were used to target each gene. Injection mixtures were prepared at a concentration of 25 ng/μL per sgRNA expression plasmid, 50 ng/μL Cas9 plasmid (Addgene #46168), 25 ng/μL *dpy-10* sgRNA plasmid (pJA58 from Addgene), and 500 mM *dpy-10(cn64)* donor oligonucleotide (synthesized by Integrated DNA Technologies, Coralville, IA). Injected P<sub>0</sub> hermaphrodites were transferred to individual Petri plates to produce F<sub>1</sub> progeny. F<sub>1</sub> progeny exhibiting a Rol or Dpy phenotype were picked to individual Petri plates four days after injection. F<sub>1</sub>s that produced Rol or Dpy F<sub>2</sub>s were genotyped for the presence of a deletion allele. Homozygous deletion mutants were isolated from the F<sub>2</sub> or F<sub>3</sub> population, and the deletion alleles were confirmed by Sanger sequencing (Laragen, Culver City, CA).

The 1343bp *flp-21(sy880)* deletion is flanked by the sequences TATGTACACTATTTAA  
GATTTGATTGTGTA and CATTCGGGGCCACAACTCCTGCTTCGATC.  
*flp-32(sy853)*, *flp-34(sy810)* and *flp-34(sy811)* deletion alleles have short DNA fragment insertions. The 460bp *flp-32(sy853)* deletion is flanked by the sequences TATGAATATGTTCCGGAGCGCATGTCAAAC and  
AACTAAAGATACACCACTAC

CACCTGAACC, with a TAACT insertion. The 1365bp *flp-34(sy810)* deletion is flanked by the sequences TCAAATTTTTTGAGGAAATCCTCCTGAAAC and AATATTTTCGA

GTTTCGAAACATTTCAAAT, with a AATATATTTTCGAGTTTCGAAACATATTTT CGAGTTTCGAAACAC insertion. The 1607bp *flp-34(sy811)* deletion is flanked by the sequences TTTGTGTCTAGCAAAAGGAGATGCTCTTTA and CATAGGCGTAGGCC

ATAGGCGTAGGCCATA, with a AATAAATTAATTAAATATCTGAAATAAAAACA AACCTCGAGAGAGAAAATTTAGAAAAAAAAACGAGACGGCTACGGACGGCT GACGTGATGGAATTATTTACGGCCAAATCTGAAAATAAAATGGATTATATTTT GTTTTAGGCCATAGACGTAGGTCATAGGCGTAGACCATAGGCGTAGGC insertion.

### ***daf-9(dh6)* culturing and harvesting for RNA-seq**

Synchronous, single-stage populations of *daf-9(dh6)* animals were grown using our previously described method for liquid culturing *daf-9(dh6)* (13). *daf-9(dh6)* animals were collected at 6 points over a branching time series along 24 hours post hatch (hph) to 60 hph. This period, as we have previously analyzed, includes L2d sensory integration, dauer-commitment, dauer maintenance, reproductive-commitment, and reproductive development (13) (**Figure 3.1A**). The dauer-developing branch was obtained by withholding dafachronic acid ( $\Delta 7$ -DA), and animals were collected at 24 hph (L2d), 26 hph (L2d), 34 hph (dauer-commitment), and 60 hph (dauer). The reproductive-developing branch was obtained by adding

100 nM  $\Delta 7$ -DA at 24 hph, and animals were collected at 26 hph (L3-committing) and 34 hph (L4). Reproductive animals at 60 hph are gravid, making them inappropriate for single-stage transcriptome analysis, and were therefore not collected.

Cultures from the dauer and reproductive branches were grown in parallel, fed at the same time, and experienced the same batches of HB101 and  $\Delta 7$ -DA in order to minimize asynchronous development between the cultures. Each time point was collected using two independently cultured biological replicates. Each biological replicate was maintained separately for at least 5 generations. Harvested animals were spun in S. Basal three times to help clear the bacteria. The worm pellets (approximately 10,000 worms per pellet) were then treated with 1 mL Trizol and 0.6 mg/mL linear polyacrylamide carrier, before being flash frozen in liquid nitrogen and stored at  $-80^{\circ}\text{C}$ . RNA was purified as previously described (13).

### **RNA-sequencing and computational analysis**

cDNA was prepared from the collected samples using the Illumina TruSeq RNA Sample Preparation kit or mRNA-Seq Sample Preparation kit. cDNA was sequenced using the Illumina HiSeq2000 to generate paired-end or single-end libraries. Paired-end libraries were not multiplexed, were sequenced at a read length of 100 bp, and were sequenced to an average depth of 76 million reads. Single-end libraries were multiplexed at 4 libraries per lane, sequenced at a read length of 50 bp, and sequenced to an average depth of 33 million reads. All raw

sequences have been deposited into the NCBI Sequence Read Archive (SRA) database (accession number SRP116980). **Appendix Table 3.1** contains the detailed metadata for the sequenced libraries. Codes used for data analysis have been deposited into GitHub at <https://github.com/WormLabCaltech/dauerRNAseq>.

**Read mapping and differential expression testing:** Reads that did not pass the Illumina chastity filter were removed using Perl. Read mapping, feature counting, library normalization, quality checks, and differential gene expression analysis was performed using R version 3.1.0, bowtie2 version 2.2.3, tophat2 version 2.0.12, SAMtools version 0.1.19, HTSeq version 0.6.1, and DESeq, as described in (38). The *C. elegans* reference genome and gene transfer format files were downloaded from Ensembl release 75 and genome assembly WBcel235. Gene dispersion estimates were obtained after pooling all sequenced samples. Each pairwise comparison for differential gene expression was performed at a Benjamini-Hochberg controlled false discovery rate  $< 0.01$ .

**RNA-seq data summaries:** Principal component analysis was performed using the DESeq package in R (37). Violin plotting was done in R using ggplot2 (95). KEGG biochemical pathway enrichment analysis was performed using clusterProfiler in R (96), at a cutoff of BH-corrected  $q$ -value  $< 0.01$ . Gene Ontology (GO) enrichment analysis was performed using the PANTHER Overrepresentation Test for GO Biological Process, at a Bonferroni-adjusted  $p$ -value cutoff of  $< 0.05$ . GO and KEGG terms were ranked based on descending fold-enrichment for GO, and ascending  $q$ -value for KEGG.



**Soft clustering:** Soft clustering was performed using the mFuzz package in R (40, 41). Gene expression data were standardized before clustering, and cluster numbers were chosen based on cluster stability, minimum cluster centroid distance, and visual clarity of the clusters. Over-represented neuronal gene classes in clusters 1 to 6 were determined by hypergeometric test, using a cutoff of Bonferroni-corrected  $p$ -value  $< 0.05$ .

**Heatmaps:** Heatmaps were drawn using the gplots and RColorBrewer packages in R (97, 98). Mean count values were used for each time point, calculated by averaging the biological replicates. Heatmap dendrograms were drawn using correlation distances and average-linkage hierarchical clustering. Expression values were centered and scaled for each gene.

**Gene expression correlation analysis:** Spearman correlation scores were computed using Python 2.7.9 and the Scipy library (99) by ranking the transcripts per million (TPM) values in each RNA-seq experiment, and then calculating the Pearson correlation on the ranked values for each pairwise combination of genes:  $\rho = \text{covariance}(\text{gene1}, \text{gene2}) / \sigma_{\text{gene1}} \sigma_{\text{gene2}}$ , where  $\sigma$  represents standard deviation.  $p$ -values were computed by comparing average correlation scores to the bootstrap distribution of average scores for random sets of 31 genes (mimicking the size of the *flp* family), and calculated as the fraction of times that bootstrapping produced a score greater than or equal to the score being tested. Because the *ins* and *nlp* families have more than 31 genes, the  $p$ -value is an upper estimate. Bootstrapping was performed 10,000 times. The RNA-seq datasets that were used were our *daf-9(dh6)* RNA-seq data, re-quantified using kallisto (100) into TPM

counts; and processed RNA-seq data from 246 publically available libraries (23), obtained using WormBase SPELL and converted to TPM counts (101). Genes detected in less than 80% of the experiments were discarded.

**Dotplot analysis:** Dotplot analysis of the *flp* coding sequences was performed using Gepard (63). Coding sequences from the 31 total *flp* genes (taking only the a isoform for genes with multiple isoforms) were used in the analysis.

### **Dauer entry assay on pheromone plates**

The preparation of crude pheromone and the dauer entry assay were performed with modifications to previously described methods (102). Crude pheromone was extracted from exhausted liquid culture medium, re-suspended with distilled water and stored at -20°C. Pheromone plates (NGM-agar with added crude pheromone and no peptone) were freshly prepared the day before each experiment and dried overnight at room temperature. Heat-killed *E. coli* OP50 was used as a limited food source for the dauer entry assays, and was prepared by re-suspending OP50 overnight cultures in S. Basal to 8 g/100 mL, and heating at 100°C for 5 minutes. On the day of the experiment, seven to ten young adults were picked onto each plate, and allowed to lay approximately 50-60 eggs before being removed. 20 µl of heat-killed OP50 was added to the plates as a food source for the un-hatched larvae. After 48 hours of incubation at 25.5°C, dauers and non-dauers were counted on each plate based on their distinct morphologies.

Dauer entry can exhibit day-to-day variation caused by environmental conditions such as humidity or temperature (25). To control for this variation, wild type controls were run in every trial. The wild type results from the same batch of pheromone were pulled together for better statistical power, and each statistical analysis was done with samples treated with the same batch of pheromone.

### **Statistical analysis for dauer entry assay**

The mean and 99% confidence interval of the dauer entry percentage were calculated non-parametrically for each genotype by pooling the data from all the plates and computing 10,000 bootstrap replicates (103). Pairwise comparisons were performed through a non-parametric permutation test with 10,000 replicates. The difference in dauer entry probability between two genotypes was estimated using a Bayesian approach (104) to compute the posterior probability of dauer entry for each genotype. Bootstrapping, permutation, and Bayesian statistics were performed using Python 3.5 and the SciPy library (105).

For each genotype, the data from all of the plates tested for that genotype were pooled and the number of dauers and non-dauers was converted into a Boolean array (1 for dauer, 0 for non-dauer). Non-parametric bootstrapping was used to sample the data array (with replacement) to calculate a corresponding dauer entry percentage. This procedure was repeated 10,000 times to construct a dauer entry percentage distribution, from which the mean and 99% confidence interval were calculated.

For each comparison between two genotypes, data arrays from the two genotypes were concatenated, shuffled, and split into two datasets of original size as before concatenation, and a difference of means was calculated between the two new datasets. This procedure was repeated 10,000 times to generate a distribution of differences of means that simulated the null hypothesis. The  $p$ -value was calculated as the fraction of the distribution where the simulated difference was greater than or equal to the observed difference.

A binomial likelihood was used with a uniform prior for values in the range [0, 1], so that the log posterior probability distribution was proportional to the log binomial distribution in the allowed range. The data for each genotype were pooled, and the posterior distribution was sampled using Markov chain Monte Carlo (MCMC). The difference between mutant and wild-type was computed by subtracting the respective MCMC samples.

### **Dauer behavior assays**

Crude pheromone plates were used to induce synchronized dauers for behavior assays: for each pheromone plate, 20  $\mu$ L of heat-killed OP50 (8 g/100 mL) were spotted and 12-15 young adult animals were picked onto the plate to lay eggs at 20°C for 12 hours before being removed. After 2-4 days of incubation at 25.5°C, dauers were identified by their morphology and isolated for the following assays.

**Nictation assay:** Nictation assay was performed on micro-dirt chips with modifications to previously described methods (19). Dauers suspended in distilled

water were transferred onto the micro-dirt chip (4% agarose in distilled water) and allowed to nictate. Each nictating dauer was observed for at least 3 minutes or until the end of nictation. The time recording began when a dauer initiated nictation (by lifting its neck region of the body), and the total duration of each nictation event was also recorded. If the dauer stopped nictating and exhibited quiescence in a standing posture during the recording, the data were excluded from further analysis. The average nictation duration was calculated by dividing the total duration of nictation by the number of nictation events. At least 20 dauers were assayed for each genotype. The mean of average duration, the 99% confidence interval, and the pairwise *p*-value were computed non-parametrically as described for the dauer entry assay.

**CO<sub>2</sub> chemotaxis assay:** CO<sub>2</sub> chemotaxis assays were performed on dauers with modifications to previously described methods (18). Dauers were washed three times with distilled water and transferred to standard chemotaxis assay plates (106). Two gas mixtures were delivered to the plate at a rate of 0.5 mL/min through PVC tubing and holes drilled through the plate lid. The CO<sub>2</sub> gas mixture was 10% CO<sub>2</sub> and 21% O<sub>2</sub> balanced with N<sub>2</sub>, and the control gas mixture was 21% O<sub>2</sub> balanced with N<sub>2</sub> (Airgas). The two holes were positioned on opposite sides of the plate along a diameter line, with each of them positioned 1 cm from the edge of the plate. The scoring regions were set as the areas of the plate beyond 1 cm from a central line drawn orthogonally to the diameter on which the gas mixtures were presented. At the end of 1 hour, the number of animals in each scoring region was counted and the chemotaxis index was calculated as ( $N_{\text{at CO}_2 \text{ scoring region}} - N_{\text{at}}$

control gas scoring region) / (N<sub>at CO<sub>2</sub></sub> scoring region + N<sub>at control gas</sub> scoring region).

Statistical analysis (two-tailed t test) was performed using GraphPad Prism.

**Acute CO<sub>2</sub> avoidance assay:** CO<sub>2</sub> avoidance assays were performed as previously described (62), with slight modifications. Dauers were washed three times with distilled water and transferred to unseeded NGM plates. A 50 mL gas-tight syringe was filled with either a CO<sub>2</sub> gas mixture or a control gas mixture, and connected to a pipet tip using PVC tubing. Gas was pumped out through the pipet tip at a rate of 1.5 mL/min using a syringe pump, and the tip was presented to the head of forward-moving dauers. A response was scored if the animal reversed within 4 seconds. For each plate, at least 20 animals were assayed per gas mixture, with each plate counted as a trial. The avoidance index was calculated as (N<sub>reversed to CO<sub>2</sub></sub> / N<sub>presented with CO<sub>2</sub></sub>) - (N<sub>reversed to control gas</sub> / N<sub>presented with control gas</sub>). Statistical analysis (one-way ANOVA with Bonferroni post-correction test) was performed using GraphPad Prism.

### ***flp* gene expression in infective juveniles**

Orthologs/analogs of *C. elegans flp* genes exist in other nematodes (69, 80, 107). Identified *flp* orthologs/analogs in (69, 107) were matched to transcript IDs in *S. stercoralis*, *A. ceylanicum*, *G. pallida*, and *B. malayi* using BLAST via WormBase ParaSite. Published RNA-seq data was downloaded for *S. stercoralis* (73) and *G. pallida* (71) using the ENA; *B. malayi* (70) using WormBase SPELL; and *A. ceylanicum* (72) as it was published.

The read counts from the *A. ceylanicum* and *B. malayi* data were pre-processed into TPM counts. We obtained TPM counts for the *S. stercoralis* and *G. pallida* datasets using kallisto to align the read data and to quantify transcript abundances (100). Kallisto was preferable to DESeq at this stage of our analysis, as it allowed us to quickly and accurately quantify these large datasets. To increase comparability between all of the datasets, kallisto was used to re-quantify our own dauer RNA-seq data into TPM counts.





**Figure 3.1. 39% of the *C. elegans* genome is differentially expressed during dauer and reproductive development.** **(A)** Experimental design for collecting dauer- and reproductively-developing *daf-9(dh6)* animals. The timing of molt events are indicated in parentheses (13). **(B-C)** Twelve comparisons between the six time points. Arrows are directed from the reference point to the end point of each comparison. **(D)** Violin plots of the significantly up- and down-regulated genes in each comparison. The number of up- and down-regulated genes in each comparison is indicated above and below its violin plot. The fold changes between the replicates of each sequenced time point are plotted for reference (orange and green plots). Abbreviations are hph: hours post hatch, DA: dafachronic acid, cL3: L3-committing, cD: dauer-committed.

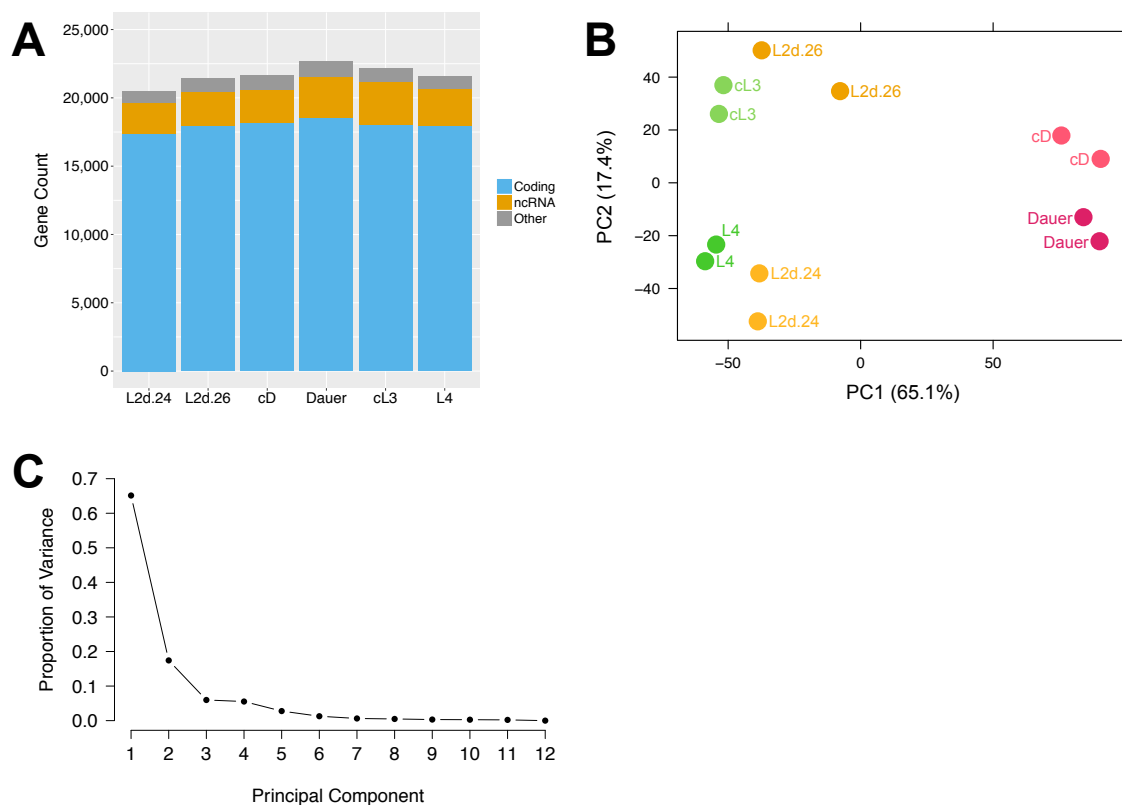


**Figure 3.2. *daf-9(dh6)* RNA-seq dataset summaries** **(A)** Detected gene counts from the six sequenced stages along dauer and reproductive development. **(B)** Principal component analysis plot of the variation in gene expression across the 12 sequenced samples. The proportion of total variation that is spanned by PC 1 and 2 are listed in parentheses. **(C)** Scree plot demonstrating the proportion of the total variation between the 12 sequenced samples that is explained by each principal component in the principal component analysis.

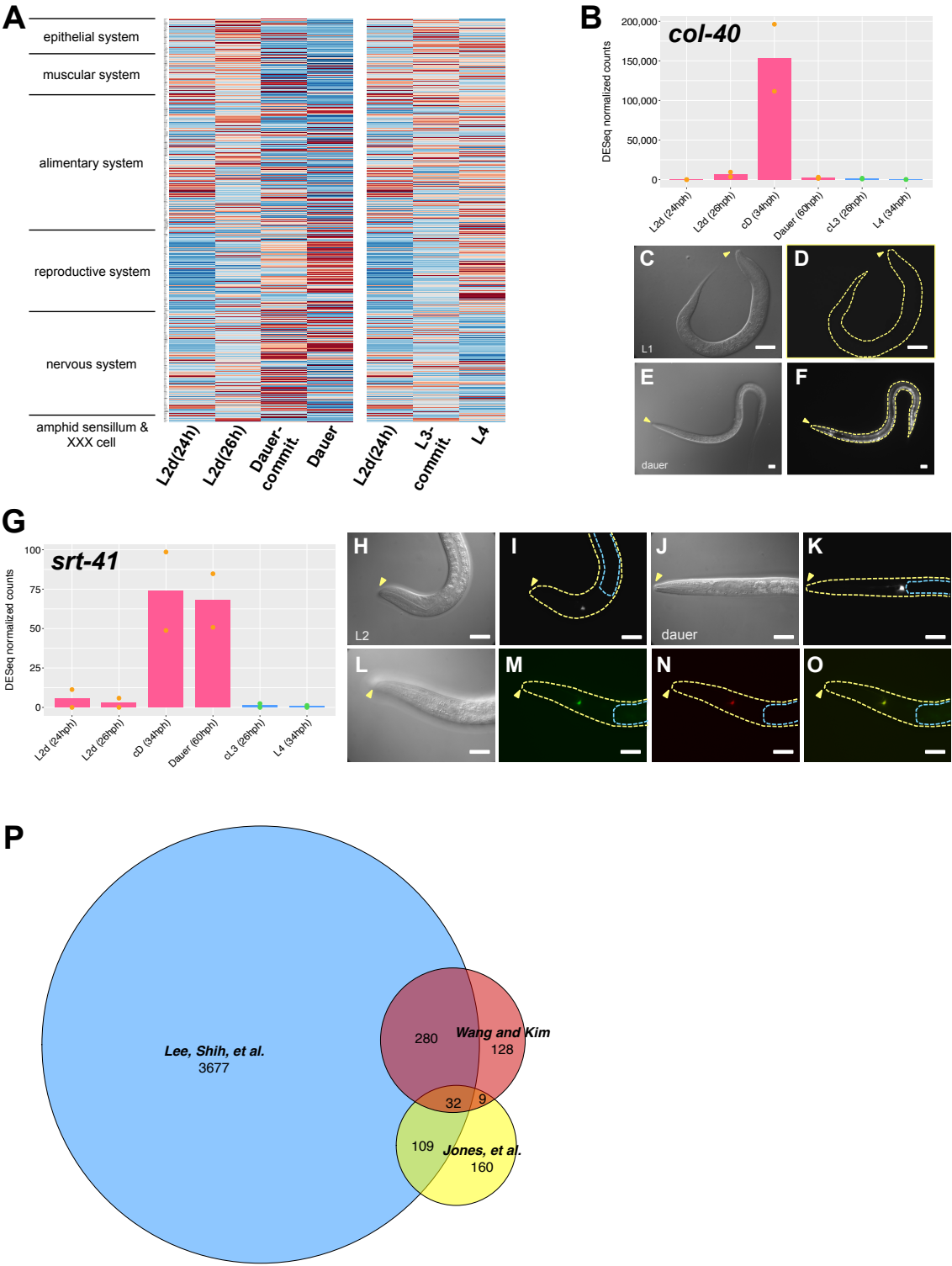


**Figure 3.3. Differential expression was detected at high accuracy and single-cell resolution** (A) The expression profiles of differentially expressed genes with putative tissue-specific expression in the epithelial system, muscular system, alimentary system, reproductive system, nervous system, amphid sensillum, and XXX cell. The expression data was scaled and heatmapped as in Figure 3. (B) Detected read counts for the *col-40* gene. Points indicate count values from each sequenced replicate. The bar height represents the mean count value for each stage. Abbreviations are hph: hours post hatch, cL3: L3-committing, cD: dauer-committed. (C-D) Bright field and fluorescence images of the *col-40* non-dauer expression pattern (shown is an L1). The body is traced in yellow dotted lines, and yellow arrows point to the mouth for reference. Scale bars represent a length of 20  $\mu$ m. (E-F) Bright field and fluorescence images of the *col-40* dauer expression pattern. (H-I) Bright field and fluorescence images of the *srt-41* non-dauer expression pattern (shown is an L2). The intestine is traced in blue dotted lines for reference. (J-K) Bright field and fluorescence images of the *srt-41* dauer expression pattern. The two fluorescence images (I) and (K) were captured using the same imaging parameters. (L-O) *srt-41p::mCherry* expression in the AWC<sup>on</sup> neuron. (M) GFP expressed from the AWC<sup>on</sup> marker *str-2p::gfp* and (N) mCherry from *srt-41p::mCherry* co-localized in the same cell, as shown in (O) the merged image. Pictured is a non-dauer, since *str-2p::gfp* changes expression to the ASI neuron in dauers (4). (P) Venn diagram comparing our dataset to SAGE data published by Jones, et al. (2001), and microarray data published by Wang & Kim (2003), drawn using the eulerr package (5). Differential expression in our data was

tested for using comparisons 2-6 and 11-12 to identify genes that were significantly up-regulated at dauer-commitment and dauer, relative to L2d and L4.

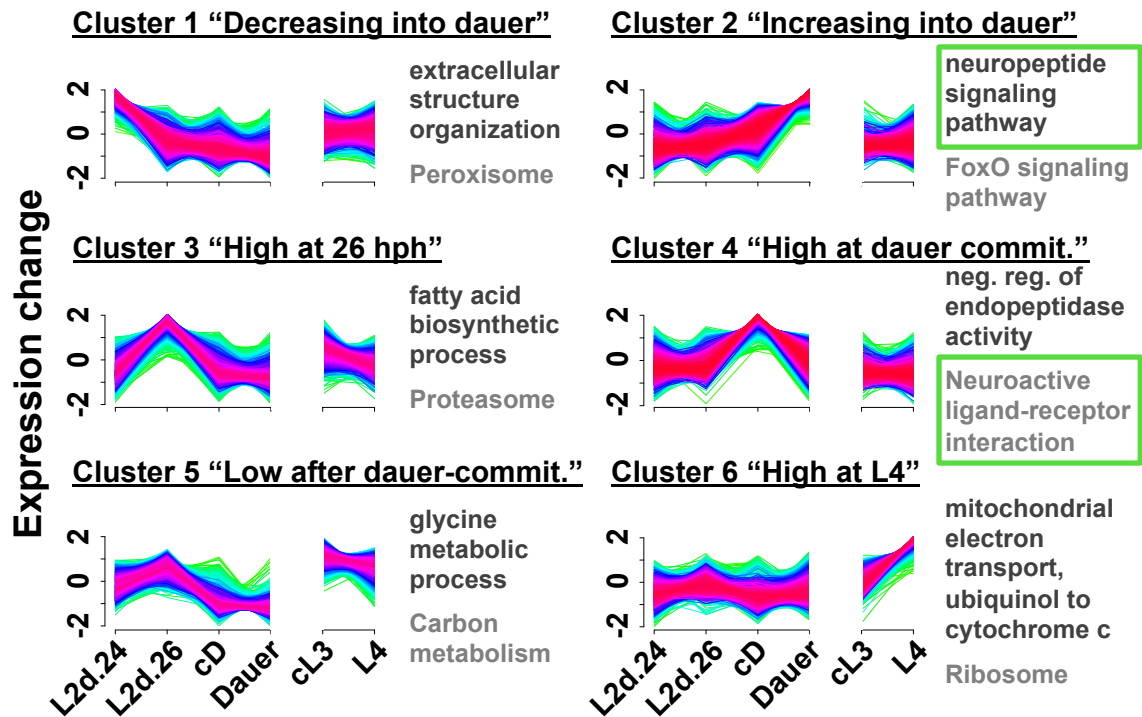
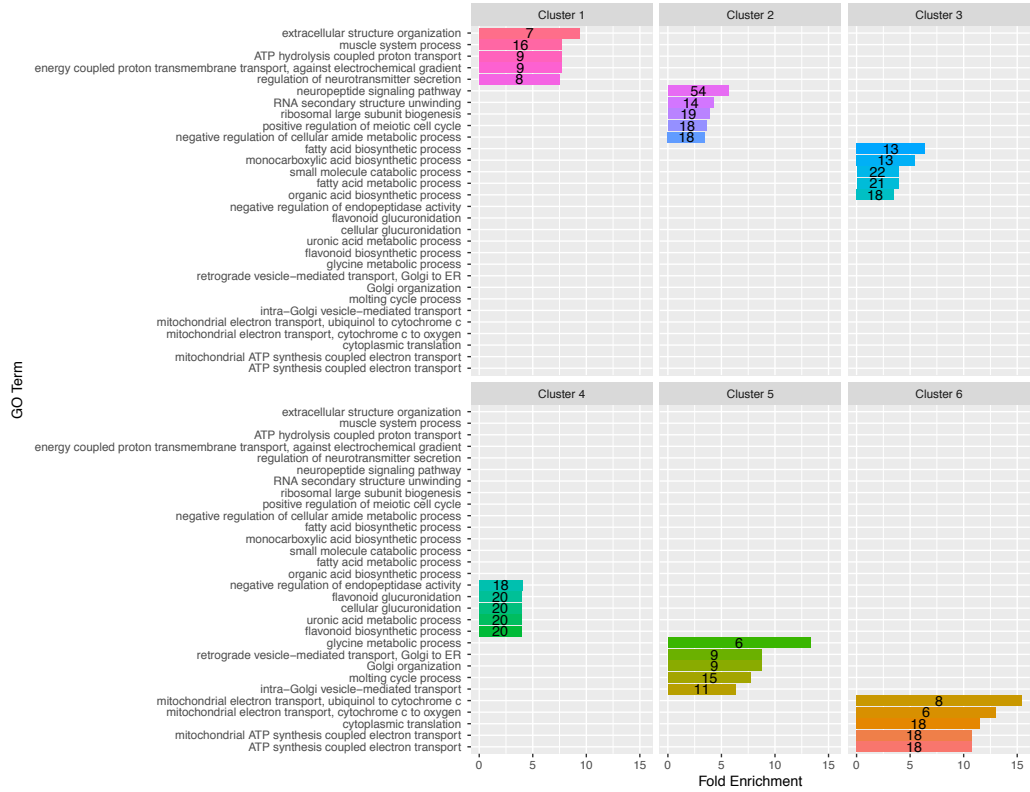


**Figure 3.4. Clustering revealed six common expression profiles during dauer and reproductive development.** Soft clustering of the 8,042 differentially expressed genes into six common expression profiles. Yellow-green lines indicate genes with low cluster membership scores, and purple-red lines indicate genes with high membership scores. The top enriched GO and KEGG terms for each cluster are listed. Abbreviations: FE: fold enrichment.

A



B



**Figure 3.5. Enriched GO terms and KEGG pathways in clusters 1 to 6.** The number in each bar indicates the number of genes with that term in the cluster. (A) The five most enriched GO terms (based on descending fold enrichment) in clusters 1 to 6, using a cutoff of Bonferroni-adjusted  $p$ -value  $< 0.05$ . (B) The five most enriched biochemical pathways (based on ascending  $q$ -value) in clusters 1 to 6, using a cutoff of BH-corrected  $q$ -value  $< 0.05$ .



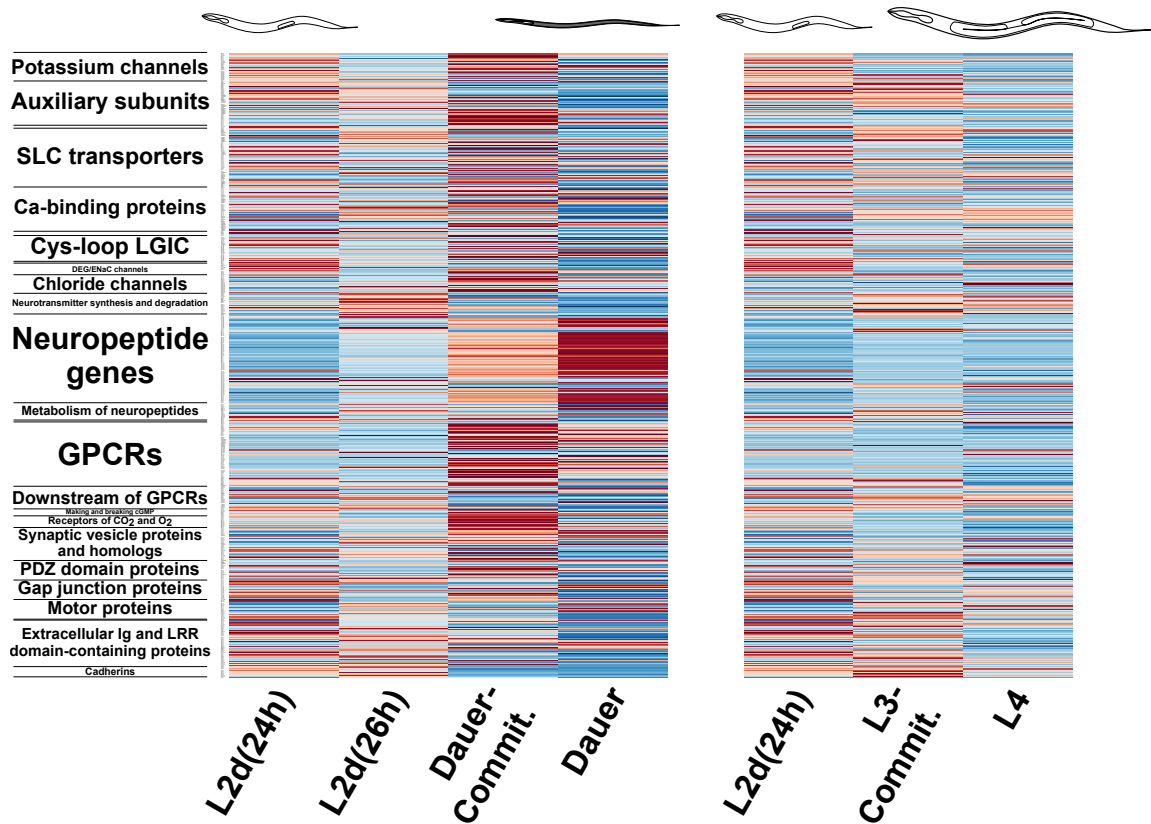


**Figure 3.6. Differential expression of the neuronal effector genome of *C. elegans* during dauer and reproductive development.** Heatmap of the expression of 606 differentially expressed neuronal effector genes. Each row represents a single gene, with the class that the gene belongs to indicated on the left. Red and blue indicate high and low expression scores, respectively.

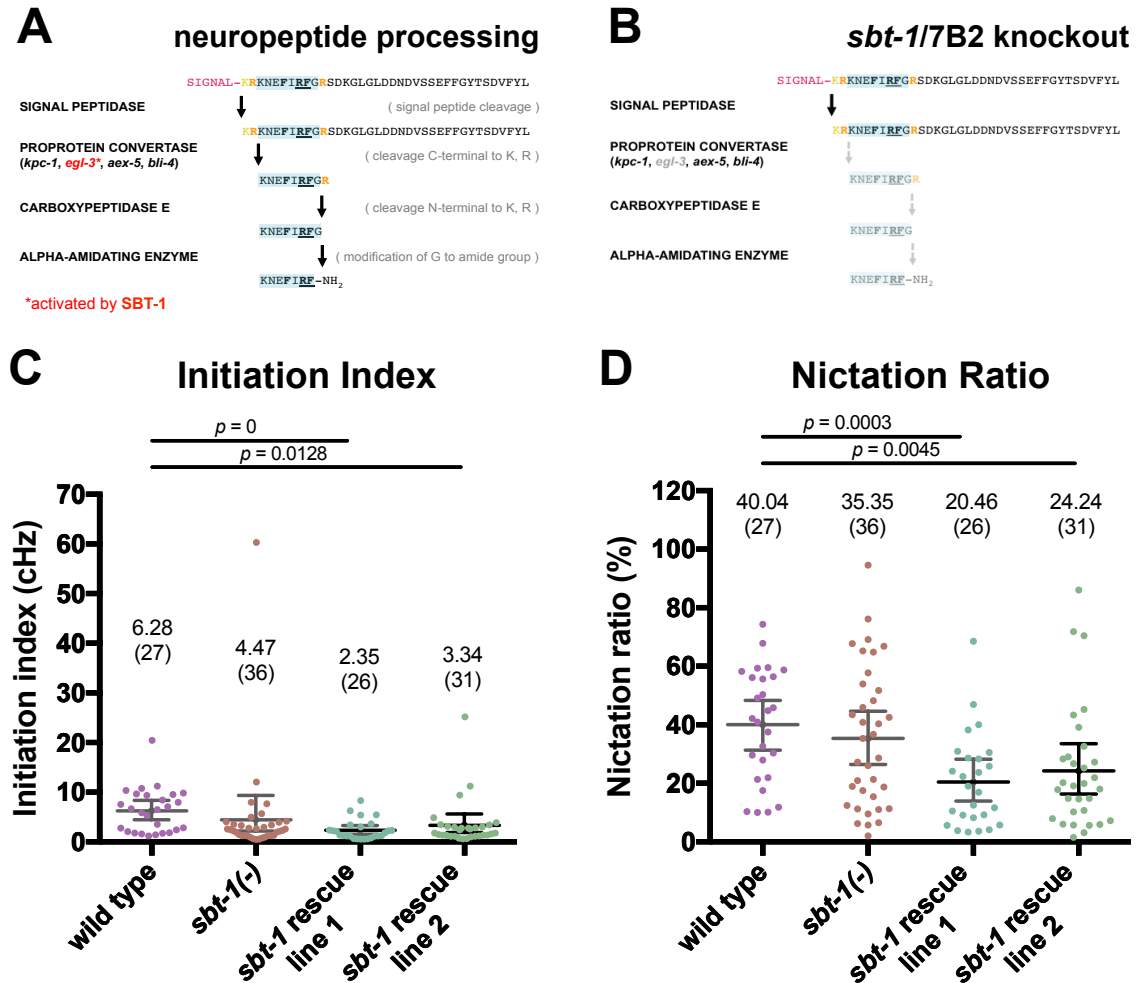


**Figure 3.7. Nictation initiation and the proportion of time spent nictating are not significantly affected in *sbt-1* null mutants.** (A and B) Neuropeptide processing in wild-type (A) and *sbt-1*-null (B) animals, using the FLP-8 peptide sequence as an example. (C and D) Nictation initiation (C) and ratio (D) measurements that were collected simultaneously with the nictation duration data in Fig. 3.8B. Bootstrapped means and 99% CIs are indicated. Statistic: permutation test.

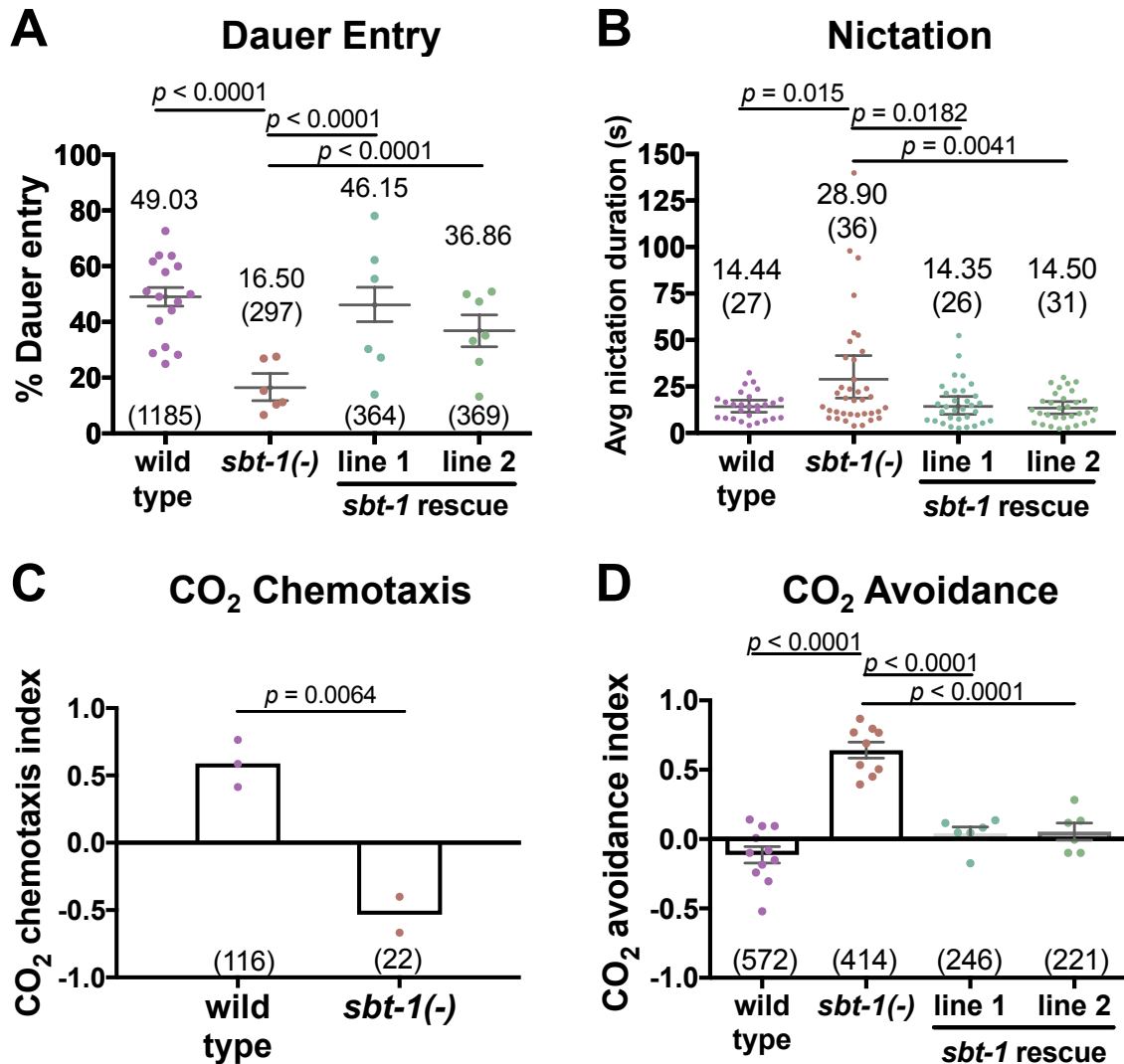


**Figure 3.8. Neuropeptide signaling promotes dauer entry and dispersal behaviors.** (A and B) Dauer-entry (A) and nictation duration (B) assays. Bootstrapped means and 99% CIs are indicated. (C and D) CO<sub>2</sub> chemotaxis (C) and avoidance (D) assays. Means and SEM are indicated. In A–D, each dot is one trial, and the number tested is in parentheses. Statistics: permutation test (A and B); two-tailed t (C); one-way ANOVA (D). Avg, average.

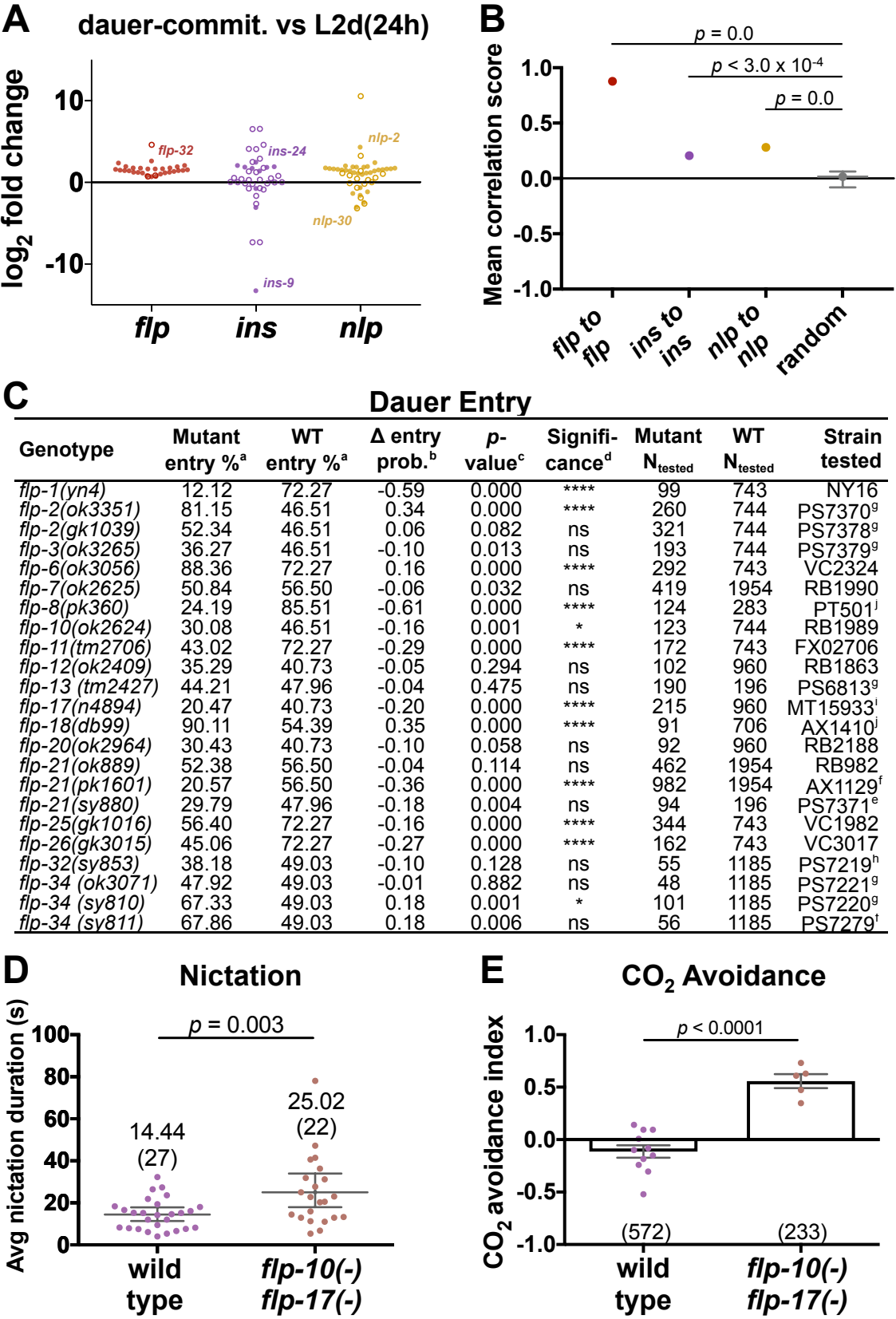


**Figure 3.9. FMRFamide-like peptides are coordinately up-regulated during dauer development.** (A) Fold changes in gene expression for all 118 *C. elegans* neuropeptide genes. Closed and open circles indicate significant and non-significant differential expression, respectively. The most up- and down-regulated genes of each family are labeled for reference. (B) Average Spearman correlation scores of genes to other genes of the same neuropeptide family, calculated across our RNA-seq dataset. Indicated is the bootstrapped mean and 99% confidence interval. (C) Survey for *flp* genes involved in the dauer entry decision. Footnotes: a–mean percentage calculated by nonparametric bootstrapping. b–the mean difference in dauer entry probability between wild type and mutant animals, calculated using Bayesian probability. c–calculated via permutation test. d–determined using a cutoff of Bonferroni-corrected  $p$ -value  $< 0.05$ : \*\*\*\* $p < 0.0001$ , \* $p < 0.05$ , ns, not significant. e to j–strains outcrossed 1, 2, 3, 4, >4, and 6 times, respectively. (D-E) Nictation duration (D) and CO<sub>2</sub> avoidance (E) assays.

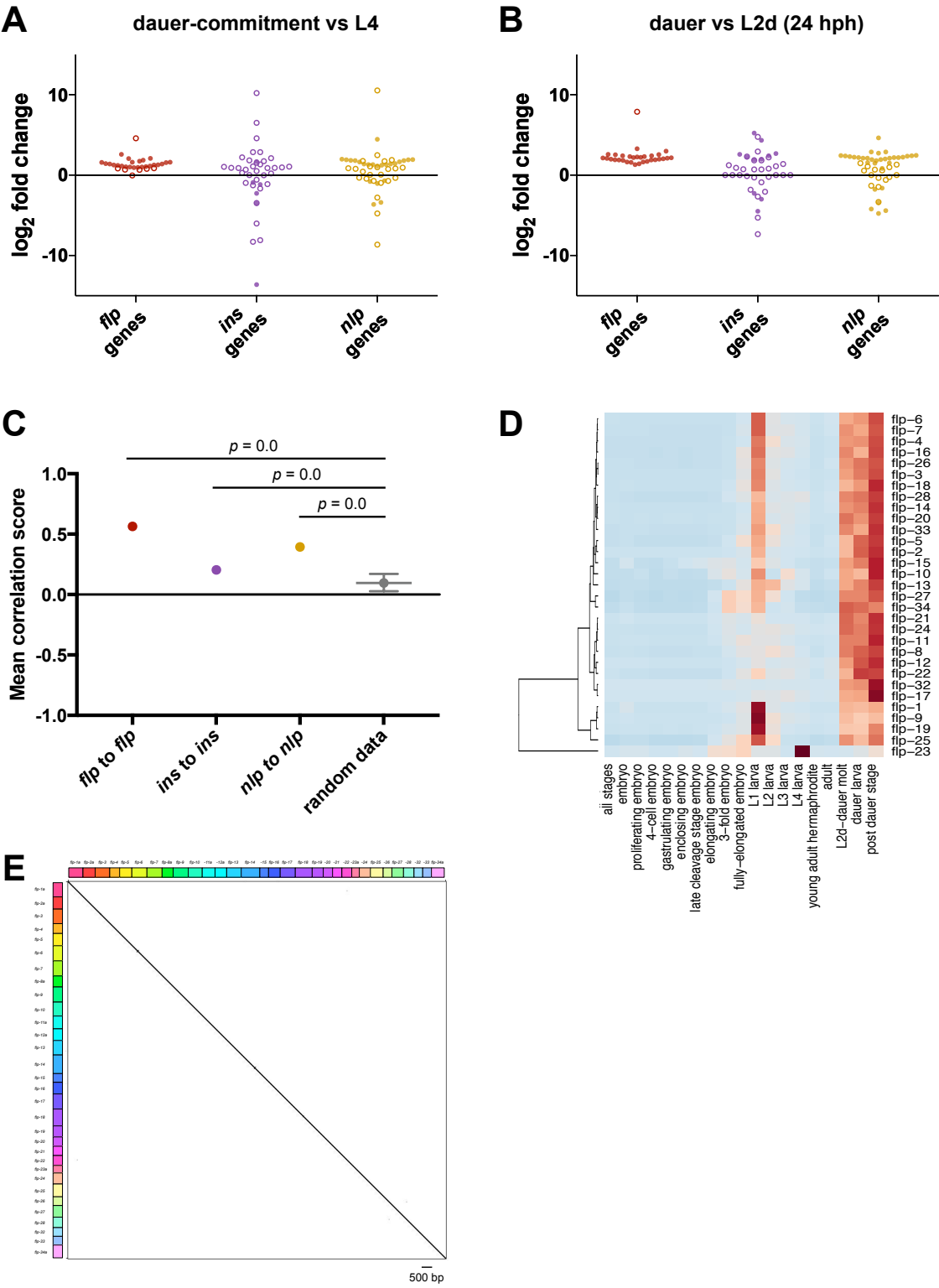


**Figure 3.10. FMRFamide-like peptides are coordinately up-regulated during dauer development.** (A) Fold changes in gene expression for all 118 *C. elegans* neuropeptide genes during dauer-commitment versus L4 and (B) dauer versus L2d. Each circle represents an individual neuropeptide gene. Closed and open circles indicate significant and non-significant differential expression, respectively. (C) Average Spearman correlation scores of genes to other genes of the same neuropeptide family, calculated across 246 publically available RNA-seq datasets describing various *C. elegans* life stages and experimental conditions, including embryos, larvae, adults, and males (6). (D) Heatmap of *flp* median gene expression (analyzed in TPM) across the 246 RNA-seq datasets (6). The expression data was scaled and heatmapped as in Figure 3. (E) Dotplot of the coding sequences of all 31 *flp* genes, compared against each other. The x- and y-axes represent the concatenated coding sequences of the 31 *flp* genes (using only the a isoform, if multiple isoforms exist for that gene). Regions of sequence similarity are represented as a diagonal line of hits along the alignment space, and a minimum of 20 identical, consecutive nucleotides were required to generate a hit.

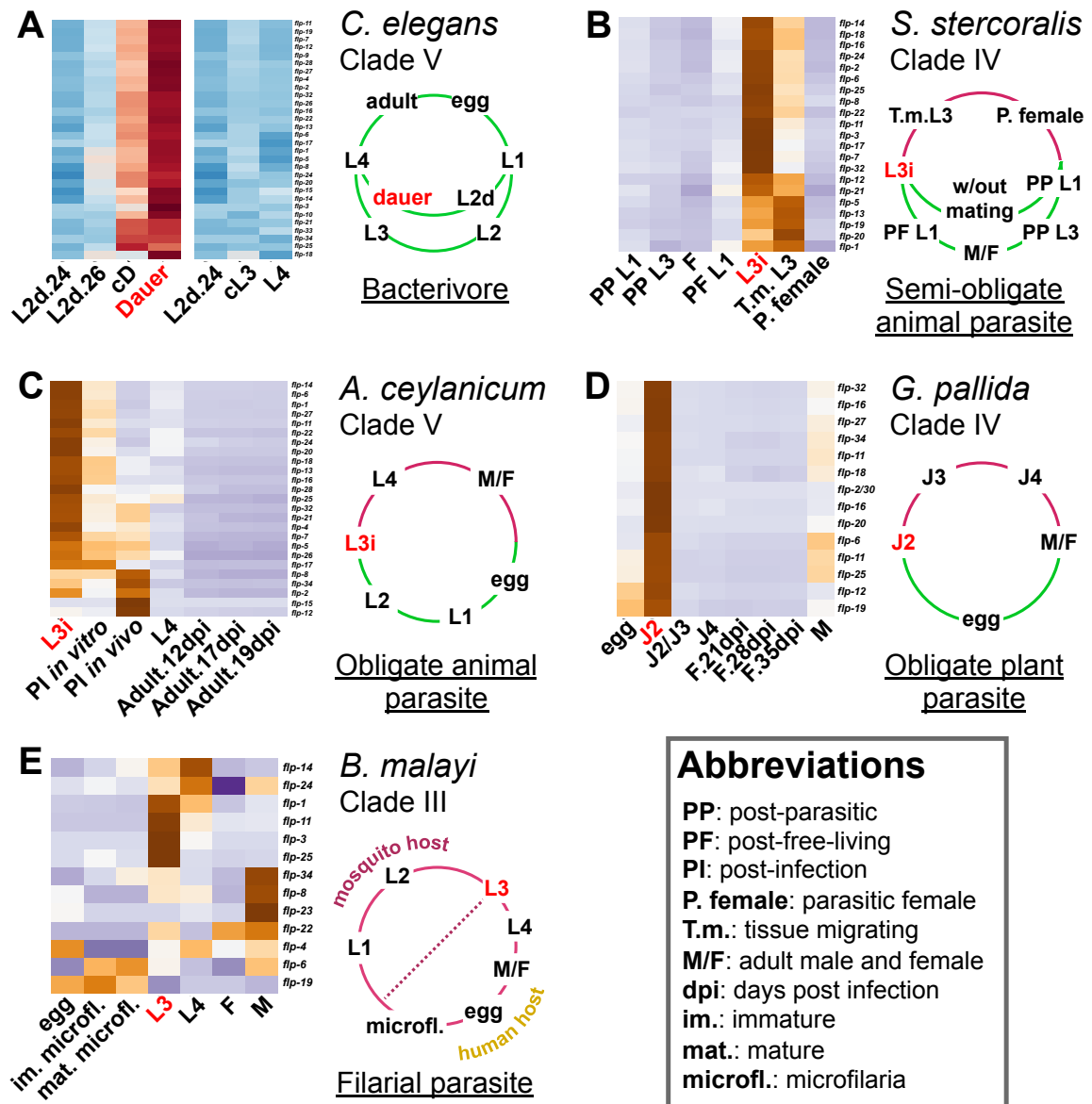


**Figure 3.11. FMRFamide-like peptides are coordinately up-regulated in host-seeking infective juveniles of parasitic nematodes.** The life cycle and clade membership (out of five major clades of Nematoda (108)) of each species are indicated to the right of each heatmap. Green life cycle regions indicate stages that are free-living or external to a host. Red life cycle regions indicate stages internal to a host. The dauer and infective juvenile stages are highlighted in red boxes. (A)



Expression of *flp* genes in the free-living *C. elegans* (from our data). Red and blue indicate high and low expression scores, respectively. (B-E) Expression of *flp* orthologs/analogs in the transcriptomes of (B) the semi-obligate animal parasite *Strongyloides stercoralis*, (C) the obligate animal parasite *Ancylostoma ceylanicum*, (D) the obligate plant parasite *Globodera pallida*, and (E) the filarial parasite *Brugia malayi*. Orange and purple indicate high and low expression scores, respectively. Transcriptomic data from (70-73).

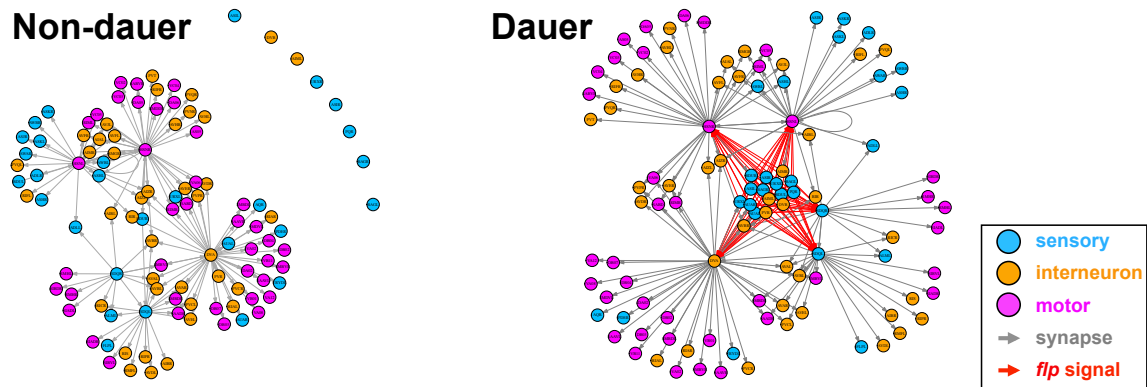


**Figure 3.12. Model of circuit changes during dauer development via non-synaptic FLP signaling.** The FLP-10 ligand EGL-6 receptor circuit is shown as an example. The synaptic connections that are indicated are (in pre-synaptic to post-synaptic order) from *flp-10* expressing neurons to *egl-6* expressing neurons to directly downstream synaptic targets. Expression pattern, connectomic, and biochemical data was used from (7-9), WormWiring, and WormBase.

### 3.7 References

1. McLaughlin KA, *et al.* (2015) Causal effects of the early caregiving environment on development of stress response systems in children. *Proceedings of the National Academy of Sciences of the United States of America* 112(18):5637-5642.
2. McQuaid RJ, McInnis OA, Stead JD, Matheson K, & Anisman H (2013) A paradoxical association of an oxytocin receptor gene polymorphism: early-life adversity and vulnerability to depression. *Frontiers in neuroscience* 7:128.
3. Reichmann F & Holzer P (2016) Neuropeptide Y: A stressful review. *Neuropeptides* 55:99-109.
4. Teicher MH, Samson JA, Anderson CM, & Ohashi K (2016) The effects of childhood maltreatment on brain structure, function and connectivity. *Nat Rev Neurosci* 17(10):652-666.
5. Gilbert SF (2000) *Developmental Biology*. (Sinauer Associates, Sunderland (MA)).
6. Fusco G & Minelli A (2010) Phenotypic plasticity in development and evolution: facts and concepts. Introduction. *Philosophical transactions of the Royal Society of London. Series B, Biological sciences* 365(1540):547-556.

7. Janzen FJ & Phillips PC (2006) Exploring the evolution of environmental sex determination, especially in reptiles. *J Evol Biol* 19(6):1775-1784.
8. Woodward DE & Murray JD (1993) On the effect of temperature-dependent sex determination on sex ratio and survivorship in crocodilians. *Proceedings of the Royal Society of London. Series B: Biological Sciences* 252(1334):149.
9. Newman RA (1992) Adaptive plasticity in amphibian metamorphosis. *BioScience* 42(9):671-678.
10. Cassada RC & Russell RL (1975) The dauerlarva, a post-embryonic developmental variant of the nematode *Caenorhabditis elegans*. *Developmental biology* 46(2):326-342.
11. Fielenbach N & Antebi A (2008) *Caenorhabditis elegans* dauer formation and the molecular basis of plasticity. *Genes & development* 22(16):2149-2165.
12. Golden JW & Riddle DL (1984) The *Caenorhabditis elegans* dauer larva: developmental effects of pheromone, food, and temperature. *Developmental biology* 102(2):368-378.
13. Schaedel ON, Gerisch B, Antebi A, & Sternberg PW (2012) Hormonal signal amplification mediates environmental conditions during development and controls an irreversible commitment to adulthood. *PLoS biology* 10(4):e1001306.

14. Wadsworth WG & Riddle DL (1989) Developmental regulation of energy metabolism in *Caenorhabditis elegans*. *Developmental biology* 132(1):167-173.
15. Oriordan VB & Burnell AM (1990) Intermediary metabolism in the dauer larva of the nematode *Caenorhabditis-Elegans*. 2. The Glyoxylate Cycle and Fatty-Acid Oxidation. *Comp Biochem Phys B* 95(1):125-130.
16. Albert PS & Riddle DL (1983) Developmental alterations in sensory neuroanatomy of the *Caenorhabditis elegans* dauer larva. *The Journal of comparative neurology* 219(4):461-481.
17. Schroeder NE, *et al.* (2013) Dauer-specific dendrite arborization in *Caenorhabditis elegans* is regulated by KPC-1/Furin. *Current Biology* 23(16):1527-1535.
18. Hallem EA, *et al.* (2011) A sensory code for host seeking in parasitic nematodes. *Current biology : CB* 21(5):377-383.
19. Lee H, *et al.* (2012) Nictation, a dispersal behavior of the nematode *Caenorhabditis elegans*, is regulated by IL2 neurons. *Nature neuroscience* 15(1):107-112.
20. Vanfleteren JR & Braeckman BP (1999) Mechanisms of life span determination in *Caenorhabditis elegans*. *Neurobiol Aging* 20(5):487-502.

21. Klass M & Hirsh D (1976) Non-ageing developmental variant of *Caenorhabditis elegans*. *Nature* 260(5551):523-525.
22. Erkut C, *et al.* (2013) Molecular strategies of the *Caenorhabditis elegans* dauer larva to survive extreme desiccation. *PloS one* 8(12):e82473.
23. Gerstein MB, *et al.* (2010) Integrative analysis of the *Caenorhabditis elegans* genome by the modENCODE project. *Science* 330(6012):1775-1787.
24. Wang J & Kim SK (2003) Global analysis of dauer gene expression in *Caenorhabditis elegans*. *Development* 130(8):1621-1634.
25. Karp X (2016) Working with dauer larvae. *WormBook : the online review of Caenorhabditis elegans biology*:1-19.
26. Husson SJ & Schoofs L (2007) Altered neuropeptide profile of *Caenorhabditis elegans* lacking the chaperone protein 7B2 as analyzed by mass spectrometry. *FEBS letters* 581(22):4288-4292.
27. Li C & Kim K (2014) Family of FLP peptides in *Caenorhabditis elegans* and related nematodes. *Frontiers in endocrinology* 5:150.
28. Pierce SB, *et al.* (2001) Regulation of DAF-2 receptor signaling by human insulin and *ins-1*, a member of the unusually large and diverse *Caenorhabditis elegans* insulin gene family. *Genes & development* 15(6):672-686.

29. Jia K, Albert PS, & Riddle DL (2002) DAF-9, a cytochrome P450 regulating *Caenorhabditis elegans* larval development and adult longevity. *Development* 129(1):221-231.
30. Motola DL, *et al.* (2006) Identification of ligands for DAF-12 that govern dauer formation and reproduction in *Caenorhabditis elegans*. *Cell* 124(6):1209-1223.
31. Gerisch B, Weitzel C, Kober-Eisermann C, Rottiers V, & Antebi A (2001) A hormonal signaling pathway influencing *Caenorhabditis elegans* metabolism, reproductive development, and life span. *Developmental cell* 1(6):841-851.
32. Sulston JE & Horvitz HR (1977) Post-embryonic cell lineages of the nematode, *Caenorhabditis elegans*. *Developmental biology* 56(1):110-156.
33. Marinov GK, *et al.* (2014) From single-cell to cell-pool transcriptomes: stochasticity in gene expression and RNA splicing. *Genome research* 24(3):496-510.
34. Miura F, *et al.* (2008) Absolute quantification of the budding yeast transcriptome by means of competitive PCR between genomic and complementary DNAs. *BMC genomics* 9:574.
35. Aken BL, *et al.* (2016) The Ensembl gene annotation system. *Database (Oxford)* 2016.

36. Howe KL, *et al.* (2016) WormBase 2016: expanding to enable helminth genomic research. *Nucleic Acids Res* 44(D1):D774-780.
37. Anders S & Huber W (2010) Differential expression analysis for sequence count data. *Genome biology* 11(10):R106.
38. Anders S, *et al.* (2013) Count-based differential expression analysis of RNA sequencing data using R and Bioconductor. *Nat Protoc* 8(9):1765-1786.
39. Jones SJ, *et al.* (2001) Changes in gene expression associated with developmental arrest and longevity in *Caenorhabditis elegans*. *Genome research* 11(8):1346-1352.
40. Futschik ME & Carlisle B (2005) Noise-robust soft clustering of gene expression time-course data. *J Bioinform Comput Biol* 3(4):965-988.
41. Kumar L & M EF (2007) Mfuzz: a software package for soft clustering of microarray data. *Bioinformatics* 2(1):5-7.
42. Kanehisa M, Furumichi M, Tanabe M, Sato Y, & Morishima K (2017) KEGG: new perspectives on genomes, pathways, diseases and drugs. *Nucleic Acids Res* 45(D1):D353-D361.
43. Kanehisa M & Goto S (2000) KEGG: kyoto encyclopedia of genes and genomes. *Nucleic Acids Res* 28(1):27-30.



44. Kanehisa M, Sato Y, Kawashima M, Furumichi M, & Tanabe M (2016) KEGG as a reference resource for gene and protein annotation. *Nucleic Acids Res* 44(D1):D457-462.
45. Mi H, *et al.* (2017) PANTHER version 11: expanded annotation data from Gene Ontology and Reactome pathways, and data analysis tool enhancements. *Nucleic Acids Res* 45(D1):D183-D189.
46. Kaplan F, *et al.* (2011) Ascaroside expression in *Caenorhabditis elegans* is strongly dependent on diet and developmental stage. *PloS one* 6(3):e17804.
47. von Reuss SH, *et al.* (2012) Comparative metabolomics reveals biogenesis of ascarosides, a modular library of small-molecule signals in *C. elegans*. *J Am Chem Soc* 134(3):1817-1824.
48. Li C & Kim K (2008) Neuropeptides. *WormBook : the online review of C. elegans biology*:1-36.
49. Cohen M, *et al.* (2009) Coordinated regulation of foraging and metabolism in *Caenorhabditis elegans* by RFamide neuropeptide signaling. *Cell metabolism* 9(4):375-385.
50. Lee D, Lee H, Kim N, Lim DS, & Lee J (2017) Regulation of a hitchhiking behavior by neuronal insulin and TGF-beta signaling in the nematode *Caenorhabditis elegans*. *Biochem Biophys Res Commun* 484(2):323-330.

51. Braeckman BP, Houthoofd K, & Vanfleteren JR (2009) Intermediary metabolism. *WormBook : the online review of Caenorhabditis elegans biology*:1-24.
52. Ghosh S & Sternberg PW (2014) Spatial and molecular cues for cell outgrowth during *Caenorhabditis elegans* uterine development. *Developmental biology* 396(1):121-135.
53. Gupta BP, Hanna-Rose W, & Sternberg PW (2012) Morphogenesis of the vulva and the vulval-uterine connection. *WormBook : the online review of Caenorhabditis elegans biology*:1-20.
54. L'Hernault SW (2006) Spermatogenesis. *WormBook : the online review of Caenorhabditis elegans biology*:1-14.
55. Hobert O (2013) The neuronal genome of *Caenorhabditis elegans*. *WormBook : the online review of Caenorhabditis elegans biology*:1-106.
56. Kim Y, Bark S, Hook V, & Bandeira N (2011) NeuroPedia: neuropeptide database and spectral library. *Bioinformatics* 27(19):2772-2773.
57. Lindberg I, Tu B, Muller L, & Dickerson IM (1998) Cloning and functional analysis of *Caenorhabditis elegans* 7B2. *DNA and cell biology* 17(8):727-734.
58. Sieburth D, et al. (2005) Systematic analysis of genes required for synapse structure and function. *Nature* 436(7050):510-517.

59. Shen LL, Wang Y, & Wang DY (2007) Involvement of genes required for synaptic function in aging control in *Caenorhabditis elegans*. *Neuroscience bulletin* 23(1):21-29.
60. Kiontke K & Sudhaus W (2006) Ecology of *Caenorhabditis* species. *WormBook : the online review of Caenorhabditis elegans biology*:1-14.
61. Felix MA & Braendle C (2010) The natural history of *Caenorhabditis elegans*. *Current biology : CB* 20(22):R965-969.
62. Hallem EA & Sternberg PW (2008) Acute carbon dioxide avoidance in *Caenorhabditis elegans*. *Proceedings of the National Academy of Sciences of the United States of America* 105(23):8038-8043.
63. Krumsiek J, Arnold R, & Rattei T (2007) Gepard: a rapid and sensitive tool for creating dotplots on genome scale. *Bioinformatics* 23(8):1026-1028.
64. Smith ES, Martinez-Velazquez L, & Ringstad N (2013) A chemoreceptor that detects molecular carbon dioxide. *Journal of Biological Chemistry* 288(52):37071-37081.
65. Kim K & Li C (2004) Expression and regulation of an FMRFamide-related neuropeptide gene family in *Caenorhabditis elegans*. *J Comp Neurol* 475(4):540-550.

66. Ringstad N & Horvitz HR (2008) FMRFamide neuropeptides and acetylcholine synergistically inhibit egg-laying by *Caenorhabditis elegans*. *Nature neuroscience* 11(10):1168-1176.
67. Viney ME (2009) How did parasitic worms evolve? *BioEssays : news and reviews in molecular, cellular and developmental biology* 31(5):496-499.
68. Okumura E & Yoshiga T (2014) Host orientation using volatiles in the phoretic nematode *Caenorhabditis japonica*. *J Exp Biol* 217(18):3197-3199.
69. McCoy CJ, *et al.* (2014) New insights into the FLPerGic complements of parasitic nematodes: informing deorphanisation approaches. *EuPA open proteomics* 3:262-272.
70. Choi YJ, *et al.* (2011) A deep sequencing approach to comparatively analyze the transcriptome of lifecycle stages of the filarial worm, *Brugia malayi*. *PLoS neglected tropical diseases* 5(12):e1409.
71. Cotton JA, *et al.* (2014) The genome and life-stage specific transcriptomes of *Globodera pallida* elucidate key aspects of plant parasitism by a cyst nematode. *Genome biology* 15(3):R43.
72. Schwarz EM, *et al.* (2015) The genome and transcriptome of the zoonotic hookworm *Ancylostoma ceylanicum* identify infection-specific gene families. *Nature genetics* 47(4):416-422.

73. Stoltzfus JD, Minot S, Berriman M, Nolan TJ, & Lok JB (2012) RNAseq analysis of the parasitic nematode *Strongyloides stercoralis* reveals divergent regulation of canonical dauer pathways. *PLoS neglected tropical diseases* 6(10):e1854.
74. Bain O & Babayan S (2003) Behaviour of filariae: morphological and anatomical signatures of their life style within the arthropod and vertebrate hosts. *Filaria journal* 2(1):16.
75. Felix MA & Duveau F (2012) Population dynamics and habitat sharing of natural populations of *Caenorhabditis elegans* and *C. briggsae*. *BMC biology* 10:59.
76. Nusbaum MP, Blitz DM, Swensen AM, Wood D, & Marder E (2001) The roles of co-transmission in neural network modulation. *Trends in neurosciences* 24(3):146-154.
77. Salio C, Lossi L, Ferrini F, & Merighi A (2006) Neuropeptides as synaptic transmitters. *Cell Tissue Res* 326(2):583-598.
78. Landgraf R & Neumann ID (2004) Vasopressin and oxytocin release within the brain: a dynamic concept of multiple and variable modes of neuropeptide communication. *Frontiers in neuroendocrinology* 25(3-4):150-176.

79. Bargmann CI (2012) Beyond the connectome: how neuromodulators shape neural circuits. *BioEssays : news and reviews in molecular, cellular and developmental biology* 34(6):458-465.
80. Jekely G (2013) Global view of the evolution and diversity of metazoan neuropeptide signaling. *Proceedings of the National Academy of Sciences of the United States of America* 110(21):8702-8707.
81. Dockray GJ (2004) The expanding family of -RFamide peptides and their effects on feeding behaviour. *Experimental physiology* 89(3):229-235.
82. Elphick MR & Mirabeau O (2014) The evolution and variety of RFamide-type neuropeptides: insights from deuterostomian invertebrates. *Frontiers in endocrinology* 5:93.
83. Cardoso JC, Felix RC, Fonseca VG, & Power DM (2012) Feeding and the rhodopsin family g-protein coupled receptors in nematodes and arthropods. *Frontiers in endocrinology* 3:157.
84. Guillermin ML, Castelletto ML, & Hallem EA (2011) Differentiation of carbon dioxide-sensing neurons in *Caenorhabditis elegans* requires the ETS-5 transcription factor. *Genetics* 189(4):1327-1339.
85. White JG, Southgate E, Thomson JN, & Brenner S (1986) The structure of the nervous system of the nematode *Caenorhabditis elegans*. *Philosophical transactions of the Royal Society of London. Series B, Biological sciences* 314(1165):1-340.

86. Dalzell JJ, McMaster S, Fleming CC, & Maule AG (2010) Short interfering RNA-mediated gene silencing in *Globodera pallida* and *Meloidogyne incognita* infective stage juveniles. *International journal for parasitology* 40(1):91-100.
87. Morris R, *et al.* (2017) A neuropeptide modulates sensory perception in the entomopathogenic nematode *Steinernema carpocapsae*. *PLoS Pathog* 13(3):e1006185.
88. Sudhaus W (2010) Preadaptive plateau in Rhabditida (Nematoda) allowed the repeated evolution of zooparasites, with an outlook on evolution of life cycles within Spiroascarida. *Palaeodiversity* 3, Supplement:117-130.
89. De Ley P (2006) A quick tour of nematode diversity and the backbone of nematode phylogeny. *WormBook : the online review of Caenorhabditis elegans biology*:1-8.
90. Han Z, Boas S, & Schroeder NE (2015) Unexpected variation in neuroanatomy among diverse nematode species. *Front Neuroanat* 9:162.
91. Brenner S (1974) The genetics of *Caenorhabditis elegans*. *Genetics* 77(1):71-94.
92. Mello C & Fire A (1995) DNA transformation. *Methods in cell biology* 48:451-482.

93. Maduro M & Pilgrim D (1995) Identification and cloning of *unc-119*, a gene expressed in the *Caenorhabditis elegans* nervous system. *Genetics* 141(3):977-988.
94. Arribere JA, *et al.* (2014) Efficient marker-free recovery of custom genetic modifications with CRISPR/Cas9 in *Caenorhabditis elegans*. *Genetics* 198(3):837-846.
95. Wickham H (2009) *ggplot2: Elegant Graphics for Data Analysis* (Springer-Verlag New York).
96. Yu G, Wang LG, Han Y, & He QY (2012) clusterProfiler: an R package for comparing biological themes among gene clusters. *OMICS* 16(5):284-287.
97. Warnes GR, *et al.* (2016) gplots: Various R programming tools for plotting data.
98. Neuwirth E (2014) RColorBrewer: ColorBrewer Palettes. R package version 1.1-2.
99. Jones E, Oliphant T, & Peterson P (2001) SciPy: open source scientific tools for Python.
100. Bray NL, Pimentel H, Melsted P, & Pachter L (2016) Near-optimal probabilistic RNA-seq quantification. *Nature biotechnology* 34(5):525-527.
101. Pachter L (2011) Models for transcript quantification from RNA-Seq. *arXiv*. eprint arXiv:1104.3889(eprint arXiv:1104.3889):eprint arXiv:1104.3889.



102. Golden JW & Riddle DL (1984) A pheromone-induced developmental switch in *Caenorhabditis elegans*: Temperature-sensitive mutants reveal a wild-type temperature-dependent process. *Proceedings of the National Academy of Sciences of the United States of America* 81(3):819-823.
103. Efron B & Tibshirani RJ (1994) *An introduction to the bootstrap* (CRC press).
104. Sivia DS & Skilling J (2006) *Data analysis: a Bayesian tutorial* (Oxford University Press).
105. Jones E, Oliphant T, & Peterson P (2001) SciPy: open source scientific tools for Python.
106. Bargmann CI, Hartweg E, & Horvitz HR (1993) Odorant-selective genes and neurons mediate olfaction in *Caenorhabditis elegans*. *Cell* 74(3):515-527.
107. McVeigh P, et al. (2005) Analysis of FMRFamide-like peptide (FLP) diversity in phylum Nematoda. *International journal for parasitology* 35(10):1043-1060.
108. Blaxter M & Koutsovoulos G (2015) The evolution of parasitism in Nematoda. *Parasitology* 142 Suppl 1:S26-39.

*Chapter 4***GENETIC MARKERS ENABLE THE VERIFICATION AND  
MANIPULATION OF THE DAUER ENTRY DECISION**

(This work was done in collaboration with Shih P.Y.)

## 4.1 Introduction

Phenotypic plasticity enables organisms to respond to changing environments through activation of different phenotypes or alternative developmental courses (1). For example, nutritional factors contribute to the development of morphological distinct ants castes in some species (2), and also influence neuronal plasticity in human (3).

*Caenorhabditis elegans* can go through two different developmental trajectories depending on the conditions of the environment. In favorable environments, they proceed from L1, L2, L3, and L4 larvae stages to reproductive adults. When the animal senses harsh stimuli, including high temperature, low food, and high amount of pheromone, L1 larva can enter an alternative pre-dauer stage, L2d, and commit to become a dauer if the unfavorable conditions persist. The dauer entry decision is a whole animal decision that involves remodeling of individual tissues to transform the entire animal to have dauer-specific physiology and behaviors. The specialized physiology, the thickened cuticle for example, makes dauer more resistant to environmental insult (4, 5), and the special behaviors enable dauers to disperse to better environments and resume reproductive development (6, 7).

Genes involved in dauer development, including genes in insulin and TGF-beta signaling pathways, have been identified through intense genetic screening (8–11). However, our knowledge regarding how the dauer entry decision is made and how the decision is coordinately executed across different tissues is still limited (12). First, it is difficult to identify L2d, the stage when environmental signals are integrated and the dauer-commitment decision is made, because of its lack of

distinct features (13). Additionally, it can be labor-intensive to look for non-dauer features in dauers that fail to coordinately remodel all the tissues. SDS sensitivity and fluorescent beads are two available tools for dauer hypodermis and pharynx selection (14, 15), but not for other tissues.

We previously reported the time-resolved gene expression profiles from animals going through dauer or reproductive development (16). From the rich dataset, we were able to find genes that are specifically regulated in either of the developmental tracks as potential readouts of the decision. Here we describe four molecular markers that can track the decision at the level of different tissues, and are predictive of the decision. We verified that the markers could also be used to drive gene expression during the dauer entry decision, and to parse incomplete dauer development phenotypes. Our findings provide strong molecular tools for studying phenotypic plasticity during a whole animal decision.

## 4.2 Results

### Dauer and reproductive markers demonstrated specific expression patterns

Unfavorable conditions promote L1 larvae to develop into pre-dauer L2d. Depending on whether the environment improves and enough dafachronic acid (DA) growth hormone gets amplified, L2d larvae can progress to either reproductive or dauer development. In our previous study, we controlled the animals' binary developmental choice by withholding or adding synthetic DA at 24 hours post hatch (hph) to *daf-9(dh6)* mutant, which lack intrinsic DA, and we profiled the transcriptional changes from animals going through dauer (L2d, dauer-committed, and dauer) or reproductive (L3-committing and L4) development (16). To find good markers for dauer, we selected candidate genes based on the following criteria: (i) genes that have high expression specifically during dauer or reproductive development; (ii) genes that are expressed in large tissues, including collagen genes, for convenient observation under low magnification; and (iii) genes that might shed light on dauer biology, including transcription factors and unknown genes.

First, 156 of 164 genes in the collagen (*col*) family were detected and differentially expressed in the RNA-seq dataset. Within those, five collagen genes (*col-2*, *col-37*, *col-85*, *col-40* and *col-183*) have the highest transcripts per million (tpm) counts at the dauer-commitment, while having low counts in other stages (**Figure 4.1**). Indeed, *col-2* and *col-40* have previously been reported to have specific expression in dauer (16, 22). We made a *col-183p::mcherry*

transcriptional reporter strain, and we observed strong mCherry expression exclusively in dauer but not other stages (**Figure 4.2A-C**). *col-85* also has similarly high dauer expression, but dauers expressing *col-85p::mcherry* were abnormally sensitive to SDS treatment (data not shown), possibly caused by promoter quenching or toxicity. Because SDS-resistant is a standard way for selecting and verifying dauers, we excluded *col-85* in further experiments.

Second, we detected 274 transcription factor genes that are differentially expressed during dauer and reproductive development. We clustered those genes by their expression profiles, looked for dauer marker candidates, and found 119 that fit our criteria (**Figure 4.3**). We chose to focus on *ets-10*, a member of the ETS-domain family of transcription factors. The *ets-10* gene had the highest tpm counts during dauer-committed and dauer relative to other stages (**Figure 4.2D**). We observed that *ets-10* is expressed in different tissues during dauer and non-dauer (**Figure 4.2E-F** and **Figure 4.4**). During dauer, *ets-10p::gfp* was expressed in two sets of neurons and the intestine (**Figure 4.2E-F**). In non-dauers, its expression was only observed in uterine cells in L4 animals and spermatheca in adults (**Figure 4.4**).

We also investigated the transcription factor *nhr-246*. The tpm counts of *nhr-246* only increased during dauer development and was at its highest level at the dauer-commitment time point (**Figure 4.2G**). Other than intestinal expression in embryo and L1 stages, *nhr-246p::gfp* was only detected in dauer in intestine and muscle (**Figure 4.2H-I** and **Figure 4.5**).

In addition to dauer-specific genes, we also looked for genes that are downregulated specifically in dauer. Out of the five genes we tested — *asp-1*, *F53F1.4*, *sqt-3*, *dpy-13* and *col-156* — *F53F1.4* marker animals were the healthiest, and had the highest tpm reads in reproductive development (**Figure 4.6** and **Figure 4.2J**). We found that *F53F1.4p::gfp* is expressed in the hypodermis at all stages (**Figure 4.2K-L**), and the fluorescence intensity was reduced in dauer (data not shown). Because of its expression profile, we propose the gene name *led-1*, which stands for “Low Expression in Dauer”.

To sum up, we have developed three dauer markers (*col-183p::mcherry*, *ets-10p::gfp*, and *nhr-246p::gfp*) that have increased expression level and distinct expression patterns in dauers. We have also detected intensity changes in *led-1p::gfp* that mark non-dauers from dauers.

### ***col-183*, *ets-10* and *nhr-246* label the dauer commitment decision**

Because the dauer marker genes have high expression levels at dauer-commitment, we expected that the fluorescence of these genes might be useful for indicating the dauer-commitment event. If the markers do label the animals that are committed to dauer, then: (i) all dauers will have fluorescence expression (**Figure 4.7A**) and (ii) fluorescent animals will still become dauer even if the environment improves (**Figure 4.7B**). We found that the fluorescence markers were turned on in all the dauers examined (100% for all three markers strains, with 174-311 animals examined per marker) (**Figure 4.7C**). Moreover, after we transferred animals from unfavorable to favorable condition as soon as the

fluorescence was detected, we observed that 96% to 100% of the animals still entered dauer despite the shift to reproduction-promoting environment (*col-183p::mcherry* 100%, n=22; *ets-10p::gfp* 100%, n=18; *nhr-246p::gfp* 96%, n=26) (**Figure 4.7D**). These data suggest that *col-183* and *ets-10* label the dauer commitment decision, and *nhr-246* labels the decision or slightly before commitment.

### **The promoters of the dauer markers can be used to manipulate the dauer decision**

Reproductive development in *C. elegans* requires the synthesis of DA, the product of DAF-9/cytochrome P450. The timing of *daf-9* expression and the amplification of DA in the hypodermis has been shown to coincide with the critical period of time when L2d animals decide to go through reproductive instead of dauer development (23) (**Figure 4.8A-B**). However, it is not known whether ectopically expressing *daf-9* during dauer-commitment can alter developmental trajectory. We therefore used the *col-183* promoter to overexpress *daf-9* in hypodermis during dauer-commitment when *daf-9* would otherwise be expressed at its lowest (**Figure 4.8C**). We then examined the animals' decision between dauer and reproductive development under dauer-inducing conditions. We observed that animals with *daf-9* overexpression were 0.5 times as likely to become dauers compared to those with control *gfp* (*col-183p::daf-9* bootstrap mean = 30%, n = 336; *col-183p::gfp* bootstrap mean = 59%, n = 262) (**Figure 4.8D**). This data suggests that the promoters of the dauer markers can be used



to drive ectopic gene expression during dauer-commitment, and that *daf-9* hypodermal expression can shift animal development from dauer to adulthood.

### **The dauer markers can be used to study the coordination between tissues**

The dauer entry decision is a whole-animal decision, with all the tissues coordinating dauer development programs. Previous studies have identified partial dauers, where one or more of the tissues fail to coordinate and therefore exhibit non-dauer features. Known partial dauer phenotypes include continued pharyngeal pumping, indistinct dauer alae on the cuticle, and L2/L3-like pharynx, neuron, intestine, or excretory gland morphologies. For example, *daf-9(e1406)*/cytochrome P450 dauers have a non-dauer intestine, cuticle, pharynx, and neurons (24); *daf-15(m81)*/RAPTOR dauers fail to remodel the cuticle, pharynx, neurons intestine and excretory gland (24); *daf-18(e1375)*/PTEN dauers have an unremodeled, still pumping pharynx, and an intestine that is neither fully dauer nor L3 (25).

Because identifying partial dauers relies on close examination of the animal's morphology, it can be time-consuming and requires experience. We therefore utilized the dauer-specific *ets-10p::gfp* expression in neurons and intestine to pinpoint partial dauer phenotypes.

In *daf-9(e1406)* dauers, we confirmed their partial dauer phenotype in the intestine: we observed a 3-fold decrease in *ets-10p::gfp* expression in the intestine compared to wild type dauers (average intensity in wild type = 9017 arbitrary units (a.i.), n = 26; average intensity in *daf-9(e1406)* = 2998 a.i., n = 25)

(**Figure 4.9A-B** and **Figure 4.9K**), providing a clear indication of the non-dauer feature of *daf-9(e1406)* intestines.

We were also able to confirm the intestinal partial dauer phenotype of *daf-15(m81)* animals as well: we observed a 4-fold reduction in *ets-10p::gfp* intestinal expression compared to wild type (average intensity in wild type = 7166 a.i., n = 12; average intensity in *daf-15(m81)* = 1512 a.i., n = 16) (**Figure 4.9C-D** and **Figure 4.9K**). Additionally, we confirmed the neuronal partial dauer phenotype of *daf-15(m81)*, as neuronal *ets-10p::gfp* fluorescence was present in all wild type animals (n=20), but was undetectable (16 out of 20 animals) or dimly expressed (4 out of 20) in *daf-15(m81)* (**Figure 4.9G-H** and **Figure 4.9L**).

In *daf-18(e1375)*, we observed a slight increase in *ets-10p::gfp* intestinal expression (average intensity in wild type = 3299 a.i., n = 11; average intensity in *daf-18(e1375)* = 5169 a.i., n = 9) (**Figure 4.9E-F** and **Figure 4.9K**), and the disappearance of neuronal expression in most of the animals (9 out of 10) (**Figure 4.9I-J** and **Figure 4.9L**). These results not only confirmed the partial dauer characteristic of *daf-18(e1375)* intestine, but also revealed the previously unknown non-dauer characteristic of *daf-18(e1375)* neurons.

From our results, we have identified *ets-10p::gfp* as a tool for studying the execution of the dauer decision in different tissues. We propose a model for how *ets-10* expression is differentially regulated in the dauer intestine and neurons by DAF-9, DAF-15 and DAF-18 (**Figure 4.9M**). In the dauer intestine, DAF-15 and DAF-9 promote *ets-10* expression and DAF-18 inhibit *ets-10*; both DAF-15 and DAF-18, but not DAF-9, positively regulate *ets-10* expression in the dauer

nervous system. This model suggests that the same signal (e.g. DA produced by DAF-9/cytochrome P450) can have distinct effects on the differentiation of different tissues in dauer.

### 4.3 Discussion

We have described four genetic markers that label dauer or non-dauer animals, and which can be used for conveniently assaying the dauer entry decision. We demonstrated that the dauer markers in fact mark the dauer-commitment decision using condition-shift experiments. Beyond fluorescence labeling, we were able to use the promoter region to manipulate the commitment decision, and to tease apart the tissue-specific defects of partial dauer mutants.

We picked members of the hypodermis-expressed collagen gene family as one of our dauer marker candidates because they fit our criteria of being expressed at high levels and in a large tissue. In addition, they offered the opportunity to learn more about the role of hypodermal *daf-9* expression in the developmental decision. When animals commit to reproductive development, *daf-9* functions by promoting a positive feedback amplification loop in the hypodermis to lock in the decision (23). Even under dauer-inducing conditions, when we introduced *daf-9* expression under the control of *col-183* promoter, we were able to shift the animal's decision toward reproduction.

Notably, dauer-specific collagen expression has been reported before for *col-2* (22), but we are the first to connect the expression of a collagen gene with the dauer-commitment decision. We speculate that the biological function of *col-183* is to shape the stress-resistance and impermeability of dauer cuticle starting from the commitment decision (4, 26).

We also looked at the transcription factor gene class for additional marker candidates. We found that both *ets-10* and *nhr-246* demonstrated dauer-specific

expression patterns during dauer-commitment, suggesting their function in execution and maintenance of the dauer program. For instance, the expression of *ets-10* and *nhr-246* in intestine might help establish the specialized intestine structure and metabolism of dauers. We speculate that they participate in remodeling the dauer intestine or switching metabolism from the TCA cycle to long-term lipid metabolism (27, 28).

The full coordination of tissue physiology and function is important for dauer survival. Using these markers, we can study how tissue-coordination is achieved during dauer development. Partial dauers represent breaks in tissue-coordination, and by using the markers we can read out their phenotypes on a molecular level. Using *ets-10* markers, we were able to not only recapitulate known partial dauer phenotypes in *daf-9*, *daf-15* and *daf-18*, but identify the previously unknown function of DAF-18 in remodeling dauer neurons. Moreover, we found that DA and insulin signals (controlled by *daf-9* and *daf-15*, *daf-18*, respectively) are combined in discrete ways to control *ets-10* expression in different tissues. It would be intriguing to figure out how different tissues might use different *cis*-regulatory elements and signaling receptors to interpret the same signal to meet their specialized needs.

We have described three dauer-specific markers and one reproductive-specific marker selected from our previously published dauer RNA-seq time course. We have demonstrated that these markers are useful for tracking the dauer-commitment decision, driving gene expression during dauer-commitment, and for teasing apart partial dauer phenotypes tissue by tissue. 117 transcription

factor genes and 6 collagen genes also fit the selection criteria we used to pick our markers. This selection opens up the exciting potential of using these genes for further tracking, manipulating, and parsing the dauer entry decision.

## 4.4 Materials and Methods

### Animal strains.

*C. elegans* strains were grown using standard protocols with the *Escherichia coli* strain OP50 as a food source (17). The wild type strain is N2 (Bristol). Other animal strains are listed below.

### Transgenic strains.

*Transcriptional reporter strains.* All of the transcriptional reporters were built using fusion PCR (18). Primers used to amplify the promoter regions and the amplified promoter sizes were as follows: *col-183p* (*col-183* promoter, 1695bp)

forward- AATCGCAAACCTTCAACGAAGAG,

reverse- tcacccttgagaccattaagcGGTTGACTGGTTGCTGTTGCT;

*ets-10p* (1111bp)

forward- GGTTGACTGGTTGCTGTTGCT,

reverse-agtcgacctgcaggcatgcaagct GTTTGTCAGCTAGTTTGCGG;

*nhr-246p* (3069bp)

forward- GTTTGTCAGCTAGTTTGCGG,

reverse- agtcgacctgcaggcatgcaagctATTGTTGAAATTGAAAATTATTTTGAA;

*F53F1.4p* (1851bp)

forward- ATTATGTAGGCCCAATATAAAGTTTGA,

reverse- agtcgacctgcaggcatgcaagct GTTGAAAATGTTGAAAGTCAAAAGAG.

The promoter regions of *ets-10*, *nhr-246* and *F53F1.4* were fused to *gfp::unc-54* 3'UTR (amplified from pPD95\_75 from Addgene), and the promoter region of

*col-183* was fused to *mCherry::unc-54* 3'UTR (amplified from pGH8 from Addgene). Injection mixture was prepared at a concentration of 20 ng/μL reporter construct, 50 ng/μL *unc-119(+)* rescue construct, and 130 ng/μL 1-kb DNA ladder carrier DNA. Transgenic strain was obtained by microinjecting the mixtures into the adult gonads of *unc-119(ed4)* animals. The *ets-10p::gfp* and *F53F1.4p::gfp* were further integrated into the genome by X-ray (19, 20). The fluorescent transcriptional reporter strains generated were as follows: PS6725 *unc-119(ed4); syEx1337[col-183p::mcherry; unc-119(+)]*; PS7127: *unc-119(ed4); syls360[ets-10p::gfp; unc-119(+)]* (outcrossed 3 times); PS7921 *unc-119(ed4); syEx1539[nhr-246p::gfp; unc-119(+)]*; PS7920 *unc-119(ed4)*; PS6724: *unc-119(ed4); syls263[F53F1.4p::gfp; unc-119(+)]* (outcrossed 10 times).

*Transcriptional reporter in partial dauer mutant backgrounds.* The strains with *ets-10p::gfp* expression in *daf-15(m81)* or *daf-9(e1406)* background were generated by crossing PS7127 with DR732 *daf-15(m81) unc-22(s7)/nT1* or AA823 *daf-9(e1406) dhEx354[sdf-9::daf-9cDNA::GFP; lin-15(+)]*. The strain with *ets-10p::gfp* expression in *daf-18(e1375)* background was obtained by microinjecting the injection mixture (20 ng/μL reporter construct, 50 ng/μL *ofm-1p::rfp* coelomocyte co-injection marker, and 130 ng/μL 1-kb DNA ladder carrier DNA) into the adult gonads of CB1375 *daf-18(e1375)*.

*daf-9 overexpression strain.* *col-183* promoter region were cloned into the pSM vector that contains *gfp* or *daf-9* cDNA. *daf-9* cDNA sequence was obtained from



Wormbase and amplified with forward primer ATGCACTTGGAGAACCGTG and reverse primer TTAGTTGATGAGACGATTTCCG. Injection mixture was prepared at a concentration of 20 ng/μL *col-183p::gfp* or *col-183p::daf-9* cDNA, 50 ng/μL *ofm-1p::rfp* coelomocyte co-injection marker, and 130 ng/μL 1-kb DNA ladder carrier DNA. Transgenic strain was obtained by microinjecting the mixtures into the adult gonads of wild type animals. The transgenic strains generated were PS7949 *syEx1628[col-183p::gfp; ofm-1p::rfp]* and PS7931 *syEx1629[col-183p::daf-9 cDNA; ofm-1p::rfp]*.

### **Dauer induction.**

The preparation of crude pheromone and the induction of dauers on pheromone plates were performed with previously described methods (16, 21). Briefly, crude pheromone plates (NGM-agar with added crude pheromone and no peptone) were used to induce synchronized dauers: For each pheromone plate, 20 μL of heat-killed OP50 (8 g/100 mL) were spotted and 12-15 young adult animals were picked onto the plate to lay eggs at 20°C for 3 (for *environmental condition shift*) or 12 hours (for examining fluorescence expression in dauer) before being removed. The plates were then moved to 25.5°C incubation for 48 hours.

### **Verification of dauer markers.**

#### *SDS assay on fluorescent animals*

Dauers induced on pheromone plate were identified by morphology and examined for the presence of fluorescence expression. The fluorescence animals were

further transferred to unseeded plates and treated with 1% SDS. The numbers of total and survived animals were scored after 15 minutes.

*Environmental condition shift of fluorescent animals.*

The fluorescence expression in the transcriptional reporter strains was detectable under dissecting microscope staring around 30-32 hours after egg laid. At 33-34 hour, we transferred the fluorescent animals from dauer-inducing pheromone plates to reproduction-inducing plates, which contain high amount of bacteria and no pheromone. 24 hours after the transfer, the animals were treated with 1% SDS, and the numbers of total and survived animals were scored after 15 minutes.

**Quantification of fluorescence intensity.**

The fluorescence intensity of *ets-10p::gfp* was measured using ZEISS ZEN microscope software. The regions of interests were drawn on both the intestine and the background area, and the net fluorescence intensity was calculated as the subtraction of the two measurements.

**Dauer formation assay.**

The preparation of crude pheromone and the dauer entry assay were performed with previously described methods (16, 21). On the day of the experiment, seven to ten young adults were picked onto each pheromone plate (NGM-agar with added crude pheromone and no peptone), and allowed to lay approximately 50-60 eggs before being removed. 20 µl of heat-killed OP50 was added to the plates as

a food source for the un-hatched larvae. After 48 hours of incubation at 25.5°C, dauers and non-dauers were counted on each plate based on their distinct morphologies. The permutation test was used to calculate statistics as previously describe (16).

#### 4.5 Figures

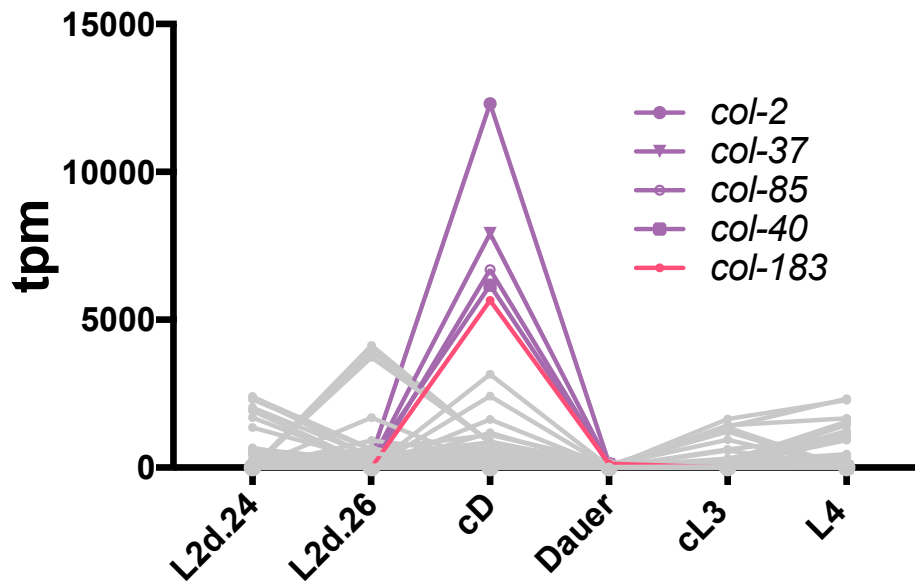


**Figure 4.1. Expression profiles of collagen genes**

Expression profiles of all the collagen genes detected. Each line represents one collagen gene. The top five genes with the highest expression level were highlighted in purple (*col-2*, *col-37*, *col-85*, and *col-40*) and pink (*col-183*). The rest of the genes were colored in grey for simplicity. All the expression data plotted were from our previous paper (16).

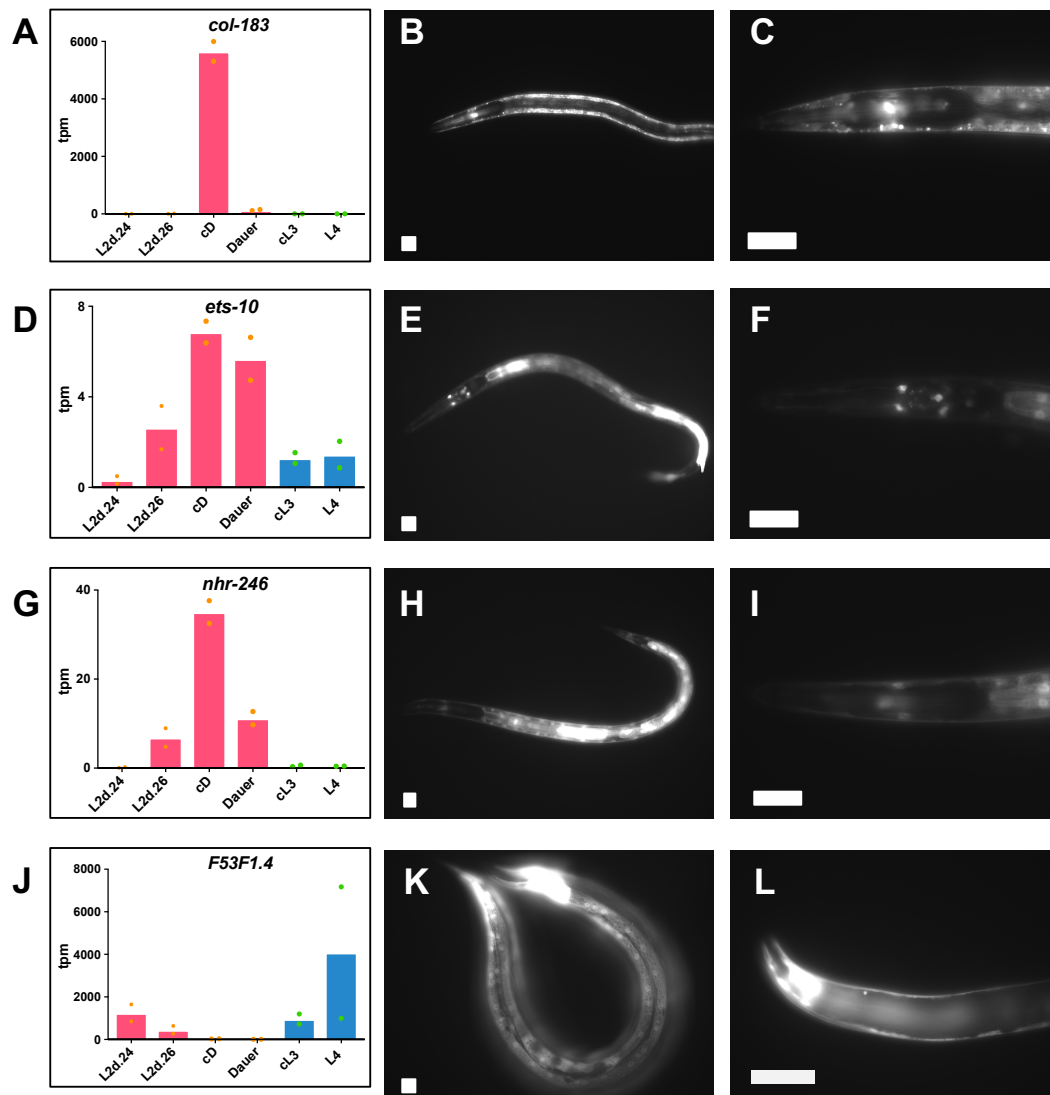


**Figure 4.2. *col-183*, *ets-10*, *nhr-246* and *led-1(F53F1.4)* Genetic markers demonstrates dauer- or reproductive-specific expression pattern**

**(A-C) *col-183*:** detected read counts of the *col-183* gene across developmental stages **(A)**, and fluorescence images of the *col-183* expression pattern in dauer **(B-C)**. **(D-F) *ets-10*:** detected read counts of the *ets-10* gene across developmental stages **(D)**, and fluorescence images of the *ets-10* expression pattern in dauer **(E-**

**F). (G-I) *nhr-246*:** detected read counts of the *nhr-246* gene across developmental stages **(G)**, and fluorescence images of the *nhr-246* expression pattern in dauer **(H-I)**. **(J-L) *led-1(F53F1.4)*:** detected read counts of the *F53F1.4* gene across developmental stages **(J)**, and fluorescence images of the *led-1(F53F1.4)* expression pattern in dauer **(L)**. In read count figures **(A, D, G, and J)**, points indicate the values from each sequenced replicate, and the bar height represents the mean count value for each developmental stage. Red and blue bars represent dauer and reproductive development, respectively. tpm, transcripts per million; L2d.24, L2d at 24 hours post hatch (hph); L2d.26, L2d at 26 hph; cD, dauer-committed; cL3, L3-committing. All the plotted read counts data were from Lee and Shih *et al.* (16). Scale bar: 0.1mm.

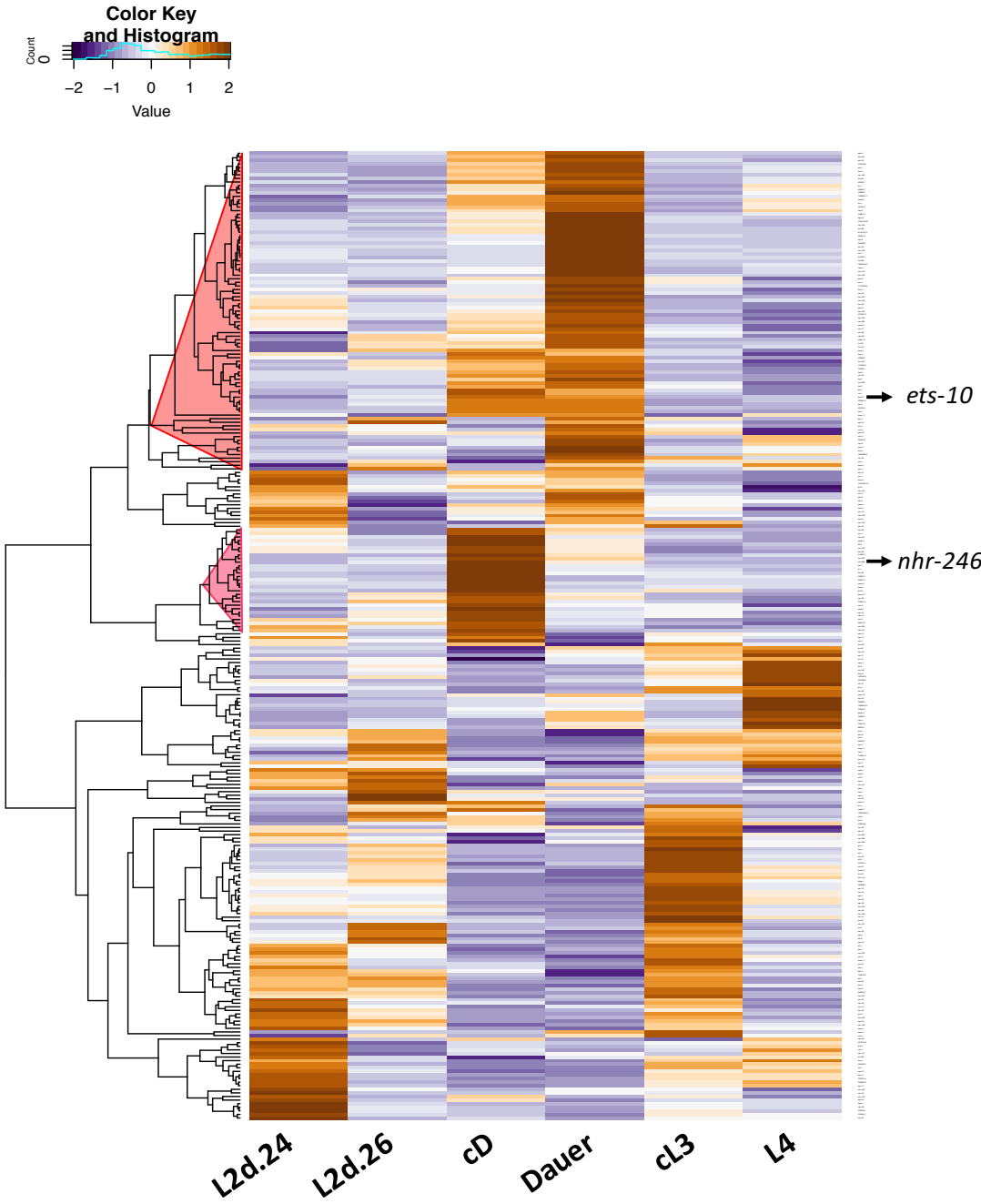


**Figure 4.3 Expression profiles of transcription factors**

The expression profiles of genes encoding transcription factors were scaled and plotted on the heatmap. High and low expression level were shown in brown and purple color, respectively. Each row represents one single gene, and the genes were clustered based on their expression patterns. *ets-10* and *nhr-246* belong to the two gene clusters that have increased expression in dauer and dauer-committed (cD) stage, respectively. The heatmap was generated using packages in R, as described previously (16).



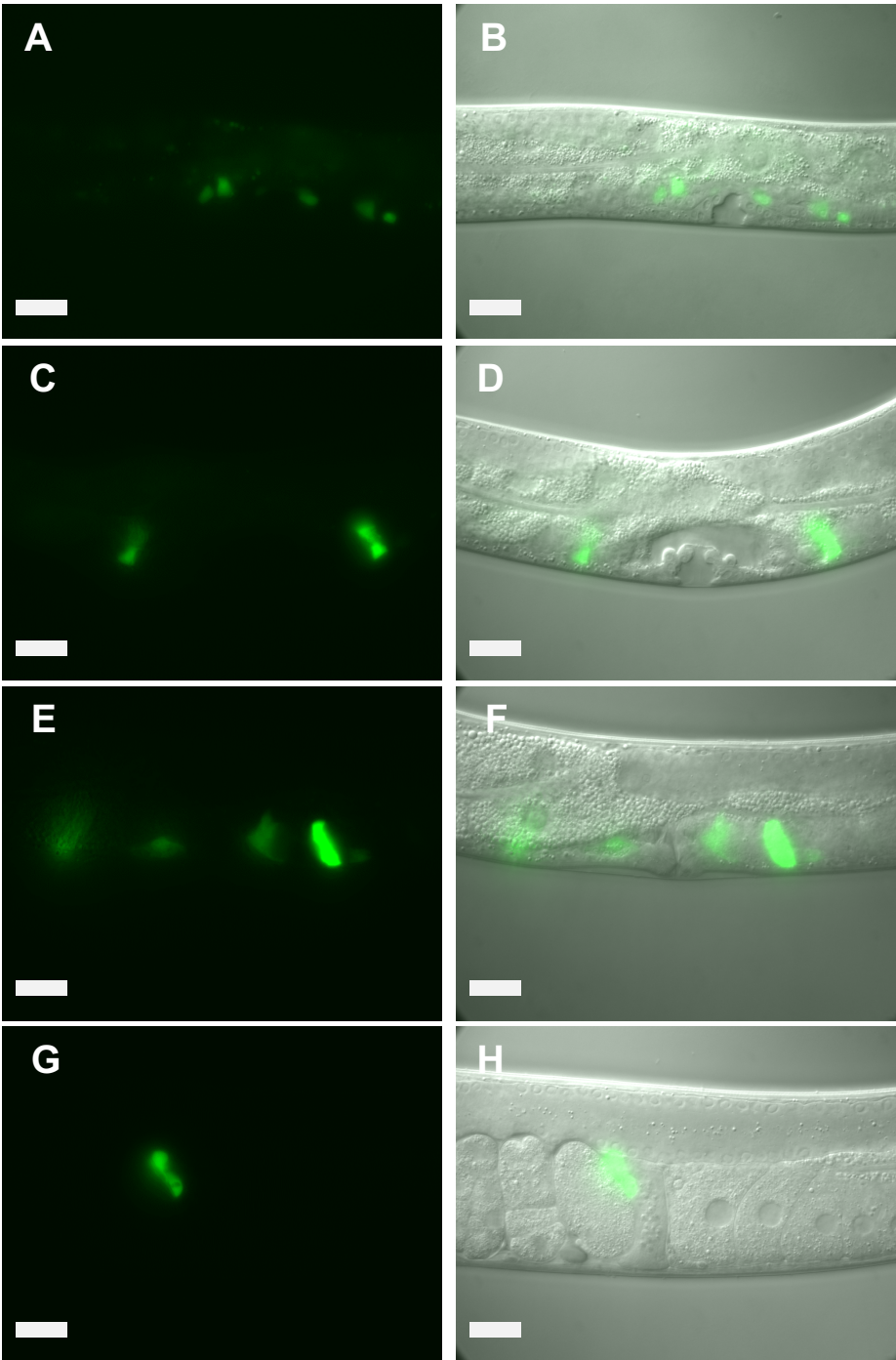


**Figure 4.4. *ets-10* expression pattern in non-dauer stages (L4-adult)**

Fluorescence (**A, C, E, and G**), and the corresponding brightfield and fluorescence merged images (**B, D, F, and H**) of *ets-10* across different life stages: early-mid L4 (**A-B**), mid-L4 (**C-D**), L4 lethargus (**E-F**) and adult (**G-H**). Scale bar: 0.02mm.

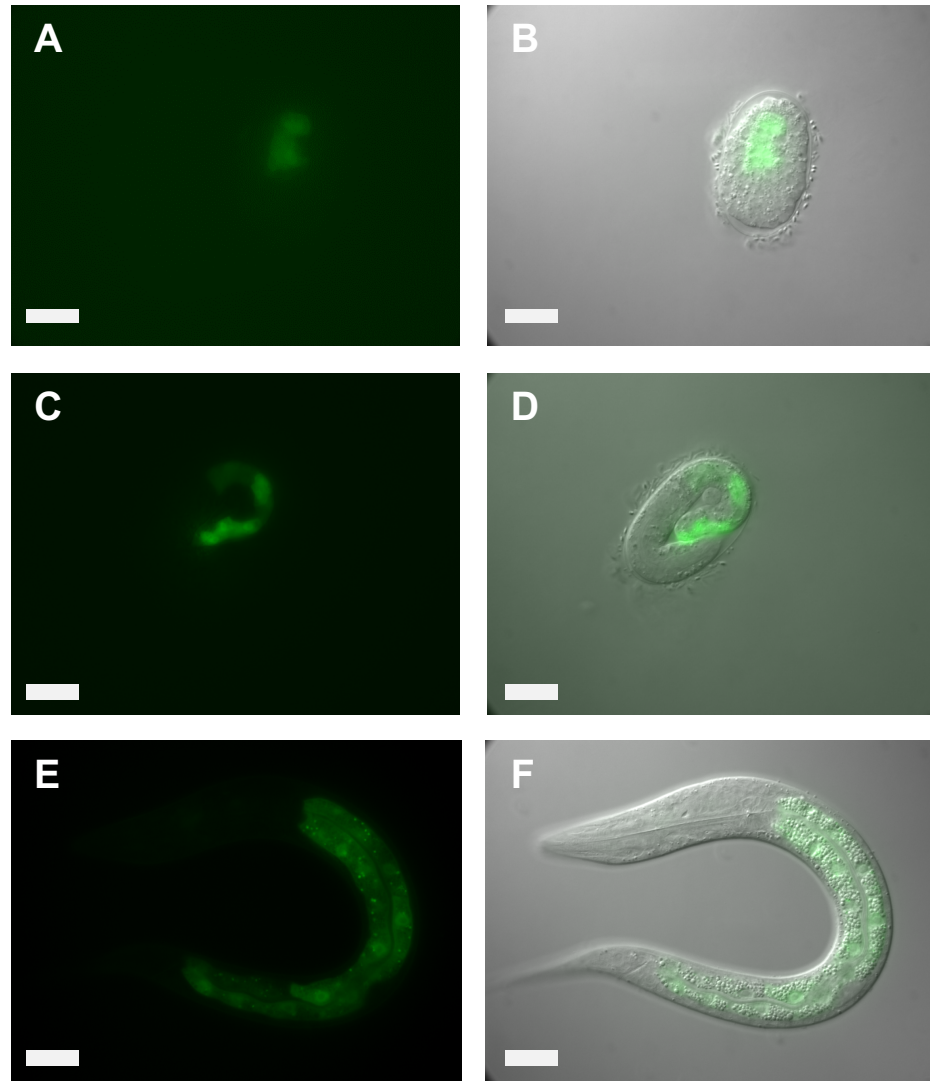


**Figure 4.5. *nhr-246* expression pattern in non-dauer stage (embryo-L1)**

Fluorescence (A, C, and E), and the corresponding brightfield and fluorescence merged images (B, D, and F) of *nhr-246* across different life stages: embryo (A-D) and L1 (E-F). Scale bar: 0.02mm.

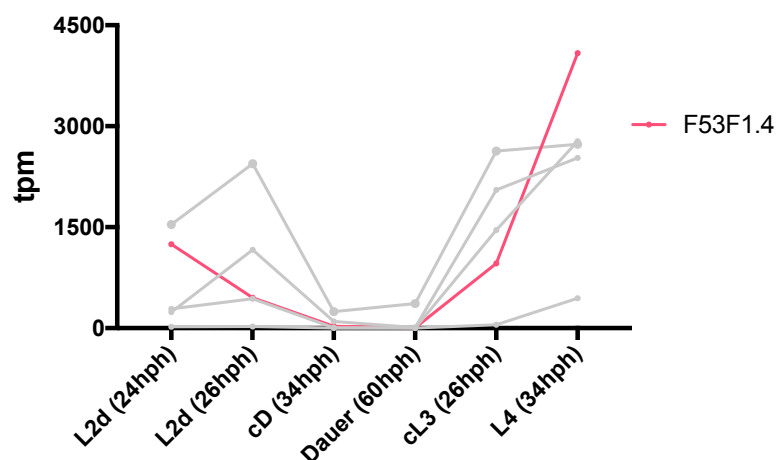


**Figure 4.6. Expression profiles of genes that are down-regulated in dauer**

Expression profiles of genes that are down-regulated specifically in dauer. Each line represents the average read counts of one single gene across different stages. *led-1(F53F1.4)*, the one we studied, was labeled in pink, and the rest of the genes were colored in grey for simplicity.

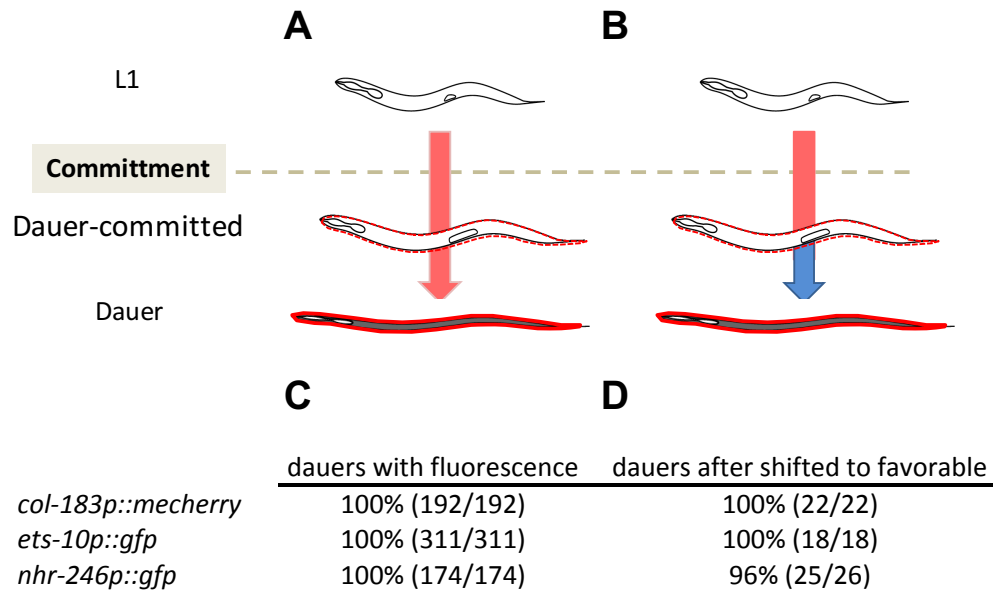


**Figure 4.7. The appearance of fluorescence correlates with the dauer-commitment decision and stays on in dauer**

**(A-B)** Cartoon diagram showing the experimental design with red hypodermal marker as an example. The red and blue arrows indicate the developmental progression in unfavorable and favorable conditions, respectively. **(C-D)** The results from each of the marker strains. The numbers in parentheses represent the number of animals with positive results / total number of animals tested.

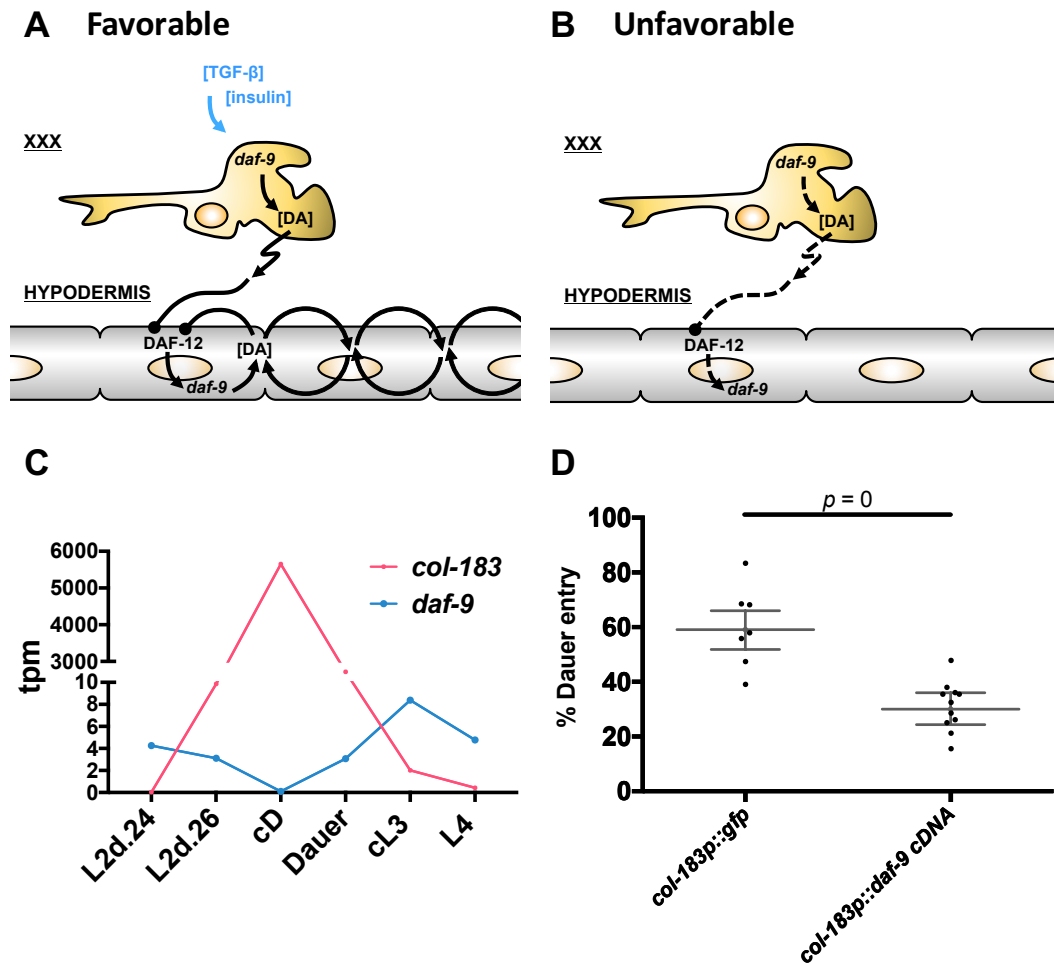


**Figure 4.8. Overexpressing *daf-9* in the hypodermis during commitment increases the reproduction decision**

**(A-B)** Cartoon diagram showing the amplification of dafachornic acid in hypodermis through TGF-beta and insulin signaling under favorable condition **(A)**, and the lack of dafachornic acid amplification in dauer-inducing environment **(B)**.

**(C)** Average detected read counts of the *col-183* and *daf-9* gene across developmental stages. **(D)** Dauer entry assay on animals with *col-183* promoter driving expression of *gfp* or *daf-9* cDNA. The long horizontal line indicates the

bootstrapped mean, and the error bar shows the 99% confidence intervals. Each dot is one trial, and the data were collected from at least three different days. Statistics: permutation test. XXX: XXX cell; DA, dafachronic acid; tpm, transcripts per million.

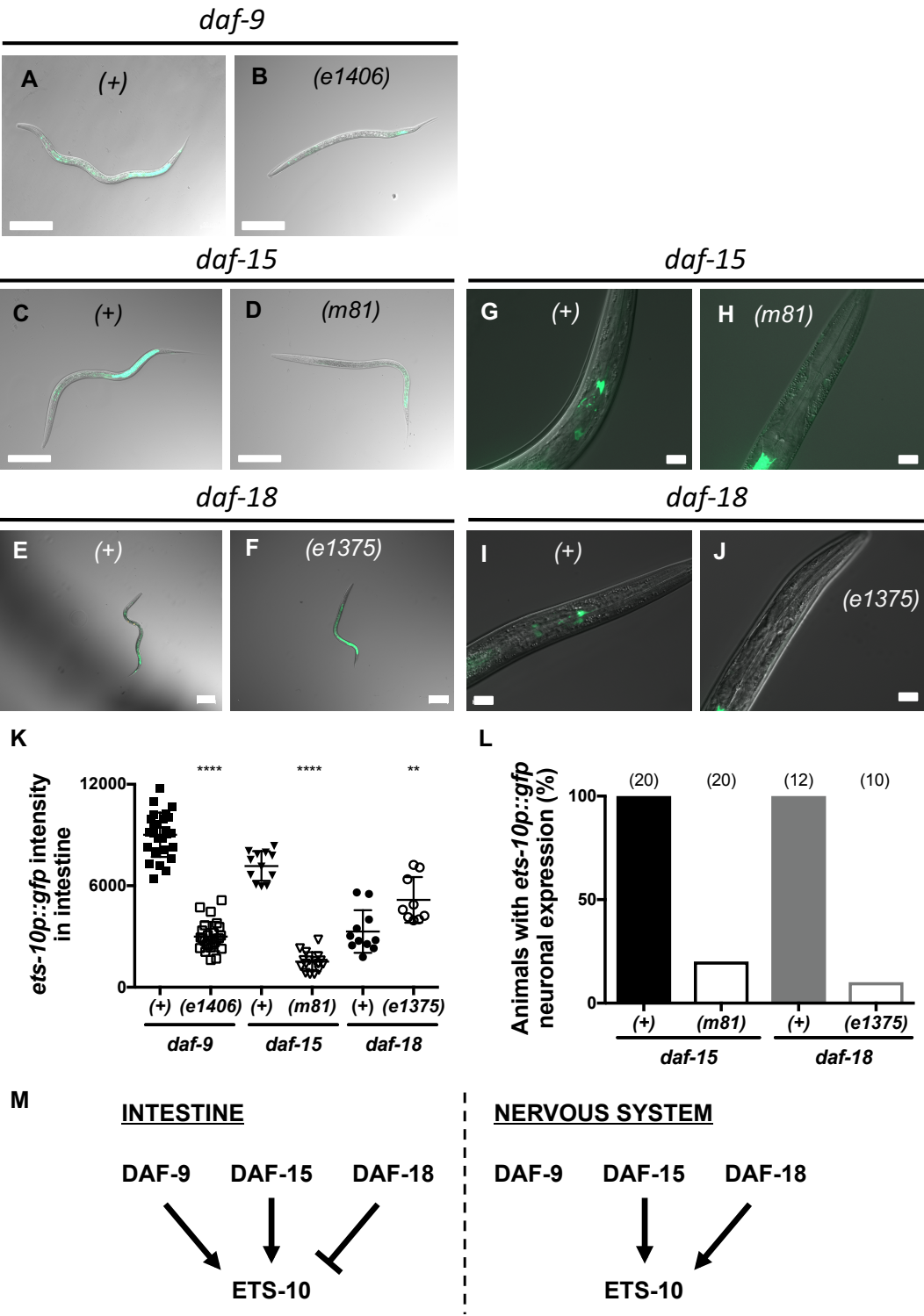




#### Figure 4.9. Partial dauers mis-express dauer markers

**(A-J)** Representative images of *ets-10p::gfp* expression pattern in wild type **(A, C, E, G and I)**, *daf-9(e1406)* **(B)**, *daf-15(m81)* **(D and H)**, *daf-18(e1375)* **(F and J)** animals. **(K)** Quantification of *ets-10p::gfp* intestinal fluorescence intensity in wild type, *daf-9(e1406)* and *daf-15(m81)* animals. Each dot represented one animal. The error bars showed standard deviation. Statistic: nonparametric two-tailed t test. \*\*\*\*  $p < 0.0001$ ; \*\*  $p < 0.01$  **(L)** The percentage of wild type, *daf-15(m81)* and *daf-18(e1375)* animals with *ets-10p::gfp* neuronal expression. The number in parenthesis indicates the number of animals examined. **(M)** A proposed model for how DAF-9, DAF-15, and DAF-18 influence ETS-10 expression in the intestine and nervous system. Scale bar: 100um **(A-F)** and 10um **(G-J)**.

#### 4.6 References

1. Kelly SA, Panhuis TM, Stoeckl AM (2012) Phenotypic plasticity: molecular mechanisms and adaptive significance. *Comprehensive Physiology* 2(2):1417–39.
2. Schwander T, Lo N, Beekman M, Oldroyd BP, Keller L (2010) Nature versus nurture in social insect caste differentiation. *Trends in ecology & evolution* 25(5):275–82.
3. Nithianantharajah J, Hannan AJ (2006) Enriched environments, experience-dependent plasticity and disorders of the nervous system. *Nature reviews Neuroscience* 7(9):697–709.
4. Cox GN, Staprans S, Edgar RS (1981) The cuticle of *Caenorhabditis elegans*. II. Stage-specific changes in ultrastructure and protein composition during postembryonic development. *Developmental biology* 86(2):456–70.
5. Page AP, Johnstone IL (2007) The cuticle. *WormBook*:1–15.
6. Hallem EA, et al. (2011) A sensory code for host seeking in parasitic nematodes. *Current biology : CB* 21(5):377–83.
7. Lee H, et al. (2011) Nictation, a dispersal behavior of the nematode *Caenorhabditis elegans*, is regulated by IL2 neurons. *Nature neuroscience* 15(1):107–12.

8. Fielenbach N, Antebi A (2008) *Caenorhabditis elegans* formation and the molecular basis of plasticity. *Genes & development* 22(16):2149–65.
9. Ren P, et al. (1996) Control of *Caenorhabditis elegans* larval development by neuronal expression of a TGF-beta homolog. *Science* 274(5291):1389–1391.
10. Li W, Kennedy SG, Ruvkun G (2003) *daf-28* encodes a *Caenorhabditis elegans* insulin superfamily member that is regulated by environmental cues and acts in the DAF-2 signaling pathway. *Genes Dev* 17(7):844–858.
11. Schackwitz WS, Inoue T, Thomas JH (1996) Chemosensory neurons function in parallel to mediate a pheromone response in *Caenorhabditis elegans*. *Neuron* 17(4):719–728.
12. Androwski RJ, Flatt KM, Schroeder NE (2017) Phenotypic plasticity and remodeling in the stress-induced *Caenorhabditis elegans* dauer. *Wiley interdisciplinary reviews Developmental biology*. doi:10.1002/wdev.278.
13. Karp X (2018) Working with dauer larvae. *WormBook*:1–19.
14. Cassada RC, Russell RL (1975) The dauerlarva, a post-embryonic developmental variant of the nematode *Caenorhabditis elegans*. *Developmental biology* 46(2):326–42.

15. Nika L, Gibson T, Konkus R, Karp X (2016) Fluorescent beads are a versatile tool for staging *Caenorhabditis elegans* in different life histories. *G3* 6(7):1923–33.
16. Lee JS, et al. (2017) FMRFamide-like peptides expand the behavioral repertoire of a densely connected nervous system. *Proceedings of the National Academy of Sciences of the United States of America* 114(50):E10726–E10735.
17. Brenner S (1974) The genetics of *Caenorhabditis elegans*. *Genetics* 77(1):71–94.
18. Hobert O (2002) PCR fusion-based approach to create reporter gene constructs for expression analysis in transgenic *Caenorhabditis elegans*. *BioTechniques* 32(4):728–30.
19. Maduro M, Pilgrim D (1995) Identification and cloning of *unc-119*, a gene expressed in the *Caenorhabditis elegans* nervous system. *Genetics* 141(3):977–88.
20. Mello C, Fire A (1995) DNA transformation. *Methods in cell biology* 48:451–82.
21. Schroeder NE, Flatt KM (2014) In vivo imaging of dauer-specific neuronal remodeling in *Caenorhabditis elegans*. *Journal of visualized experiments : JoVE* (91):e51834.

22. Kramer JM, Cox GN, Hirsh D (1985) Expression of the *Caenorhabditis elegans* collagen genes *col-1* and *col-2* is developmentally regulated. *The Journal of biological chemistry* 260(3):1945–51.
23. Schaedel ON, Gerisch B, Antebi A, Sternberg PW (2012) Hormonal signal amplification mediates environmental conditions during development and controls an irreversible commitment to adulthood. *Plos Biology* 10(4). doi:10.1371/journal.pbio.1001306.
24. Albert PS, Riddle DL (1988) Mutants of *Caenorhabditis elegans* that form dauer-like larvae. *Developmental biology* 126(2):270–93.
25. Vowels JJ, Thomas JH (1992) Genetic analysis of chemosensory control of dauer formation in *Caenorhabditis elegans*. *Genetics* 130(1):105–23.
26. Blaxter ML (1993) Cuticle surface proteins of wild type and mutant *Caenorhabditis elegans*. *J Biol Chem* 268(9):6600–6609.
27. Popham JD, W JM (1979) Aspects of the fine structure of the dauer larva of the nematode *Caenorhabditis elegans*. *Canadian Journal of Zoology* 57(4):794–800.
28. Braeckman BP (2009) Intermediary metabolism. *WormBook*:1–24.

*A p p e n d i x A***EXTREMOPHILE NEMATODES IN AND AROUND MONO LAKE  
DEMONSTRATE ADAPTATION TO AN ARSENIC-RICH  
ENVIRONMENT**

(This work was done in collaboration with Shih P.Y., Shinya R., Badroos J.M., Goetz E., and Sapir A.)

## A.1 Abstract

Studying extremophile organisms have expanded our understanding of the limits and adaptability of life. Nevertheless, the dynamics of animal habitation of harsh environments and the mechanisms of resilience and plasticity underlying this habitation remain largely unknown. Here we describe the discovery of extremophile nematodes in and around Mono Lake, CA, a unique basic, arsenic-rich, and hypersaline environment. In contrast to the limited number of animal species previously reported to live in the lake, we have isolated at least eight species of nematodes, including five previously unidentified species. Finding live nematodes in the same niches of Mono Lake in two consecutive years show that the lake hosts a stable population of worms. Phylogenetic analyses show that the nematodes belong to diverse clades across the phylum Nematoda, supporting a model of multiple colonization events. Consistent with this model, different mouth morphologies of these nematodes suggest diverse feeding strategies including bacterial grazers and predatory nematodes. We were able to culture one species of Mono Lake worms, *Auanema tufa* n. sp., and found that it is resistant to arsenite (As(III)) and arsenate (As(V)) — the two primary arsenic species in the lake. Integration of niche environmental conditions with the prevalence of worms at each of these niches suggests that arsenic resistance preceded the adaptation to other environmental conditions in the lake. Our finding highlights the previously unappreciated complexity of the animal life in the unique ecosystem of Mono Lake and provides insights into the dynamics and type of adaptations of animals to extreme environments.

## A.2 Introduction

Among the largest habitats on Earth are “extreme” environments where the physical and chemical conditions differ from the habitable zone of humans. These environments include, for example, the Deep Sea, sub-terrestrial niches, the high atmosphere, and specific terrestrial lakes. However, we know very little about the organisms that live in these habitats (extremophiles) and their strategies for adapting and thriving in such hostile environments, partly due to sampling challenges and limited access to these habitats. Moreover, the difficulties of growing and maintaining organisms from extreme habitats in the laboratory limit our understanding of the dynamics and the mechanisms underlying the adaptation of these organisms to their niches.

One phylum of organisms that seem to be particularly adapted to thrive in extreme environments are nematodes. These roundworms have been found in a variety of hostile environments, including deep subterranean niches (1, 2), extreme arid soil (3), frozen Antarctic water (4) and the Deep Sea (5, 6). Moreover, nematodes were found to dominate many of the habitats with environmental conditions so harsh as to almost not support animal life including the subterranean surface (7) and anoxic underwater sediments (8).

Nematodes have developed several protective strategies of modified life cycle to ensure the survival of the current or subsequent generations. For example, in response to unfavorable environmental conditions *Caenorhabditis elegans* enters an alternative developmental stage, the dauer, that allows its survival in harsh conditions (9, 10). Specific adaptive genetic programs facilitate the unique



physiology of the dauer state including the development of specialized morphology such as thickening of the cuticle, and an anaerobic metabolism. These adaptations result in an animal that is highly resistant to environmental insults and long-lived. The diverse lifestyle and feeding strategies of nematodes that range from free-living bacterial and fungal feeders, predator nematodes, to parasitic worms of plant and animal hosts often result in the cohabitation of worms in the same ecological niche. It is not clear, however, what specific adaptations enable nematodes to survive and thrive in extreme environments. Moreover, the sequences of events that underlie the habitation of nematodes in hostile environments remain largely unknown.

Mono Lake, a natural basin located in the Inyo National Forest of California, is an extreme environment that is high in pH, salt, and arsenic (11). It was formed as a closed basin since at least 50,000 years ago (12), but in 1941 some freshwater streams feeding the lake were diverted, making the drop of the lake level even more severe (13). The result of this level drop not only concentrated the salts (14, 15), but also facilitated arsenic to dissolve from sediments to its aqueous forms (16). Arsenic is a chemical element that is toxic to most organisms. At a biochemical level, inorganic arsenic in concentrations found in Mono Lake replace phosphate in several reactions and may react with critical thiols in proteins and inhibit their activity. Thus, arsenic has a negative pleiotropic effect on living organisms causing genotoxicity, altered DNA methylation and cell proliferation, oxidative stress, apoptosis, and mutagenesis (17). The level of arsenic in Mono Lake is approximately 0.2 mM, which is 1,500 times higher than the maximum limit

for drinking water (18). Consistent with the harshness of the environment, the number of living animals reported in the lake has been limited to two animal species, the alkali fly (*Ephydra hians*) and brine shrimp (*Artemia monica*) (19). The adaptation of these two species is polyphyletic, suggesting that an independent habitation of the lake took place in a process of strong purifying selection. Nevertheless, the sequence of events of this colonization process and the type of the specific adaptations that enable these animals to live in Mono Lake remain largely unknown.

Here we report eight species isolated in and around Mono Lake. These species were isolated from polyphyletic nematode clades, suggesting that Mono Lake has been inhabited by nematodes independently and multiple times. One of these species, *Auanema tufa* is culturable in laboratory conditions and exhibits resistance to arsenic, highlighting a probable hallmark of adaptation of animals to arsenic-rich environments.

### A.3 Results

#### Nematodes were isolated from three sampling sites around Mono Lake

Mono Lake covers 13 miles east to west and 8 miles north to south, and the lake shores are characterized by variable levels of human intervention and environment conditions. To survey for animal life in the sediments of Mono Lake, we collected soil from three different sites around Mono Lake to sample across various levels of human activities, and chemical and physical conditions. The three sites located in the north-east (site A), south (site B), and west (site C) (**Figure A.1A** and **Figure A.2**). Not approachable by vehicles, site A (Pristine Beach) on the north-east side of the lake is a large, sandy open field with the least visitors and observable biological activity of the three sites. Site B (Navy Beach) on the south attracts the most tourists. It contains emerged tufa structures, which are the precipitation products of calcium-bearing springs and the lake's carbonated waters (19). Site C (Old Marina) on the west has a rocky shore with small tufa structures. In all the sites we found the brine shrimps *Artemia monica* in the lake water and upper surface of the sediment, larvae of the *Ephydra hians* alkali fly in the sediments, and adult alkali flies on the lake's shores.

At each sampling site, we collected soil samples from three zones with various distances relative to the shore: dry zone, tide zone and in-lake (**Figure A.1B**). Within each niche, we sampled different sub-niches, for example, "in-lake" sampling involved the sampling of sediments in an increasing distance from the shoreline. We isolated live nematodes from all three sampling sites. From site A, most samples were collected from the tide zone and in-lake, and nematodes were

isolated in samples across -1 to 100 m away from the shore in sediments under water columns of 0 to 110 cm deep (**Figure A.1B-C**). Nematodes were also found from site B dry and tide zones, and from dry, tide and in-lake zones in site C. In contrast to the sediments, we did not find nematodes along the water columns. During the survey of the soil samples, we found that nematodes that were isolated in the wet tide zone and in-lake niches coexist with brine shrimp and the larvae of the alkali fly. These three taxa were the only animals isolated from the samples demonstrating the harshness of the environment that apparently can host a limited number of animal species that developed specific adaptations.

Mono Lake is not an isolated ecological system; it collects the waters of several streams from the nearby mountains, and it is amenable for different human interventions. To rule out the possibility that the isolated nematodes are the result of an environmental contamination, for example due to human activity, we sampled the isolated Pristine Beach site (**Figure A.1A**). Sampling this site in two consecutive years, 2016 and 2017, we found nematodes at Pristine Beach at both years indicating that the lake hosts an ecologically-stable community of nematodes (**Figure A.1C**). From the many morphologically different nematodes we found, we choose to characterize eight morphologically distinct species by DNA analysis (species a-h. **Figure A.1D** (species b), **Figure A.1E** (species e) and **Figure A.3**). One species was isolated from in-lake in site A (species g), six species were isolated in site B (species a-f), and one was from both site B and C (species h). Importantly, in 2017, we found two of the species (species e and f) again, from different locations (site B tide zone in 2016 and site C dry zone in 2017) (**Figure**

**A.4E).** This observation suggests that particular species of nematodes are ecologically stable and widespread in the lake.

#### **Some of the nematodes in Mono Lake live in pH 10.**

To understand the environmental conditions at the niches inhabited by Mono Lake nematodes, we measured the pH and soil salinity of our samples (**Table A.1**). Consistent with previous reports, the average pH of the samples fell within the range of 9-10 across different zones and sites (minimum:  $9.0 \pm 0.7$  from site B tide zone, maximum:  $10.01 \pm 0.1$  from site C dry zone), except for one sample from site B dry zone (pH=7.815). In contrast, the salinity of the samples varied by site and zone (**Figure A.4A**). Overall, samples from site A were more saline (tide zone  $15.0 \pm 3.0$  ppt and in-lake  $11.5 \pm 3.5$  ppt), and samples from site B were less saline (dry zone 1.0 ppt, tide zone  $0.9 \pm 0.7$  ppt and in-lake  $2.7 \pm 1.9$  ppt). This chemical analysis is consistent with the geography of Mono Lake in which site A, the most secluded from human interventions and the entry points of freshwater streams, is the most chemically extreme among the three sites we sampled. Nevertheless, site A hosts a large population of nematodes in the tide zone and in the lake, suggesting that nematodes were adapted to thrive even at extreme niches of the lake.

#### **Mono Lake's nematodes belong to different nematode clades and represent diverse lifestyles**

We integrated morphological and phylogenetic tools to study the biodiversity of

the isolated nematodes and their lifestyle in the Mono Lake ecosystem. Within the eight species, we identified a variety of mouth structures (**Figure A.5**), including grinders (**Figure A.4B**, species a), teeth (**Figure A.4C**, species d) and long esophagus (**Figure A.4D**, species f). The mouth structure of nematodes is an indicator of its feeding style (28). Base on the mouth structure analysis, we predict that species a and species d are a bacterial feeder and a predator, respectively. Species d may develop its tooth to prey on nematodes that are bacterial feeders in cases of harsh environmental conditions similar to what was shown for the interaction between the predatory nematode, *Pristionchus pacificus*, and its prey, *C. elegans* (29). Species e belongs to the family Mermithidae (see below), whose members have been observed to parasitize arthropods, such as spiders and grasshopper (30). This structure raises the possibility that species e could be parasitic of the other animals living in the lake. Taken together, our data show that the ecosystem of Mono Lake is much more complex than previously thought encompassing bacterial grazers, predators of other animals, and probably parasitic nematodes.

### **Five nematodes isolated are likely new species**

We used molecular signatures, including ribosome large subunit (LSU) 28rDNA and small subunit (SSU) 18rDNA, to identify the species in order to understand the course and dynamics of lake colonization by these nematodes. The sequence analysis suggested that three of the isolated nematodes are known species, and five of the isolated nematodes are likely new species (**Figure A.4E**, **Figure A.6**).

Moreover, the isolates are from across the phylogeny of Nematoda (Blaxter and Helder classification (31)(32)) (**Figure A.4E-F**). The known species include Clade V/9 nematodes *Mononchoides americanus* (species c, **Figure A.11-12**) and *Diplogaster rivalis* (species d, **Figure A.13-14**), and Clade II/1 nematode *Prismatolaimus dolichurus* (species f, **Figure A.17**). Two of the new species belong to Clade V/9, including *Auanema* sp. (species a, **Figure A.7-8**) and *Pellioditis* sp. (species b, **Figure A.9-10**). We assigned the other three new species in family instead of genus because of the lack of phylogenetically close species: species e is in *Mermithidae* family, which belongs to Clade I/2 (**Figure A.4F** and **Figure A.15**); species g and h are in *Diplolaimelloides* family, which is classified between Clade II and III/5 (**Figure A.4F** and **Figure A.18-19**). We concluded that species g and h are different because the sequence similarity between them is 96.77%, which is less than our criteria of 98% (**Figure A.20**). Taken together, the diverse distribution across the phylum Nematoda suggests that the colonization of Mono Lake by nematodes happened independently and multiple times.

### ***Auanema tufa* is culturable in lab**

The difficulty in replicating the exact conditions of extreme environments in order to culture the organisms that live in these habitats is a major obstacle in the study of life in the extremes. Thus, employing different culturing methods and conditions, we sought to establish a stable culturing system of Mono Lake nematodes in the laboratory. Of the eight species identified, we were able to

culture in our laboratory, using *C. elegans* culturing methods, one species which we identified as belonging to the *Auanema* genus (species a). Because this *Auanema sp.* shares only 89% (LSU) and 96%(SSU) sequence identity with its closest related *A. rhodensis* (**Figure A.6-8**), we concluded that *Auanema sp.* is a new species. Based on the tufa-rich environment we isolated it from, we named the species *Auanema tufa*. Notably, while its close related nematode species have been found in diverse habitats, only *A. tufa* was isolated from extreme environment (**Figure A.21**). The reproductive lifespan of *A. tufa* at 22.5°C is around 2.5-3 days, which is comparable to *C. elegans*. *A. tufa* shares some similarities with *A. rhodensis* and *A. freiburgensis* but also show some unique characteristics of their reproduction traits (33). The adult of all three species has a vulva located at mid-body and a two-armed gonad (**Figure A.21B-C**). *A. rhodensis* and *A. freiburgensis* have three genders (hermaphrodite, male and female), whereas *A. tufa* might be hermaphroditic or parthenogenic. We have observed male in *A. tufa*, but it appears very rarely. Moreover, *A. tufa* live-birth hatched larvae from their vulva (ovoviviparity) (**Figure A.21B**) instead of laying embryos like other nematodes of the *Auanema* genus such as *A. rhodensis* and *A. freiburgensis*. Ovoviviparity has been considered an adaptation to thrive in extreme environments (34, 35), thus yet representing another conceivable adaptation of *A. tufa* to the conditions of the lake.

#### ***A. tufa* is an arsenic-resistant nematode**

Mono Lake water and sediments are unique environments of high pH, salinity,



and high concentrations of arsenic species, primarily As(III) and (V) (11). It is known that a high concentration of arsenic is toxic to most living organisms thereby limiting animal life in arsenic-rich environments. To understand how Mono Lake nematodes survive in this hostile environment, we exposed *A. tufa* and a control nematode, the culturable soil worm *C. elegans*, with increasing concentrations of As(III) and As(V) solutions and examined their ability to survive over time. After 2.5 hours of exposure, we observed increased survival of *A. tufa* in both 1.5 and 3 mM of As(III) solutions in comparison to *C. elegans* (**Figure A.22A-B**). Even more striking is the ten fold more resistance of *A. tufa* to As(V). Specifically, *A. tufa* could withstand a concentration of 30mM As(V) compared to *C. elegans* (**Figure A.22C-D**). As a control we incubated the two strains in water and we detected 100% survival of the two species within the time window of the assay (**Figure A.22E**). *A. tufa* was isolated from near the surface of the tide zone, where As(V) is reported to be the dominant arsenic species (36). The results strongly suggest that evolving of mechanisms of arsenic resistance is a critical step in the adaptation of nematodes, including *A. tufa*, to the conditions of Mono Lake.

An increasing body of evidenc show that in *C.elegans*, SKN-1 is a transcription factor dedicated to promote many protective stress responses. Specifically, an activated form of *skn-1* mediates arsenic resistance in *C. elegans* (37). Thus, it is possible that activation of SKN-1 is one of the mechanisms that collectively underlie the adaptation of Mono Lake nematodes to Arsenic. To test if *skn-1* gene activity could explain the observed arsenic resistance of *A. tufa*, we compared the survival rate of *A. tufa* with different strains of *C. elegans*. These strains include the

wild-type background as a control and an *skn-1* allele, *lax188*, in which the SKN-1 protein is activated constitutively. We choose to expose the worms to 10mM As(V) solution in which the survival rate of *A. tufa* is significantly higher than wild-type *C. elegans* worms (**Figure A.22C**). Consistent with previous reports, we found that the activation of SKN-1 leads to arsenic resistance. Importantly, *A. tufa* survive better than wild-type and *skn-1* gain of function *C. elegans* worms (**Figure A.22F**). Thus, activation of the *skn-1* pathway might play a critical role in the adaptation of *A. tufa* and other Mono Lake nematodes to the extreme environmental conditions in the lake.

#### A.4 Discussion

Because Mono Lake is an extreme natural environment it was thought to host limited animal biodiversity. Here we report that, in addition to what was previously known, nematodes live in Mono Lake. We found spatial and temporal stable populations of nematodes all across the lake (A, B, and C sites) and at various zones (dry zone, tide zone, and in-lake), indicating there are multiple niches within the ecosystem of Mono Lake where nematodes can thrive. Mono Lake nematodes have multiple lifestyles for survival, as suggested by their diverse morphologies. In total we identified, using molecular phylogeny, eight species that belong to diverse clades across the phylum Nematoda. This polyphyletic diversity suggests that multiple colonization events took place in Mono Lake. Moreover, we found that one of the nematodes, *Auanema tufa* is culturable in lab and is more resistant to arsenic than *C. elegans*.

Due to the high level of protection of Mono Lake, we believe that our sampling was far from being saturated. Indeed, when we isolated the same species (species in *Mermithidae* and *Tripylidae*) in subsequent years, we did not find them in the same site. Our unsaturated sampling may also explain why the nematodes we observed at low abundance in the first year (*A. tufa*) were not observed in the subsequent year.

We suspect that there are several ways for the nematodes to adapt to Mono Lake. First, it is possible that nematodes around Mono Lake develop pre-adaptations to arsenic, which may allow them to evolve and further adapt to the high pH and salinity conditions in-lake. That could explain the adaptation strategy

of the arsenic-resistant *A. tufa* found in site B, where the salinity is the lowest and the pH varies the most among the three sampling sites. Secondly, upregulation of arsenic resistance genes, such as *skn-1*, may be a critical aspect of this adaptation. Further investigation is required to test directly if *skn-1* or other stress-related genes are involved. Finally, entering the dauer stage, a stress-resistant and developmentally arrested period (38)(39), might help nematodes survive in Mono Lake and find relatively favorable places within the harsh environment via dauer-specific dispersal behaviors (40). Our sampling technique did not favor the isolation of dauers, but it is possible that dauer formation is one strategy of resistance that facilitated the habitation of the lake by dauer-forming nematodes.

The fact that nematodes have been found in several harsh environments, including Mono Lake, raises the question: what makes nematodes good extremophiles? Because nematode genomes can very quickly and dramatically through high rates of gene acquisition and loss (41), it is likely that nematodes can adapt to challenging conditions. Moreover, the small size of nematodes is probably beneficial, allowing the utilization of neuroendocrine signaling to engage and enact whole animal survival programs in response to stress. Lastly, as mentioned before, dauer animals have well-equipped physiology and behaviors to cope with stress.

We have investigated extremophile biology in nematodes and have identified yet another harsh environment where nematodes can survive. We identified eight species from across the diversity of Nematoda, suggesting that Mono Lake was invaded independently and multiple times. The arsenic resistance of *A. tufa* that lives in the relatively safe harbor of the B site suggests that preadaptation to

arsenic could lead to the genomic evolution necessary to survive the pH and salinity of inner Mono Lake.

## **A.5 Material and Method**

### **Sites and sampling**

Soil and water samples were collected from three sites around Mono Lake (**Figure A.1**) in August 2016, June 2017 and July 2017. Site A, which we named Pristine Beach, ( $38^{\circ} 3' 27.91''$  N,  $119^{\circ} 1' 50.66''$  W), site B is at Navy Beach ( $37^{\circ} 56' 21.90''$  N,  $119^{\circ} 1' 25.93''$  W), and site C is at Old Marina ( $37^{\circ} 59' 12.80''$  N,  $119^{\circ} 8' 18.70''$  W).

At each site, soil samples were collected from inside the lake, tide zone, and dry zone, with each sample weight ranging from 15 to 375 g. Total numbers of samples collected from each site were: 25 from site A (9 in 2016 and 16 in 2017), 34 from site B (19 in 2016 and 15 in 2017), and 22 from site C (7 in 2016 and 15 in 2017). The sampling permits were issued to Amir Sapir by the California Fish and Wildlife Department (SCP-13436) and from the Californian State Parks Department. All of the sample information, including location, pH, salinity, and the presence of nematodes, is listed in Table S1.

### **Soil salinity and pH measurement**

Each soil sample was mixed with Milli-Q water in a 1:2 ratio (weight:volume) for salinity and pH measurements (20). Soil salinity was estimated by measuring the conductivity with two meters: Orion conductivity meter model 126 (for 2016 samples) and TPS WP-81 conductivity meter (for 2017 samples). Soil pH was measured using VWR pH meter model 8015.

## **Nematode isolation and species identification**

Nematodes were isolated directly from the soil samples either using a dissecting microscope on-site or in the laboratory by the Baermann funnel method for overnight extraction (21). The isolated nematodes were further identified by morphology and molecular signatures. For molecular analysis, individual worm lysate was prepared in worm lysis solution (100µl DirectPCR lysis reagent (Viagen Biotech), 10.5µl proteinase K (10 mg/ml) and 5µl 1M DTT). The gene fragments of ribosome large subunit (LSU) 28rDNA and small subunit (SSU) 18rDNA were amplified (22)(23) and sequenced. MEGA7 was used to build phylogenetic tree from the resulting sequences (24). The tree was estimated by using Maximum Likelihood (ML) analysis and 1,000 bootstrap replicates, and the species identification was done with General Time Reversible model (25). The isolated nematode is considered as a new species when it exhibits <98% sequence similarity compared with its nearest neighbor (26, 27).

## **Nematode culture**

### *Maintenance*

Both *C. elegans* wild-type strain N2 (Bristol) and *Auanema tufa* n. sp. were grown using standard *C. elegans* culturing protocol with *Escherichia coli* strain OP50 as a food source (19). *Auanema tufa* was maintained at 22.5°C.

### *Freezing*

*Auanema tufa* was frozen using Trehalose-DMSO method (personal

communication with Dr. Kevin F. O'Connell). Briefly, *Auanema tufa* n. sp. from freshly starved plates was washed off with M9 buffer (3 g  $\text{KH}_2\text{PO}_4$ , 6 g  $\text{Na}_2\text{HPO}_4$ , 5 g NaCl and 1 ml 1 M  $\text{MgSO}_4$  in 1L ddH<sub>2</sub>O) and collected in a 15ml centrifuge tube. The worm pellet was washed once, re-suspended with Trehalose-DMSO freezing buffer (15.1 g Trehalose (Fisher BioReagents, PA, Cat# BP2687-25) and 17.7 ml DMSO in 500 ml M9 buffer), and transferred to cryogenic vials. The vials were stored in -80°C freezer after 30 minutes incubation at room temperature.

### **Survival assay**

As(III) and As(V) solutions were prepared by dissolving sodium (meta)arsenite (Sigma-Aldrich, MO, Cat S7400) and sodium arsenate dibasic heptahydrate (Sigma-Aldrich, MO, Cat# S9663) in Milli-Q water, respectively. Adults of *C. elegans* wild-type N2, *skn-1(lax188)*, and *Auanema tufa* were washed with Milli-Q water for 4 times and transferred to 12-well tissue culture plates (Corning, NY) containing 0.9 ml of Milli-Q water and various concentration of As(III) or As(V) per well. Each well has on average 34 animals, ranging from 10 to 66. Final concentrations of 1.5 and 4.5 mM of As(III), and 10 and 30 mM of As(V) was used to treat animals. Animals were incubated at 22°C and the numbers of surviving animals, determined by their physiology and touch-provoked movement (in response to eyelash touch), were counted at different time points (1, 2.5, 5 and 7 hours).



A.6 Figures

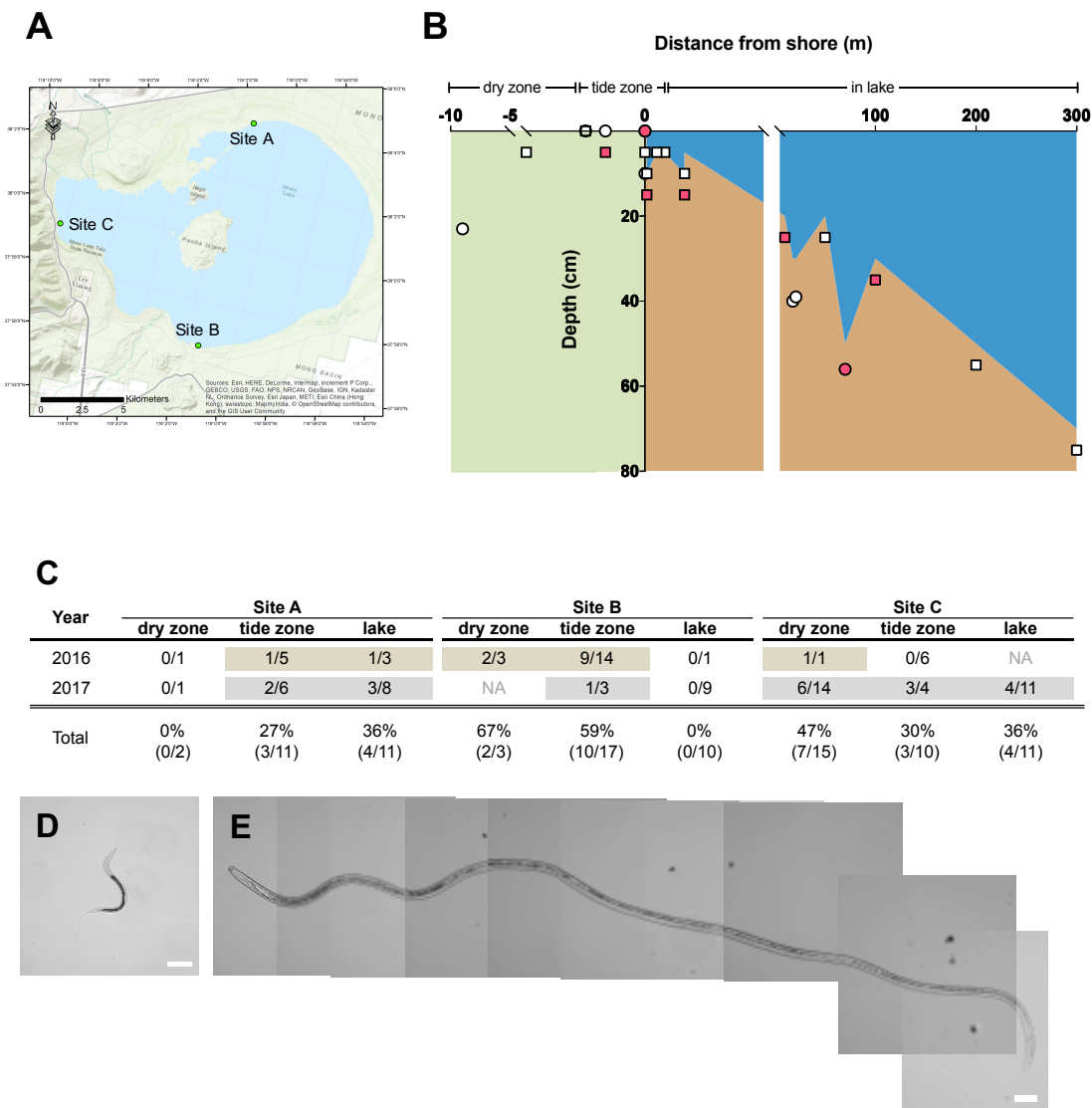


**Figure A.1. Nematodes were isolated from in and around Mono Lake. (A)** The locations of the three sampling sites A, B and C around Mono Lake. Samples were collected in August 2016 and June 2017. **(B)** Plot showing the locations at site A where samples were collected, relative to the shore (x-axis) and surface (y-axis). The boundaries of three different kinds of locations, dry zone, tide zone, and in-lake, were shown by the brackets. Blue indicates lake water and brown indicates

the soil. Circles and squares represent samples collected in 2016 and 2017, respectively. The samples in which nematodes were found were colored in pink.

**(C)** Summary table of the origins of the samples. Samples were collected from dry zone, tide zone or lake from each site. The numbers in the cells indicate the number of samples with nematodes isolated versus the total number of samples collected. The locations that have nematodes found were highlighted in beige for 2016 samples and grey for 2017 ones. NA, non-applicable. **(D-E)** Representative images of two nematodes isolated. One was isolated from site B dry and tide zones in 2016 **(D)**, and the other one was isolated from site B tide zone in 2016 and site C dry zone in 2017 **(E)**.

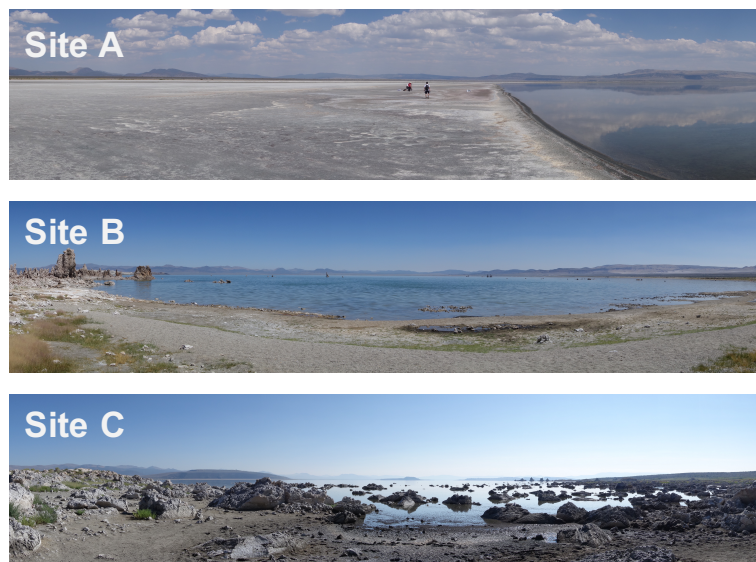
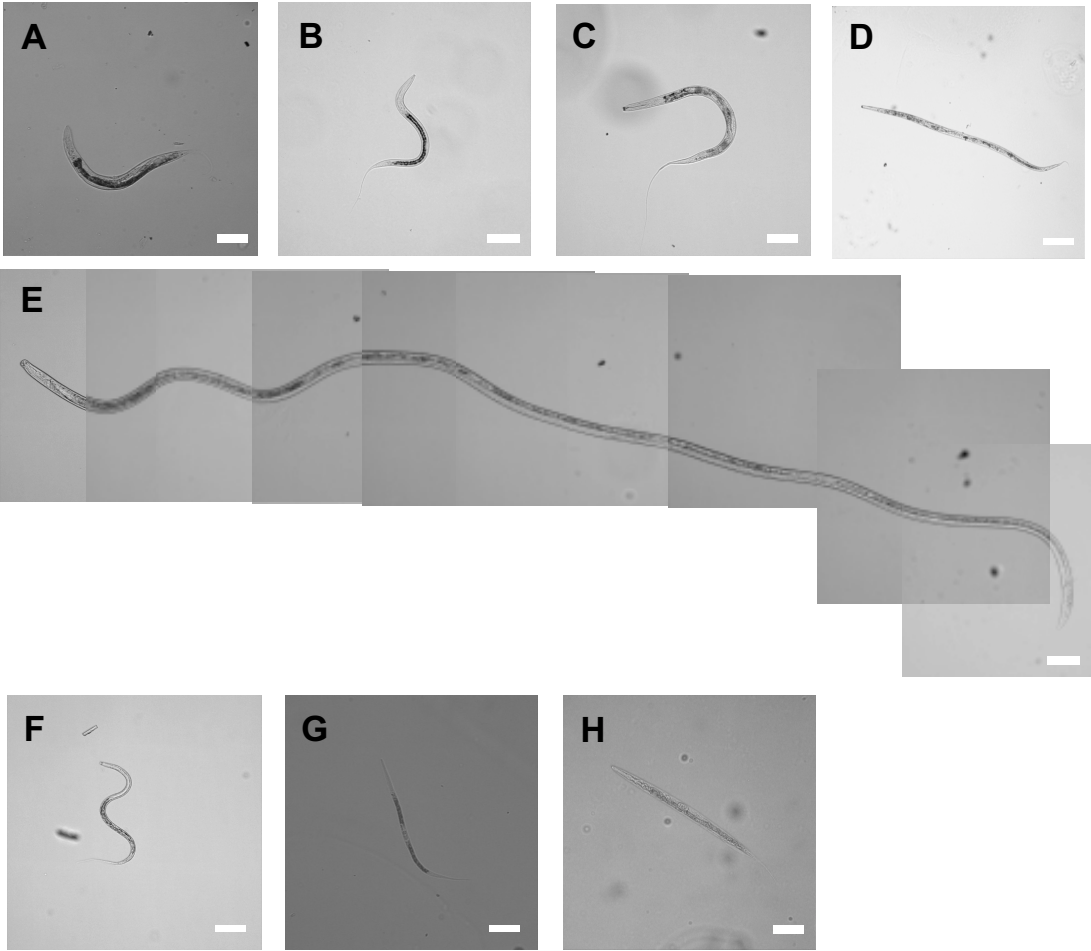


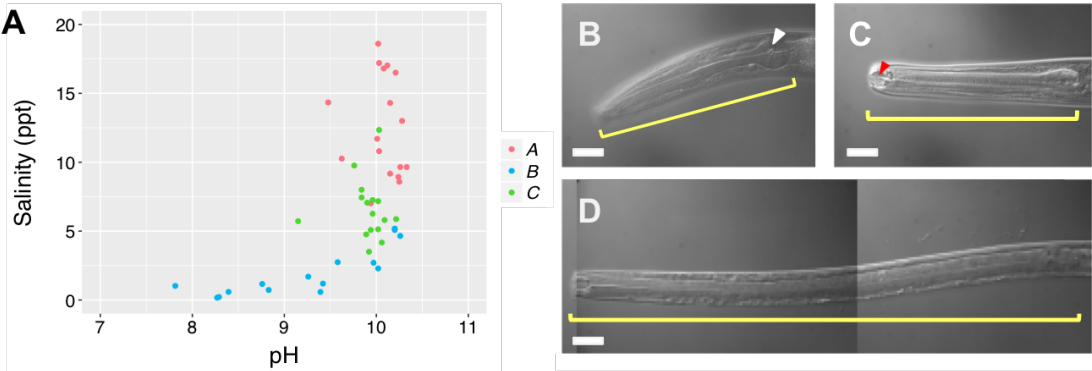
**Figure A.2. Pictures of three sampling sites around Mono Lake.** Pictures of site A (10 Mile Road), site B (Navy Beach), and site C (Old Marina).



I

Species	Clade		Site A		Site B		Site C		
	Blaxter <sup>3</sup>	Helder <sup>4</sup>	tide zone	lake	dry zone	tide zone	dry zone	tide zone	lake
a. <i>Auanema</i> sp. <sup>1,2</sup>	V	9				B8 (2016) B14 (2016)			
b. <i>Pellioditis</i> sp. <sup>1,2</sup>	V	9			B20 (2016)	B9 (2016)			
c. <i>Mononchoides americanus</i> <sup>1,2</sup>	V	9			B20 (2016)	B7 (2016) B9 (2016)			
d. <i>Diplogaster rivalis</i> <sup>1,2</sup>	V	9				B8 (2016)			
e. species in Mermithidae <sup>1,2</sup>	I	2				B9 (2016)	C131 (2017) C133 (2017)		
f. <i>Prismatolaimus dolichurus</i> <sup>1</sup>	II	1				B7 (2016)	C130 (2017)		
g. species in Monhysteridae <sup>2</sup>	(II, III)	5		A9 (2016)					
h. species in Monhystreidae <sup>2</sup>	(II, III)	5				B8 (2016)	C7 (2016)		

**Figure A.3. Nematodes isolated from the three sites are diverse in morphology. (A-H)** Morphology of species a-h under low magnification. **(I)** Identification and classification of the eight nematodes isolated. The species were identified by either 28S LSU rRNA (Footnote 1) or 18S SSU rRNA (Footnote 2). The classification system was based on the ones introduced by Blaxter (Clade I-V) or Heider (Clade 1-13). Some species fall between Clade II and III, which were indicated with parenthesis in the table. The sample number, location, and the year collected were indicated in the corresponding cell. Highlighted squares denote sites where the species was observed. Samples from 2016 are in beige, and those from 2017 are in grey. Scale bar: 100 $\mu$ m



**E**

Species	Clade		Site A		Site B		Site C		
	Blaxter <sup>3</sup>	Helder <sup>4</sup>	tide zone	lake	dry zone	tide zone	dry zone	tide zone	lake
a. <i>Auanema</i> sp. <sup>1,2</sup>	V	9				B8 (2016) B14 (2016)			
b. <i>Pellioditis</i> sp. <sup>1,2</sup>	V	9			B20 (2016)	B9 (2016)			
c. <i>Mononchoides americanus</i> <sup>1,2</sup>	V	9			B20 (2016)	B7 (2016) B9 (2016)			
d. <i>Diplogaster rivalis</i> <sup>1,2</sup>	V	9				B8 (2016)			
e. species in Mermithidae <sup>1,2</sup>	I	2				B9 (2016)	C131 (2017) C133 (2017)		
f. <i>Prismatolaimus dolichurus</i> <sup>1</sup>	II	1				B7 (2016)	C130 (2017)		
g. species in Monhysteridae <sup>2</sup>	(II, III)	5		A9 (2016)					
h. species in Monhystreidae <sup>2</sup>	(II, III)	5				B8 (2016)	C7 (2016)		

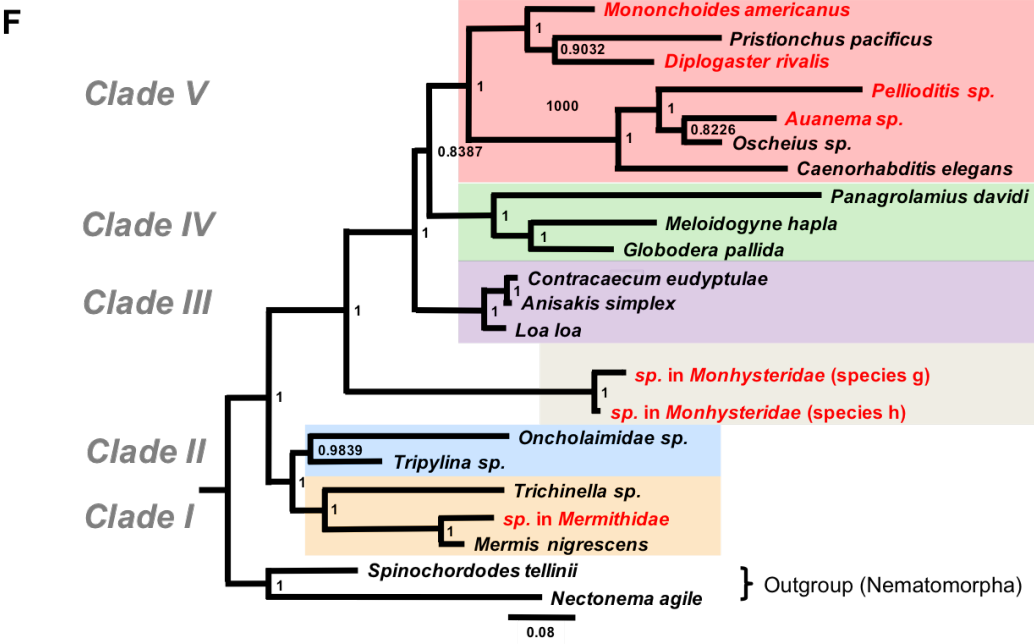
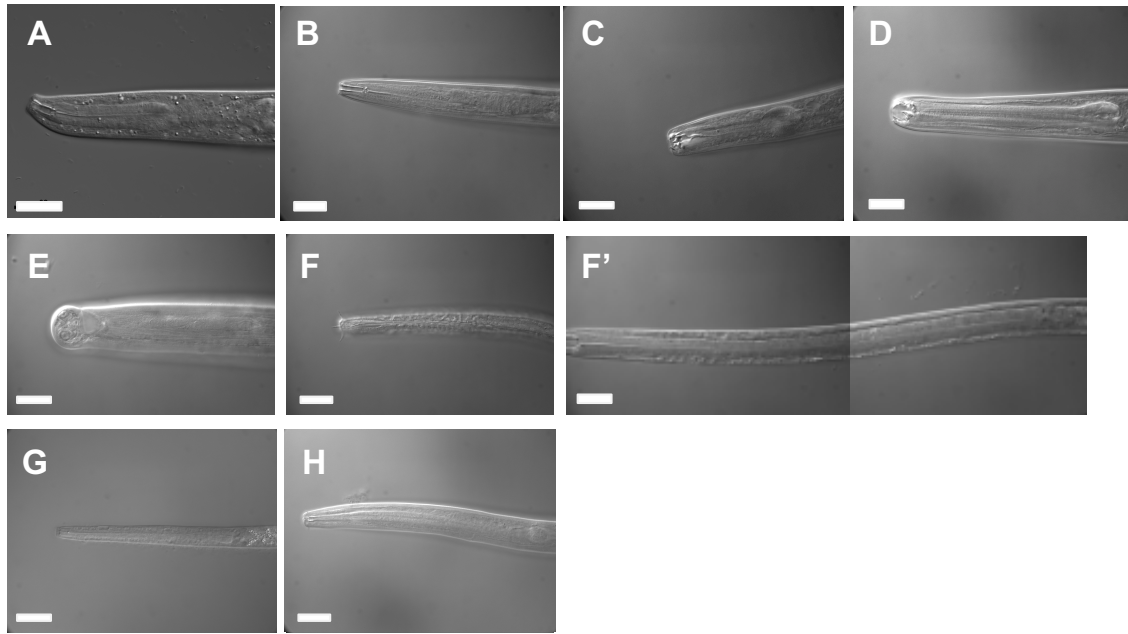


**Figure A.4. The nematodes isolated are phylogenetically and morphologically diverse. (A)** Plot showing the salinity and pH of all the samples collected. Each dot represents the measurements from one single sample, and the color corresponds to the site where the sample were collected from. **(B-D)** Mouth/head structures of three representative nematodes (Species a, d and f, respectively). The white and red arrowheads indicate the grinder and tooth, respectively. The yellow bracket shows the length of the esophagus. Scale bar: 20 $\mu$ m. **(E)** Identification and classification of the eight nematodes isolated. The species were identified by either 28S LSU rRNA or 18S SSU rRNA. The classification system was based on the ones introduced by Blaxter (Clade I-V) or Heider (Clade 1-13). Some species fall between Clade II and III, which were indicated with parenthesis in the table. The sample number, location, and the year collected were indicated in the corresponding cell. Highlighted squares denote sites where the species was observed. Samples from 2016 are in beige, and those from 2017 are in grey. **(F)** Phylogenetic tree of the eight of the nematodes based on SSU sequences. The nematodes we isolated were highlighted in red. The numbers show the bootstrap score out of 1000 runs. Footnotes: 1, confirmed by LSU rRNA sequence; 2, confirmed by SSU rRNA sequence; 3, reference (31) ; 4, reference (32)

Sample number	Location	From shore (cm)	Under ground (cm)	Water depth (cm)	pH	Salinity (ppt)	Presence of neamtdoes	Number of nematodes/species
A1	tide zone	0	0	0	ND	ND	NO	
A2	tide zone	-150	0	0	ND	ND	NO	
A3	tide zone	0	10	0	ND	ND	NO	
A4	tide zone	0	0	0	9.477	14.342	YES	1 / 1
A5	tide zone	-100	0	0	ND	ND	NO	
A6	dry zone	-900	23	0	ND	ND	NO	
A7	in lake	1800	10	30	ND	ND	NO	
A8	in lake	7000	6	50	9.624	10.26	YES	~5 / 1
A9	in lake	2100	9	30	ND	ND	NO	
A100	tide zone	5	10	0	10.21	16.5	NO	
A101	tide zone	5	5	0	10.08	16.8	YES	1 / 1
A102	dry zone	-300	5	0	10.12	17.02	NO	
A103	tide zone	50	0	5	10.15	14.3	NO	
A104	tide zone	0	5	0	10.02	18.6	NO	
A105	in lake	30	0	5	10.01	11.7	NO	
A106	tide zone	-150	0	0	10.03	17.2	NO	
A107	tide zone	-100	0	5	10.03	10.8	YES	4 / ND
A108	in lake	100	5	10	10.28	13	YES	33 / ND
A109	in lake	1000	5	20	10.33	9.65	YES	1 / 1
A110	in lake	5000	5	20	10.24	8.93	NO	
A111	in lake	10000	5	30	10.25	8.58	YES	4 / ND
A112	in lake	20000	5	50	9.94	7.02	NO	
A113	in lake	30000	5	70	10.15	9.17	NO	
A114	in lake	100	5	5	10.26	9.65	NO	
B1	tide zone	0	0	0	ND	ND	NO	
B2	tide zone	0	0	0	ND	ND	NO	
B3	in lake	300	0	10	ND	ND	NO	
B4	tide zone	0	8	0	ND	ND	NO	
B5	tide zone	20	10	0	ND	ND	YES	2 / 1
B6	tide zone	10	10	0	ND	ND	YES	1 / 1
B7	tide zone	0	5	0	9.3925	0.581	YES	~15 / 2
B8	tide zone	-100	5	0	ND	ND	YES	20 / ≥2
B9	tide zone	-100	5	0	5.967 <sup>a</sup>	0.779	YES	~50 / 3
B10	tide zone	0	0	0	ND	ND	YES	1 / 1
B12	tide zone	0	0	0	ND	ND	YES	1 / 1
B13	tide zone	-75	8	0	ND	ND	NO	
B14	tide zone	-75	0	0	8.394	0.586	YES	~200 / ≥3
B15	tide zone	0	0	0	ND	ND	NO	
B16	dry zone	-300	6.5	0	ND	ND	YES	2 / ND
B19	dry zone	-300	5	0	ND	ND	NO	
B20	dry zone	0	0	0	7.815	1.022	YES	~20 / 2
B21	tide zone	-120	4	0	ND	ND	YES	1 / 1
B100	in lake	30	10	0	9.42	1.19	NO	
B101	tide zone	0	10	0	8.83	0.725	NO	
B102	in lake	300	10	0	8.27	0.166	NO	
B103	in lake	50	10	30	9.58	2.74	NO	
B104	in lake	10	10	10	9.97	2.7	NO	
B106	in lake	10	10	10	8.76	1.16	NO	
B107	in lake	30	10	10	9.26	1.692	NO	
B108	tide zone	-100	10	0	8.29	0.214	YES	40 / 1
B111	tide zone	0	10	0	10.02	2.29	NO	
B112	in lake	100	10	40	10.2	5.08	NO	
B113	in lake	300	10	50	10.26	4.65	NO	
B114	in lake	1000	10	100	10.2	5.18	NO	
C1	tide zone	0	5	0	ND	ND	NO	
C2	tide zone	0	0	0	ND	ND	NO	
C3	tide zone	-30	0	0	ND	ND	NO	
C4	tide zone	0	4	0	ND	ND	NO	
C6	tide zone	0	5	0	ND	ND	NO	
C7	dry zone	-200	5	0	10.2145	5.87	YES	3 / 2
C8	tide zone	0	3	0	9.175	22.361 <sup>a</sup>	NO	
C100	in lake	300	0	0	10.06	4.17	YES	1 / 1
C101	tide zone	5	0	0	9.89	4.76	YES	2 / ND
C102	dry zone	-20	0	0	10.02	7.17	YES	8 / 1
C103	in lake	10	20	0	10.02	5.13	NO	
C104	dry zone	-1000	0	0	10.03	12.34	YES	52 / ND
C105	in lake	20	20	20	9.92	3.5	NO	
C106	tide zone	0	0	0	9.15	5.72	YES	1 / 1
C108	in lake	100	0	20	9.94	5.08	NO	
C109	in lake	100	10	0	9.96	7.26	NO	
C110	in lake	300	10	40	9.9	7.06	YES	2 / ND
C111	in lake	1000	0	50	10.09	5.8	YES	2 / ND
C112	in lake	3000	10	50	9.84	7.44	YES	1 / 1
C113	in lake	5000	0	50	9.96	6.26	NO	
C114	in lake	7000	10	70	9.84	8	NO	
C115	in lake	10000	10	100	9.76	9.76	NO	
C130	dry zone	-300	5	0	ND	ND	YES	~400 / 1
C131	dry zone	-500	5	0	ND	ND	YES	131 / 2
C132	tide zone	-30	5	0	ND	ND	NO	
C133	dry zone	-1000	5	0	ND	ND	YES	10 / 1
C134	dry zone	-1000	15	0	ND	ND	NO	
C135	dry zone	-1000	28	0	ND	ND	NO	
C136	dry zone	-500	15	0	ND	ND	YES	1 / 1
C137	dry zone	-500	48	0	ND	ND	NO	
C138	dry zone	-50	5	0	ND	ND	NO	
C139	dry zone	-50	48	0	ND	ND	NO	
C140	dry zone	-50	28	0	ND	ND	NO	
C141	dry zone	-50	15	0	ND	ND	NO	
C142	dry zone	-10000	2	0	ND	ND	NO	
C143	tide zone	-30	5	10	ND	ND	YES	1 / 1



**Table A.1. Detailed information of the soil samples collected.** Sample numbers include the information of both sampling site (A, B, or C) and sampling year (2016 samples start from 1, 2017 samples start from 100). The sign of the distance from the shore indicates the direction of the sampling site in respect to the lake: positive is into the lake, and negative is away from the lake. Footnote: a, outliers, excluded from further analysis. ND: not determined.



I

Species	Clade		Site A		Site B		Site C		
	Blaxter <sup>3</sup>	Helder <sup>4</sup>	tide zone	lake	dry zone	tide zone	dry zone	tide zone	lake
a. <i>Auanema</i> sp. <sup>1,2</sup>	V	9				B8 (2016) B14 (2016)			
b. <i>Pellioditis</i> sp. <sup>1,2</sup>	V	9			B20 (2016)	B9 (2016)			
c. <i>Mononchoides americanus</i> <sup>1,2</sup>	V	9			B20 (2016)	B7 (2016) B9 (2016)			
d. <i>Diplogaster rivalis</i> <sup>1,2</sup>	V	9				B8 (2016)			
e. species in Mermithidae <sup>1,2</sup>	I	2				B9 (2016)	C131 (2017) C133 (2017)		
f. <i>Prismatolaimus dolichurus</i> <sup>1</sup>	II	1				B7 (2016)	C130 (2017)		
g. species in Monhysteridae <sup>2</sup>	(II, III)	5		A9 (2016)					
h. species in Monhystreidae <sup>2</sup>	(II, III)	5				B8 (2016)	C7 (2016)		

**Figure A.5. Nematodes isolated from the three sites are diverse in morphology. (A-H)** Morphology of species a-i under high magnification. (F) and (F') were taken from the same animal but on different focal planes. **(I)** Identification and classification of the eight nematodes isolated. The sample number, location, and the year collected were indicated in the corresponding cell. Scale bar: 20µm

Species	Sequence identity (%)	
	LSU	SSU
a	89	96
b	88	95
c	90	98 (to <i>Mononchoides americanus</i> )
d	92	99 (to <i>Diplogaster rivalis</i> )
e	85	93
f	99 (to <i>Prismatolaimus dolichurus</i> )	NA
g	NA	92
h	NA	96

**Figure A.6. Percent of sequence identity of each isolate compared to its closest related species.** Based on LSU and SSU sequences. NA: not applicable

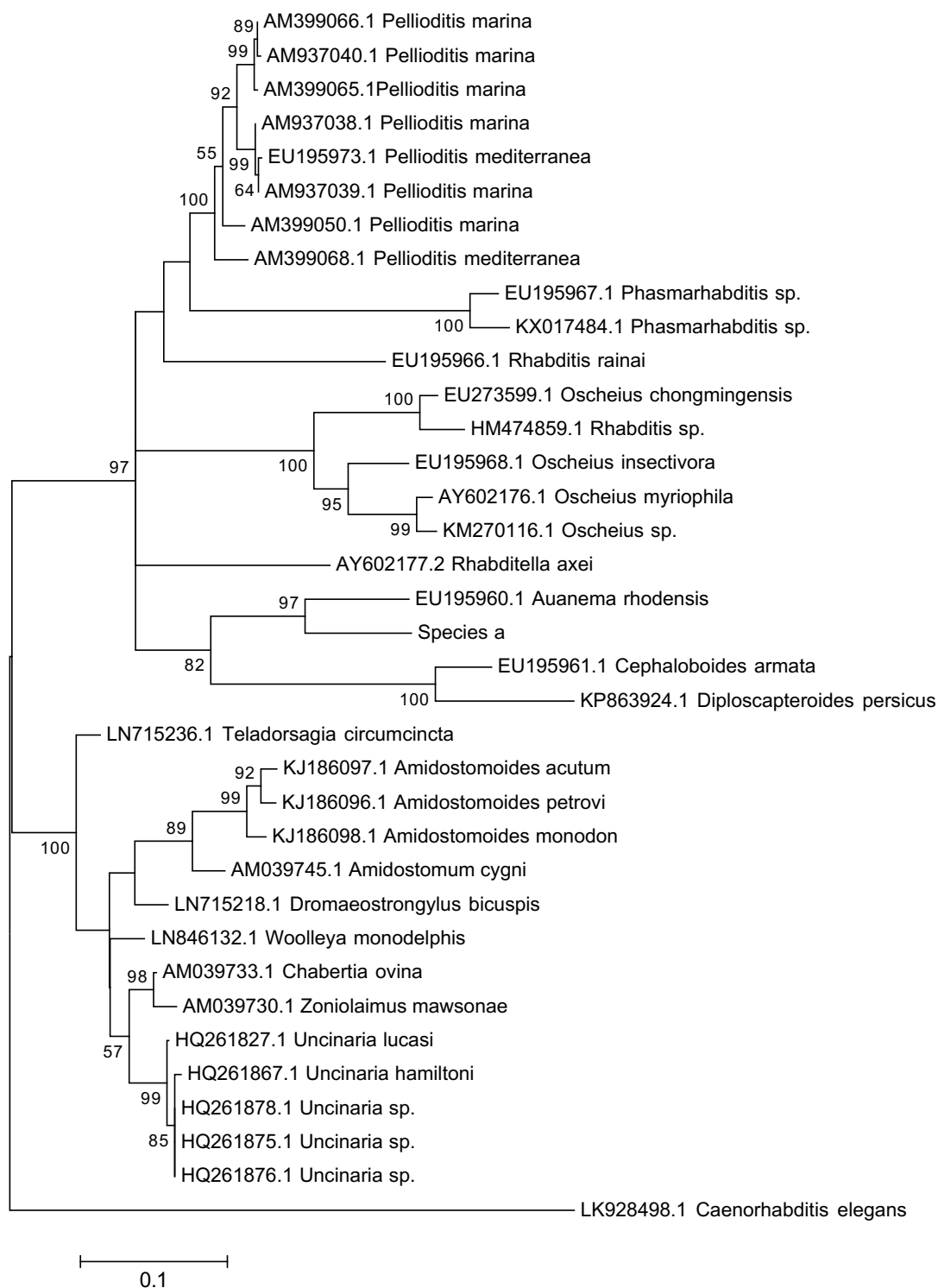


**Figure A.7. Phylogenetic tree of species a (based on LSU sequence)**

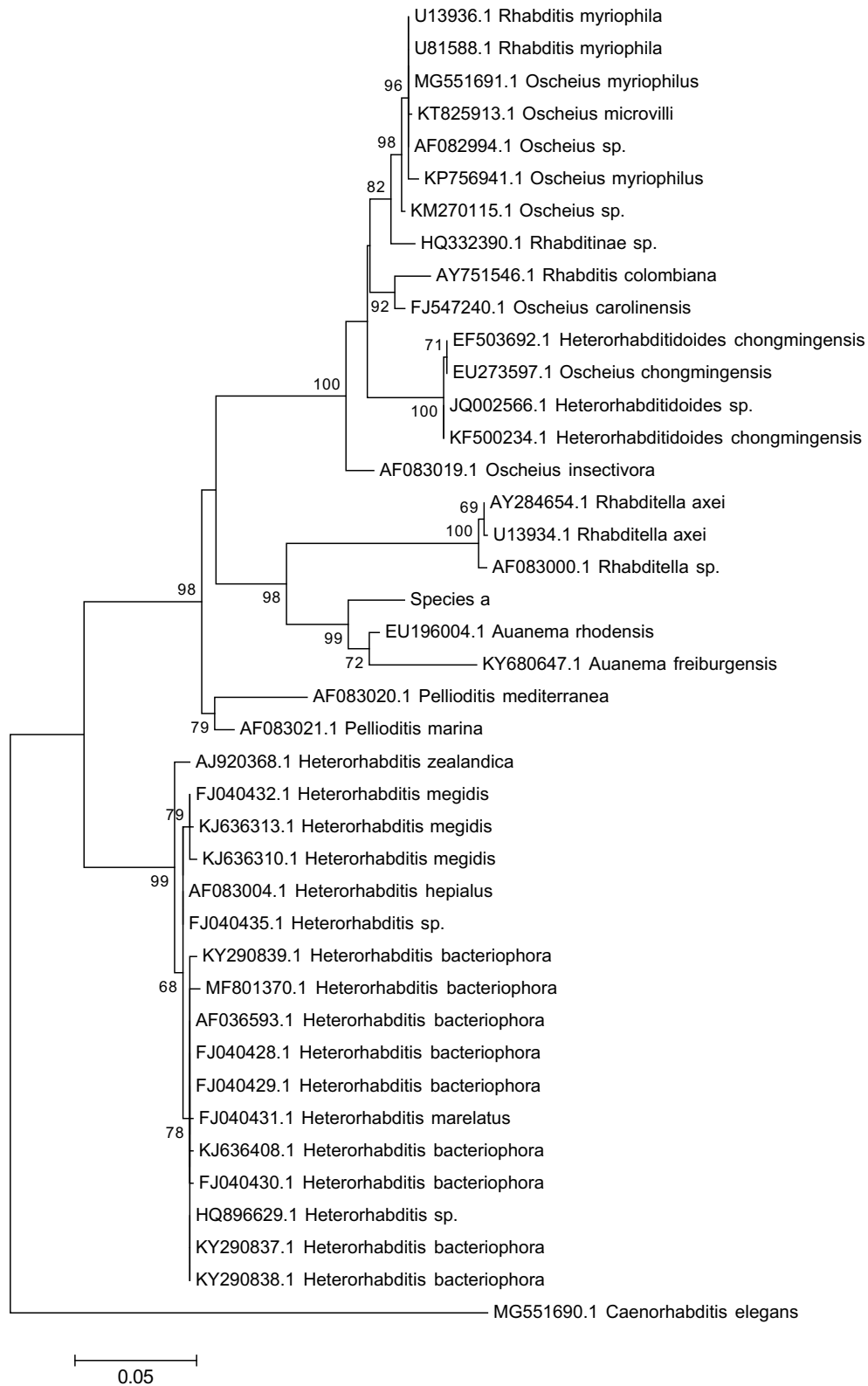


**Figure A.8. Phylogenetic tree of species a (based on SSU sequence)**

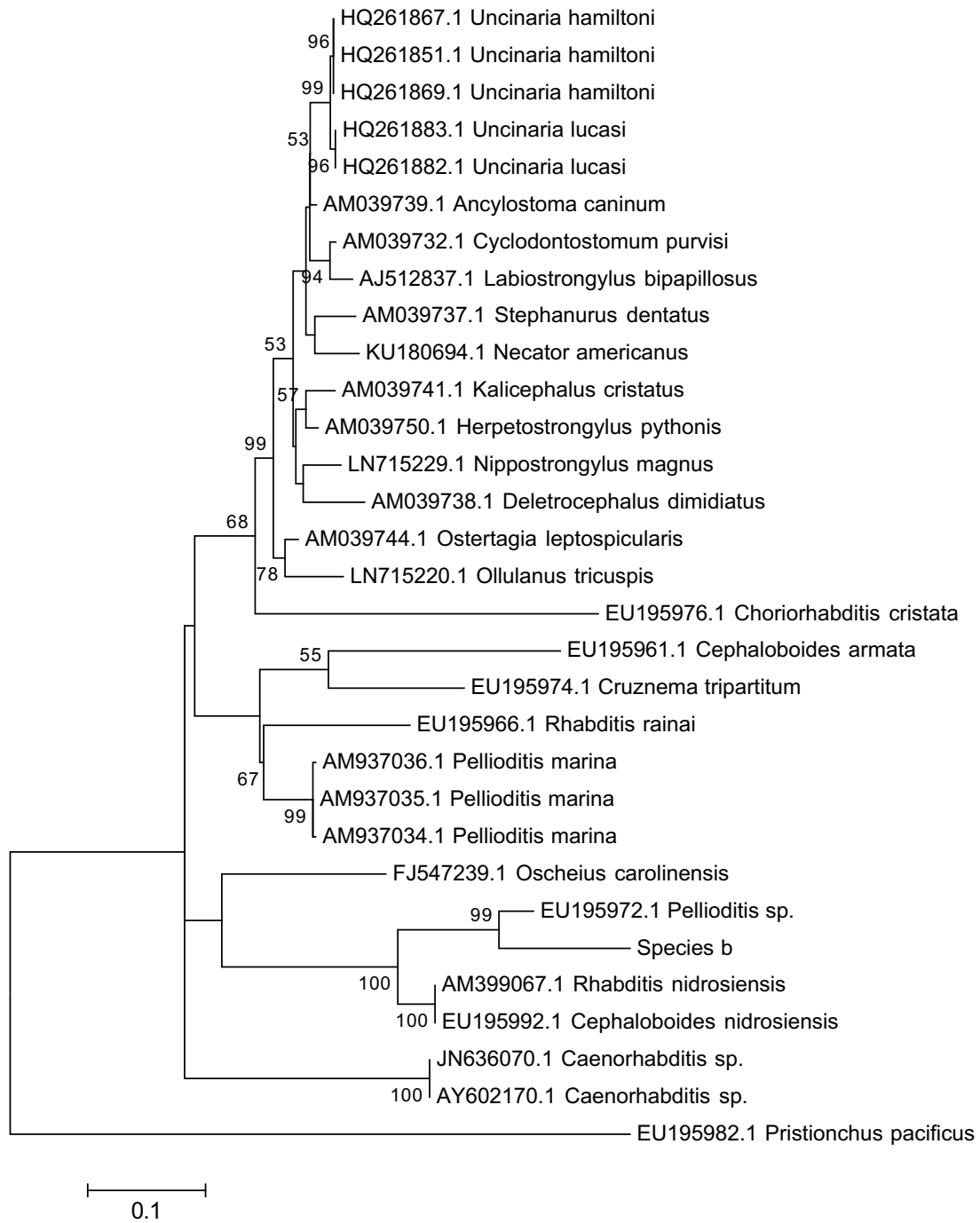


**Figure A.9. Phylogenetic tree of species b (based on LSU sequence)**

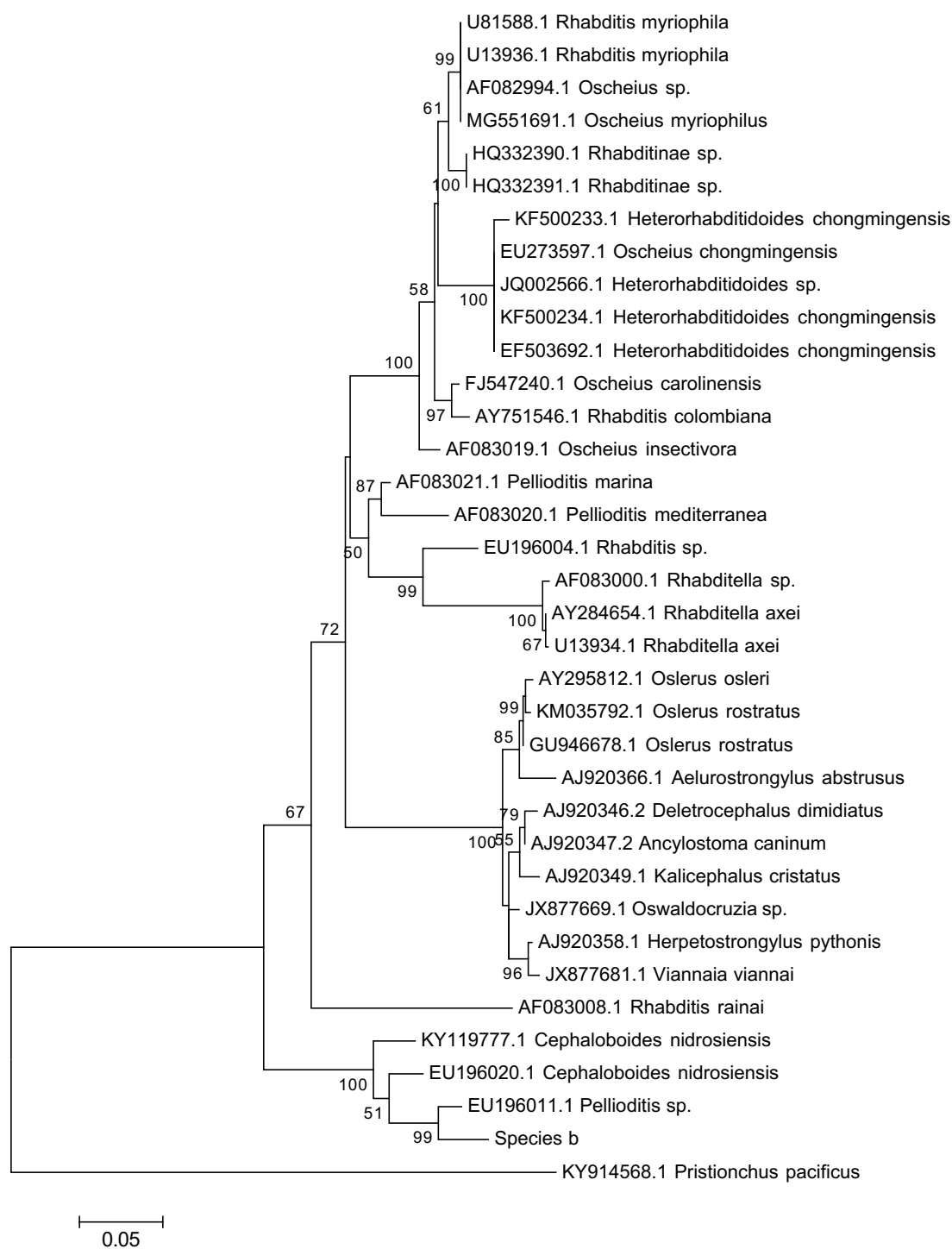


**Figure A.10. Phylogenetic tree of species b (based on SSU sequence)**

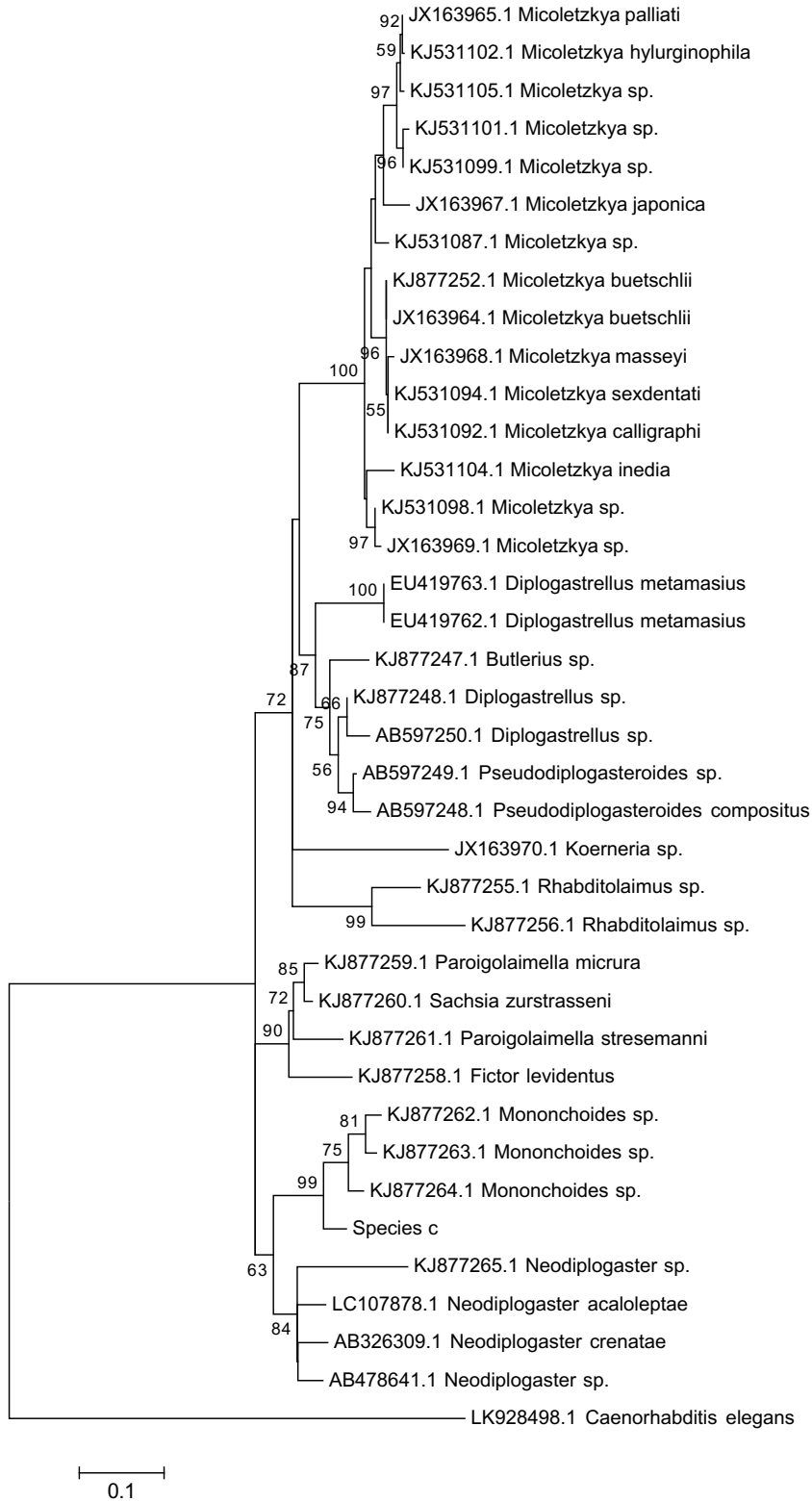


**Figure A.11. Phylogenetic tree of species c (based on LSU sequence)**



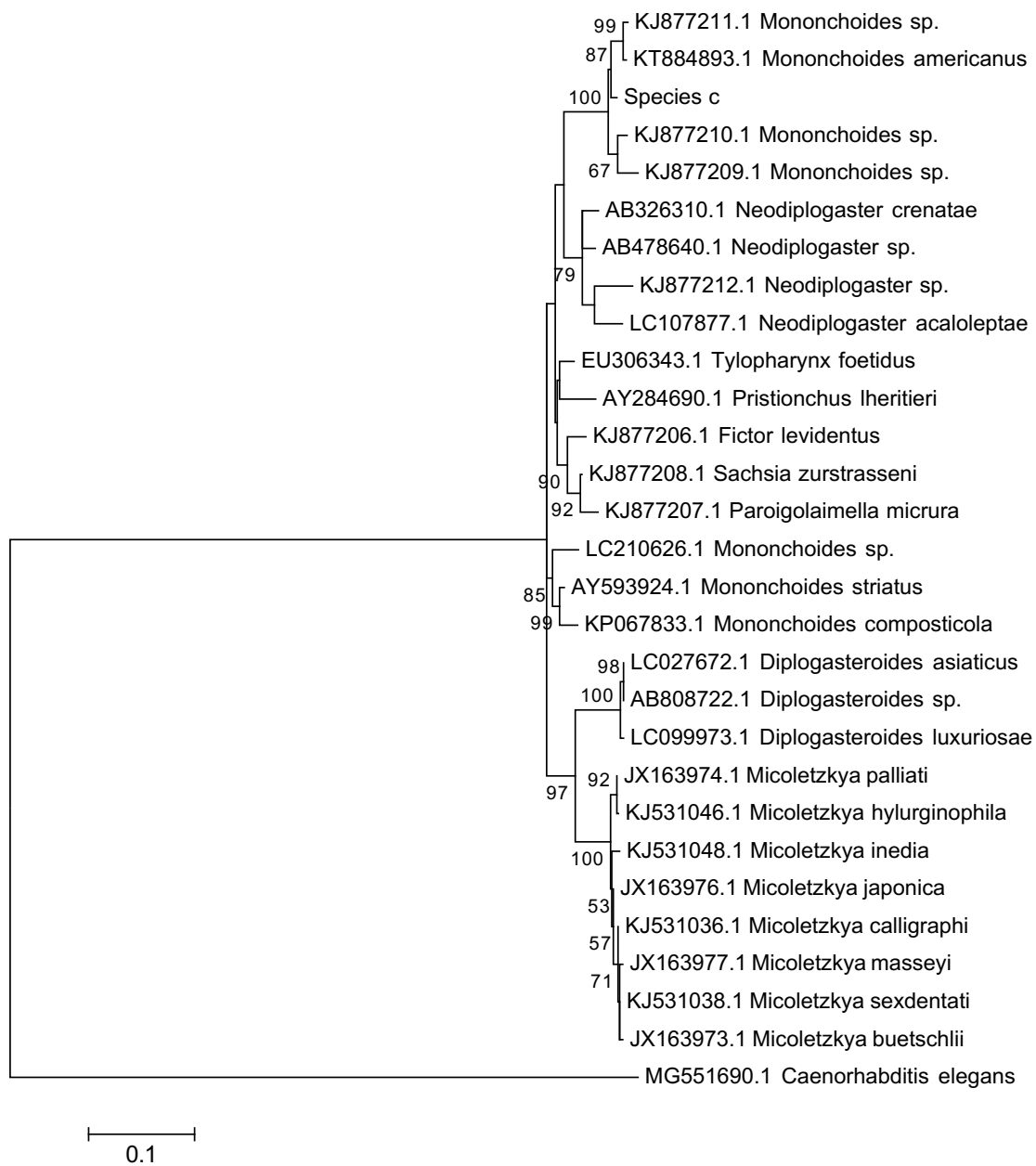


**Figure A.12. Phylogenetic tree of species c (based on SSU sequence)**

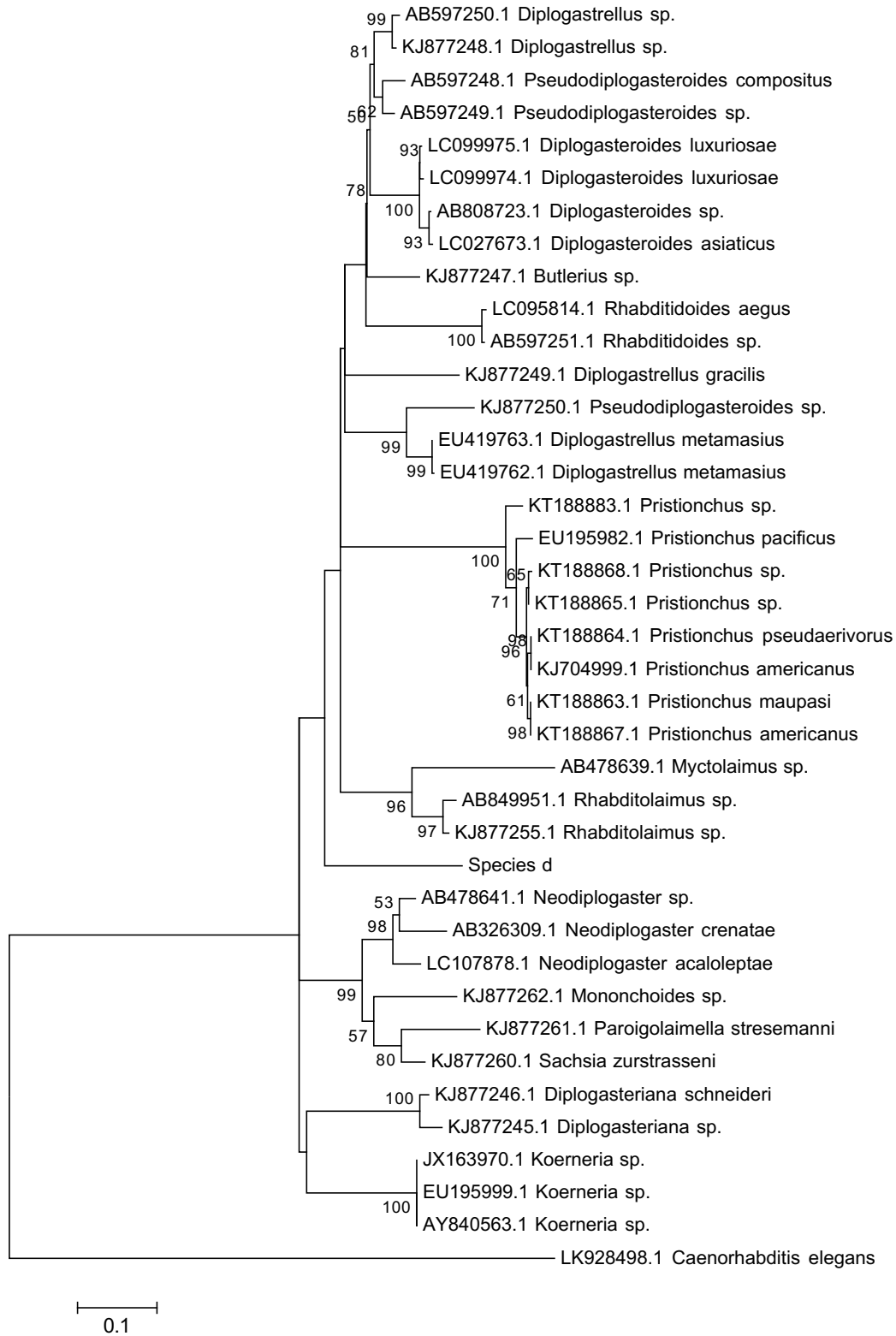


**Figure A.13. Phylogenetic tree of species d (based on LSU sequence)**

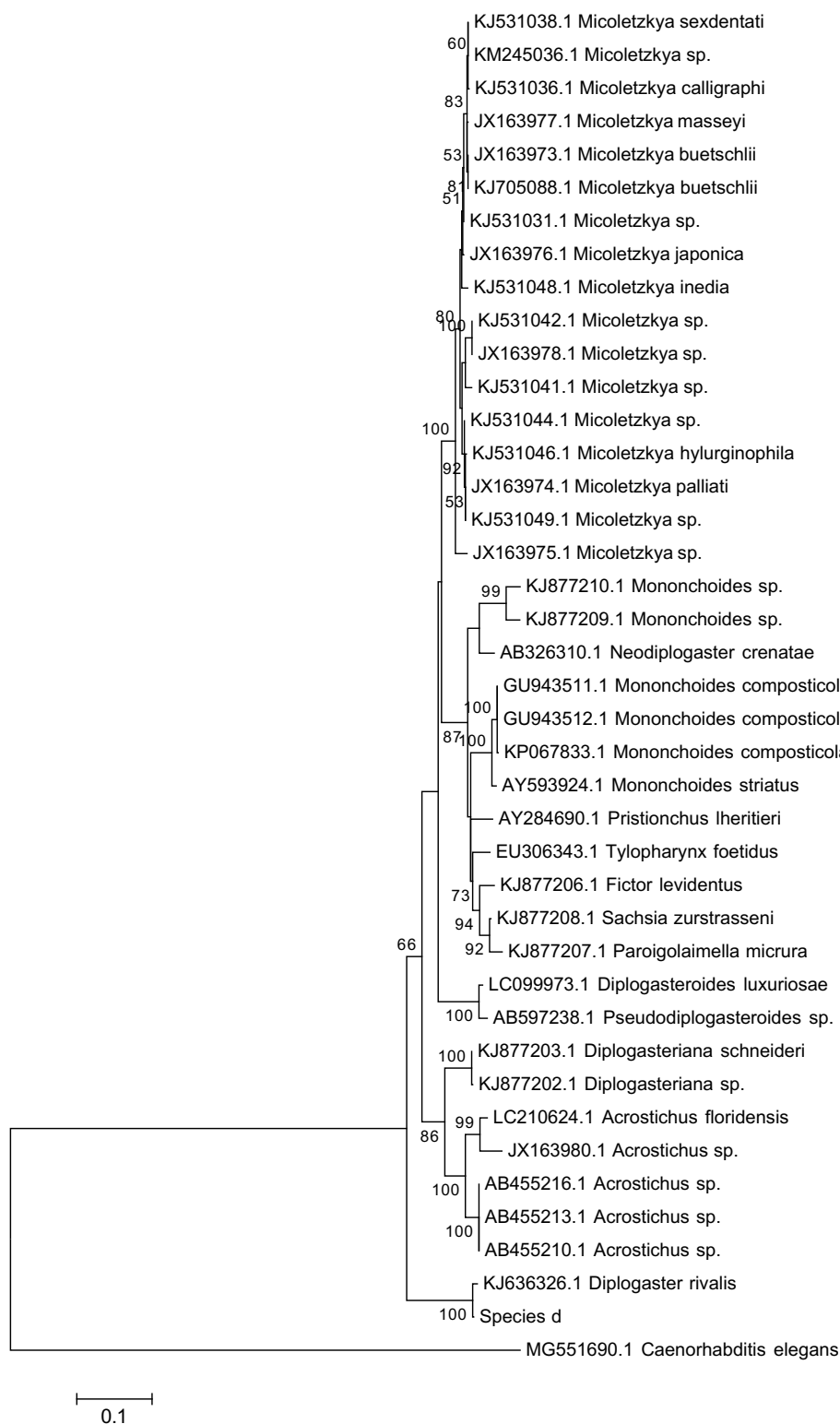


**Figure A.14. Phylogenetic tree of species d (based on SSU sequence)**

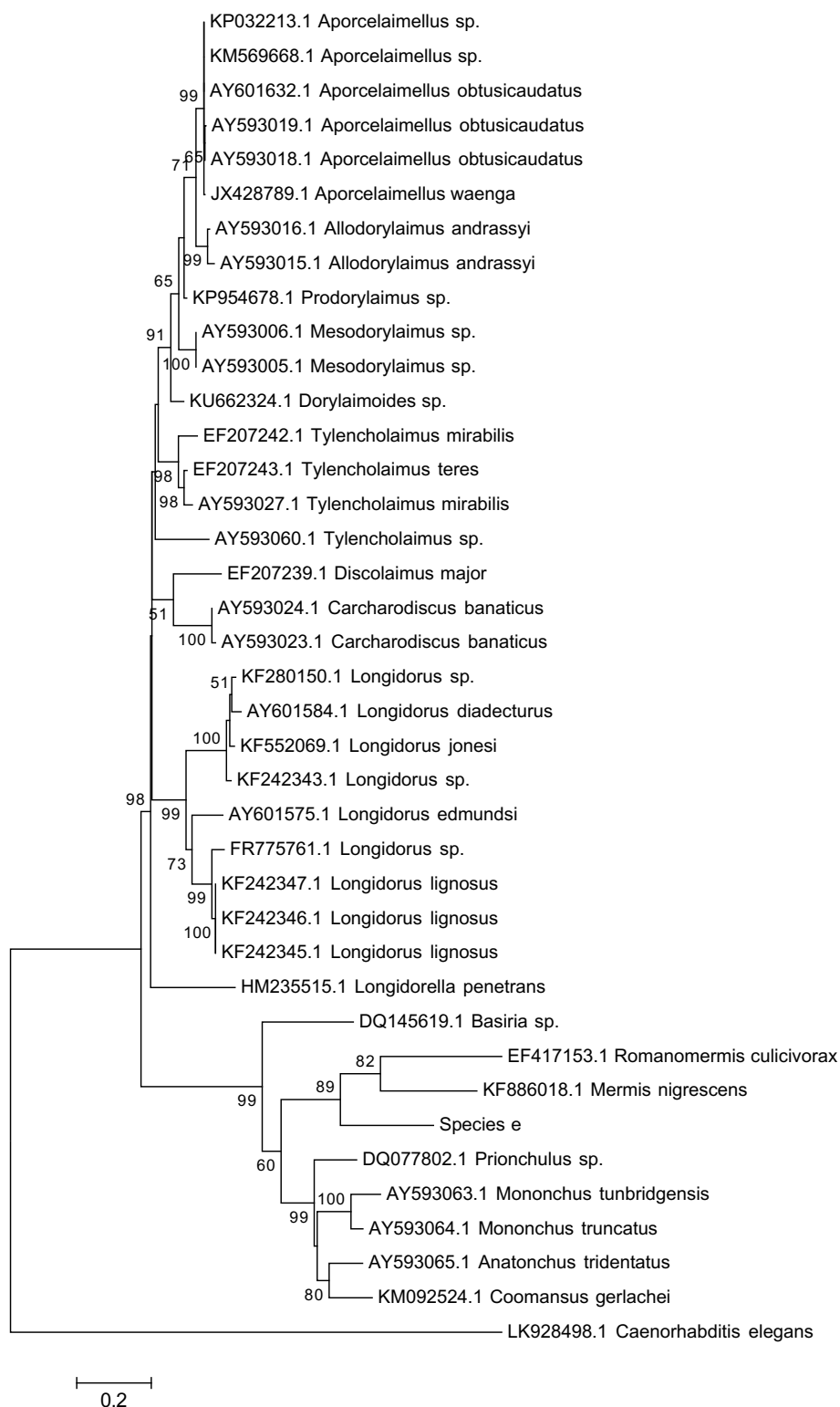


**Figure A.15. Phylogenetic tree of species e (based on LSU sequence)**

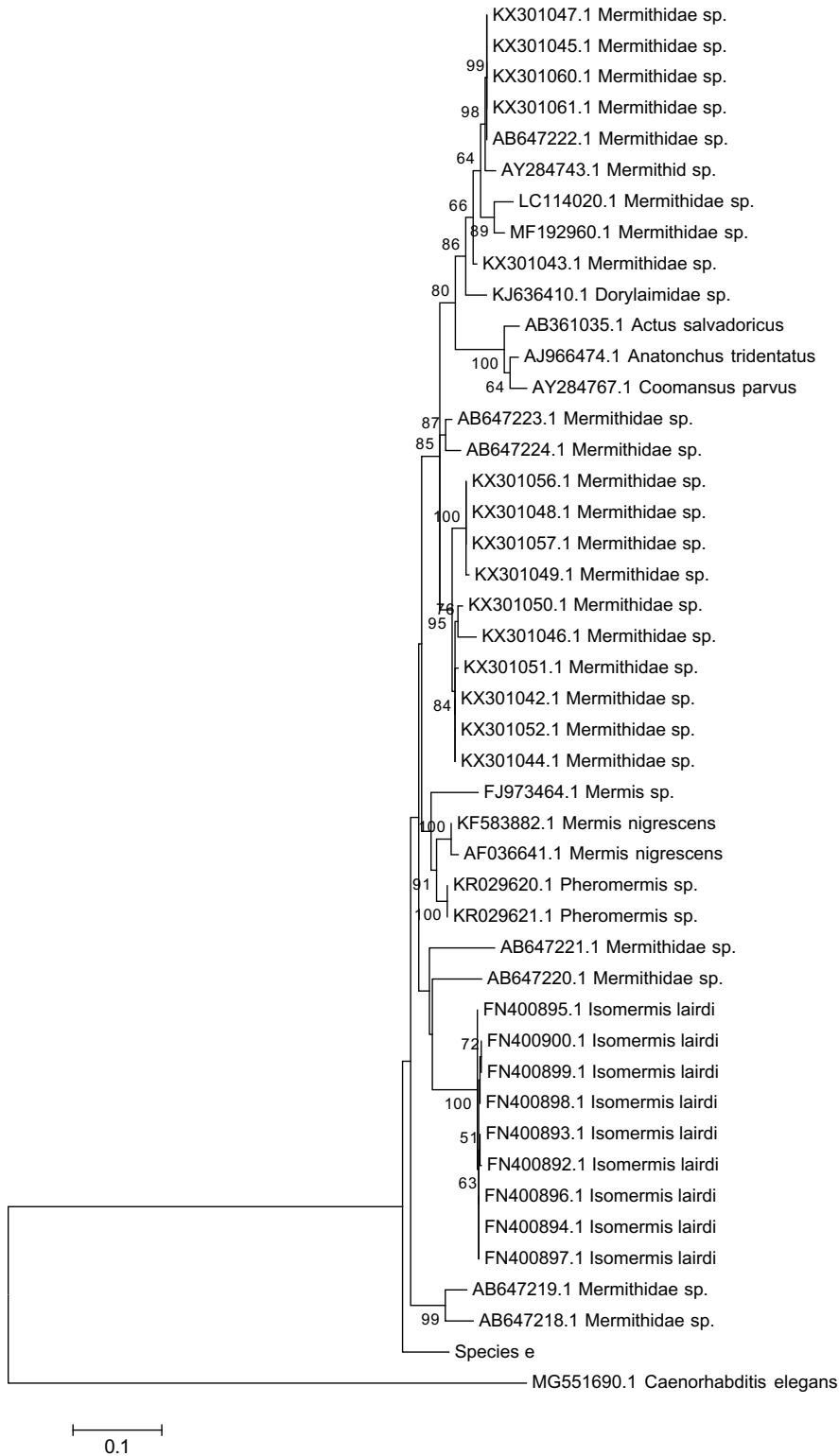


**Figure A.16. Phylogenetic tree of species e (based on SSU sequence)**

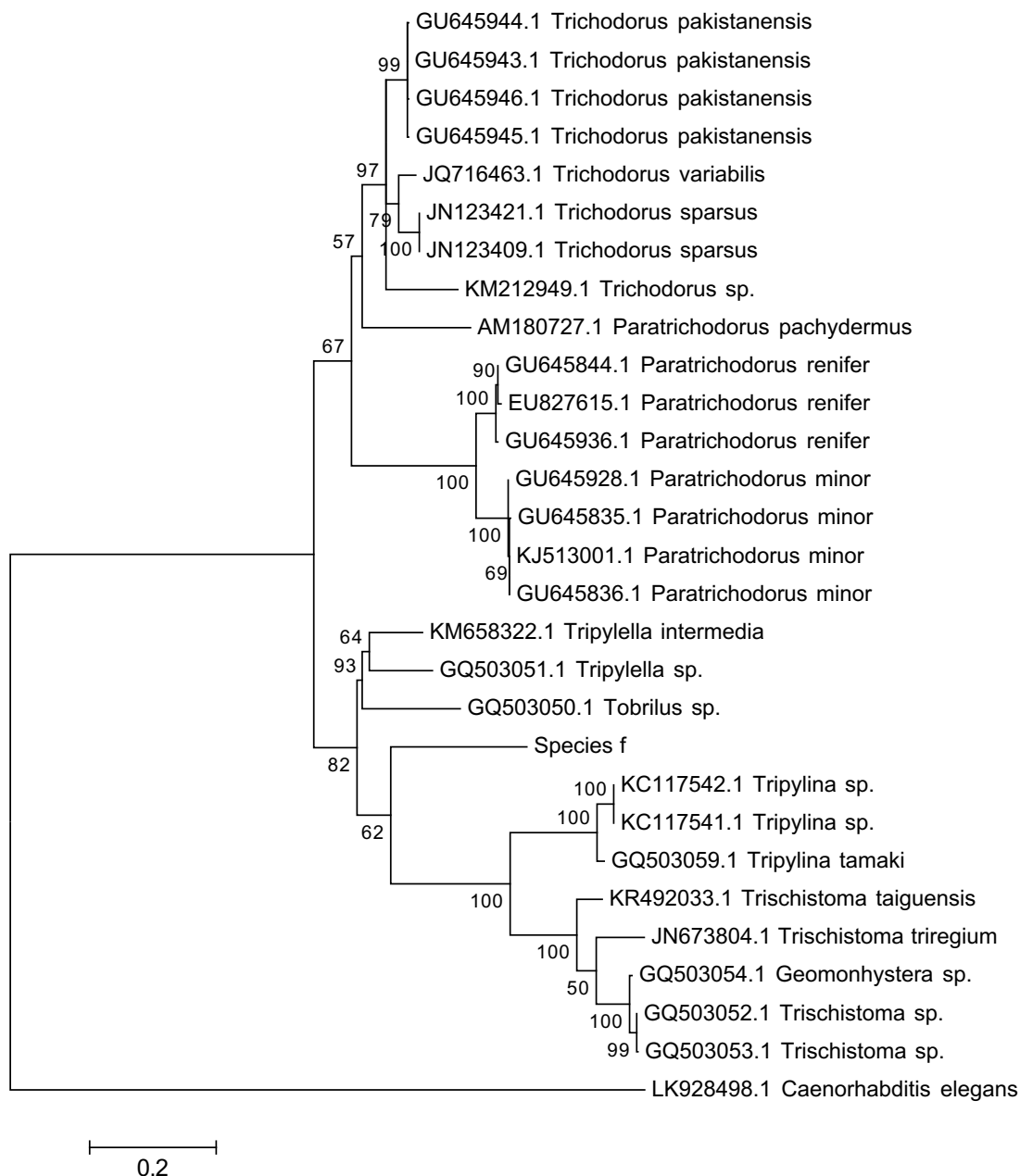


**Figure A.17. Phylogenetic tree of species f (based on LSU sequence)**

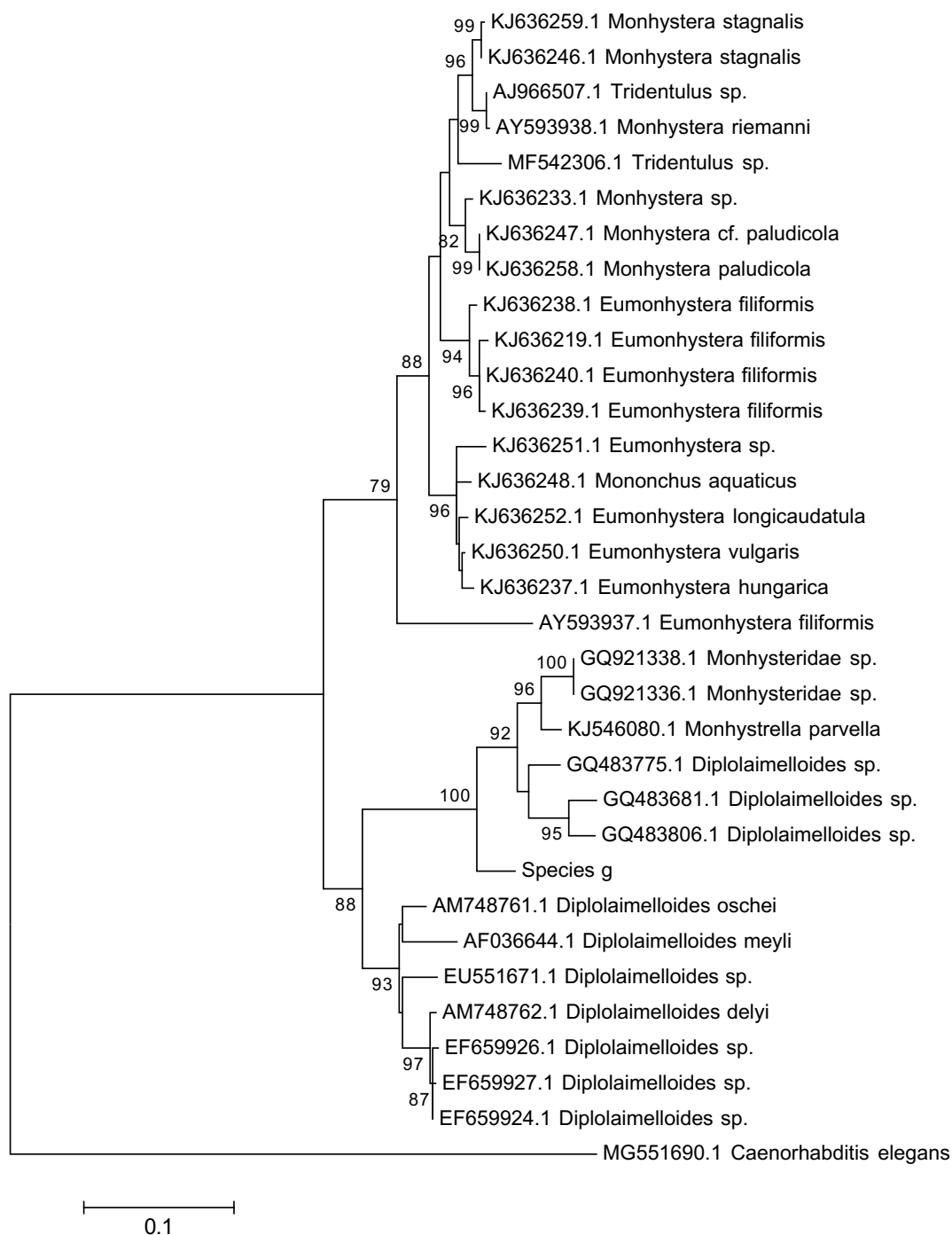


**Figure A.18. Phylogenetic tree of species g (based on SSU sequence)**

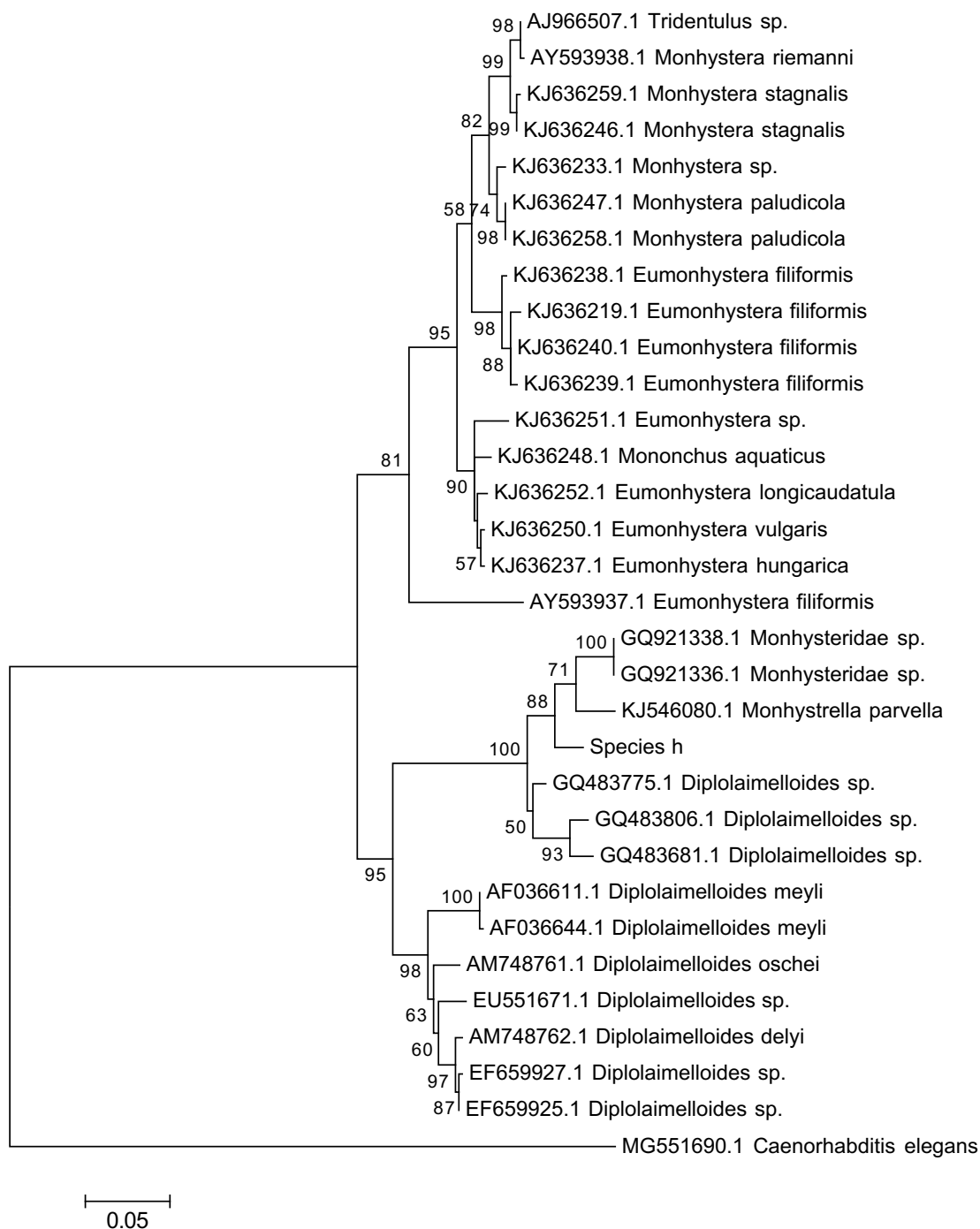


**Figure A.19. Phylogenetic tree of species h (based on SSU sequence)**



g	-----ATACAACAGCCGTTGTTTCTTGGATCTCTTCTACTTGGA	42
h	----AGCCGCGATAGCTCATTACAACAGCCGTTGTTTCTTGGATCTCTTCTACTTGGA	56
i	AGTGAGCCGCGATAGCTCATTACAACAGCCGTTGTTTCTTGGATCTCTTCTACTTGGA	60
	*****	
g	TAAGTGTGGTAATTCTAGAGCTAATACATGCAATCAAGCCCTGAACCTACGTGACGGGCG	102
h	TAAGTGTGGTAATTCTAGAGCTAATACATGCAACCAAGCCCTGAACCTACGTGACGGGCG	116
i	TAAGTGTGGTAATTCTAGAGCTAATACATGCAACCAAGCCCTGAACCTACGTGACGGGCG	120
	*****	
g	CATTTATTAGAACAAAACCATCCGGCTTTGC--CGTGCTTTGGTGACTCTGAATAACTGA	160
h	CATTTATTAGAACAAAACCATCTGGCCTCGCGCCATCTAATGGTGACTCTGAATAACTGA	176
i	CATTTATTAGAACAAAACCATCTGGCCTCGCGCCATCTAATGGTGACTCTGAATAACTGA	180
	*****	
g	GCCGATCGCACGGGCTTGTCCCGGCGACATATCTTTCAAGTGCTGCCTTATCAGGTTTC	220
h	GCCGATCGCACGGGCTCGTCCCGGCGACGTATCTTTCAAGTGCTGCCTTATCAGGTTTC	236
i	GCCGATCGCACGGGCTTGTCCCGGCGACATATCTTTCAAGTGCTGCCTTATCAGGTTTC	240
	*****	
g	GTTGGCGGTTTATGTGACCGCCAAGCCTGTAACGGGTAACGGAGGATCAGGGTCTGACTC	280
h	GTTGGCGGTTTATGTGACCGCCAAGCCTGTAACGGGTAACGGAGGATCAGGGTCTGACTC	296
i	GTTGGCGGTTTATGTGACCGCCAAGCCTGTAACGGGTAACGGAGGATCAGGGTCTGACTC	300
	*****	
g	CGGAGAGGGAGCCTGAGAAACGGCTACCACCTCTAAGGAAGGCAGCAGGCGCGCAAATTA	340
h	CGGAGAGGGAGCCTGAGAAACGGCTACCACCTCTAAGGAAGGCAGCAGGCGCGCAAATTA	356
i	CGGAGAGGGAGCCTGAGAAACGGCTACCACCTCTAAGGAAGGCAGCAGGCGCGCAAATTA	360
	*****	
g	CCCACTCTTGGAGCAAGGAGGTAGTGACGAAAAATACCAAGGTCAGGCTCATTGAGCTTG	400
h	CCCACTCTTGGAGCAAGGAGGTAGTGACGAAAAATACCAAGGTCAGGCTCATCGAGCTTG	416
i	CCCACTCTTGGAGCAAGGAGGTAGTGACGAAAAATACCAAGGTCAGGCTCATCGAGCTTG	420
	*****	
g	ACCATTGGAATGAGAACAATCTAAATCCTTTAACGAGGATCTAGTGAGGGCAAGTCTGG	460
h	ACCATTGGAATGAGAACAATCTAAATCCTTTAACGAGGATCTAGTGAGGGCAAGTCTGG	476
i	ACCATTGGAATGAGAACAATCTAAATCCTTTAACGAGGATCTAGTGAGGGCAAGTCTGG	480
	*****	
g	TGCCAGCAGCCGCGGTAATCCAGCTCCGCAAGTGATTCTTACTGTTGCGTTTAAAT	520
h	TGCCAGCAGCCGCGGTAATCCAGCTCCGCAAGTGATTCTTACTGTTGCGTTTAAAT	536
i	TGCCAGCAGCCGCGGTAATCCAGCTCCGCAAGTGATTCTTACTGTTGCGTTTAAAT	540
	*****	
g	AGCTCGTAGTTGGATCTGCGTGTTTAGCGCGTGGTGCTGCTTTTGTGGTTACTGCGACG	580
h	AGCTCGTAGTTGGATCTGCGTGTTTAGCGCGTGGTGCTGCTTTTGTGGTTACTGCGACG	596
i	AGCTCGTAGTTGGATCTGCGTGTTTAGCGCGTGGTGCTGCTTTTGTGGTTACTGCGACG	600
	*****	
g	CGACACAGTGTTGCTTCTGCCACGATGCTCTCGCGAGTGTCGTGTCGATAAGCAGAGTT	640
h	CGACACAGTGTTGCTTCTGCCACGATGCTCCACACAAGG-----	635
i	CGACACAGTGTTGCTTCTGCCACGATGCTC-----	631
	*****	
g	TACTTTGAACAAATCAGAGTGCTCAAAACGGGCGTTTCGCTCGAATGTTCTTGCATGGAA	700
h	-----	635
i	-----	631
g	TAATGGAATA	710
h	-----	635
i	-----	631

Figure A.20. Species g and h SSU sequence alignment

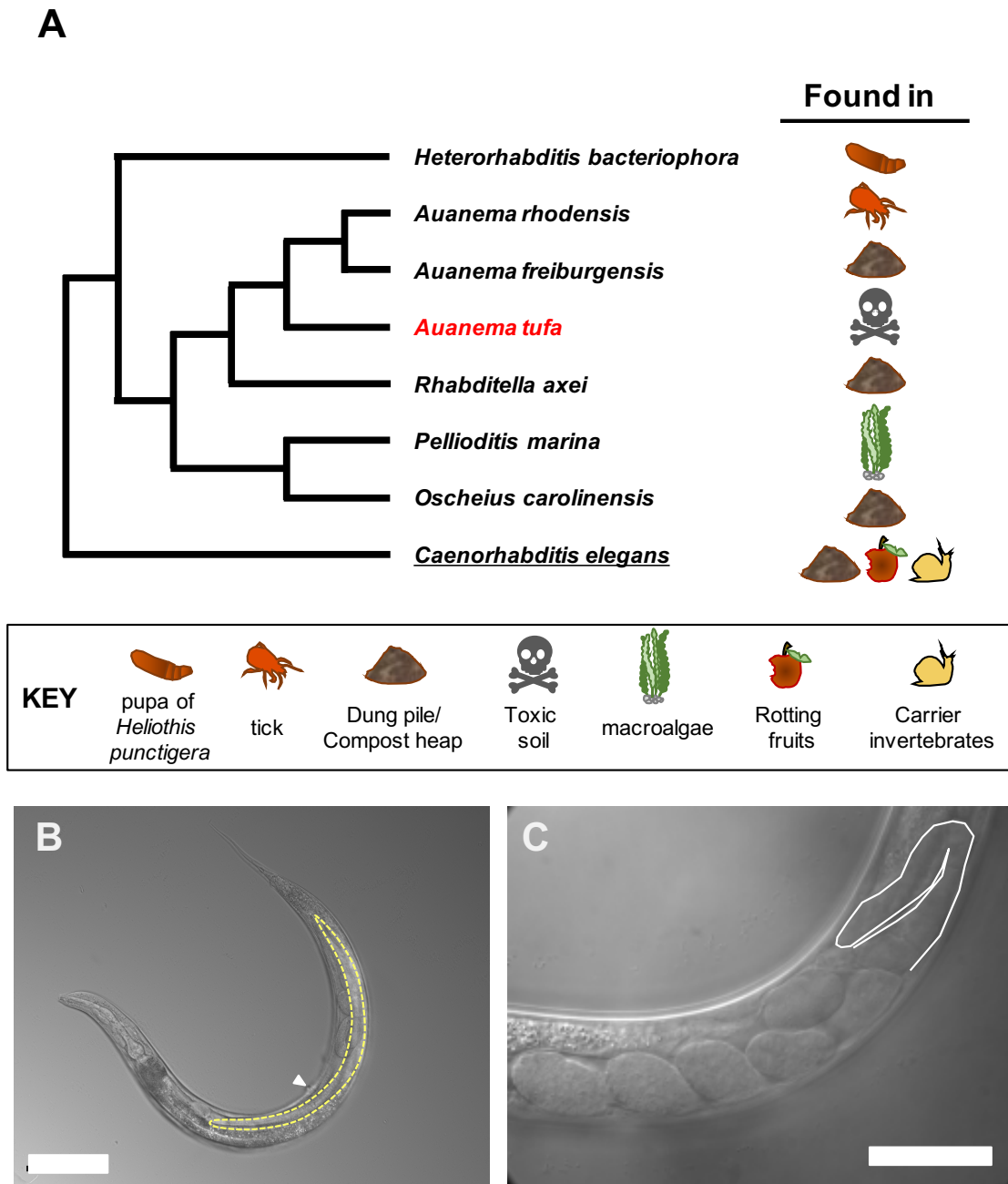


**Figure A.21. Characteristics of *Auanema tufa*.** (A) Simplified phylogenetic tree showing the phylogenetic relationships of *Auanema tufa* (highlighted in red) and selected Rhabditina based on SSU sequences. (B) One of the two arms of the *A. tufa* adult gonad. The gonad arm is outlined with white line. Scale bar: 20 $\mu$ m. (C)

The representative image of an adult *A. tufa*. The position of the vulva was indicated by the white arrow. Scale bar: 100 $\mu$ m

• *Auanema* sp.  
• *Caenorhabditis elegans*

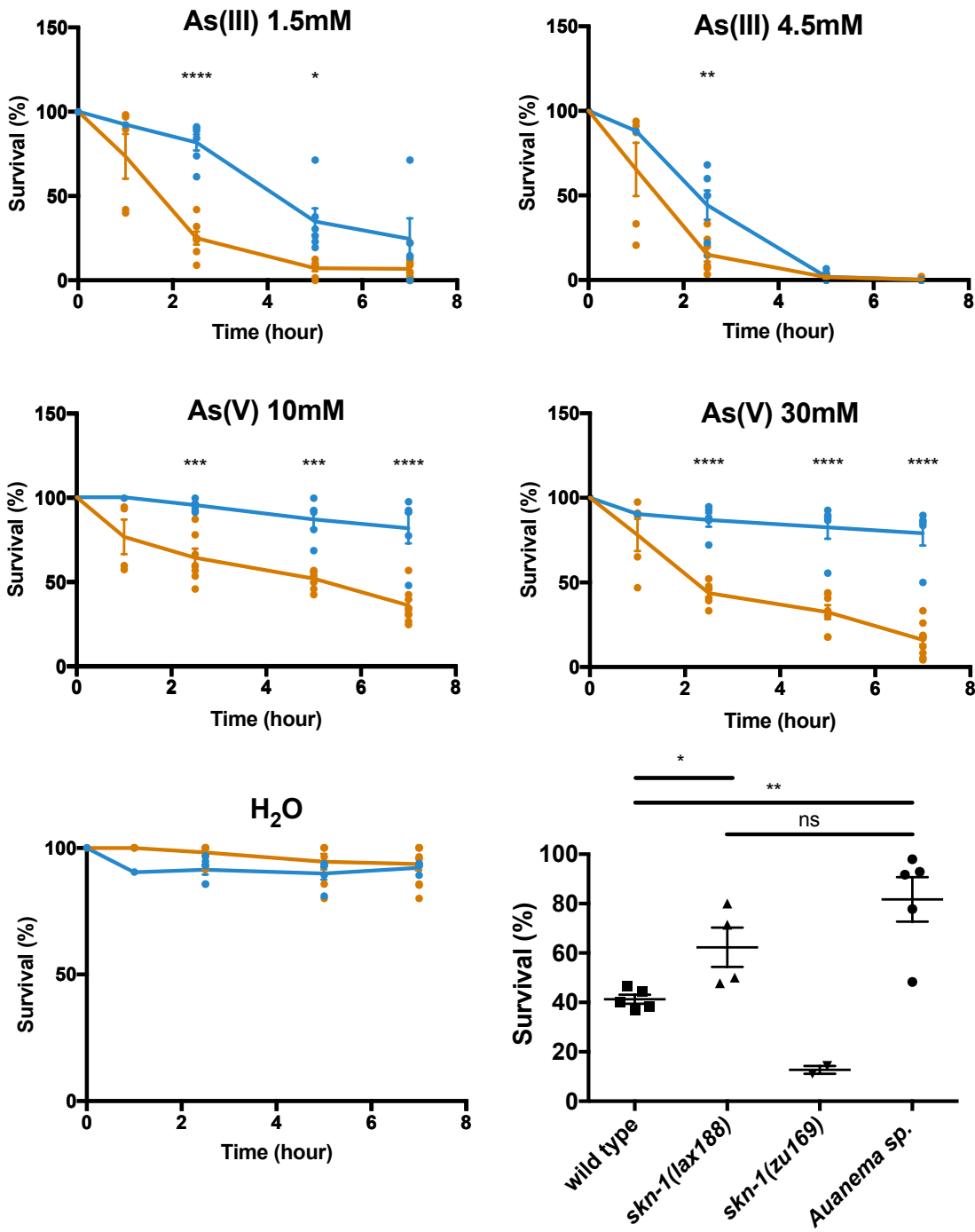


**Figure A.22. *A. tufa* is resistant to arsenic. (A-D)** The survival curve of *A. tufa* (blue) and *C. elegans* (orange) in 1.5mM As(III) (A), 4.5mM As(III) (B), 10mM As(V) (C), or 30 mM As(V) (D). **(E)** The survival of *Auanema sp.* (blue) and *C. elegans* (orange) in water over time. Statistics: two-way ANOVA with Bonferroni correction. “\*” <0.05, “\*\*” <0.01, “\*\*\*” < 0.001, “\*\*\*\*” <0.0001. **(F)** The survival percentage of *C. elegans*, wild-type animals, *skn-1* mutants (with gain-of-function (*lax188*) and *A. tufa* with 10mM As(V) treatment for seven hours. WT, wild-type; gf, gain-of-function. Statistics: One-way ANOVA with Tukey’s post hoc test after the validation of normal distribution using the SPSS software “\*” p<0.05. Error bars indicate the standard error of the mean.

## A.7 References

1. Borgonie G, et al. (2011) Nematoda from the terrestrial deep subsurface of South Africa. *Nature* 474(7349):79–82.
2. Borgonie G, et al. (2015) Eukaryotic opportunists dominate the deep-subsurface biosphere in South Africa. *Nature communications* 6:8952.
3. Treonis AM, Wall DH (2005) Soil nematodes and desiccation survival in the extreme arid environment of the antarctic dry valleys. *Integrative and comparative biology* 45(5):741–50.
4. Wharton D, Ferns D (1995) Survival of intracellular freezing by the Antarctic nematode *Panagrolaimus davidi*. *The Journal of experimental biology* 198(Pt 6):1381–7.
5. Sapir A, et al. (2014) Microsporidia-nematode associations in methane seeps reveal basal fungal parasitism in the deep sea. *Front Microbiol* 5:43.
6. Vanreusel A, De Groote A, Gollner S, Bright M (2010) Ecology and biogeography of free-living nematodes associated with chemosynthetic environments in the deep sea: a review. *PLoS ONE* 5(8):e12449.
7. Borgonie G, et al. (2015) Deep subsurface mine stalactites trap endemic fissure fluid Archaea, Bacteria, and Nematoda possibly originating from ancient seas. *Frontiers in microbiology* 6:833.

8. Danovaro R, et al. (2010) The first metazoa living in permanently anoxic conditions. *BMC Biol* 8:30.
9. Riddle DL, Albert PS (1997) Genetic and environmental regulation of dauer larva development. *C. Elegans II*, eds Riddle DL, Blumenthal T, Meyer BJ, Priess JR (Cold Spring Harbor (NY)). 2nd Ed. Available at: <http://www.ncbi.nlm.nih.gov/pubmed/21413222>.
10. Vanfleteren JR, Braeckman BP (1999) Mechanisms of life span determination in *Caenorhabditis elegans*. *Neurobiol Aging* 20(5):487–502.
11. Oremland RS, Stolz JF, Hollibaugh JT (2004) The microbial arsenic cycle in Mono Lake, California. *FEMS microbiology ecology* 48(1):15–27.
12. Reheis MC, Stine S, Sarna-Wojcicki AM (2002) Drainage reversals in Mono Basin during the late Pliocene and Pleistocene. *GSA Bulletin* 114(8):991–1006.
13. Cloud P, Lajoie KR (1980) Calcite-impregnated defluidization structures in littoral sands of mono lake, California. *Science* 210(4473):1009–1012.
14. Nielsen LC, DePaolo DJ (2013) Ca isotope fractionation in a high-alkalinity lake system: Mono Lake, California. *Geochimica et Cosmochimica Acta* 118:276–294.
15. Jellison R, Melack JM (1993) Meromixis in hypersaline Mono Lake, California. 1. Stratification and vertical mixing during the onset, persistence,

- and breakdown of meromixis. *Limnology and Oceanography* 38(5):1008–1019.
16. Smedley PL, Kinniburgh D (2002) A review of the source, behaviour and distribution of arsenic in natural waters. *Applied Geochemistry* 17(5):517–568.
  17. Hughes MF (2002) Arsenic toxicity and potential mechanisms of action. *Toxicol Lett* 133(1):1–16.
  18. Council NR (2001) *Arsenic in Drinking Water: 2001 Update* (The National Academies Press, Washington, DC) doi:10.17226/10194.
  19. Wiens JA, Patten DT, Botkin DB (1993) Assessing ecological impact assessment: Lessons from Mono Lake, California. *Ecological applications* : a publication of the Ecological Society of America 3(4):595–609.
  20. Raymond MW DA and Marshall, CJ (2013) Factors determining nematode distributions at Cape Hallett and Gondwana station, Antarctica. *Antarctic Science* 25(3):347–357.
  21. Hooper DJ (1986) Extraction of free-living stages from soil. In *Laboratory Methods for Work with Plant and Soil Nematodes*, ed Southey JF (HMSO, London), pp 5–30.



22. Nunn GB (1992) Nematode molecular evolution: an investigation of evolutionary patterns among nematodes based upon DNA sequences. Ph.D. (University of Nottingham, United Kingdom).
23. Floyd R, Abebe E, Papert A, Blaxter M (2002) Molecular barcodes for soil nematode identification. *Molecular ecology* 11(4):839–50.
24. Hall BG (2013) Building phylogenetic trees from molecular data with MEGA. *Molecular biology and evolution* 30(5):1229–35.
25. Guindon S, Gascuel O, Rannala B (2003) A simple, fast, and accurate algorithm to estimate large phylogenies by maximum likelihood. *Syst Biol* 52(5):696–704.
26. Schlaberg R, Simmon KE, Fisher MA (2012) A systematic approach for discovering novel, clinically relevant bacteria. *Emerg Infect Dis* 18(3):422–430.
27. Marande W, López-García P, Moreira D (2009) Eukaryotic diversity and phylogeny using small- and large-subunit ribosomal RNA genes from environmental samples. *Environ Microbiol* 11(12):3179–3188.
28. Yeates GW, Coleman, DC (1982) Role of nematodes in decomposition. *Nematodes in Soil Ecosystems*, ed Freckman DW (University of Texas Press Austin), pp 55–80.

29. Bento G, Ogawa A, Sommer RJ (2010) Co-option of the hormone-signalling module dafachronic acid-DAF-12 in nematode evolution. *Nature* 466(7305):494–497.
30. Nickle WR (1972) A contribution to our knowledge of the Mermithidae (Nematoda). *J Nematol* 4(2):113–146.
31. Blaxter ML, et al. (1998) A molecular evolutionary framework for the phylum Nematoda. *Nature* 392(6671):71–5.
32. Holterman M, et al. (2006) Phylum-wide analysis of SSU rDNA reveals deep phylogenetic relationships among nematodes and accelerated evolution toward crown Clades. *Molecular biology and evolution* 23(9):1792–800.
33. Kanzaki N, et al. (2017) Description of two three-gendered nematode species in the new genus *Auanema* (Rhabditina) that are models for reproductive mode evolution. *Sci Rep* 7(1):11135.
34. Gaever SV, Moodley L, Beer D de, Vanreusel A (2006) Meiobenthos at the Arctic Håkon Mosby Mud Volcano, with a parental-caring nematode thriving in sulphide-rich sediments. *Marine Ecology Progress Series* 321:143–155.
35. Zeppilli D, et al. (2015) Rapid colonisation by nematodes on organic and inorganic substrata deployed at the deep-sea Lucky Strike hydrothermal vent field (Mid-Atlantic Ridge). *Mar Biodiv* 45(3):489–504.

36. Oremland RS, et al. (2000) Bacterial dissimilatory reduction of arsenate and sulfate in meromictic Mono Lake, California. *Geochimica et Cosmochimica Acta* 64(18):3073–3084.
37. Inoue H, et al. (2005) The *C. elegans* p38 MAPK pathway regulates nuclear localization of the transcription factor SKN-1 in oxidative stress response. *Genes Dev* 19(19):2278–2283.
38. Golden JW, Riddle DL (1984) The *Caenorhabditis elegans* dauer larva: developmental effects of pheromone, food, and temperature. *Dev Biol* 102(2):368–378.
39. Fielenbach N, Antebi A (2008) *C. elegans* dauer formation and the molecular basis of plasticity. *Genes & development* 22(16):2149–65.
40. Campbell JF, Gaugler R (1993) Nictation behaviour and its ecological implications in the host search strategies of entomopathogenic nematodes (*Heterorhabditidae* and *Steinernematidae*). *Behaviour* 126(3/4):155–169.
41. Rödelsperger C, Streit A, Sommer RJ (2013) Structure, function and evolution of the nematode genome. ELS, ed John Wiley & Sons, Ltd (John Wiley & Sons, Ltd, Chichester, UK). doi:10.1002/9780470015902.a0024603.